EXPERIMENTAL INVESTIGATION IN COMBUSTION CHARACTERISTICS OF ETHANOL-GASOLINE BLENDS FOR STRATIFIED CHARGE ENGINE VIA CONSTANT VOLUME COMBUSTION CHAMBER

PIYABOOT ORNMAN

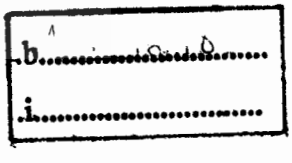

A THESIS SUBMITTED IN FULFILLMENT
OF THE REQUIREMENT FOR THE DEGREE OF
MASTER OF ENGINEERING IN AUTOMOTIVE ENGINEERING
INTERNATIONAL COLLEGE
KING MONGKUT'S INSTITUTE OF TECHNOLOGY LADKRABANG
2011

KMITL-2011-IC-M-004-009

Thesis	Experimental investigation in combustion characteristics of ethanol-gasoline blends for stratified charge engine via constant volume combustion chamber
Student	Mr.Piyaboot Ornman
Student ID.	51061911
Degree	Master of Engineering
Program	Automotive Engineering (International Program)
Year	2011
Thesis Advisor	Asst.Prof.Dr. Chinda Charoenphonphanich
	Prof.Dr. Hidenori Kosaka
	Dr. Nuwong Chollacoop

ABSTACT

The increasing of global energy demand and stringent pollution regulations have promoted research on alternative fuels. In Thailand, Ethanol, can be produced from many sources of national agriculture products as renewable fuel, which was strongly promoted by government due to its many merits for use in transportation field. In this study, combustion characteristics of ethanol-gasoline blend (20%, 85%, and 100%) as well as pure gasoline (E0) were investigated by using a swirl-generated constant volume combustion chamber. Flame propagations of different fuel blends were observed by high speed Schlieren photography technique while pressure history data were recorded for detailed combustion analysis. Combustion behavior, combustion duration and rate of pressure rise of all tested fuels were investigated in various swirl intensities and equivalence ratios. In addition, effect of swirl intensities and ethanol concentration on lean misfire limit were also discussed. The results showed that the high concentration of ethanol blend with the high swirl intensity can significantly extended lean misfire limit while lowering combustion variations. Furthermore, combustion duration can be accelerated by increasing the percentage of ethanol in fuel blend. Through this study, a better understanding of stratified charge combustion fuelled with ethanol/gasoline blends can be achieved.

ACKNOWLEDGEMENTS

Initially, I would like to express, first and foremost, to my supervisor Prof. Dr. Chinda Charoenphonphanich and Professor Hidenori Kosaka for his extensive advice, guidance and encouragement throughout my thesis

I am extremely grateful to thank Dr. Nuwong Chollacoop and National Metal and Materials Technology Center (MTEC), THAILAND for the financial, measuring equipments and also intensive suggestion support that made my study meet well accomplishment

I wish to express my gratitude to assistance from my senior at KMITL automotive laboratory, P'Naren, P'Wittawat, P'Thanawat and P'Pratan for their sincere advice and technical support such as the electronic controller and material cost quotation. I am pleased to have this opportunity to thank the many colleagues, and bachelor subordinate who have helped me with this dissertation . Special thanks to N'Yutthana, N'Pattanit and N'Theerakul for their kind assist, their time and invaluable advice throughout my experiment. I would like to special thanks to Miss Panida Singra for giving me the strength, motivation and support to overcome the difficult moments and to make the most of this experience.

I am also wish to thank Pathumwan Institute of Technology for their support in pressure measuring device and data acquisition system.

Last but not least, I cannot thank enough to my family for their love, interests and supports throughout my life.

CONTENTS

Page

CONTENTS(continued)

Page

CONTENTS(continued)

Page

CONTENTS(continued)

LIST OF FIGURES

Figures Page

LIST OF FIGURES(continued)

Figures Page

LIST OF FIGURES(continued)

Figures Page

LIST OF FIGURES(continued)

Figures Page

LIST OF FIGURES(continued)

Figures Page

Chapter 1

Introduction

1.1 Background

From the IEA (International Energy Agency) and Exxon Mobile Corporation reports, Global energy demand has been increasing continuously for the last decade. Projection view to the year 2030 of energy demand show that the consumption in oil is significantly growing, especially in transportation field, the growing rate is approximately 1.7% per year. The effect from this rising of energy consumption that should be concerned are the fossil fuel shortage and the environmental issues. Because of majority sources of energy use in transportation sector is come from the crude oil, fossil fuel, which cannot be re-produced in a few years. It mean that the balance between demand and supply will be deteriorated in the near future. Furthermore, in environmental issues, emission from the vehicle or transportation sector will be increasing for the same time of fossil fuel usage. However, it is unfortunately to said that even excellent combustion technology can be provided the complete combustion, green house gas, CO_2 emission cannot be reduced by utilize of this fossil fuel. Due to the carbon monoxide that generated in exhaust gas is come from the non-renewable source, fossil fuel or crude oil. Carbon will be produced in one-way path and cannot re-cycle back to the environment.

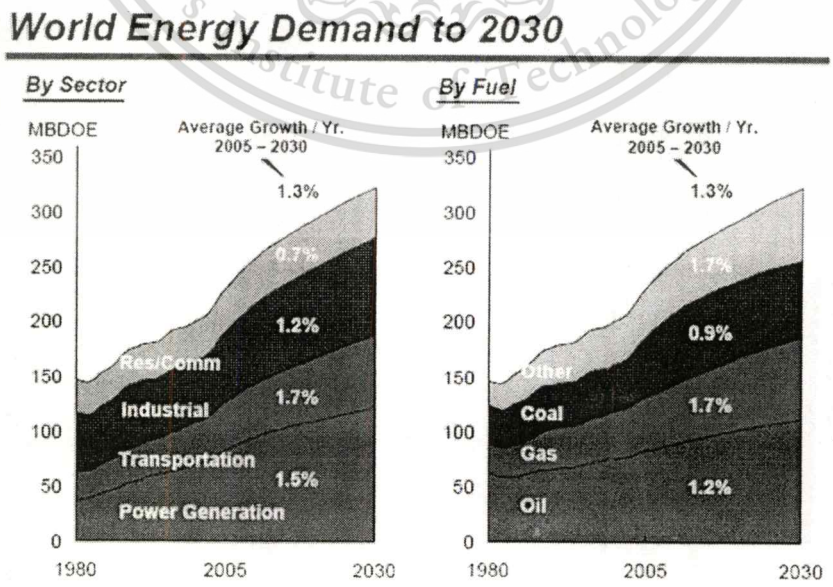

Figure 1.1 Global energy demand, View to the year 2030.

For the last decade year, there are many attempts to reduce fossil fuel usage and its emission. One of this is development in combustion technology. In the last few years, the targets of research are focused on high engine efficiency, low fuel consumption and low level of emission. The gasoline stratified charge and lean burn engine are challenging one to overcome both fuel consumption and exhaust gas emission. For stratified charge engine, it is well known that lean, stratified combustion can reduce fuel consumption and gain some merits in gasoline spark-ignited, direct injection engines for several reasons. First, unthrottled operation allows for a significant reduction in pumping loss, especially at low loads. Second, the lean mixture being compressed has a higher ratio of specific heats. This allows for a more efficient compression and expansion process [1]. In theory, for an Otto-cycle engine, the efficiency η_{th} can be written as $\eta_{th} = 1-(1/r_c^{\kappa-1})$ where r_c is compression ratio and κ is specific heat ratio. As an engine operates leaner, the specific heat ratio of combustion mixture becomes higher. If the specific heat ratio (κ) can further be raised, the heat efficiency and engine power output can be improved [2]. In addition, volumetric efficiency in stratified charge engine could be increased by cooling effect from direct injection process [2, 3]. Although this combustion can achieve many kinds of advantage for combustion characteristics, it produces much unburned hydrocarbon and soot because of inhomogeneous charge mixture in the combustion chamber. The main problem is a misfiring under lean operation even if whole air-fuel mixture is very lean [4]. In stratification, air-fuel ratio tends to be over-rich in the middle of the mixture and over-lean in the periphery bordering surrounding air. It is essential to minimize the above mentioned air-fuel ratio difference by enhancing the stratification degree, defined by the ratio of fuel quantity involved in nearly stoichiometric mixture zone to total fuel quantity. As the stratification degree becomes low, unburned fuel amount increases and fuel economy deteriorates.

As describe in prior paragraph, limitation of spark ignition direct injection are soot formation and HC emission. To overcome this limitations, low HC concentration fuel and renewable energy are very interesting. the development of alternative fuel engines has attracted more attention. Alcohol, especially ethanol, was the challenging candidate in alternative fuel since it can be produced from many sources of biomass, and is indeed the renewable energy. In combustion advantages, high heat of vaporization can be support the cooling effect of air charge in combustion

chamber. Since, the volumetric efficiency will be increased. With low HC chain of ethanol fuel, vaporization in high temperature will be accelerated by reducing the time of mixture formation prior the combustion process, thus it isn't need the time to mixture distribution like the high HC fraction fuels. Moreover, high octane rating in ethanol fuel can be supported high compression ratio operation without knock phenomena. Consequently, thermal efficiency can be improved by utilizing this alternative fuel with the high compression ratio engine. For emission aspects, since the ethanol fuel has the lower HC concentration compare with conventional gasoline. Tendency of soot formation and also HC emission will be reduced.

Considering in global impacts, due to ethanol can be produced from the biomass and renewable source. Carbon emitted from the combustion will be balanced and not produced more greenhouse gas. Since the engine use hydrocarbon in the fuel to combust with air and then emit carbon dioxide to the exhaust pipe, then this CO_2 will be absorbed by the plant to use in photo-synthesis process. After that, CO_2 will be converted back to hydrocarbon store within the plant. And finally, this plant or biomass will be synthesis as renewable fuel like ethanol. This cycle of carbon is called "Carbon neutral", it's mean that combust gas, especially CO_2, from biomass is not be generated more. However, CO2 in environment still balance and not change. In Thailand, Ethanol, can be produced from many sources of national agriculture products as renewable fuel, the raw materials for ethanol production, cassava and sugarcane, are also the main economic crops in Thailand. Furthermore, ethanol was strongly promoted by government due to its many merits for use in transportation field and can be improved national economic by reduced imported oil dependency. As a result, using ethanol in stratified-charge, spark-ignition, direct-injection engines is capable of achieving significant gains in both volumetric and thermal efficiencies and also reducing the CO_2 emission simultaneously. Nevertheless, it is advantageous to combine the advantage of direct injection stratified charge combustion with oxygenated fuels, ethanol. it is necessary to investigate the combustion characteristics in order to obtain the stable lean combustion for minimizing the HC emission due to misfiring.

In this study, the effect of swirl ratio on the combustion characteristics was investigated in the ethanol /gasoline blends, which vary from pure gasoline (E0) to pure ethanol (E100) in the swirl-generated constant volume combustion chamber.

With the pressure analysis data, rate of pressure rise (dp/dt), combustion duration and mass fraction burned rate were analyzed while high speed video camera was used to observe flame propagation during combustion processes.

1.2 Objectives

1.2.1. To investigate effect of ethanol blends on combustion characteristics in direct injection stratified charge (DISC) combustion

1.2.2. To study the influence of swirl intensity on mixture stratification and also combustion characteristics

Chapter 2

Literature Reviews

2.1 Introduction

Stratified charge combustion has been recognized as mean of both improving engine efficiency and lowering exhaust emissions. However, there are many factors that affect to the combustion process, such as physical properties of the fuel, swirl intensity, ignition timing, equivalent ratio, ambient temperature and pressure etc. Consequently, control combustion stability of this combustion has been challenging. In view of the wide range of investigation to improve combustion stability and efficiency, the literature reviews will be focused on influence of ethanol content with lean stratified combustion and effect of the swirl intensities on the combustion characteristics.

In this chapter, the reviewed papers will be presented the fundamental of stratified charge combustion and their strategies including the numerical model in SI engine. Definition of combustion characteristics in constant volume combustion chamber base on pressure history data will be described. Then, the potential and properties of ethanol as a fuel in the internal combustion engine are also reviewed. Finally, In order to improve combustion stability, Mixture stratification and influenced parameters are considered.

2.2 Stratified charge combustion

Since the 1920s, attempts have been made to develop a hybrid internal combustion engine that combines the advantage features of the spark-ignition engine and the diesel. So, The stratified-charge engine is something of a hybrid between the homogeneous charge spark-ignition engine and the diesel engine. From the historical perspectives, Direct injection stratified charge combustion were proposed and implemented by Texaco Controlled Combustion System (TCCS) and MAN-FM of Maschinenfabrik Auguburg-Nurnburg [3].

This combustion type can operate in leaner than conventional homogeneous charge SI engine .Furthermore, it can controlled engine load without throttling as the diesel engine. Since, the emission will become the same level of SI engine as indicated in Figure 2.9 while efficiency was close to the diesel engine.

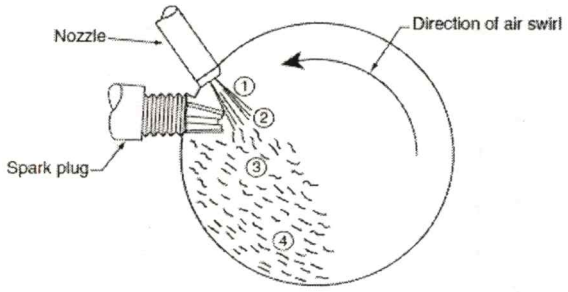

Figure 2.2 Stratified-charge engine combustion chamber (Benson and Whitehouse, 1979).

One example of a stratified-charge engine combustion chamber is shown schematically in plan view in Figure 2.2, taken from Benson and Whitehouse(1979) . As shown in Figure 2.2,The mixture burns near the spark plug and downstream of the spark plug as a premixed flame, while in the rest of the cylinder the mixture is very lean. The fact that fuel is introduced at one point in the chamber and burnt immediately means that the overall air-fuel ratio can be very lean, while the local ratio is near, and is a direct result of the stratified nature of the charge. The stratified charge engine is thus able to operate over a much wider range of air-fuel ratios than a conventional spark-ignition engine. This results in higher efficiency due to leaner overall air–fuel ratios and reduced pumping losses, since less throttling is required.

2.2.1 Stratified charge technique and strategies

In early strategy of combustion in direct injection engine , Operation mode should be divided into two major condition. Figure 2.3 show the schematic of its operations , stratified charge is achieved by a late injection during the compression stroke while the homogeneous is operated during late intake stroke or early injection to realize and uniform homogeneous mixture

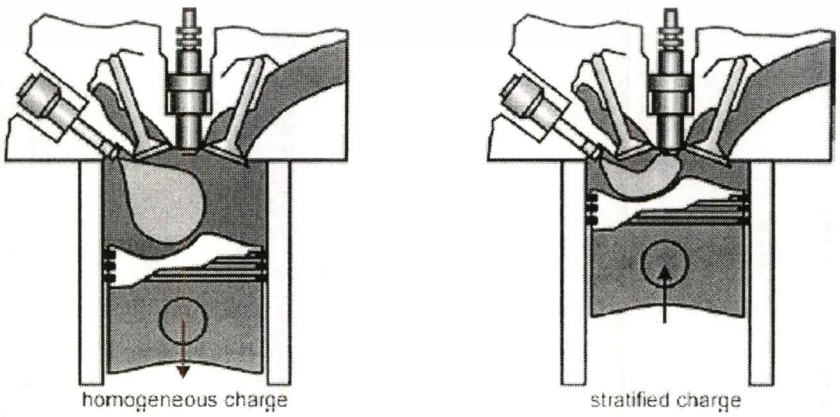

Figure 2.3 Homogeneous (early injection) and Stratified-charge mode (late injection)

Dependent on load and engine speed, different operating modes have to be applied in order to realize a stable and satisfactory engine operation within the complete engine map, Figure 2.4, In the case of full load a homogeneous stoichiometric or even fuel-rich mixture inside the complete combustion chamber is necessary in order to include the complete air charge in the combustion process and to achieve maximum torque. Early injection during the intake stroke is applied in order to have enough time to inject the required large fuel quantities and to achieve a homogeneous fuel-air mixture. At medium and low part load the stratified-charge mode offers the possibility to reduce pumping losses significantly. However, the operating range of this mode is limited in engine speed and load.

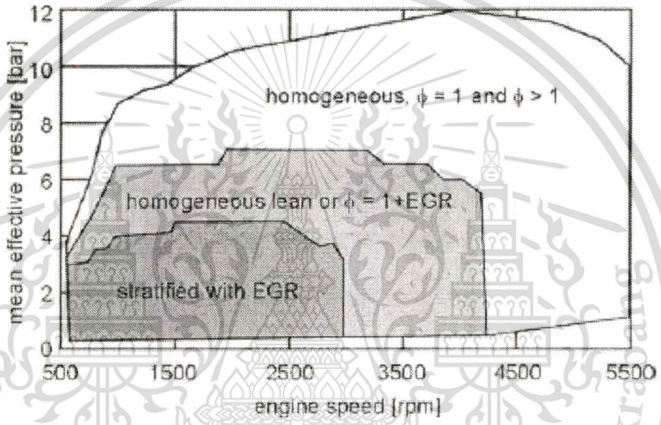

Figure 2.4 Operation mode within the engine map [3]

At increasing engine speed, the in-cylinder flow field becomes more and more turbulent, and above approx. 3000 rpm it can no more be utilized to keep the mixture cloud compact. Above break mean effective pressures (BMEP) of approx. 5 bar, the injected fuel quantity becomes too large in order to realize a sufficient mixture formation prior to ignition, and soot is produced.

As show in Figure 2.5, there are three basic approaches of controlling the stratified-charge combustion, wall-guided, air-guided, and spray-guided techniques.

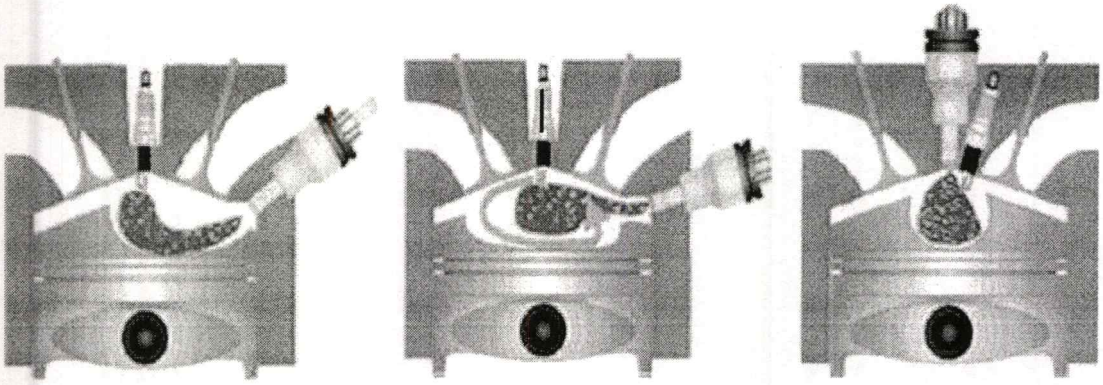

Figure 2.5 Classification of stratified charge combustion, (a) Wall-guide technique, (b) Air-guide technique and (c) Spray-guide technique.

2.2.1.1 Wall-Guided Technique

Figure 2.5 (a) shows the basic arrangement of the injector and the spark plug in wall-guided technique (wide arrangement). This approach uses a specially shaped piston surface in order to transport the fuel to the centrally arranged spark plug. Because a considerable amount of fuel is injected on the piston surface and cannot completely evaporate until ignition occurs, this technique suffers from increased emissions of unburned hydrocarbons and CO, and the full potential of reducing fuel consumption cannot be reached. However, the wall-guided concept is a very reliable approach regarding the robustness of the combustion concept and the prevention of misfiring.

2.2.1.2 Air-Guided Technique

The fuel is injected into an in-cylinder airflow, which transports the compact spray plume to the spark plug as show in Figure 2.5 (b) there is no wall wetting affect. The generation of a stable air motion that keeps the spray plume compact and transports it to the spark plug while enhancing a homogeneous air-fuel mixing inside the cloud. Therefore, the efficiency and reliability of this concept can be achieved. Two main in-cylinder air motions are possible, the swirl and the tumble. In the case of a flat cylinder head, the swirl flow is usually utilized, while a pent roof cylinder head also allows the application of a stable tumble flow.

In this technique, however, the generation of a stable airflow that enhances mixture formation inside the spray cloud, keeps it compact at the same time, and transports it to the spark plug, such that ignition can occur at a thermodynamically optimum timing, is nearly impossible to realize for all speed and load points within

the stratified operation range. Furthermore, the generation of swirl or tumble increases losses due to throttling and thus reduces fuel economy.

2.2.1.3 Spray-Guided Technique

Figure 2.5 (c) shows the spray-guided technique. This approach is the concept that theoretically allows for the attainment of the highest fuel economy. However, this approach is the most complicated to realize, and for this reason it has only been investigated and tested in research engines so far. The spray-guided concept is characterized by a narrow arrangement of the injector and the spark plug as show in the figure. The spray is directly transported to the spark plug by its kinetic energy. Thus, Special combustion chamber and piston geometries are not necessary. Due to the narrow arrangement, the time between injection and ignition, and thus the time for mixture formation, is extremely small. For this reason, high injection pressures will be necessary to provide enough energy for mixture formation and to avoid the production of soot. The generation of these high injection pressures causes problems regarding system friction and wear, because of low lubricity of gasoline.

Because the time of arrival of the spray at the spark plug is only dependent on injection timing and not on complicated air motions, there are no restrictions in ignition timing, and the thermodynamically optimal timing can be realized much easier than in the case of the wall-air-guided concepts. Hence, the spray-guided technique offers the largest possible decrease of fuel consumption at part load. Because the spray does not impact on a wall, and because a strong in-cylinder air motion is not required, heat losses to the engine and pumping losses are the smallest of all three concepts.

2.2.2 Performance of ideal internal combustion engine

The overall thermal efficiency of any reciprocating internal combustion engine is primarily a function of three parameters. First is compression ratio, second is specific heat ratio or air/fuel ratio and the last is combustion duration. The ideal efficiency of an internal combustion engine is usually determined using an "air-standard" analysis, in which pure air is used as the working fluid. A simple thermodynamic analysis of the ideal air-standard Otto cycle, which is a theoretical model for a spark-ignition engine, shows the efficiency to be

$$\eta = 1 - \frac{1}{r_v^{\gamma-1}}$$

where r_v = compression ratio and $\gamma = C_p / C_v$ (specific heat ratio).

The "compression ratio," r_v, more accurately described as the "volumetric compression ratio," is the ratio between the maximum cylinder volume at bottom dead centre (BDC) and the minimum volume at top dead centre (TDC). All of the heat is assumed to be added to the cycle at constant volume at TDC. This simple analysis shows that for high efficiency, the compression ratio should be as high as possible.

The ideal thermal efficiency of the air-standard Otto cycle as a function of compression ratio is shown in Figure 2.6, compared to that for the air-standard Diesel cycle with various values of the cutoff ratio. Although, for a given compression ratio, the efficiency of the air-standard Diesel cycle is less than that of the Otto cycle, in practice, the diesel engine has a higher efficiency because it operates at a much higher compression ratio.

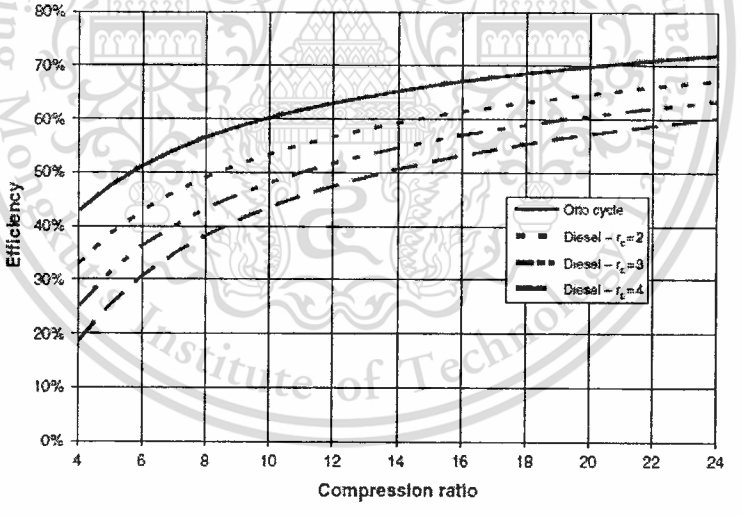

Figure 2.6 Variation of efficiency with compression ratio for a constant volume air standard cycle.

The analysis also indicates that for high efficiency, the ratio of specific heats of the working fluid should be as high as possible. In practice, it turns out that γ for air (1.4) is greater than γ for the air-fuel mixture for typical HC fuels. This means that the value of γ will be higher for mixtures with more air (i.e., lean mixtures) than for rich mixtures. The analysis predicts then that thermal efficiency is higher for lean mixtures (mixtures with excess air) than for rich mixtures. Figure 2.7, taken from

Heywood (1988), shows the theoretical efficiency for an ideal Otto cycle engine using fuel and air as the working fluid, rather than just air, as a function of the fuel - air equivalence ratio, ϕ, for a range of compression ratios, r_v, from 6:1 to 24:1. An equivalence ratio of 1.0 provides a stoichiometric mixture, while values greater than 1.0 are rich mixtures and values less than 1.0 are lean mixtures.

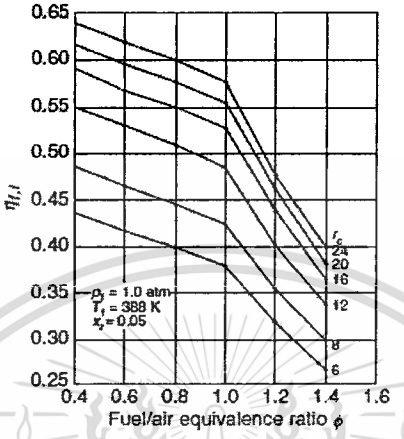

Figure 2.7 Variation of thermal efficiency with equivalence ratio for a constant volume fuel-air cycle with 1-octene fuel [2].

Figure 2.7 clearly shows the trend of higher thermal efficiency as the mixture becomes leaner. This much steeper drop in efficiency for ϕ greater than 1.0 is a result of the presence of unburned fuel in the mixture. In other words, for rich fuel-air mixtures, there is not enough oxygen present to support complete combustion of all of the fuel. This figure indicates another reason for diesel engine efficiency being greater than Otto cycle efficiency, since the un-throttled diesel engine always operates at a very lean overall fuel-air ratio, particularly at part load.

The length of the burning time, or combustion duration, also has an effect on thermal efficiency. The ideal situation would be to release all the energy into the cylinder instantaneously at TDC of the compression stroke. Since all fuels have a finite burning rate, this is not possible, and the power output obtained for a given amount of fuel burned is reduced compared to the ideal cycle, resulting in a reduction in thermal efficiency. The results of these effects are shown schematically in Figure 2.8, taken from Campbell (1979), which shows the power output as a function of spark advance, for three different values of combustion duration, $\Delta\theta_c$ .The combustion duration and spark advance are given in terms of crank angle degrees, and degrees before TDC, respectively. As the combustion duration is increased, the optimum value of the spark timing also increases, as shown in the

diagram. The figure clearly shows that reduced combustion duration results in higher power output, and therefore increased thermal efficiency.

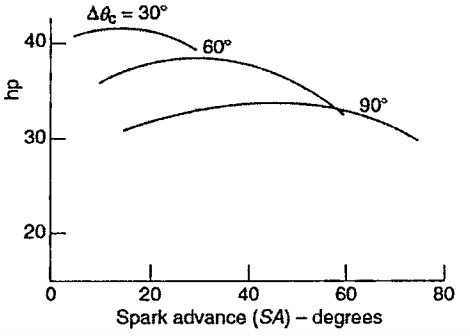

Figure 2.8 Influence of spark advance and combustion duration on power outout (Campbell,1979).

Since burning rates are generally highest close to the stoichiometric air-fuel ratio, operating an spark ignition (SI) engine lean, with an equivalence ratio of less than one, results in increased combustion duration. As can be seen from Figure 2.8, this then reduces power output and thermal efficiency, thereby tending to counteract the increased efficiency of lean operation due to an increased ratio of specific heats, as seen in Figure 2.7 It is important, therefore, when choosing to operate an SI engine under lean-burn conditions to design the combustion system to provide a high burning rate.

2.2.3 Spark ignition engine emissions

The emission levels of a spark-ignition engine are particularly sensitive to air–fuel ratio. This can be seen in Figure 2.9, taken from Heywood (1988), which shows schematically the level of emissions from a spark-ignition or Otto cycle engine as a function of relative air–fuel ratio. At rich air–fuel ratios, with ϕ greater than 1.0, unburned HC levels are high since there is not enough air to completely burn all the fuel. Similarly, CO levels are high, because there is not enough oxygen present to oxidize the CO to CO_2.

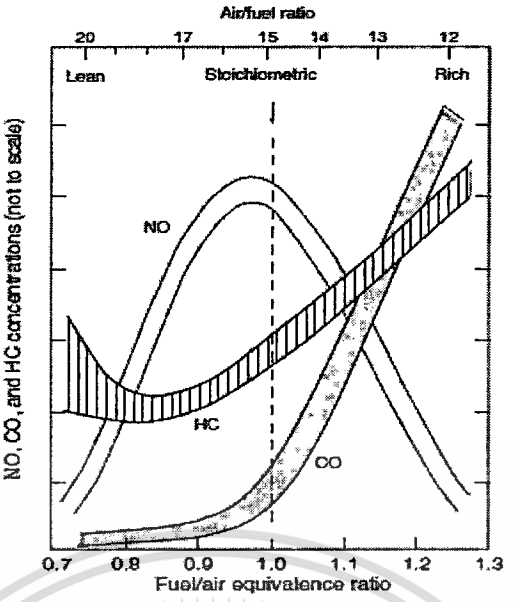

Figure 2.9 Emissions as a function of fuel–air equivalence ratio ϕ [2].

For lean mixtures, with ϕ less than 1.0, there is always excess air available, so that CO almost completely disappears, while HC emissions reach a minimum near ϕ=0.9. For ϕ less than about 0.9, some increased misfiring occurs because of proximity to the lean misfire limit, and HC emissions begin to rise again. The main factor in production of NO is combustion temperature: the higher the temperature, the greater the tendency to oxidize nitrogen compounds into NO. Since the combustion temperature is at a maximum near stoichiometric conditions where ϕ=1.0, and falls off for both rich and lean mixtures, the NO curve takes the bell shape shown in Figure 2.9.

2.2.4 Numerical model in stratified charge combustion

In the year 2002, H.Choi et al.[5] proposed the three-dimensional analysis model for the direct injection stratified charge in order to simulate the characteristics of flame propagation, diffusion reaction, concentrations of products in the burned region, and burned-gas temperature. In that numerical study, the flame speed can be developed from the laminar burning velocity as follow

$$S_\ell = \alpha \exp[-\xi(\phi-\phi_m)^2 - \exp\{-\zeta(\phi-\phi_m)\} - \zeta(\phi-\phi_m)] \quad (1)$$

Where,

$$\alpha = \alpha_0 \left(\frac{T}{T_0}\right)^{\alpha_T} \left(\frac{P}{P_0}\right)^{\beta_P}$$
$$\xi = \xi_0 \left[1 - C_T \left(\frac{T}{T_0} - 1\right)\right] \left(\frac{P}{P_0}\right)^{\beta_P} \quad (2)$$
$$\zeta = \zeta_0 \left[1 - C_T \left(\frac{T}{T_0} - 1\right)\right] \left(\frac{P}{P_0}\right)^{\beta_P}$$

S_ℓ is the laminar burning velocity and ϕ_m is the equivalence ratio where the laminar burning velocity is maximum.

Though these model, the equation can cover the asymmetric characteristics of laminar flame speed over lean and rich equivalence ratios. However, for a stratified mixture, the equivalence ratio that governs the laminar flame speed inevitably fluctuates within each computational grid because of convection and diffusion effects. Therefore, the spatial distribution of equivalence ratios and their variations can be accounted for by the fact that flame propagation is fastest in the region where mixture fraction has the highest probability of being stoichiometric. By introducing the mean mixture fraction, $\tilde{Z}$, and the Favre-averaged mixture fraction variance, $\tilde{Z}''^2$, the mean laminar flame velocity in a grid cell where the mixture is non-homogeneous can be expressed as following equation

$$\overline{S}_{\ell(\tilde{Z})} = \int_0^1 S_{\ell(Z)} P_Z(\tilde{Z}, \tilde{Z}''^2) dZ \quad (3)$$

However, this equation did not express the asymmetric characteristics of equivalent ratio Therefore, the mean laminar flame speed $\overline{S}_{\ell(\tilde{Z})}$ was approximated by

$$\overline{S}_{\ell(\tilde{Z})} = S_{\ell,\phi m} \eta \left\{P_{Zst}(\tilde{Z}, \tilde{Z}''^2)\right\} \exp[-\xi_l(\phi - \phi_m)^2 - \exp\left\{-\zeta_l(\phi - \phi_m)\right\} - \zeta_l(\phi - \phi_m) \quad (4)$$

Where ξ_l and ζ_l are fixed as 0.2, and 1.7, respectively.

The flame propagation simulation result of these study are agree with experimental studies of other researchers. Comparison of numerical result and previous study are shown in Figure 2.10.

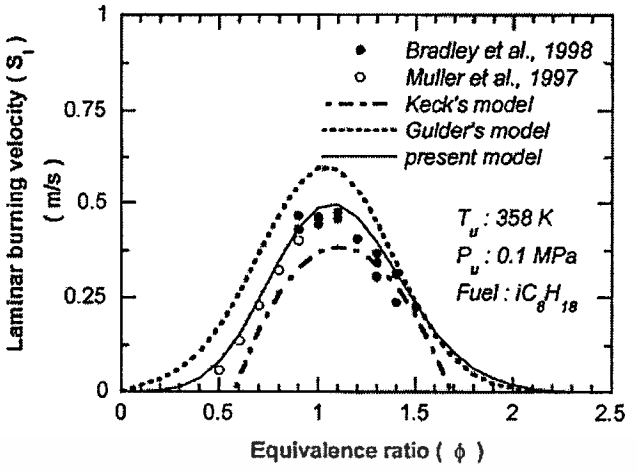

Figure 2.10 Comparison of the laminar flame-speed correlations for iso-octane

2.2.5 Influenced parameter in direct injection stratified charge combustion

In order to achieve the stable combustion phenomena, several parameters that affect to combustion phenomena should be studied and investigated. Michael C. Drake et al.[6] employ the CFD simulation to investigate the optimum ignition timing in order to reach the stable combustion. As indicated in Figure 2.11, The swirl index (SI) were not significant change the equivalent ratio and velocity at the spark plug but the ignition timing (dash line) was the most important parameter to ignite the mixture and keep the stable combustion. In the table 1, the CoV was reach the minimum at 0.9 when equivalent ratio around spark plug is 0.9-1.6. However, In their result, the mixture velocity will be decreased by the time left. In Figure 2.12, The comparison result of CFD model and experimental study show that the strong swirl flow (high SI) can be advanced combustion process .In addition, The peak pressure can be affected by the swirl index but significant as expect.

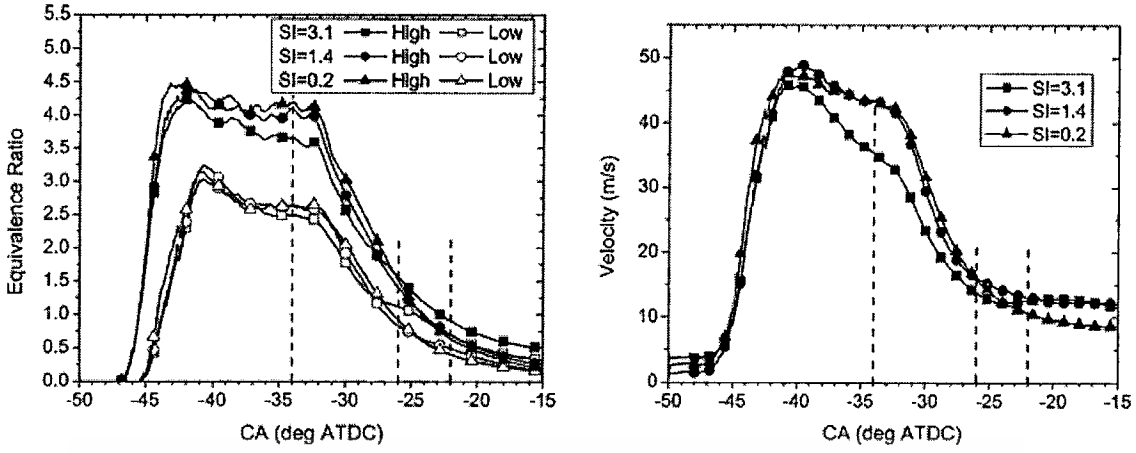

Figure 2.11 Equivalence ratio and velocity near the spark plug at various swirl index(SI)

Table 1 Effect of ignition timing on mixture distribution and misfire.

SA (BTDC)	Φ at spark	Velocity at spark (m/s)	Misfires (%)	Partial burns (%)	IMEP (kPa)	COV(IMEP) (%)
34	2.7–4.2	35–44	4	0	300	23
26	0.9–1.6	14–16	0	0	321	0.9
22	0.4–0.8	10–13	0.3	10	279	16
20	0.3–0.5	9–12	5	24	211	41

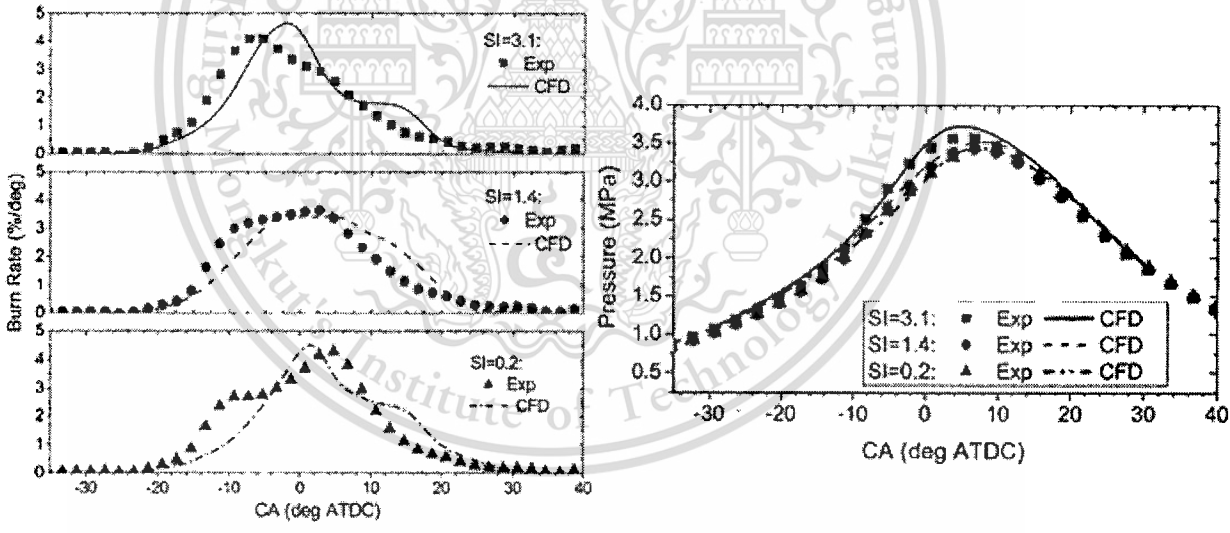

Figure 2.12 Comparison result between CFD model and experimental study of iso-octane

Naoki Shiraishi et al [4] studied the combustion efficiency of gasoline direct injection by means of constant volume combustion vessel. in year 2001, from experimental result, the researchers note that the rate of pressure rise and heating efficiency were affected by changing in injection-sparking interval time. Figure 2.13 show the relationship between pressure rise rate $\left(\frac{dP}{dt}\right)$ and injection-ignition interval (

τ_{int}) and relationship between heating efficiency (η_h) and injection-ignition interval. As the injection-ignition timing increase, the efficiency was decreased. In this study, effects of ambient temperature were also collected.

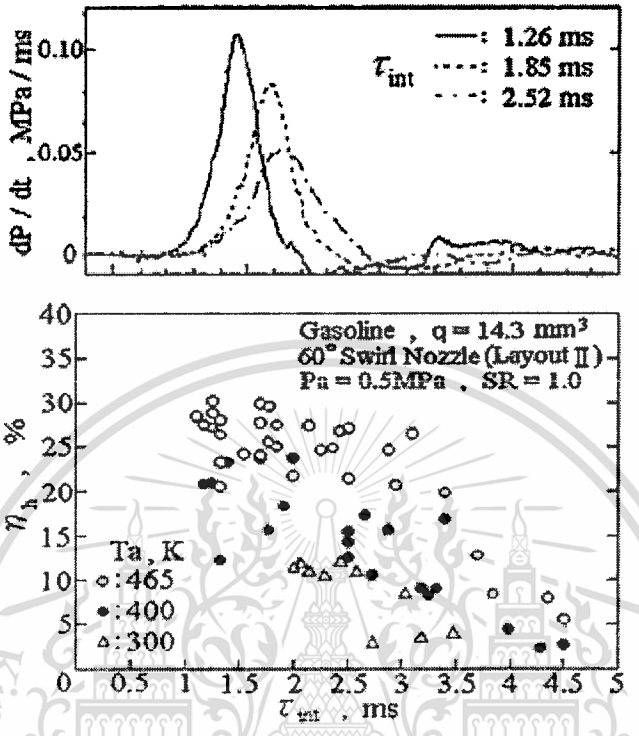

Figure 2.13 Effect of injection-ignition timing on (a) pressure rise rate and (b) heating efficiency

For another result that show effect of injection timing was from Z. Huang et al's [7]. study, the researchers claim that When the injection was relatively early the heat release pattern showed a slower burn in the initial stage and a faster burn in the late stage. There would be two factors causing this behavior: one is the degree of charge stratification of the mixture; the other is the decaying of the turbulence generated by the fuel jet. Since the injection timing was earlier, decaying of the formed turbulence and weaker charge stratification were considered to occur in the cylinder, resulting in a heat release pattern similar to that of flame propagation in the homogeneous mixture In contrast to this, when the injection timing was relatively late the heat release rate showed a faster burn in the initial stage and a slower burn in the late stage, which is contrary to the early injection case. This pattern reminds us of diesel combustion in which two kinds of heat release process are usually identified: pre-mixed phase at the initial and diffusive phase at the subsequent. Thus, for the case of late injection a mixture formed in the initial stage can burn rapidly

due to strong turbulence and then in the subsequent stage the fuel probably burns like a diffusion flame as diesel combustion.

Jeonghoon Song and Dae Hee Lee [8] studied effect of the spark energy, spark gap and electrode geometry on combustion duration by using Schlieren photography technique. From the investigation, can be summarized that as the ignition energy increases the burning rate can be accelerated, duration time in the initial stage was reduced approximately 7-8%. For a sharpened tip of the electrode, the discharge energy increases together with the efficiency of electrical energy conversion. Consequently, the kernel growth becomes faster. In addition, the breakdown energy, can be increased by extended the spark gap. Consequently, flame kernel in extended spark gap was developed faster than in the small spark gap.

2.3 Combustion characteristics in constant volume combustion chamber (CVCC)

For analyzing the combustion, The real engine, have many parameters that affect to the combustion characteristics such as manifold design, valve shape and duration, piston geometry, et cetera. In the recent years, many researchers try to avoid that undesirable effects and concentrate on only the fuel and combustion within combustion chamber. Experimental studies which carry on the constant volume combustion chamber may easier control parameter than that the real engine. The word "Constant Volume Combustion Chamber" or "CVCC" was first introduced in 2002 by publication of Jeonghoon Song and Dae Hee Lee [8]. The experimental setup of their study was shown in Figure 2.14 (a). Later in the year 2004, Kihyung Lee et al [9]. Study the effect of mixture stratification in a constant volume combustion chamber. In this study, the experimental apparatus were more complicated than that the previous as show in Figure 2.14 (b).

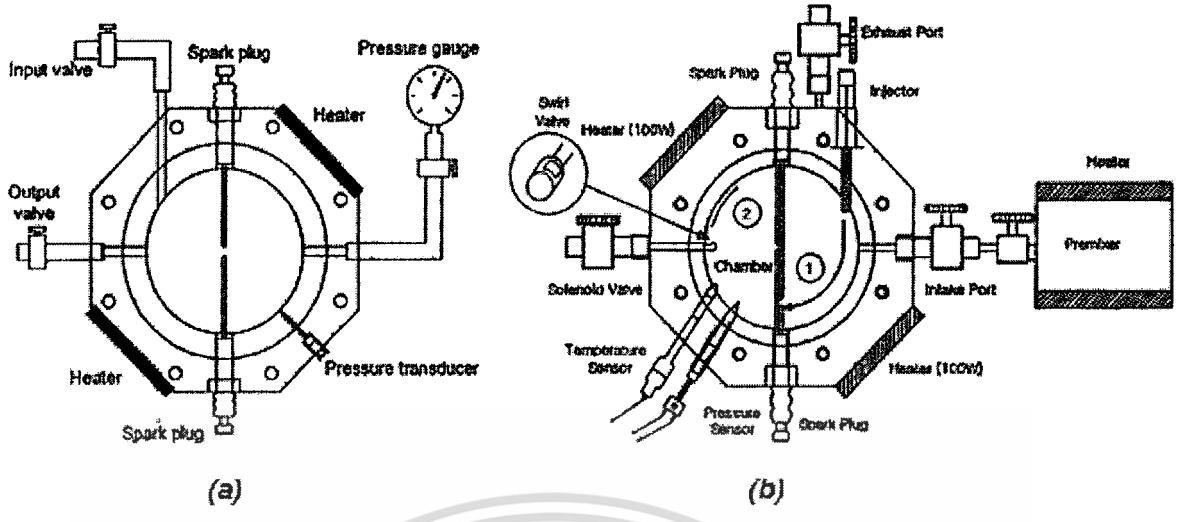

Figure 2.14 Experimental setup of Constant volume combustion chamber

(a)J.Song and D.Lee, 2002 (b) Kihyung Lee et al, 2004

Majority components in the constant volume combustion chamber was pressure transducer, It is very useful tool for analyze the combustion behavior with combustion chamber and another were the quartz glasses for spray and flame visualization. In the later, high speed video camera and laser diagnosis system may be required.

2.3.1 Pressure rise rate, Rate of heat release (ROHR) and Stratification degree.

Due to combustion analysis in constant volume combustion chamber was based on the pressure history data that collect from the high-resolution pressure transducer. Thus, rate of heat release cannot be relatively calculated with the crank angle as same as in the real engine. And also the stratification degree. For applying the Thermodynamics, rate of heat release and stratification degree, can be expressed in term of pressure rise rate $\left(\frac{dP}{dt}\right)$. The relationship between rate of heat release (ROHR) and pressure rise rate $\left(\frac{dP}{dt}\right)$ was derived from principal of ideal gas law and Thermodynamics as follow equation [10],[11].

From the first law of thermodynamics

$$\text{Heat supply rate} = \text{Heat release rate} + \text{Heat transfer} \qquad (5)$$

Neglect the heat transfer during combustion, The deviation for turbulent combustion by this treatment is small due to the short combustion

$$\text{Heat release rate} = \text{Heat supply rate}$$

$$\left(\frac{dQ}{dt}\right)_{\text{release}} = mc_v \frac{dT}{dt} + P\frac{dV}{dt} \tag{6}$$

Applying the ideal gas equation to the gas mixture and differentiating about time

$$PV = mRT$$

$$P\frac{dV}{dt} + V\frac{dP}{dt} = mR\frac{dT}{dt} \tag{7}$$

Thus,

$$\left(\frac{dQ}{dt}\right)_{\text{release}} = \left(\frac{c_v P}{R}\frac{dV}{dt}\right) + \left(\frac{c_v V}{R}\frac{dP}{dt}\right) + P\frac{dV}{dt} \tag{8}$$

And relation of specific heat, $\frac{c_p}{c_v} = k$ and $c_p = c_v + R$

$$\frac{c_v}{R} = \left(\frac{1}{k-1}\right)$$

$$\left(\frac{dQ}{dt}\right)_{\text{release}} = 0 + \left(\frac{c_v V}{R}\frac{dP}{dt}\right) + 0 \tag{9}$$

$$\left(\frac{dQ}{dt}\right)_{\text{release}} = \left(\frac{V}{k-1}\right)\frac{dP}{dt}$$

Consequently, if the volume was fixed at constant and specific heat ratio was not change significantly, The rate of heat release can be reflected by the information of rate of pressure rise.

Naoki Shiraishi et al [4] and Kihyung Lee et al [9]. Were introduce definition of stratification degree as the ratio of the fuel quantity forming the mixture with air fuel ratio near stoichiometric value against total fuel quantity injected. The requisites to enhance this ratio are, First, to reduce the amount of unburnt fuel, and second, to enhance the ratio of mixture area with air fuel ratio near stoichiometric value against flammable mixture area. The mixture with air-fuel ratio nearer stoichiometric value brings about higher burning velocity. Therefore, a stratification concept in order to satisfy both of the requisite (a) and (b) is assumed to be "how to enhance more the burning velocity in broader mixture area". Taking this concept into consideration, the

maximum volumetric burning velocity $(Sv)_{max}$ is assumed to be reasonable as a stratification degree.

The maximum volumetric burning velocity $(S_v)_{max}$ is assumed to be reasonable as a stratification degree

Volumetric burning velocity is given by

$$S_v = A_f \cdot S_u \tag{10}$$

Where A_f is the flame front area and S_u is the burning velocity

The mass burned fraction is given by

$$\dot{m}_f = A_f \cdot S_u \cdot \rho_u \frac{1}{AF+1} = S_v \cdot \rho_u \frac{1}{AF+1} \tag{11}$$

From Thermodynamics,

$$\text{Heat release rate} = \text{Heat supply rate} \tag{12}$$

And relationship between rate of heat release and pressure rise rate

$$\begin{aligned} H_u \dot{m}_f &= \left(\frac{dQ}{dt}\right)_{\text{release}} \\ H_u S_v \cdot \rho_u \frac{1}{AF+1} &= \left(\frac{V}{k-1}\right)\frac{dP}{dt} \end{aligned} \tag{13}$$

Where H_u is lower heating value and ρ_u is mixture density at fresh side of the mixture.

In stratification mixture, following assumption may be accepted

$\mathrm{AF} = 15$ assume that at this AFR the combustion is fastest

$\rho_u = \rho_0 \left(P/P_0\right)^{1/k}$ applying the law of adiabatic change to the state of the fresh side mixture

Then, $(S_v)_{max}$, the highest S_v, is given by

$$(S_v)_{\max} = \frac{\{(AF)_{Vb\max}+1\}V}{H_u \cdot (\kappa-1)\cdot \rho_0} \cdot \left[\frac{1}{(P/P_0)^{1/\kappa}} \cdot \frac{dP}{dt}\right]_{\max} \tag{14}$$

As shown in equation 14 $(S_v)_{max}$ is determined using P and $\frac{dP}{dt}$ data obtained by pressure analysis, and $(S_v)_{max}$ is closely related to $\left(\frac{dP}{dt}\right)_{max}$. This means that the

correlation between $(S_v)_{max}$ and $\left(\frac{dP}{dt}\right)_{max}$ is investigated to clarify the possibility of replacing $(S_v)_{max}$ with $\left(\frac{dP}{dt}\right)_{max}$. Therefore, $(S_v)_{max}$ was proven to be useful as a stratification degree, representing widespread stratification feature quantitatively. The example result of relation between stratification degree and pressure rise rate was shown in Figure 2.15.

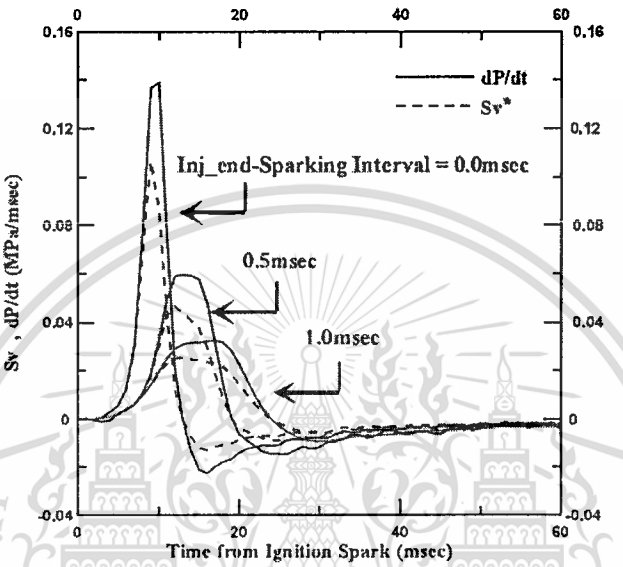

Figure 2.15 Comparison between volumetric burning velocity (S_v) and pressure rise rate (dP/dt)

Kihyung Lee 's study [9] note that as the interval after ignition start is longer, the value of S_v and $\frac{dP}{dt}$ is decreased. The reason for decreasing S_v and $\frac{dP}{dt}$ is that the stratified fuel is not formed near spark plug. Furthermore, they also observed this phenomenon through the visualization result of flame propagation near spark plug for support their assumptions.

2.3.2 Mass fraction burn, initial stage of combustion and combustion duration.

The mass fraction of the burnt fuel-air mixture was calculated from the measured pressure profile under the assumption that the pressure in the combustion chamber corresponds to the mass fraction burnt [8],[12]

$$M(t) = \frac{p(t) - p_{init}}{p_{max} - p_{init}} \tag{15}$$

where p_{init} and $p_{\max}$ are the initial and maximum pressures, respectively. The duration of flame-kernel development ($t_{0\%} - t_{10\%}$) was defined as the time period from ignition to burning of 10% of mass, and the flame propagation duration was defined as the time period beginning after burning of 10% of mass and ending after burning of 90% of mass. The time $t_{\max}$ is the period from ignition to complete burning of the entire mixture in the combustion chamber.

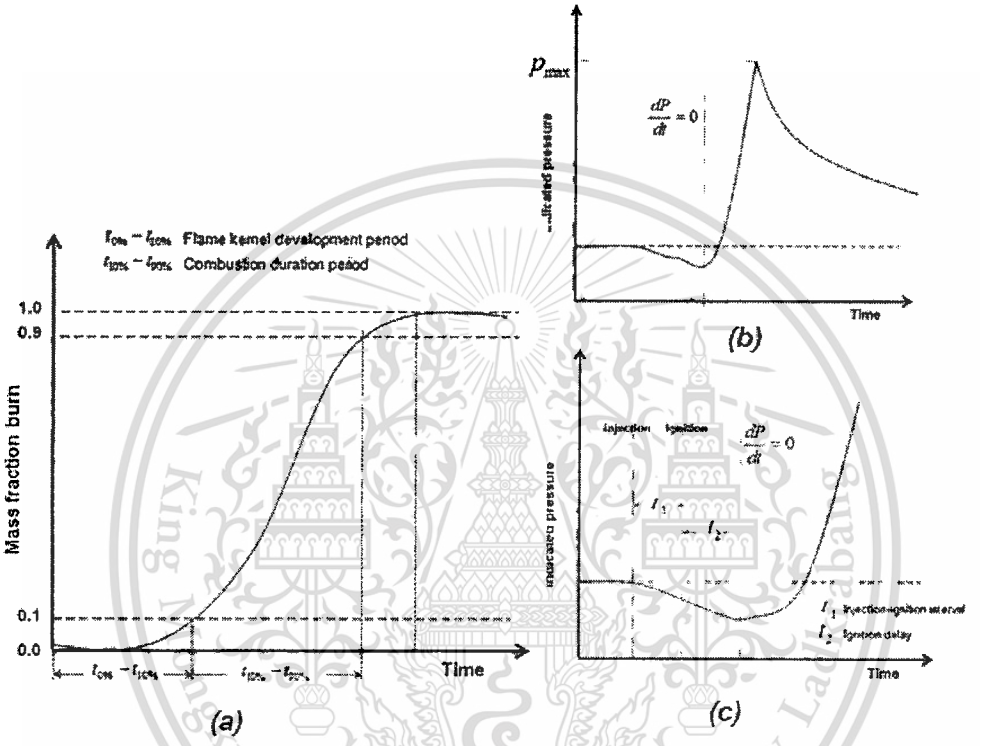

Figure 2.16 Definition of (a) combustion duration,
(b),(c) injection – ignition interval and ignition delay

For clearly understanding, the definition of combustion duration, injection - ignition interval and ignition delay, were shown by graphical of measured pressure data in Figure 2.16. Naoki Shiraishi et al.[4] and Kihyung Lee et al [9] give the definition of injection – ignition interval as elapsed time from start of injection to start of ignition. Then, as show in the Figure 2.16(c), after the ignition is started, the trace pressure will be decreased until reach the minimum or rate of pressure rise equal to zero ($\frac{dP}{dt} = 0$). The interval time form ignition start to this point can be defined as ignition delay. For the reason of pressure drop during process, Naoki Shiraishi et al[4]. discussed that this phenomena occurred by latent heat absorption by vaporized fuel just after fuel injection start.

2.3.3 Lean flammability and ignition limit.

Combustion in a spark ignition engine begins with a spark discharge which emits sufficient energy to initiate the chemical chain reaction to sustain flame propagation throughout the mixture. There are two lean limits of combustion to be considered with spark ignition engine. First is lean flammability limit and another one is lean ignition limit [Quad A. (1976)].

Lean flammability limit (LFL), an inherent fuel property which is a function of temperature and pressure, is the leanest air-fuel mixture which will sustain flame propagation, and should be independent of ignition source and combustion vessel geometry [Coward H. et al.(1952)]. In the reciprocating spark ignition engine, this operational lean limit type commonly referred to as the lean misfire limit (LML), misfire results when the air-fuel mixtures does not ignite, does not burn completely, or burns with such low flame speeds that blow down occurs before combustion is complete.

Lean ignition limit is defined by the minimum external energy which must be supplied to a critical volume to raise the mixture to its minimum ignition temperature [Chigier N.(1981)].

An exact definition of the lean misfire limit is difficult because an engine can operate in a stable mode with occasional misfire at a certain air-fuel ratio. Since, there were variety of other methods to indirectly measure and define the lean misfire limit (LML). Selected definitions of LML found in the literature are specified amount of hydrocarbon or carbon monoxide content in exhaust gases [Shimoto G. (1978)] , the number of audible misfires counted over a time period [Chaster K. (1977)] or variation of mean effective pressure or indicated mean effective pressure [Winsor R. (1973)]. Because cylinder pressure and exhaust gas content are most easily measured, the majority of work relating to lean combustion has adopted definitions using either or both measurements. When relating air-fuel ratio to cylinder pressure or exhaust gas content as the air-fuel ratio increases from stoichiometric, a point is reach where variations increase sharply, which is approximately the lean misfire limit.

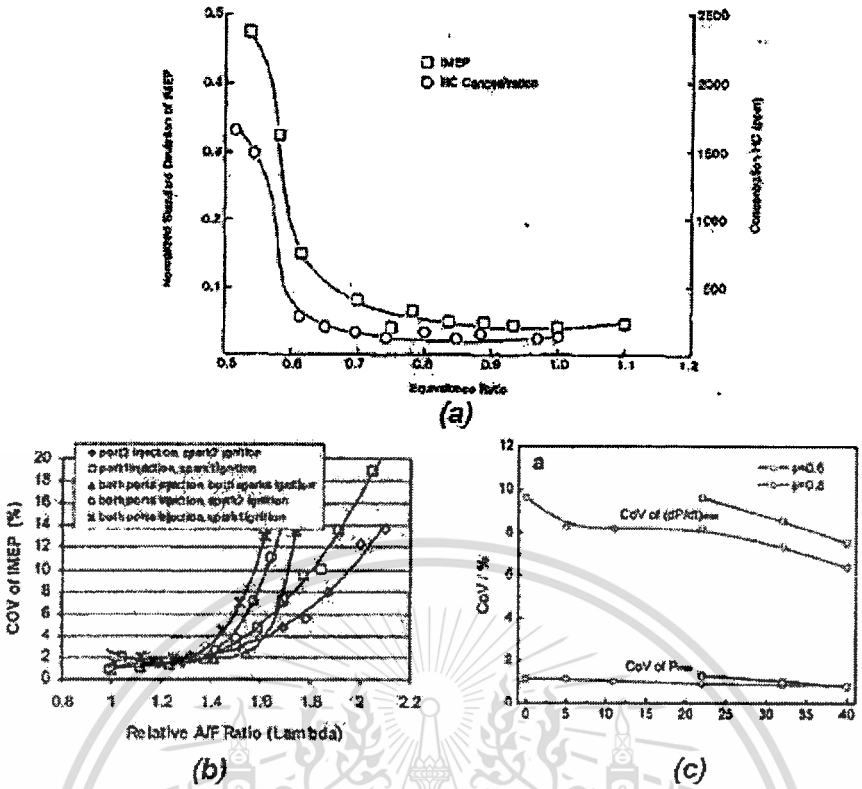

Figure 2.17 Lean limit investigation base on coefficient of variation

(a) Lewis Flight propulsion Lab (1959) (b) Y.Li and H.Zhao "Development of fuel stratification spark ignition engine"(2005) and (c) Jinhua W. et al "Study of cyclic variations of direct injection combustion fueled with natural gas-hydrogen blend using a constant volume vessel"(2008).

Figure 2.17 show some of literature result for investigating the lean miss fire limit. From all of displayed result, the lean limit investigation, were base on coefficient of variation of indicated mean effective pressure but was not define the certain number of variation as the lean limit. However, In Jinhua Wang's study[13] , the researcher had set the 20% variation as the lean limit point.

2.3.4 Cyclic variation and Coefficient of variation (CoV)

Cyclic variations in the combustion process are caused by variations in mixture motion within the cylinder at the time of spark cycle-by-cycle, variations in the amounts of air and fuel fed to the cylinder each cycle, and variations in the mixing of fresh mixture and residual gases within the cylinder each cycle, especially in the vicinity of the spark plug. Variations between cylinders are caused by differences in these same phenomena, cylinder-to-cylinder

As the mixture becomes leaner with excess air or more dilute with a higher burned gas fraction from residual gases or exhaust gas recycle, the magnitude of cycle-by-cycle combustion variations increases.

Cycle-by-cycle combustion variations are evident from the beginning of the combustion process. Analysis of flame photographs from many engine cycles taken in special research engines with windows in the combustion chamber has shown that dispersion in the fraction of the combustion chamber volume inflamed is present from the start of combustion. Dispersion in burning rate is also evident throughout the combustion process. Three factors have been found to influence this dispersion

1. The variation in gas motion in the cylinder during combustion, cycle-by-cycle

2. The variation in the amounts of fuel, air, and recycled exhaust gas supplied to a given cylinder each cycle

3. Variations in mixture composition within the cylinder each cycle-especially, near the spark plug-due to variations in mixing between air, fuel, recycled exhaust gas, and residual gas

The useful statistics tool for lean limit investigation is coefficient of variation (CoV). These parameter can be calculated directly from pressure history data. The peak pressure and indicated mean effective pressure were counted and converted to CoV by follow formula. [Heywood J.B. (1998) P.413-423]

$$\mathrm{CoV}_x = \frac{\sigma_x}{\bar{x}} \times 100\% \tag{16}$$

Where,

$$\bar{x} = \frac{1}{N}\sum_{i=1}^{N} x_i \tag{17}$$

and the standard deviation

$$\sigma_x = \sqrt{\frac{\sum_{i=1}^{N}\left(x_i - \bar{x}\right)^2}{N}} \tag{18}$$

2.4 Alternative fuel : Ethanol

The usage of ethanol in spark ignition engine can be either in the form of neat fuels, blending with base fuels (gasoline or diesel) or even as an additive (such as ETBE). Utilizing ethanol in SI engines have long been researched and developed. The main features of the ethanol that impress to the SI combustion research were the ethanol is the oxygenated fuel and have the high heat of vaporization. That means, ethanol can improve volumetric efficiency of the combustion by cooling effect. Furthermore, octane rating of ethanol was higher than conventional gasoline. Thus, the engine can either run with the higher compression ratio or more degree of spark advance. The later reasons were directly promoted to the thermal efficiency of the engine which fuelled with the ethanol. In exhaust emission aspects, NOx emission might be reduced by lower combustion temperature due to high latent heat property of the ethanol. When compare with the gasoline, CO and HC emission of the ethanol are lower . Since, ethanol contained with the oxygen and lower in carbon atom. However, Although ethanol have many merits in SI combustion, cold startibilty and aldehyde including formaldehyde emission remain the problem and challenge for utilization of ethanol in SI engine.

In Thailand, Alternative fuel, Ethanol, has been broadly promoted by the government due to environmental friendly properties of ethanol and it can reduce dependency of imported crude oil. Ethanol can be produced from many source of biomass and were the renewable energy. In addition, the raw material for produced ethanol, cassava or sugarcane was the main economic vegetation in Thailand.

Due to ethanol properties have many effect to the combustion characteristics. Thus, numerical studies of ethanol were very useful to estimate the result of its properties on combustion behavior. Hakan B.[14] have been developed theoretical model of flame propagation process in an SI engine running on gasoline/ethanol blend. In their numerical investigation, geometrical features (flame radius, flame front area and enflamed volume) of the flame, combustion characteristics (mass fraction burned and burn duration), and cylinder pressure and temperature of different ethanol/gasoline blend are predicted. The result show that blending ethanol with gasoline up to 25% by volume positively affects the geometric properties of flame and the mass burning rate, leading to faster burning. It also

produces higher cylinder pressures and temperatures compared with gasoline. As a result, the mean indicated work, and therefore engine output power and thermal efficiency, may also increase.

Although in the real engine, the combustion, was the turbulence flame propagation but laminar flame which less complicated were necessary to background study for better understanding of flame behavior. Since, in 2006, Hara Takashi and Tanoue Kimitoshi [15]studied the laminar flame speed of ethanol compare with isooctane – air mixtures. The experimental result show in Figure 2.18. As indicated in Figure 2.18, ethanols have an higher flame speed and higher flame stability than iso-octane. This behavior appears to be quite general since at low Markstein number (low Lewis number), all spherically expanding flames are intrinsically unstable, with no stabilizing influence due to thermodiffusive effects. Flame instability has many influences on combustion properties, such as burning velocities. Table 2 show the properties and Le (Lewis number) of the tested fuels.

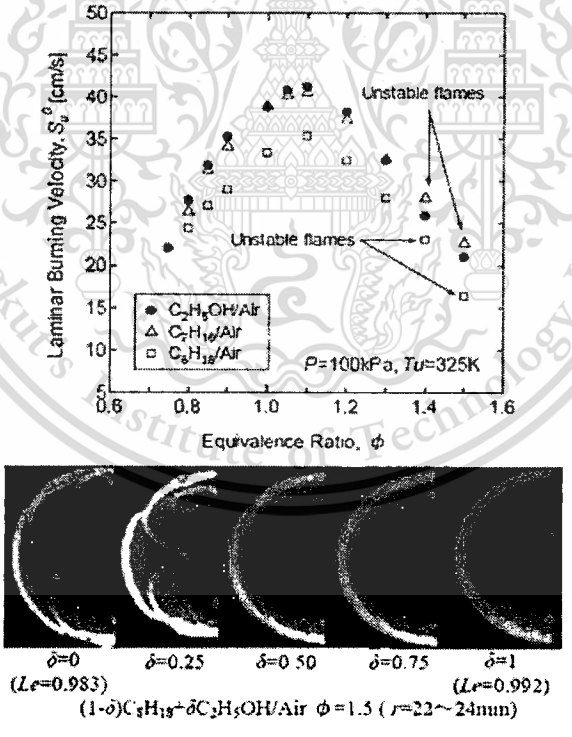

Figure 2.18 (a) Laminar burning velocity of ethanol compare with n-haptane and isooctane , (b) Schliren photographs of flame edge of different blend of ethanol and isooctane.

Table 2 Lewis number of ethanol, n-haptane and isooctane

	ϕ	ρ_b/ρ_u	α[mm²/s]	T_{ad}[K]	S_u^0[cm/s]	Le
C_2H_5OH/ Air (T_u=325K)	0.8	0.150	23.50	2051	27.7	1.775
	0.9	0.140	23.24	2177	35.3	1.761
	1.0	0.134	23.00	2256	38.8	
	1.1	0.132	22.74	2253	41.2	1.016
	1.2	0.133	22.50	2185	38.2	1.009
	1.3	0.135	22.25	2116	32.5	1.004
	1.4	0.137	22.02	2040	25.9	0.998
	1.5	0.139	21.82	1973	21.0	0.992
C_8H_{18}/Air (T_u=325K)	0.8	0.150	23.54	2074	26.6	3.060
	0.9	0.140	23.30	2208	34.1	3.042
	1.0	0.133	23.08	2292	38.9	
	1.1	0.131	22.85	2294	40.5	1.013
	1.2	0.132	22.63	2224	37.3	1.007
	1.3	0.133	22.43	2153	32.6	1.001
	1.4	0.135	22.21	2078	28.1	0.995
	1.5	0.137	22.01	2001	22.7	0.989
C_5H_{12}/Air (T_u=325K)	0.8	0.150	23.51	2071	24.4	3.206
	0.9	0.139	23.28	2205	29.1	3.189
	1.0	0.133	23.05	2289	33.3	
	1.1	0.131	22.82	2290	35.3	1.009
	1.2	0.132	22.60	2209	32.4	1.002
	1.3	0.133	22.39	2150	28.1	0.996
	1.4	0.135	22.17	2072	23.1	0.989
	1.5	0.137	21.97	1995	16.3	0.983

In combustion behavior investigation, the fuel effect on spray pattern should be taken into account. Because vaporization and spray pattern of fuels were strongly affect to the mixture distribution. Especially in direct injection engine, the ignition timing at the spark plug should be suitable to the equivalent ratio at the tip of electrode. Since, the spray pattern play an important role in mixture preparation process.

Xibin Wang et al [16] studied spray characteristics of the swirl injector fuelled with methanol and ethanol. It was explored experimentally and numerically. Experimental results show that the spray characteristics of methanol and ethanol had displayed the same trends as that of gasoline. Under the low backpressure ambient conditions, the spray behavior exhibited a hollow cone with wide spray angle and initial spray slug at the tip, while the spray presented a solid cone in the case of high back-pressure. Vortexes in the opposite direction existed in the rear part of the spray under low back-pressure ambient conditions while the vortexes formed in the middle part under high back pressure ambient conditions. however, at high injection pressure, the distinct swirl structure in the opposite direction can be clearly observed as shown in Figure 2.19. It can be concluded that increasing injection pressure will lead to the enhanced swirl intensity.

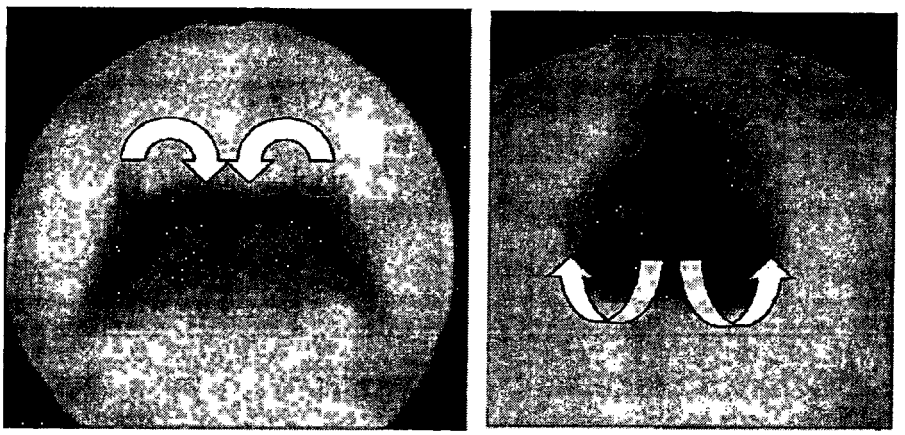

Figure 2.19 Structure and air entrainment of swirl spray at 0.1 MPa and 1.0MPa fuel injected

Figure 2.20 (a) and Figure 2.20 (b) are the shilieren images of spray development for methanol and ethanol. For comparison purposes, the shilieren images of gasoline spray development are also listed in Figure 2.20 (c).

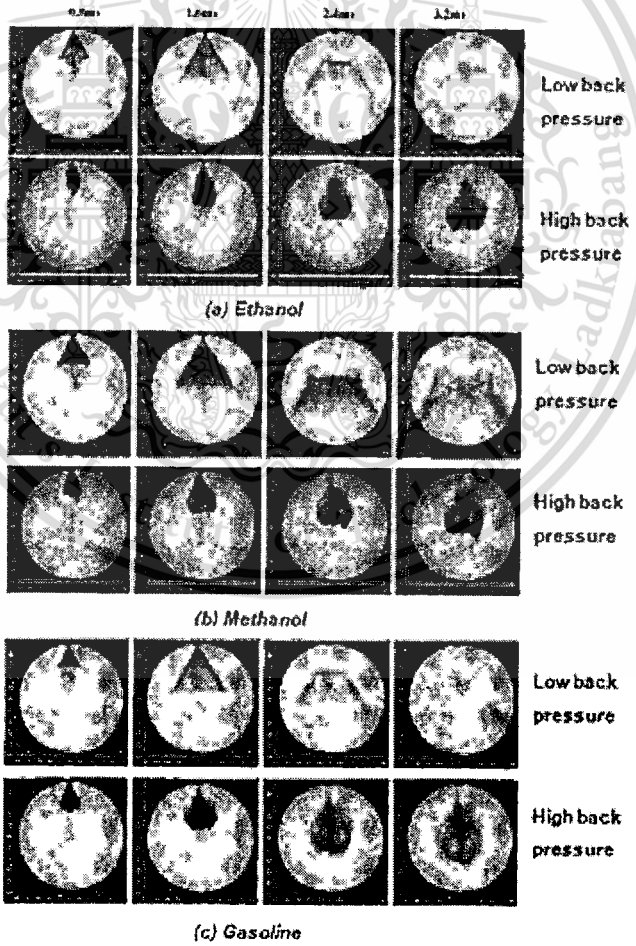

Figure 2.20 Shilieren images of spray development (a)Ethanol, (b)Methanol and (c)Gasoline

However, the vapor pressure of gasoline is even higher than methanol and ethanol, according to the fuel properties, gasoline spray should have given even shorter penetration and larger cone angle. The experimental results indicated an opposite behavior, as shown in Figure 2.21. Such phenomena may be explained by the fact that both methanol and ethanol are comprised of only one component while gasoline is a mixture of many components with various carbon atoms and structures, and its vapor pressure largely contributes to the components with relatively low boiling point which evaporate easier and faster, while the components with higher boiling point will evaporate more slowly. So the initial spray of gasoline is more distinct and the main spray of gasoline has long penetration and small cone angle.

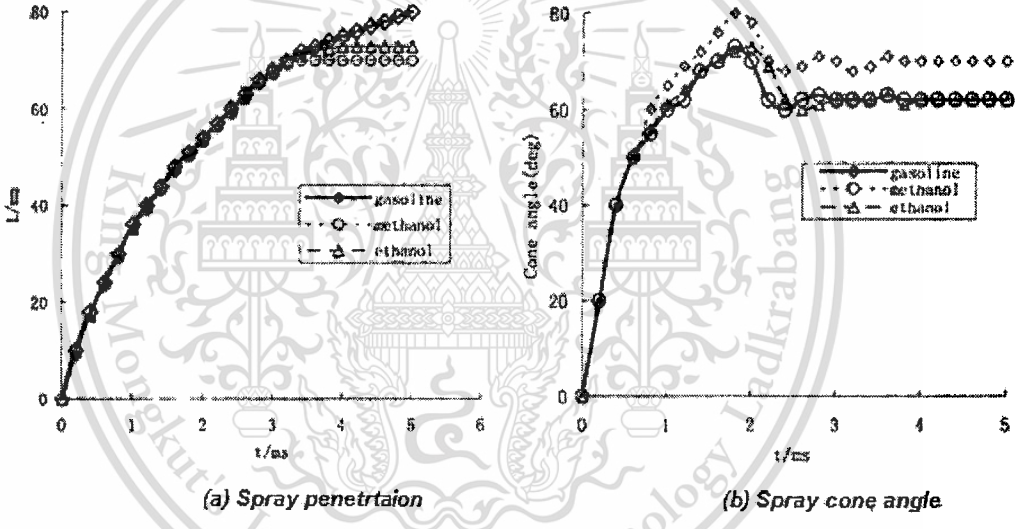

Figure 2.21 Spray cone and penetration of gasoline, methanol and ethanol

Experiments also showed that methanol had the largest cone angle, while ethanol and gasoline presented almost the same cone angle. Simulation results indicated that methanol and ethanol had a slightly larger Sauter mean diameter (SMD) than that of gasoline with swirl injector. The SMD profile of methanol coincided well with that of ethanol under low back-pressure ambient conditions, but displayed a slightly larger value under high back-pressure due to fuel evaporation.

2.5 Mixture stratification

As a result of turbulence, thermodynamic transfer rates within an engine are increased by an order of magnitude. Heat transfer, evaporation, mixing, and combustion rates all increase. As engine speed increases, flow rates increase, with a corresponding increase in swirl, squish, and turbulence. This increases the real-time rate of fuel evaporation, mixing of the fuel vapor and air, and combustion. The high turbulence near TDC when ignition occurs is very desirable for combustion. It breaks up and spreads the flame front many times faster than that of a laminar flame. The air-fuel is consumed in a very short time, and self-ignition and knock are avoided. Local flame speed depends on the turbulence immediately in front of the flame [17]. This turbulence is enhanced by the expansion of the cylinder gases during the combustion process. Turbulence intensity is a strong function of engine speed. As speed is increased, turbulence increases, and this increases the rate of evaporation, mixing and combustion. Another negative result occurs during combustion when high turbulence enhances the convection heat transfer to the walls in the combustion chamber. This higher heat loss lowers the thermal efficiency of the engine.

In 2000, Eiji Tomita, A.N., and Nobuyuki Kawahara [18] reported their study about effects of swirl flow and inhomogeneous concentration fields on combustion of propane-air Mixture in a constant-volume vessel. The experimental concept of this study was shown in Figure 2.22, the swirl velocity along the combustion vessel and its turbulence intensity were recorded, the result that shown in Figure 2.23 can be explained that how the swirl flow affect to the mixture distribution. The swirl strength was controlled by changing the times of the end of gas injection and closure of the special valve.

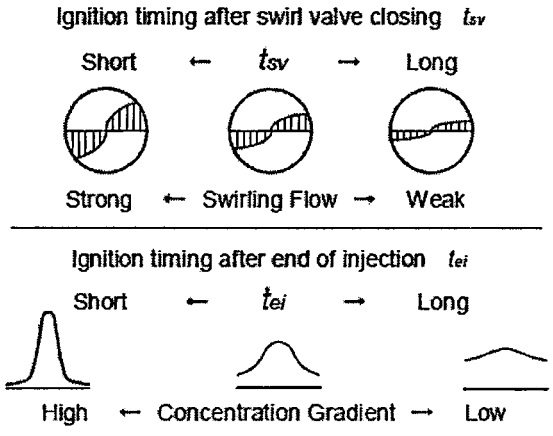

Figure 2.22 concept of experiment conditions

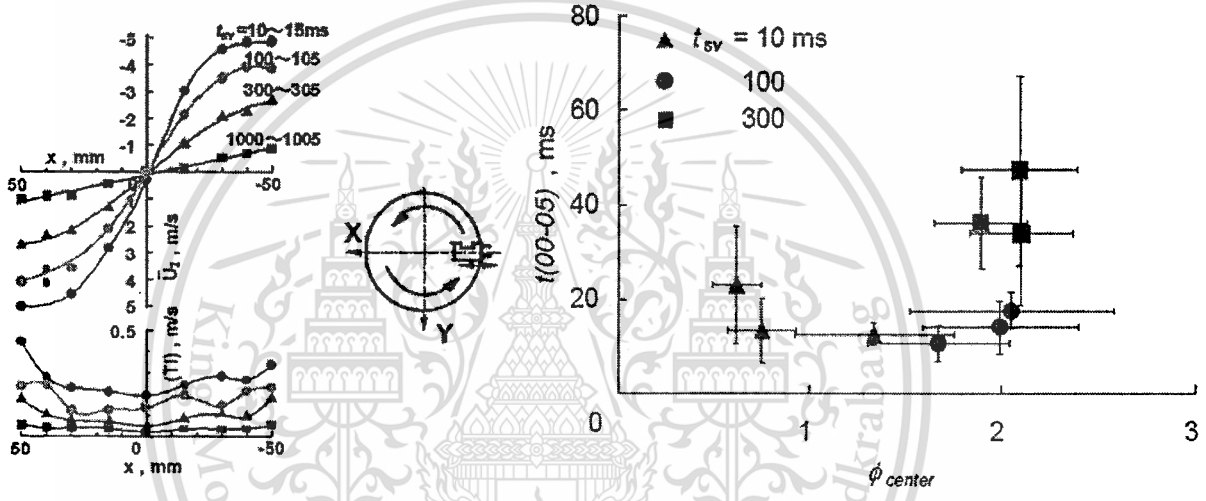

Figure 2.23 (left) Swirl intensity and turbulence intensity, (right) equivalence ratio at spark plug during initial stage of combustion.

The result shows the relation between equivalence ratio near the center measured with the LIF method and the combustion period of initial stage for various conditions in t_{sv}=10(high swirl), 100 (medium swirl)and 300ms (low swirl) in ϕ_{center}=0.3 with error bars that mean the standard deviation of concentration fluctuation near the center of the combustion chamber. In t_{sv}= 10 msec (high swirl), the standard deviation was small because the fuel near the center diffused very much. In t_{sv}= 100 msec (medium swirl), the standard deviation was large while in t_{sv}= 300 ms(low swirl), the fuel did not diffuse very much. Therefore, inhomogeneous mixture includes stoichiometric one even if it is lean or rich on the average in t_{sv}= 10 and 100ms and the averaged lean and rich limits of flammability became wide.

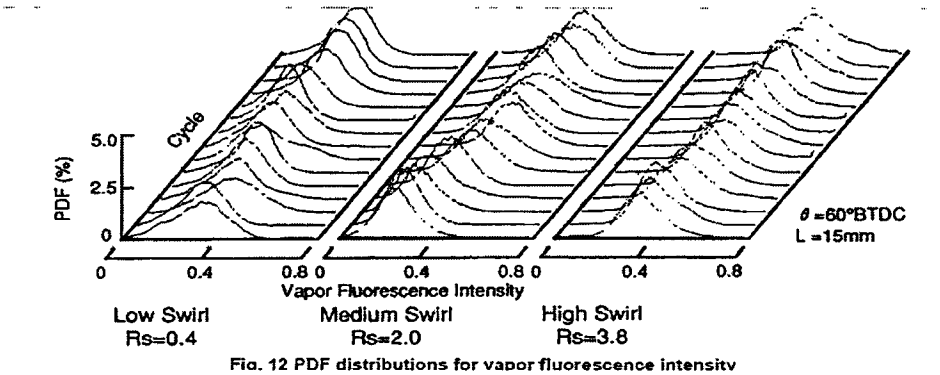

Figure 2.24 Distributions for vapor fluorescence intensity

In the real engine condition, relationship between swirl intensity and mixture distribution and combustion phenomena were reported by Masahiko Fujimoto [12]. From PDF (Provability density function) result, shown in Figure 2.24, indicates that the mixture formation was stabilized in every cycle by the swirling flow. It was also found that PDF distributions under medium and low swirling conditions were not constant in each cycle. It is considered that a large amount of liquid fuel impinged on the cylinder wall under the low swirling condition and the evaporation rate of the impinged fuel fluctuated cyclically. In Figure 2.25, it was found that the overall vapor fluorescence intensity (Iv) increased and the relative variance of the fluorescence intensity (Mv) decreased with the increasing of swirl rate.

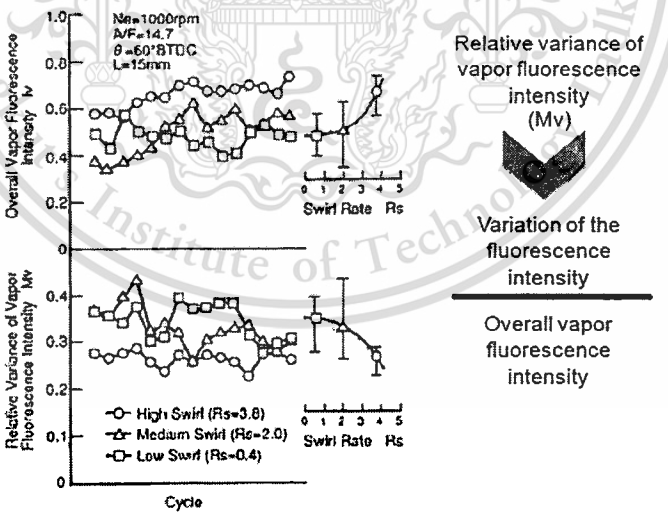

Figure 2.25 Overall vapor fluorescence intensity and Relative variance of vapor fluorescence intensity at various swirl level.

It is considered that the fuel evaporation made good progress and the homogeneity of the fuel mixture for the overall vapor concentration was improved by increasing swirl rate. Summarize form these literatures were the fuel evaporation

rate increases and the impinged fuel is reduced with increased swirl rate, and these led to increased combustion stability and reduced HC emissions.

Further reference in mixture stratification was a study on the effect of stratified mixture formation on combustion characteristics in a constant volume combustion chamber that be noticed by Kihyung Lee, er.al.[9] from their study, mixture stratification was controlled by varying proportion of premixed-mixture and direct-injected fuel in the combustion chamber while turbulence intensities were controlled by different pressure between induced inlet air pressure and combustion chamber pressure. It is founded that the arrival time to the peak combustion pressure was extremely increased as the inducing pressure increases. This is believed to the fact that the swirl flow increases the flame area and promotes air fuel mixture formation. Effect of swirl intensities, which were controlled by induced air pressure, on combustion duration was shown in Figure 2.26 below.

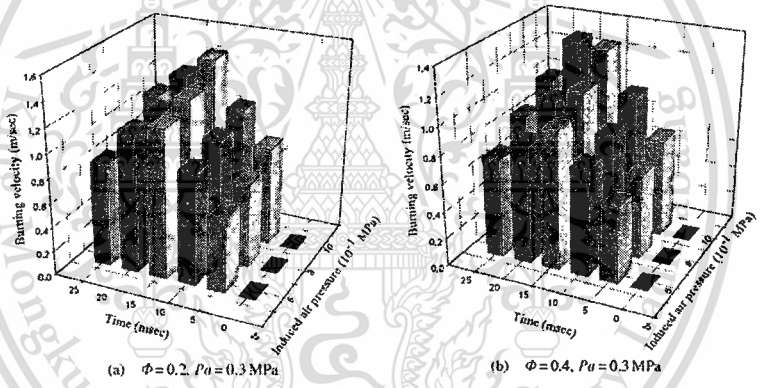

Figure 2.26 Effect of swirl intensity on the burning velocity

From this study, as the swirl intensity increases, $(S_v)_{max}$ is rapidly enhanced and the period of combustion is shortened. We also find that the stratification degree can be quantified by using burning velocity and it was controlled by induced air pressure and turbulent intensity.

Major research in this literature, Stratification levels were quantified by defined the mixture distribution in the chamber. Laser planner induced fluorescence was the one method to show air-fuel mixing phenomena. Another method to quantify the stratification degree was exhibited from pressure rise rate data, Naoki Shiraishi [4] and Kihyung Lee's [9]study, reported that the it is reasonable to quantified the stratification degree by output of combustion process, pressure rise

rate data. The detail of this quantitative calculation was show in 2.3.1, 2.3.1 Pressure rise rate, Rate of heat release (ROHR) and Stratification degree.

2.6 Schlieren photography technique.

There are many methods to derive and measure the flame velocity. The four famous method that apply in combustion research were

1. Bunsen-burner method
2. Transparent-tube method
3. Soap-bubble method
4. Constant-volume bomb method

For the first method, Flame will be stationary during combustion while three methods remaining were observed the propagation flame or non-stationary. In Soap-bubble method, high speed video camera was need, Thus, it's very complicated than two first method. The constant-volume bomb method was the most complicated method apply to flame propagation measurement due to this method have to know both rate of pressure rise and rate of flame area expansion in the same time. However, flame area expansion rate can be investigated by using direct-photograph or particle-tracking technique.

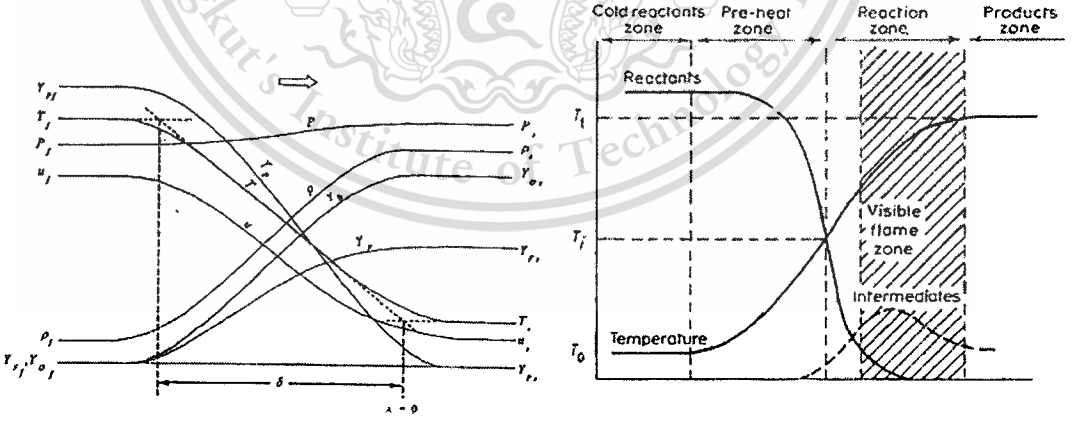

Figure 2.27 Deflagration wave structure

Even though the direct-photograph technique cannot get the high accuracy but it was the easiest technique to collect the flame shapes and also its sizes compare with another technique. This technique will observed the luminous region in luminous zone due to thermal radiation from hot gas from the combustion. However, the intensity of this luminous region was too much because it occurs

toward to the post flame. Moreover, the luminous zone was too far from the unburned mixture region as shown in Figure 2.28. This conflict to the burning velocity definition. Consider in deflagration wave in combustion process which is shown in Figure 2.27. Definition of burning velocity is relation velocity of flame expansion rate to the velocity unburned mixture. Thus, flame surface that use to measure the burning velocity should be the flame surface that occur close to the unburned mixture (x=0) as shown in Figure 2.27 and Figure 2.28

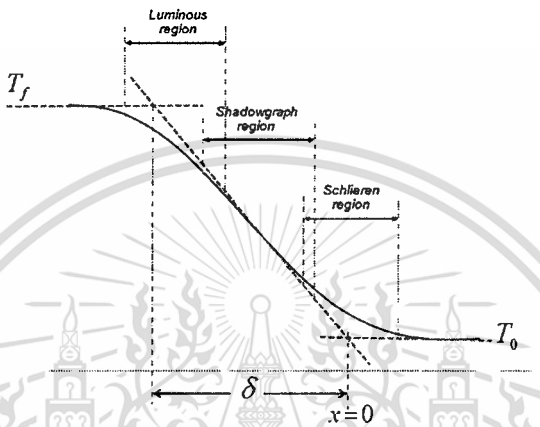

Figure 2.28 Flame region that recorded with different direct-photograph technique

For resolve that problem, special photography technique was developed. First is shadow graph technique, second is Schlieren technique and third is Interferograph technique. All of these technique were developed base on the two physical concept, Different of density within flame due to variation of temperature gradient and species, and different of reflexive index within reaction flame. Thus, when the light pass thought the flame, light from the light source will be reflex and this reflexive light will travel with longer distance compare with non-reflected light. Consequently, different time assume from different distance will be developed to principal operation of Interferograph technique. Schlieren technique will show the flame that be responded to the density gradient while the Shadowgraph technique will show the flame that be responded to the second derivative of density. Assume that the density of flame depend only on the temperature ($\rho = 1/T$). So, Shadowgraph image will display the flame edge that $\frac{dT}{dx}$ is maximum or close to inflexion point while the Schlieren technique image will show the flame edge that $\frac{d^2T}{dx^2}$ is maximum. These region were very close to the unburned region as shown in

Figure 2.28. Therefore, flame surface that be observed from Schlieren photograph technique is the most appropriate method for using to flame speed calculation even its apparatus was more complicated than Shadowgraph or Interferograph technique.

Chapter 3
Experimental apparatus and procedure

3.1 Experimental apparatus

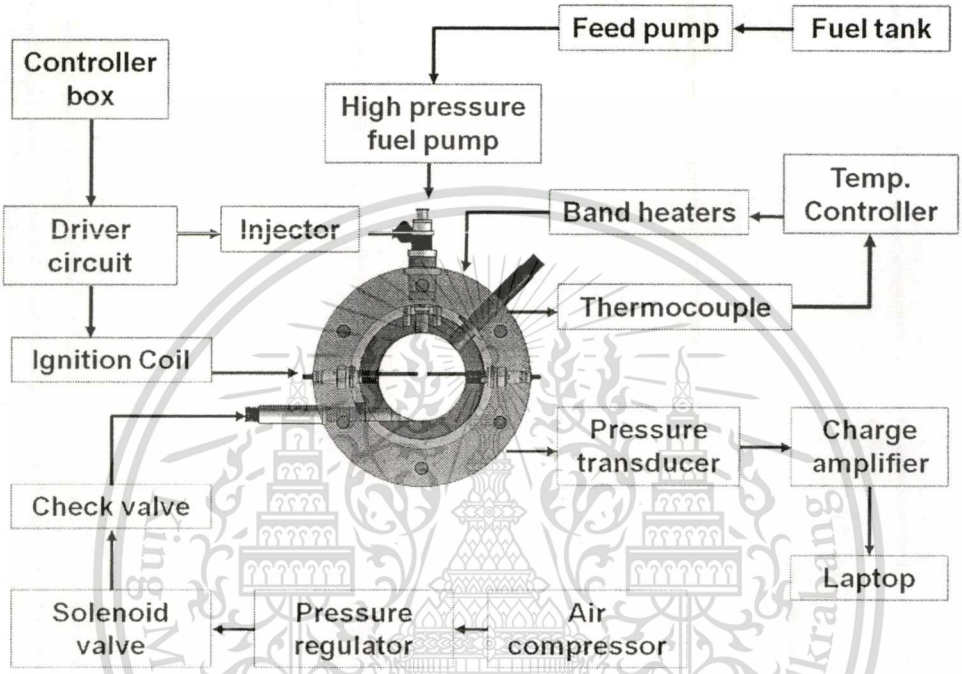

Figure 3.1 Schematic diagram of experimental apparatus.

Figure 3.1 show the schematic diagram of experimental apparatus that used in this study. It consists of six major equipments, The air supply system, fuel system, temperature control system, control module, constant volume combustion chamber and data acquisition system. The detail of each will be noted through this section.

3.1.1 Air supply system.

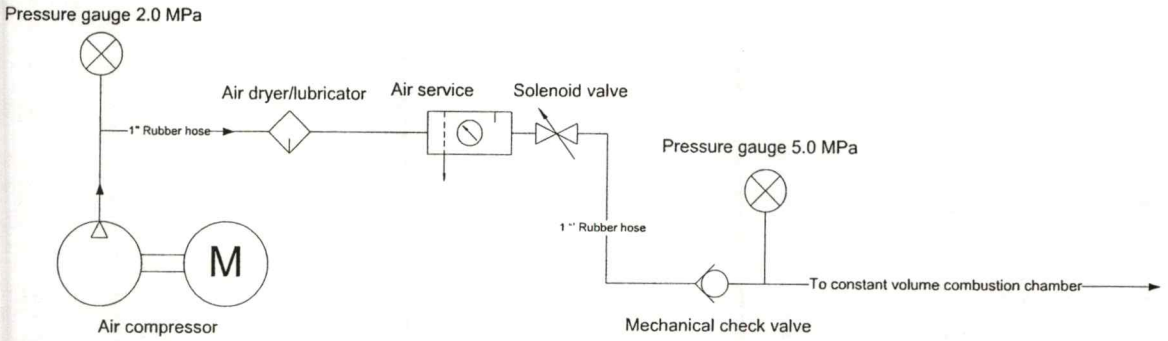

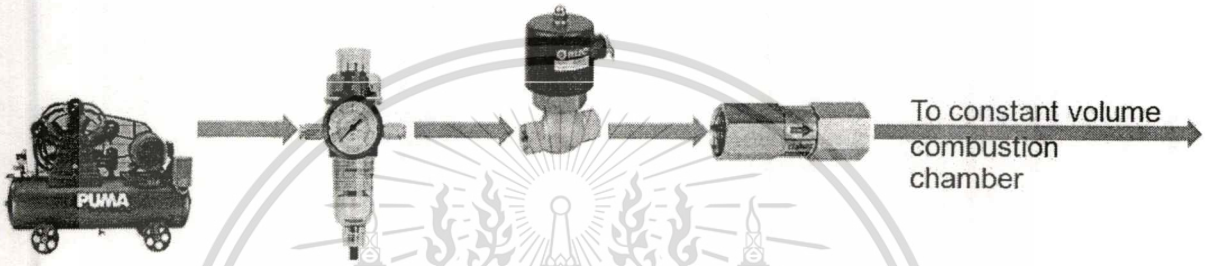

Figure 3.2 Diagram of air supply system

The air path way was shown in Figure 3.2. As illustrated in Figure 3.2, this system consist of air compressor with pressure gauge for supply and pressurize the fresh air. In this experiment, air compressor that can be pressurized up to 1.0 MPa was required. Second, is the separated pressure regulator for adjusting the air induced pressure before discharge to the constant volume combustion chamber. In addition, air dryer, air filter and pressure gauge were equipped with this regulator. Separated pressure regulator was use to adjust the air induced pressure for different swirl adjustment purpose. This pressure can be adjusted from 0.1 to 1.0 MPa of induced pressure. Third, is high pressure resistance solenoid valve which be operated by electrical signal was located before the check valve. Fourth, for avoiding incidental accident of back pressure from explode gas, mechanical check valve that can be resist both high temperature and high pressure will be used. Finally, pressure gauge with 5.0 MPa full scale length was use to determine the initial pressure before combustion process. The detail of mechanical check valve was shown in Figure 3.3. The dimension of pipe and valve were 1.0 inch through the pneumatic system.

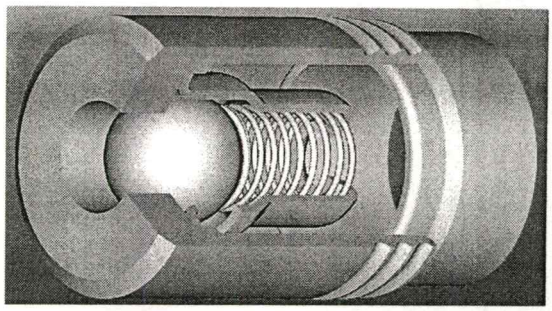

Figure 3.3 Detail view of mechanical check valve.

3.1.2 Fuel system.

Tested fuel from the fuel tank were feed by the low pressure feed pump. Discharge pressure of this feed pump was approximately 0.3 MPa with 2 ltr/min flow rate. After that, excess fuel will be regulated and drain back to fuel tank by integrated regulator within feed pump. The low pressure fuel (0.3 MPa) will be supply to the high pressure cam-driven pump that comes from Mitsubishi GDi engines. Modification for utilizing this high pressure fuel pump was required. The cam-driven case for and 1.5 kW electric motor were equipped with cam driven pump as show in Figure 3.4

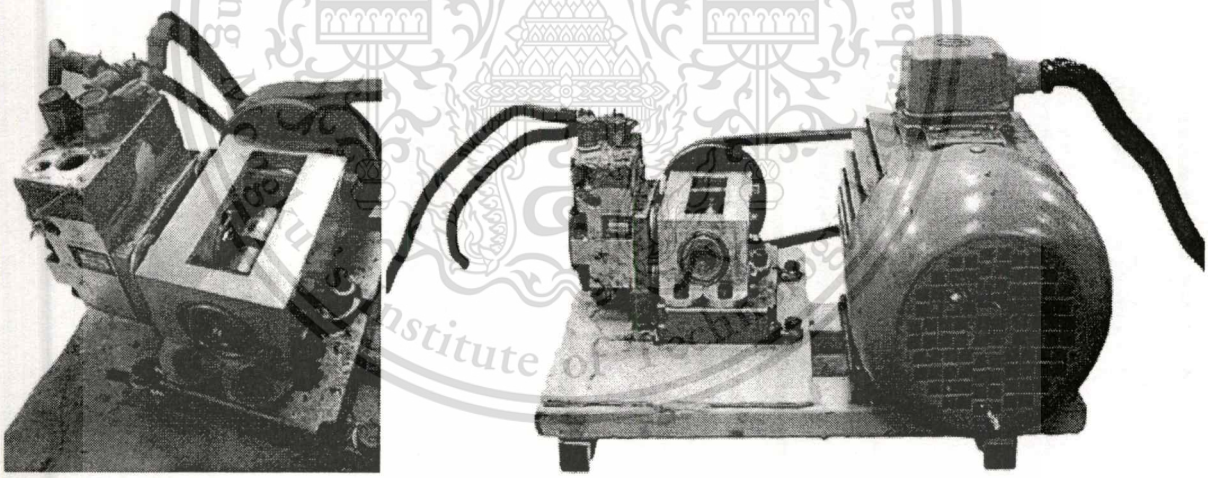

Figure 3.4 Cam-driven fuel pump with power source from 1.5 kW electric motor.

High pressure fuel was pressurized by plunger within the pump while camshaft in this study was driven by electric motor instead of the engine. For the cam-driven case, CAD image and disassembly images were illustrated in Figure 3.5. Operation length of plunger use in this pump was designed at 1 mm. Camshaft designed parameter was shown in Figure 3.6.

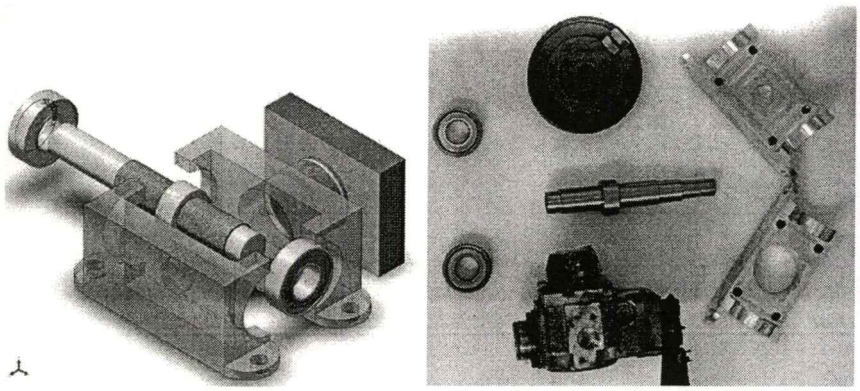

Figure 3.5 Cam-driven case (a) explode view of CAD image and (b) Assembly parts for cam-driven case.

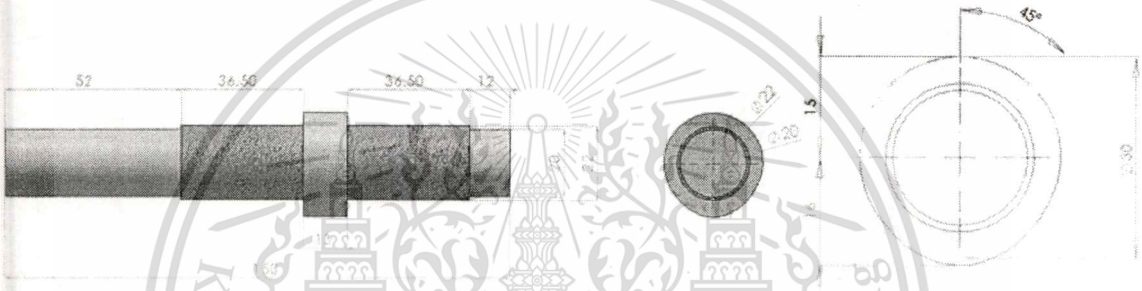

Figure 3.6 Designed dimension for camshaft.

After the fuel was pressurized, it delivered to the direct injection injector that located on the top side of combustion chamber. Along this path, 10 MPa pressure gauge was attached for observe the fuel pressure during the test while fuel pressure just before injected was control by special valve within cam-driven fuel pump. The injector that use in this experimental set up was 6 holes - hollow cone spray type injector. The detail image of injector was shown in Figure 3.7. Tangentional direction of the nozzle enhanced the fuel atomization by generated the swirl flow in form of hollow cone shape.

Finally, Figure 3.8 shows the schematic diagram of fuel route use in this experiment. The GDi injector used in this study was controlled its duration by means of the pulse width signal from the control module. The detail of operation was explained in later section.

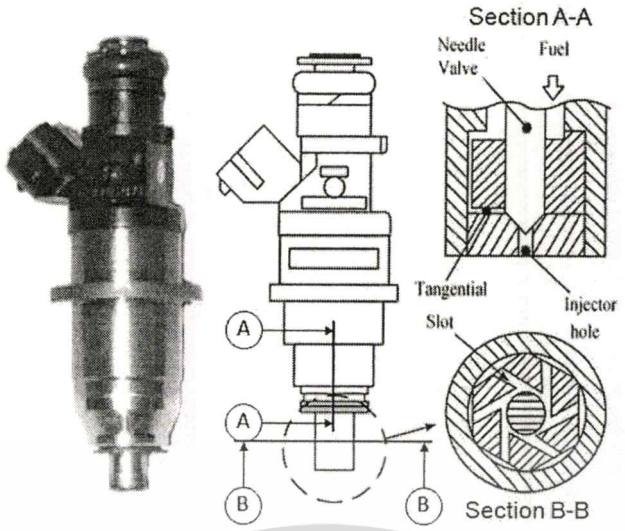

Figure 3.7 Mitsubishi GDi injector and details of nozzle tip.

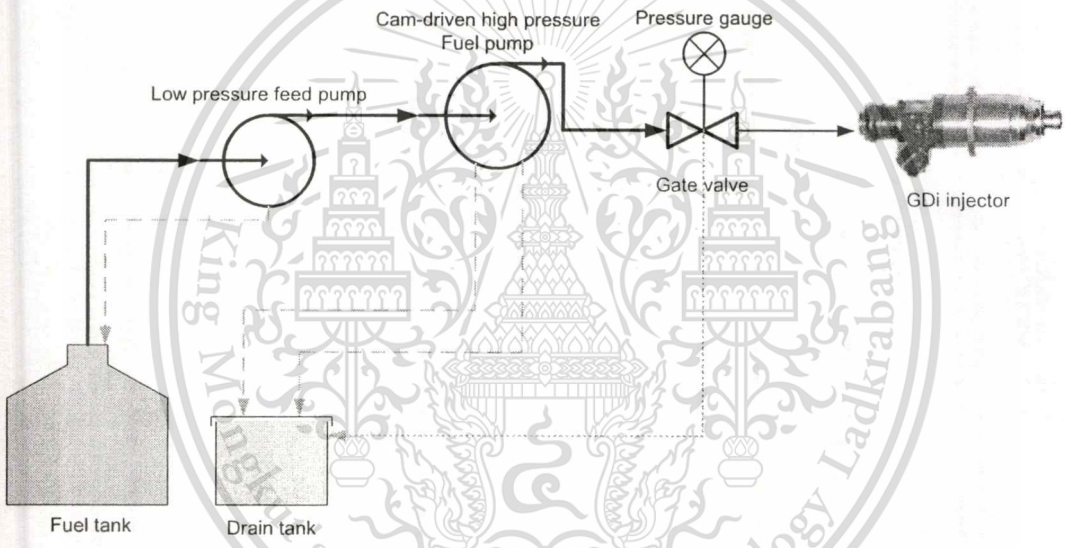

Figure 3.8 Schematic diagram of fuel system.

3.1.3 Temperature control system.

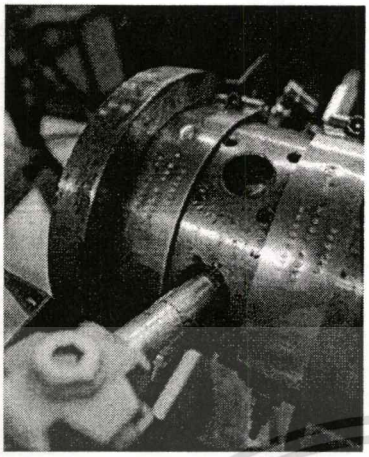

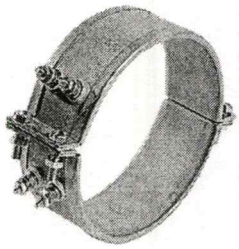

Circular length = 44 cm
Width = 5 cm
No. of heater = 2
Total area = 264 cm^2
Heat flux = 5 W/cm^2
Total Power = 1.32 kW.

a *b*

Figure 3.9 (a) Two band heater attached along the cylindrical shape of combustion chamber excepted the center and (b) dimension of each heater and total power required.

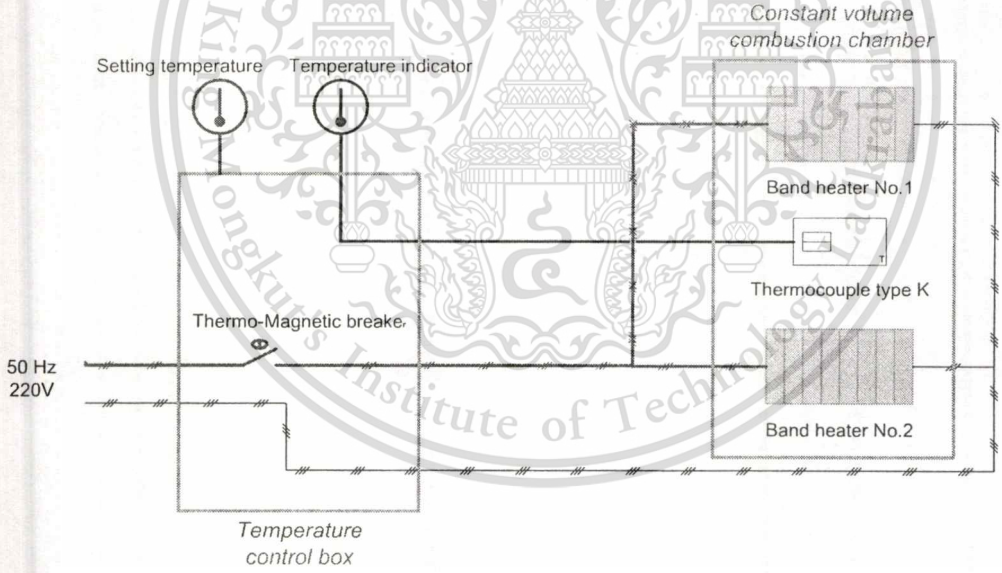

Figure 3.10 Schematic diagram of temperature control system.

Due to the tested fuels were liquid phase at normal ambient temperature and this condition wasn't consistent with the real engine condition. Hence, heat supply devices which was 1300 kW were used in this study for realize the initial temperature close to real engine conditions. From the constant volume combustion chamber geometry, cylindrical shape, two band heaters were chosen for this application. Figure 3.9 shows the images of band heaters. As show in Figure 3.9, the

chamber was allowed heat supply along the cylindrical shape except the center of the chamber. Because of some equipment such as injector, spark plugs, and measurement devices need some space for installation, holes and grooves. Thus, the center of combustion chamber wasn't contact with the band heater, As the consequence, band heater need to be separated into two pieces as show in Figure 3.9. Dimension of each band heater was 3 cm width and 44 cm curriculum length and its capacity was 5 Watt/cm^2. Thus, Total power input for two 220V band heaters was 1300 kW. In addition, constant temperature was used in all tested condition. Therefore, feedback control for keep the temperature constant was needed.

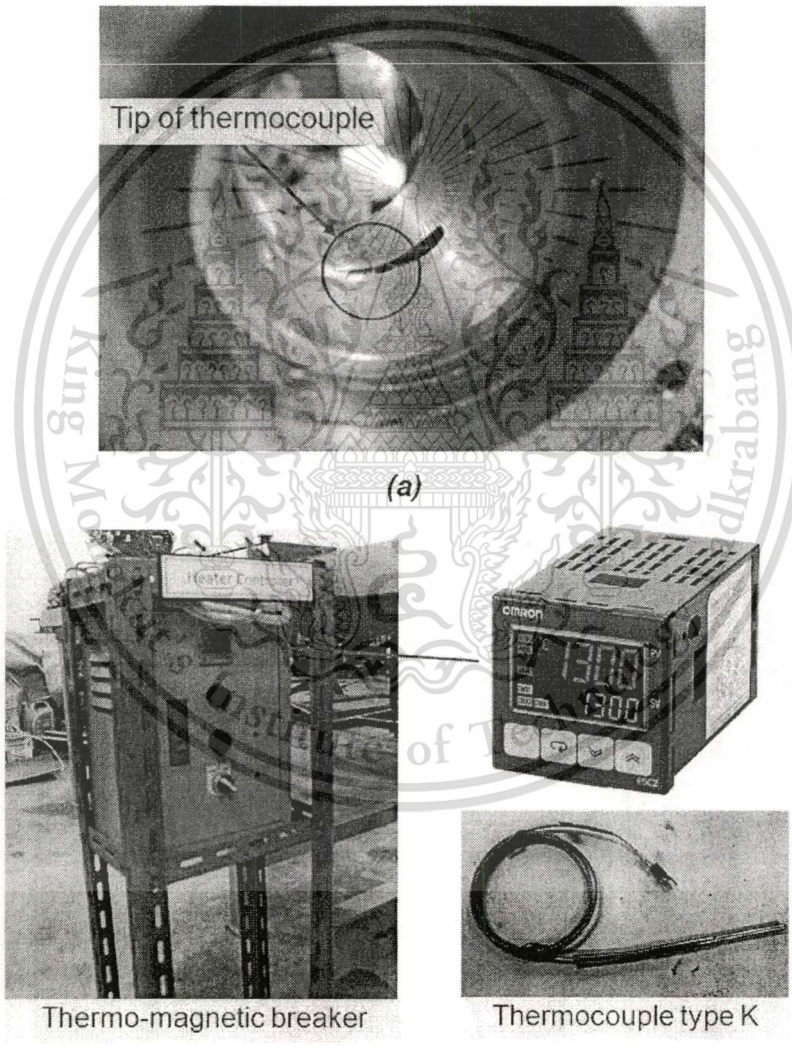

Figure 3.11 (a) Position of thermocouple and (b) thermo-magnetic breaker, temperature indicator and thermocouple for feedback control purpose.

Figure 3.10 shows the schematic diagram of temperature control system. Thermo-magnetic breaker which is 10 Amp. resistance and thermocouple type K

were equipped with this system. In this experiment, measured temperature was the air inside the combustion chamber temperature. Thermocouple were sensed only the temperature at the tip while its extended length was isolated with graphite for avoid disturbance signal form chamber wall temperature. Furthermore, digital temperature monitor was showed both designed temperature and operation temperature. The location of measurement point of air temperature and feedback control devices were shown in Figure 3.11 (a) and (b).

3.1.4 Control module.

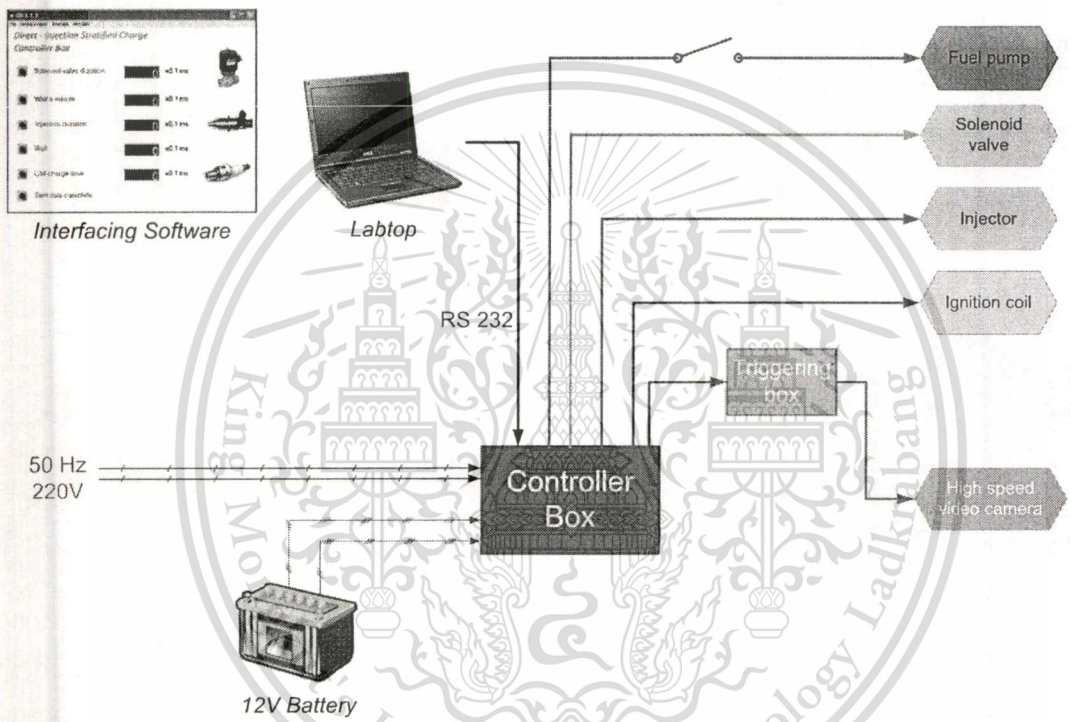

Figure 3.12 Schematic diagram of control module system.

Figure 3.12 show the schematic diagram of control module system. The power source using in this system was come from two sources. First, was the voltage converter that convert 50Hz 220V to usable 12V and 5V. This convertor was attached within controller box. The second was the separated 12V battery. Power from the convertor was used to operate feed pump, solenoid valve and injector while battery supplied voltage for only the ignition coil. The reason for chose separated battery for active only the ignition coil was it need to be prevent some risk from high voltage which can be damage to controller equipment during ignition spark. As shown in Figure 3.12 all of controlled timing were set by using interfacing software in laptop. Signal was command to the controller box via RS-232 cable. In this experiment,

interfacing software was self-building base on C and Basic language. Model of controller board was ATMEGA-128 128 bit controller. Figure 3.13 show the layout of connector and switch align on the controller box.

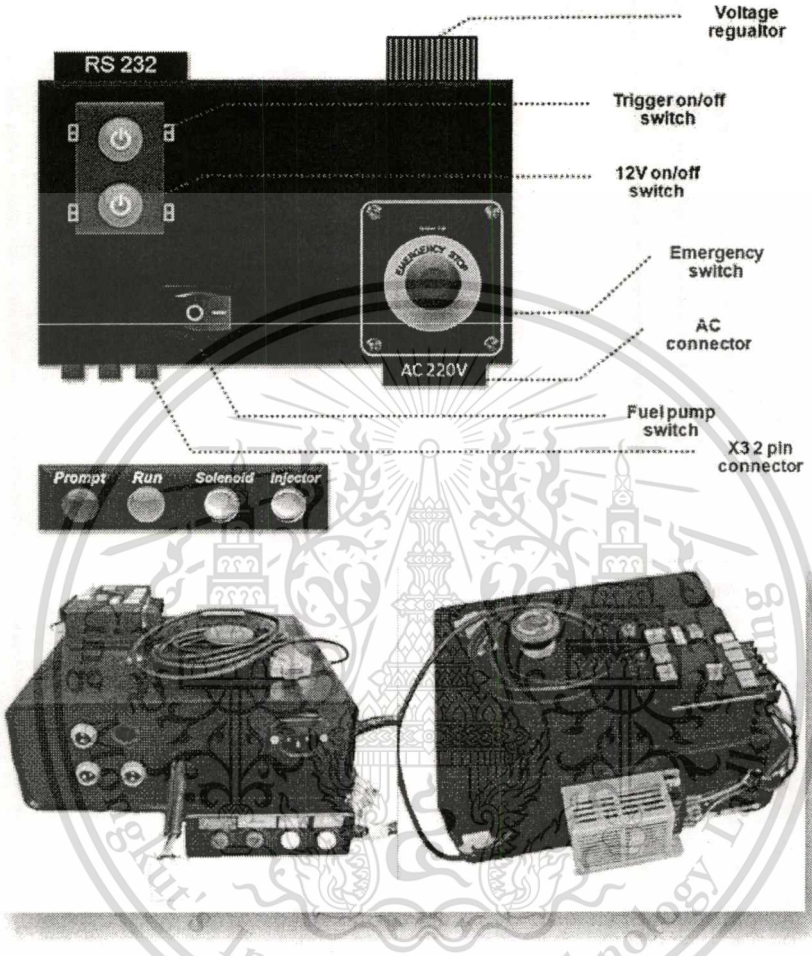

Figure 3.13 Switches and connectors layout on controller box

For the detail of driver circuit, it were illustrated in Figure 3.14 (a) and (b) . In Figure 3.14(a) was the driver circuit for driven actuator such as feed pump, injector and solenoid valve. These devices were controlled by ground signal. In the other hand, Figure 3.14 (b) show the designed diagram for use with ignition coil. This circuit was controlled by +12V signal. In addition, external triggering box for using with high speed video camera was also included in this system. Triggering time was set at constant as 30 msec. this value was also programmed in interfacing software. For avoid some incident during experiment, emergency switch was also equipped in this system.

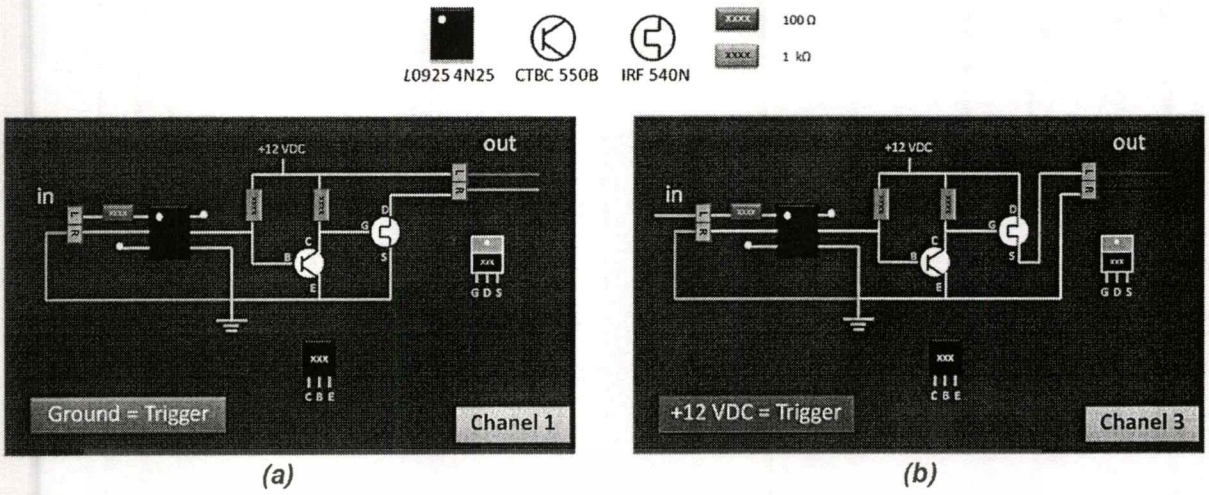

Figure 3.14 Driver circuit (a) ground controlled and (b) +12V controlled

3.1.5 Data acquisition system.

Figure 3.15 Schematic diagram of data acquisition system.

Due to the necessary for analyze the combustion characteristics occur within combustion chamber, high temperature resistance and high resolution of sampling rate were required for correct pressure history data. In this experiment, pressure transducer from KISTLER model 6052c which can be resist temperature up to 400 °C and can operated with high pressure up to 250 bar were chosen. For conditioned and amplified the pressure signal, data acquisition with charge amplifier were also used in this system as show in Figure 3.15. Sampling rate set in through this study were set at 100,000 data/second. All of data were perform in form of Ms.Excel spread sheet and then they will be processed in term of figure and chart via laptop. For detail of specification of data acquisition and pressure sensor, they were illustrated in Figure 3.16, the model of charge amplifier was DEWETRON DEWE-5000. Pressure data signal were collected in term of coulomb and convert to voltage

before conditioned with integrated DAQ (Data acquisition) card within charge amplifier, Its accuracy not exceed 2% of full scale length.

DEWETRON

DEWE-5000

Instrument facts:

- AC or DC powered
- High accuracy, 16, 22 or 24 bit resolution
- Fast sampling, 100 kS/s up to 1 MS/s per channel
- Transient recording up to 1 GS/s
- Powerful Intel® Core™2 Duo PC inside
- 80 MB/s stream-to-disk rate
- Bright 17" display
- Spare panel for customization
- 5 available PCI slots

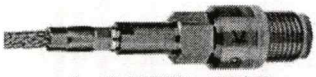

KISTLER

measure. analyze. innovate.

Technical Data

Type 6052C...		
Measuring range	bar	0 ... 250
Calibrated partial ranges	bar	0 ... 50, 0 ... 100, 0 ... 150, 0 .. 250
Overload	bar	300
Sensitivity	pC/bar	≈–20
Natural frequency (measuring element)	kHz	≈160
Linearity, all ranges (at 23 °C)	%/FSO	≤±0,3
Acceleration sensitivity		
axial	bar/g	<0,0002
radial	bar/g	<0,0005
Operating temperature range	°C	–20 ... 350
temperature min./max.		–50 ... 400
Sensitivity change		
200 °C ±50 °C	%	≤±0,5
23 ... 350 °C	%	≤±2
Thermal shock error (at 1500 1/min, p_{mi} = 9 bar)		
±p (short time drift)	bar	≤±0,5
$\pm p_{mi}$	%	≤±2
$\pm p_{max}$	%	≤±1,0
Insulation resistance at 23 °C	Ω	$>10^{13}$
Shock resistance	g	2 000
Tightening torque	N·m	1,5
Capacitance, without cable	pF	5
Weight with cable	gram	30
Connector, ceramic insulator	–	M4 x0,35

Figure 3.16 Specification of charge amplifier and pressure transducer.

3.1.6 Schlieren photography setup

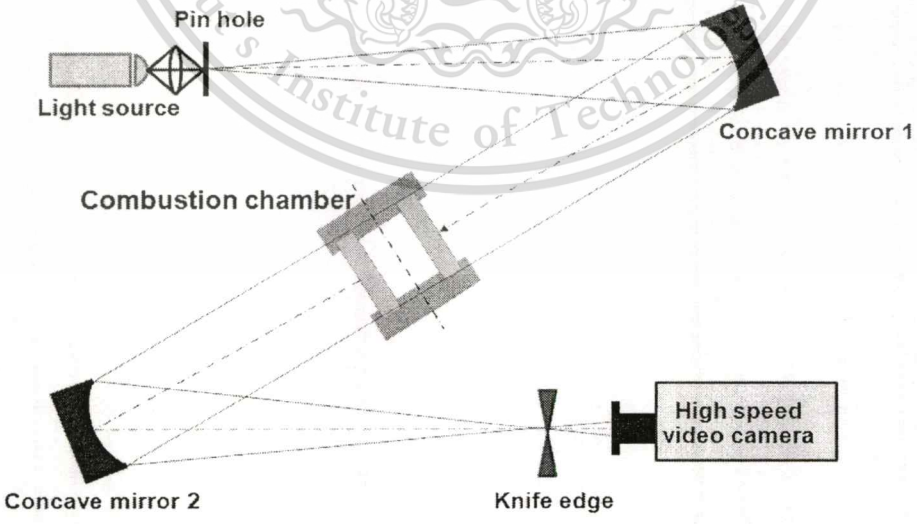

Figure 3.17 Schematic layout of Schlieren photography system.

Schematic layout of Schlieren photography set up was shown in Figure 3.17. The Schlieren photography was very useful tool for flame propagation analysis.

Because of this technique, flame edge and flame were directly measured from high speed video camera due to different of density gradient between burnt and unburned gas due to Its density were response to combustion temperature as explained in the previous section, reaction zone boundary occur at critical point of burnt gas, under assumption that the density gradient were strongly affect to the temperature Thus, Schlieren technique, photography technique that closely related to the density gradient due to change of temperature were chosen.

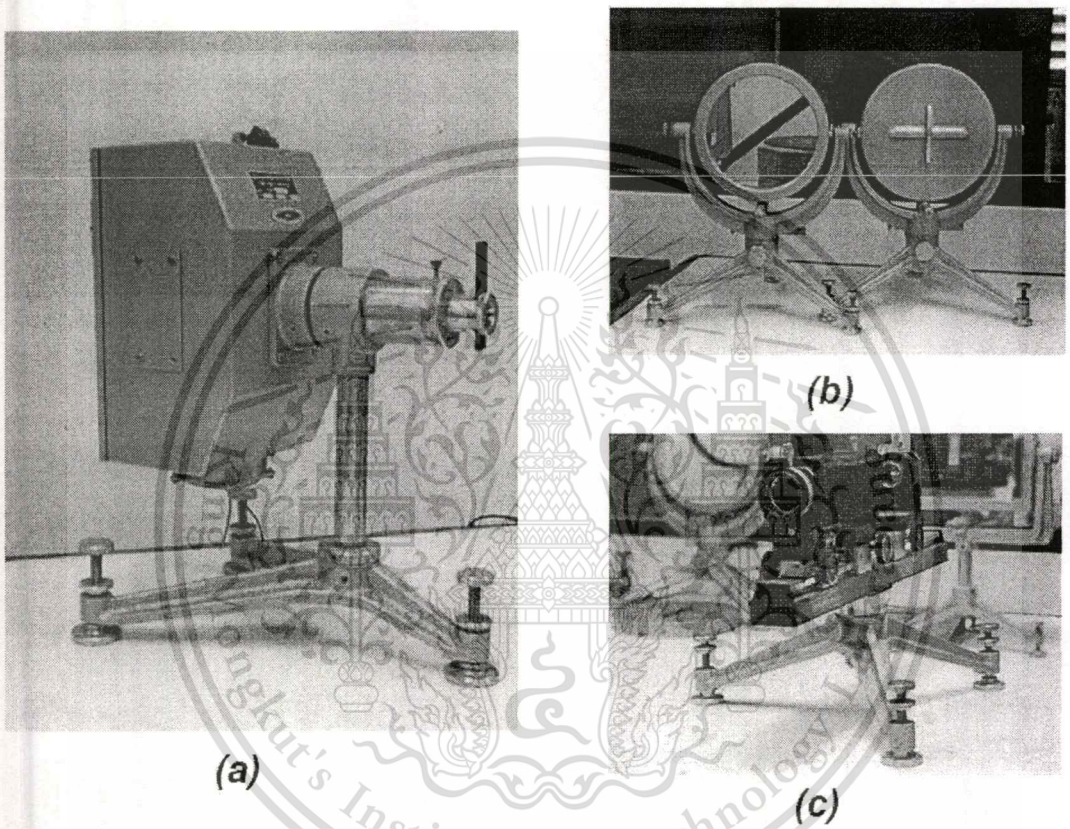

Figure 3.18 Schlieren photography equipment use in this experiment study. (a) Light source, (b) Concave mirrors and (c) knife edge.

As shown in Figure 3.18, Schlieren system was consist of three equipments. First, light source, for generated high intensity light pass through an object. Second, two concave mirrors, for reflex the light form light source into perpendicular direction to the object plan. Third, knife edge, was used to cut-off some scattering light and show more detail of density variation within an object. Two concave mirrors use in this setup has its focal length at 1,800 mm. that length was corresponding to the distance between location of concave mirror No.1 and No.2. The observed object was located at the middle of this length while knife edge was place at focal length

of concave mirror No.2 after relaxed. Position of light source, concave mirror and knife edge were addressed in Figure 3.19.

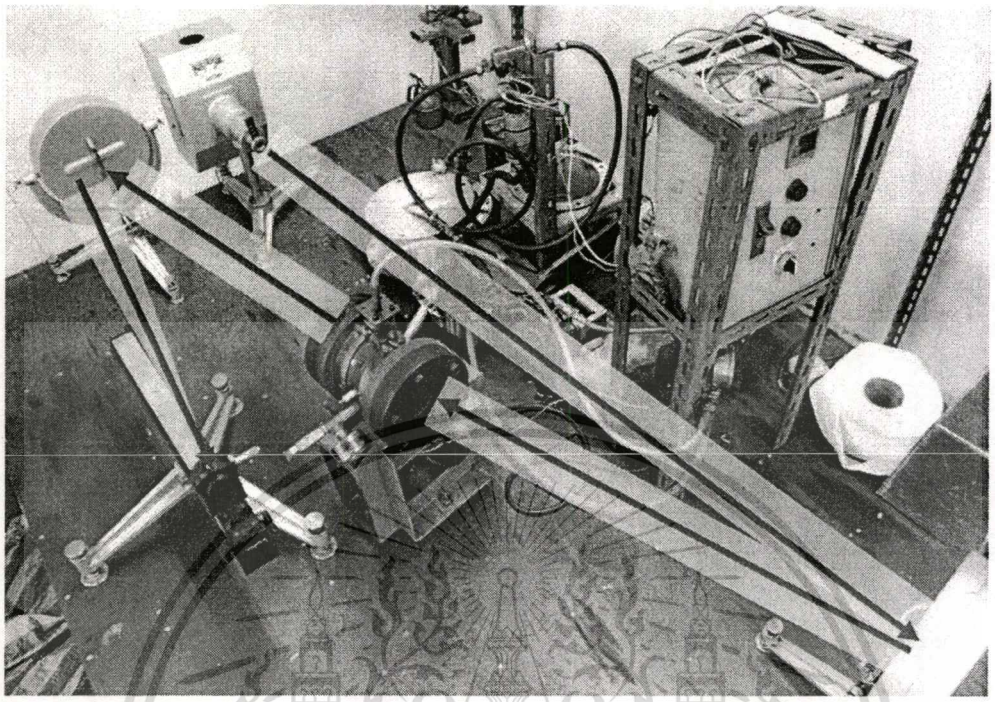

Figure 3.19 Real experiment layout of Schlieren photography.

All of device in this system were align with laser alignment for avoid distortion and provide corrected dimension images. Figure 3.20 show the real experiment setup with high speed video camera.

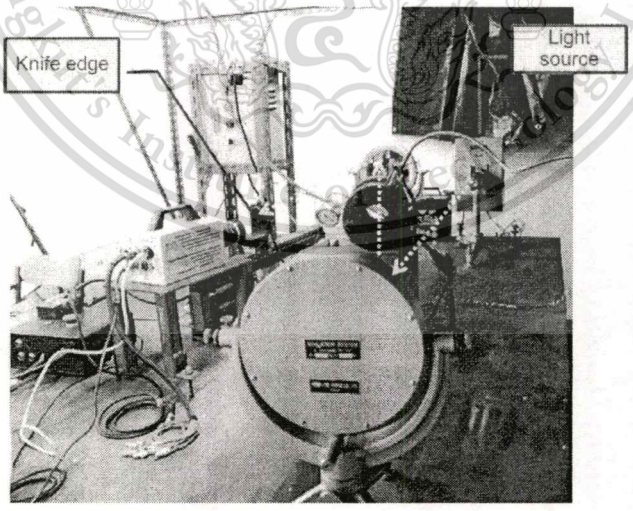

Figure 3.20 Schlieren system with high speed video camera, Position of camera were post after the knife edge.

3.1.7 High speed video camera

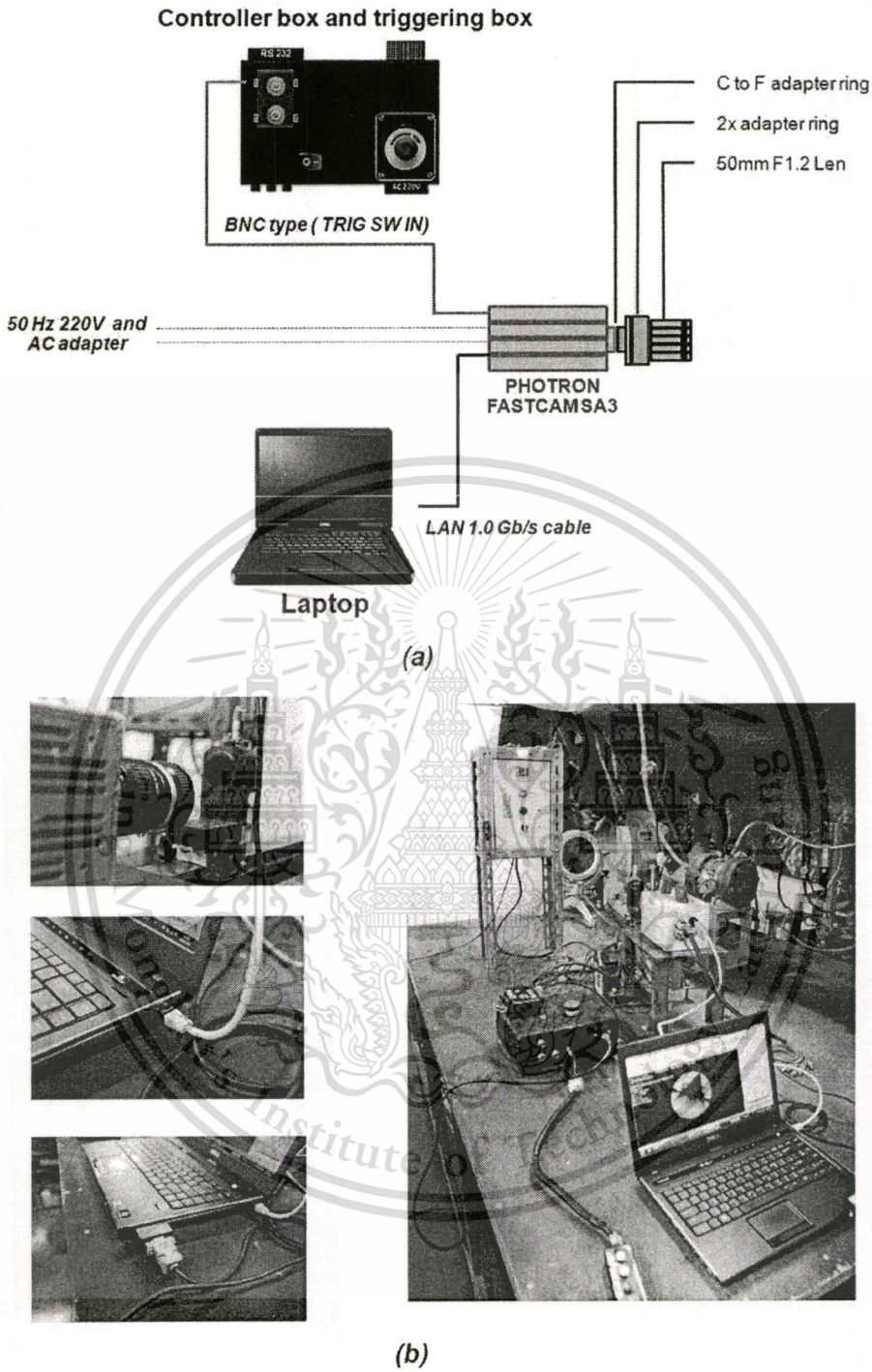

Figure 3.21 (a) Schematic diagram of high speed video camera system (b) Real equipment setup and synchronized cable.

Figure 3.21 (a) and (b) show the schematic diagram of high speed video camera setting and its position. In this study, model of high speed video camera was Photron FASTCAM SA3 – Monochrome which can record with 6,000 fps at 512x512 pixels resolution. For approximately 4 second recording time was limited by 4 Gb

integrated buffer within high speed camera itself. Triggering mode during experiment was set at "Center", event occur 2 second before ignition start and after ignition start 2 second were captured in all test condition. As display in Figure 3.21, separated laptop was used to observe and operated a high speed video camera simultaneously with another laptop, operated signal sequence for combustion. Because of transfer rate from camera to the laptop were very high, thus 1.0 Gb/sec. LAN cable was required. Triggering device, BNC type connector was interfaced between camera to external triggering box. This triggering signal was command by another laptop.

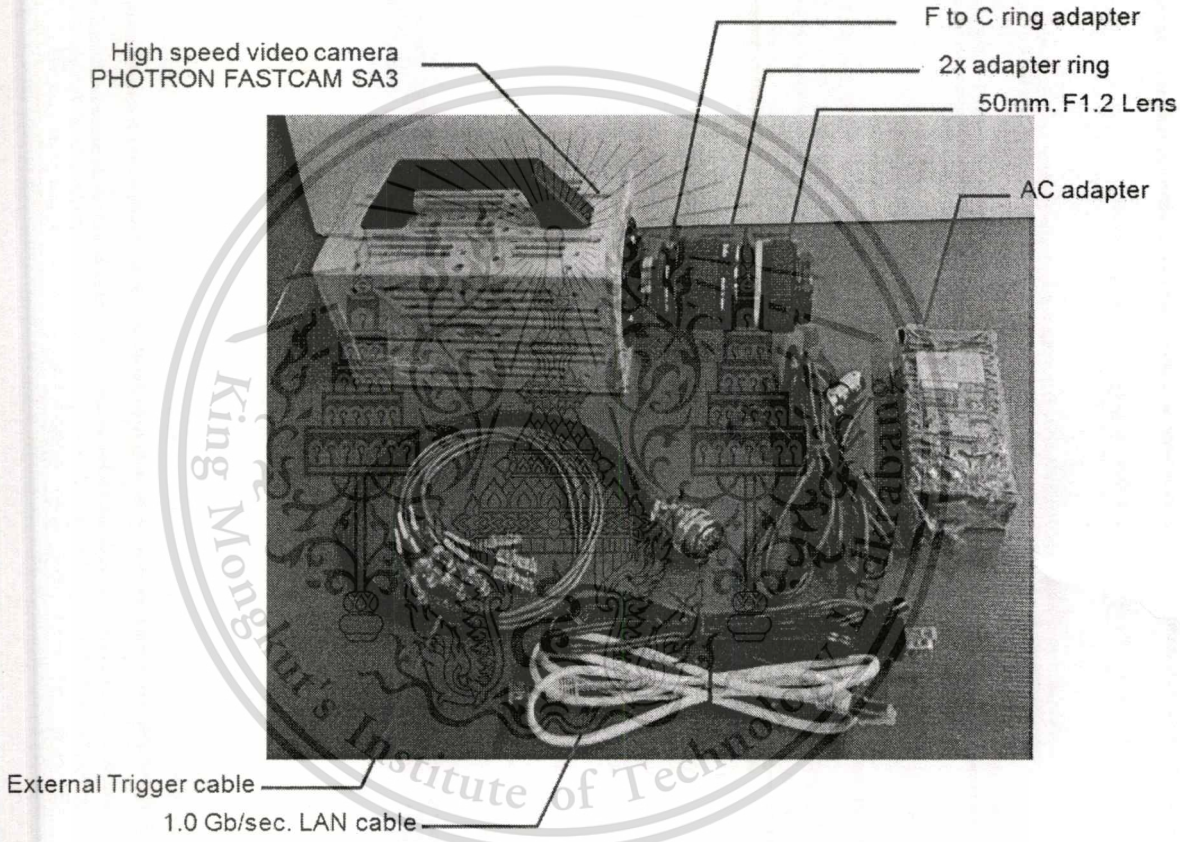

Figure 3.22 High speed video camera and necessaries.

Figure 3.22 show all of equipment that use in this system. For obtain the clearly detail of photography, fix focal length lens with 50 mm. and f=1.2 were need. In addition, 2x adapter ring was very useful to enlarge an object image equal to 2 times of original. Finally, detail of camera setting via FASTCAM viewer software was also shown below in fig.2.23

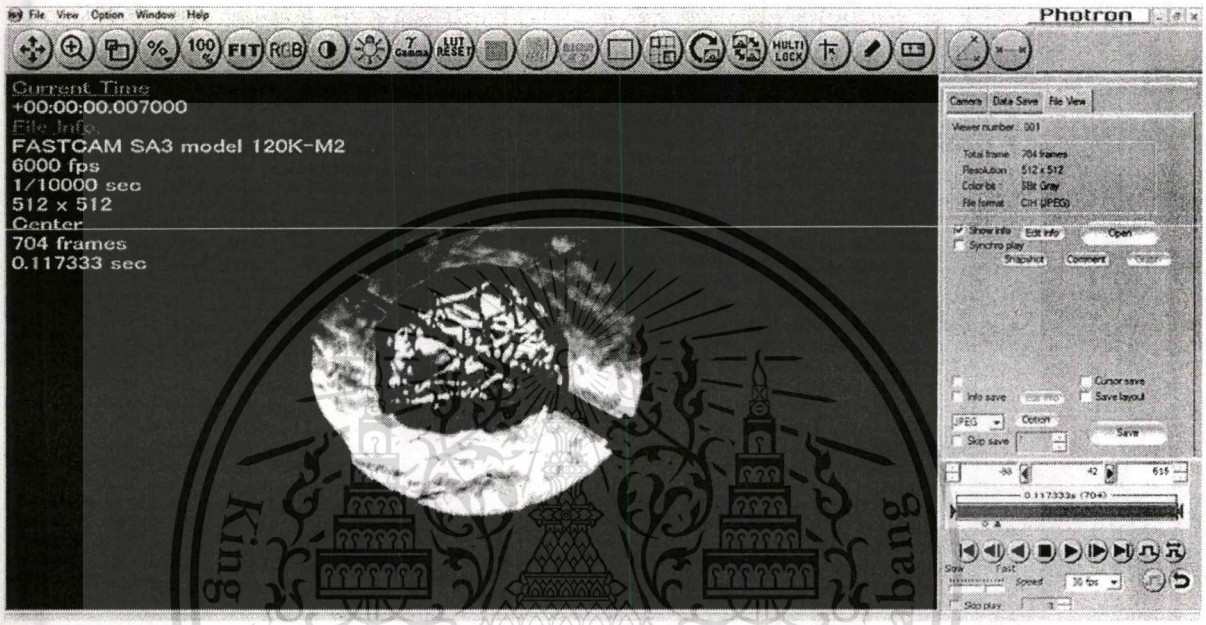

Figure 3.23 Camera setting window shown in PHOTRON FASTCAM viewer software.

3.1.8 Constant volume combustion chamber (CVCC).

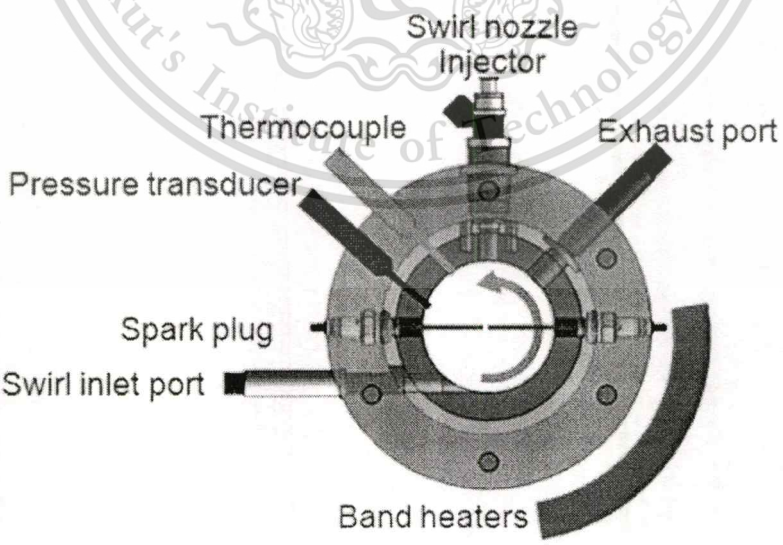

Figure 3.24 Detail view of constant volume combustion chamber (CVCC).

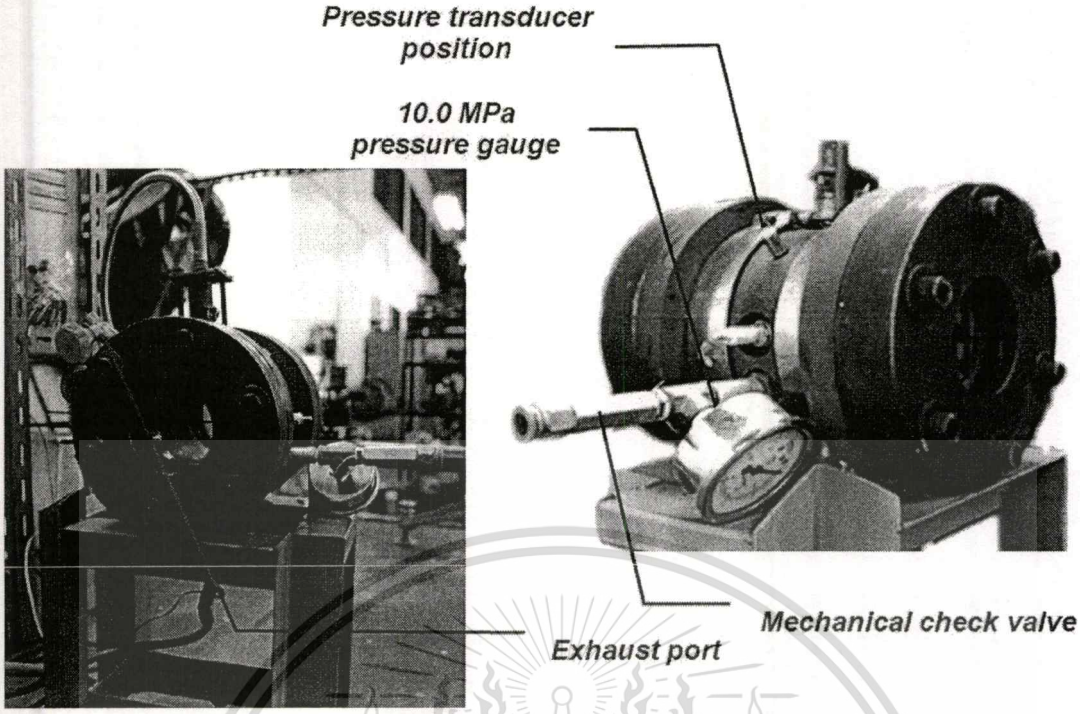

Figure 3.25 Real experiment equipment of CVCC.

In this study, the experiment was conduct on a constant volume combustion chamber instead of an actual engine. The majority reason is constant volume combustion chamber or CVCC can control many parameters and avoid some fluctuation error from external disturbance like the real engine condition. Figure 3.24 show the detail view of CVCC and its measuring devices present in this study while real experiment tools was displayed in Figure 3.25. As can be seen in Figure 3.24 and Figure 3.25, the 10.0 MPa pressure gauge was place prior to the swirl port and mechanical check valve was located before this pressure gauge for prevent back combustion pressure. The swirl port was the tangentional hole drill from the side of chamber. With this geometry, it can allow the induced air flow into the CVCC in tangent direction for realized swirl motion in the chamber. Position of swirl port and thermocouple were also shown in Figure 3.26. Dimension and assembly view of designed CVCC were illustrated in Figure 3.27. Graphite gaskets were use to sealing propose. Furthermore, these can support some shock load and prevent damage to the quartz glasses.

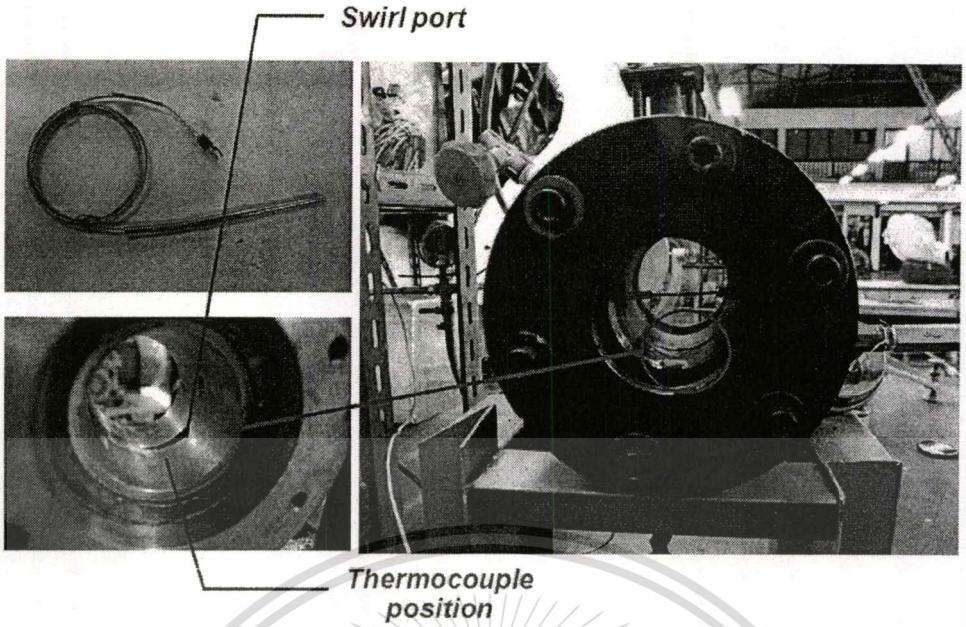

Figure 3.26 Position of swirl port and thermocouple.

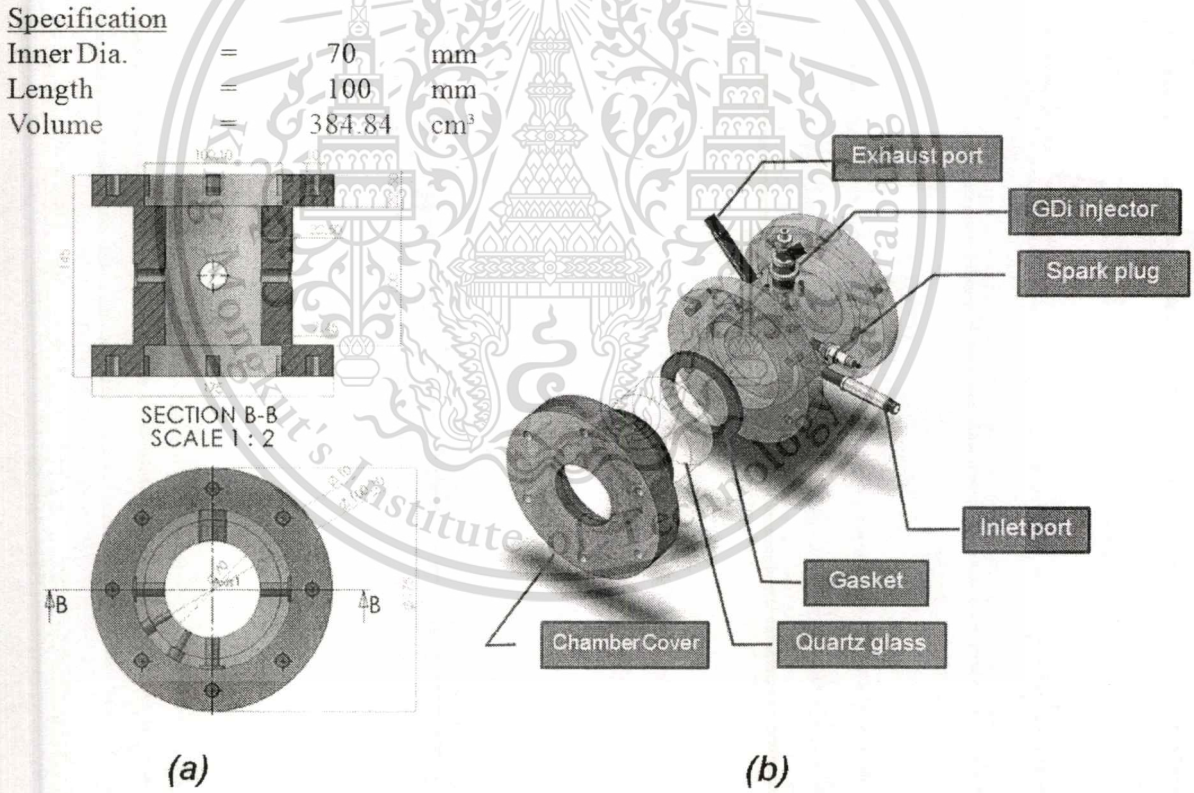

Figure 3.27 (a) Dimension of CVCC and (b) Assembly view of CVCC.

Strength simulation for material using as constant volume combustion chamber was important and very necessary. From the simulation, initial pressure condition equal to 0.5 MPa, maximum pressure occurs in CVCC should be 20-30 MPa. In Figure 3.28, CAE simulation was shown that the maximum stress appeared at measuring equipment holes and edge of quartz glass supporter. When apply pressure

at 5.0 MPa, The value show maximum stress approximately 19.78 MPa at the quartz glass supporter. Thus material of CVCC, ASTM A283 steel grade D was chosen for this application. ASTM A283 or steel SS400 has an yield strength at 230 MPa which corresponding to SF (Safety Factor) = 11 times while quartz glasses provide the safety factor equal to 58. Simulation result of quartz glass deformation was also shown in Figure 3.29.

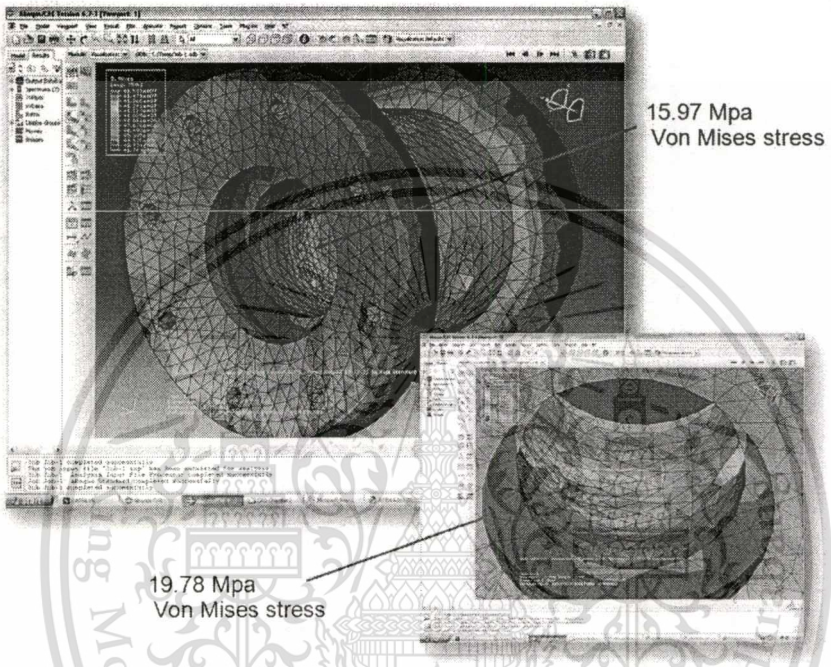

Figure 3.28 5.0 MPa, designed maximum pressure. Appeared maximum stress is 15.97 MPa acts around wall surface and instrument holes and 19.78 MPa, appears around quartz supporter.

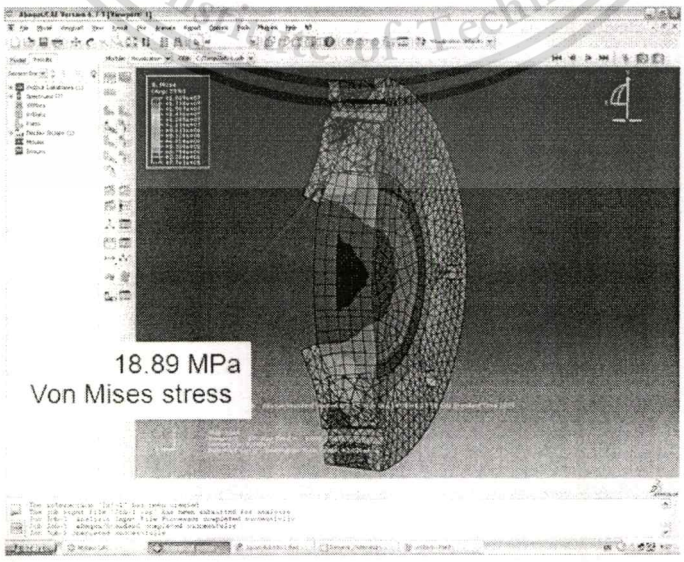

Figure 3.29 Maximum stress is 18.89 MPa acts on edge of quartz, Safety factor is 58.

For avoid impact load on the edge of quartz glasses, graphite gasket were attached at both end of quartz glass side. In order to observe flame propagation, transparent material, the quartz glasses, were necessary to use in this study. In other way, graphite gasket were act like a sealing device for prevent leakage of burnt and pressurized gas within a CVCC. These gaskets can resist temperature up to 1650 °C.

For clearly indentify, assembly view of CVCC was shown in Figure 3.27. Observation window was designed at 70 mm. of diameter while total volume of CVCC belong to 385 cc. Measuring device, Thermocouple and pressure transducer were placed at the CVCC side while GDi injector was fitted at the top side. Six M10 fastener nuts were use to fastened the CVCC to the chamber cover. Furthermore, high temperature resistance O-ring which can be operate over 200 °C were located on the chamber cover for protect the gas leakage. Specifications of material use in constant volume combustion chamber were addressed in Appendix section.

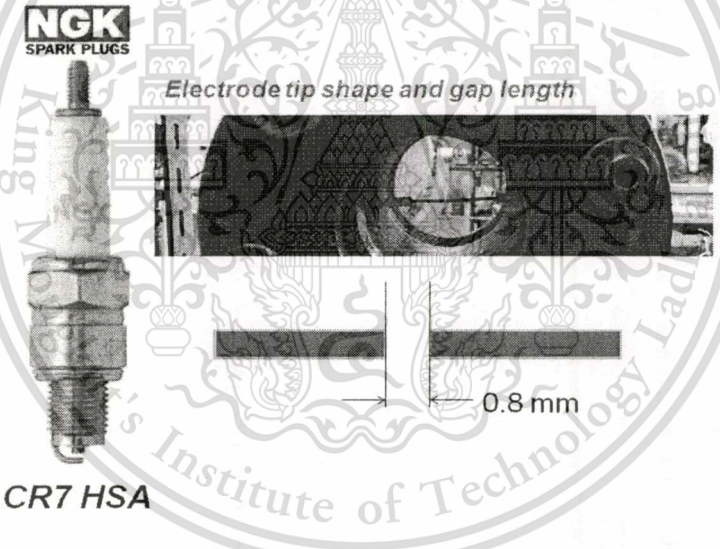

Figure 3.30 Electrode shape and spark gap use in this study.

Ignition systems in this study were the direct coil type for spark energy. Because of its convenient, install and control. For the spark plug, the electrode were extended to the center of CVCC for realize initial flame kernel like the spherical expanding shape. One spark plug was use as the energizer electrode while another spark plug was ground. The spark gap was set as constant at 0.8 mm. in all tested condition. Detail of location and electrode shape were illustrated in Figure 3.30.

3.2 Experimental condition

In stratified charge combustion, it has many parameters affect to the combustion behaviors. Following reviews was examined some parameters which have been studied by researchers and theirs effect.

3.2.1. Initial temperature, initial pressure [4]

3.2.2. Spray pattern and nozzle characteristics [1, 4, 19]

3.2.3. Turbulence intensities [12, 18]

3.2.4. Ignition timing [7, 18, 20, 21]

3.2.5. Ignition energy, spark gap and electrode shape [8]

3.2.6. Injection pressure [16]

3.2.7. Degree of mixture stratification [9]

In this study, the author wish to control many variable parameters and observe only in the effect of fuel type and swirl intensity on combustion characteristics. Therefore, a constant volume combustion chamber was employed in this study. Influenced parameter and variable parameter that be controlled in this experiment were shown in table 3.

Table 3 : Experiment condition table.

Experimental variables	Conditions
Initial temperature (K)	450
Initial pressure (MPa)	0.5
Coil charge time (msec) "e"	3
Injection pressure (MPa)	4.5
Inj – Ign Interval (msec) "d"	10
Ignition start (msec) "b"	100
Solenoid valve duration (sec) "a"	1.5
Tested fuel	E0,E20, E85, E100
Equivalent ratio	1.0, 0.8, 0.6
Swirl intensities in ΔP (bar) Swirl intensities in velocity (m/s)	1.0, 2.0, 3.0,4.0 and 5.0 4.2, 5.0, 6.3, 6.9, 8.3

From experiment condition table, the fuel type were varied from zero percentage of ethanol or pure gasoline (E0) to 20 percentage of ethanol (E20) , 85 percentage of ethanol (E85) and pure ethanol fuel (E100) for investigate effect of ethanol content on stratified charge combustion behavior. Turbulence intensities in this study were assumed that depended only on the strength of swirl flow within combustion vessel and directly related to the stratification degree. Swirl flow intensities were changed for 5 values, definite by different pressure between induced air charge and chamber pressure, for study effect of swirl intensities on combustion behaviors and their merits when apply with stratified charge combustion.

Initial temperature was set constant at 450 K ,which is higher than evaporation temperature of all tested fuel to avoid a misfire when the fuel was injected into the combustion chamber. Initial pressure was 0.5 MPa in all condition tested, this simulate combustion condition in lately stage of compression stroke. The detail explanation of setting this initial pressure show in fig.3.31. The author try to simulate the initial condition as close as possible to real engine condition. As can be seen in this figure, the starting point of compression pressure may be less than ideal Otto cycle because in the GDi engine, stratified mode operate under low to part load condition. Thus, P_1, is start at 30 to 50 kPa. and the start of ignition point is occurs around 10-20 $^{\circ}$CA BTDC. Consequently, P_2, is approximately 0.5 MPa, this is the initial pressure before ignition start. However, because of this experiment is conduct on CVCCC, some of timing for generate swirl intensity may be limited and show the longer time than real engine condition. For example, injection – ignition timing, this value may be longer for realize the mixing process. Another timing is time after solenoid vale close or start of ignition point, this value is set base on air motion velocity data. Thus, the longer timing (100 msec.) can be noticed.

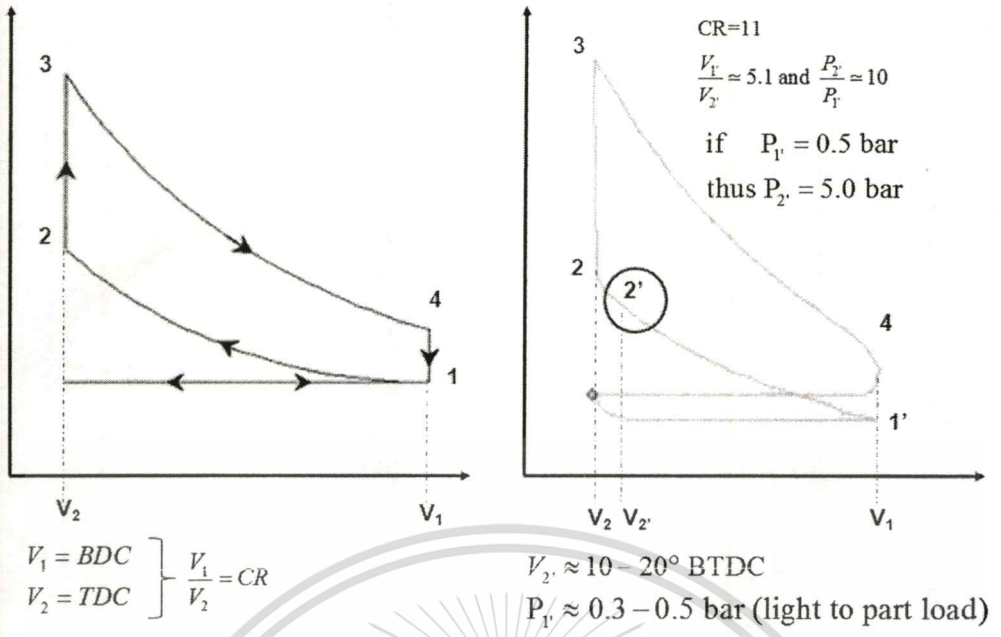

Figure 3.311 Initial pressure setup base on real engine condition.

Ignition charge time that strongly effect to the ignition energy was set constant at 3 msec., this value according to normal operation condition in GDi engine (refer to the Mitsubishi GDi manual) while spark gap was controlled at 0.6-0.8 mm. width. In addition, fuel pressure was fixed at 4.5 MPa for avoid the compressible effect of fuel mass and this value was consistent with the real GDi engine condition. For investigation on combustion characteristic in lean operation, overall equivalence ratio were varied from stoichiometric mixture or ø =1.0 to lean side ø=0.8 and ø=0.6, respectively. However, it should be noted that there exists much difference between the vessel study and a real engine. There is no influence in the vessel study from the residual gas and charging that play the influence on the cyclic variations in a real direct-injection engine. The experimental conditions such as the temperature and pressure also are much lower than those of a real engine. Thus, the studied parameters in the vessel study only reflect the mixture formation, both local equivalence ratio and degree of mixture stratification and/or mixture inhomogeneity besides the influence from swirl flow. Meanwhile, application of the vessel obtained results to a real engine still needs further investigation by including all issues inside engine combustion. Furthermore, effect of timing cannot be neglected because it strongly related to the swirl rate and ignition timing. The detail of choosing timing and control procedures have been noted in next section already.

3.3 Experiment procedure

3.3.1 Swirl setup

Swirl intensities were varied by adjusting the different pressure between pressurized air inlet and chamber pressure. Concept of swirl controlled use in this experiment was shown in Figure 3.32.

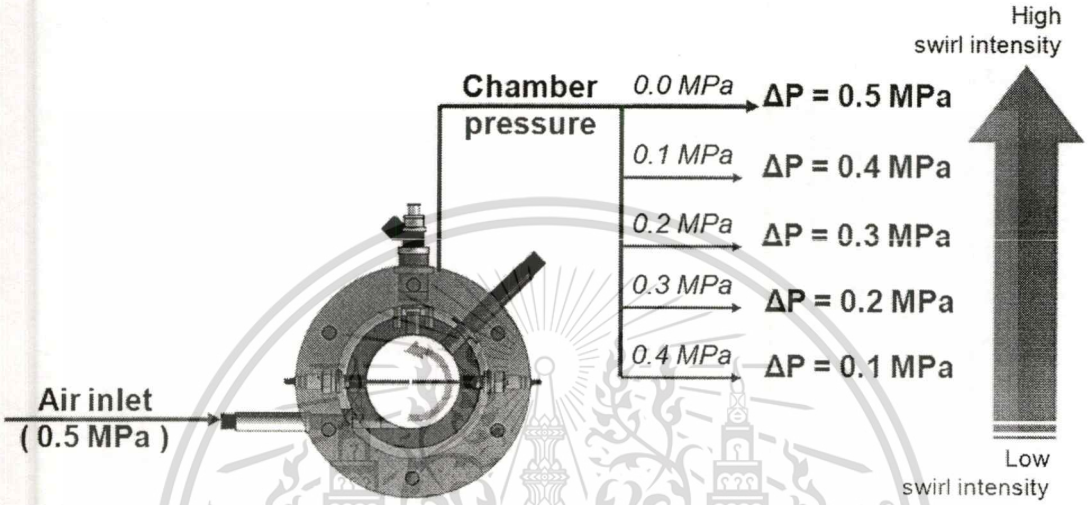

Figure 3.32 Swirl setup definition

First, pressurized air was inducted into the constant volume combustion chamber according to the swirl value (0.0, 0.1, 0.2, 0.3, or 0.4 MPa) as shown in Figure 3.322 .After that, pressure regulator will allowed second induced air to pressurized for 0.5 MPa which is consistent with the initial pressure condition. The induced charge time for 0.5 MPa fresh air was fixed at 1.5 second for ensure that constant volume vessel were filled with air. With utilizing of shadowgraph photography and high speed video camera, air motion image can be used to investigate an air velocity in each condition of swirl flow. In this study, The air velocity didn't measure by LDV or PIV method. But they were measured by observed the air stripes appeared in shadowgraph image of air flow that be taken by high speed video camera.

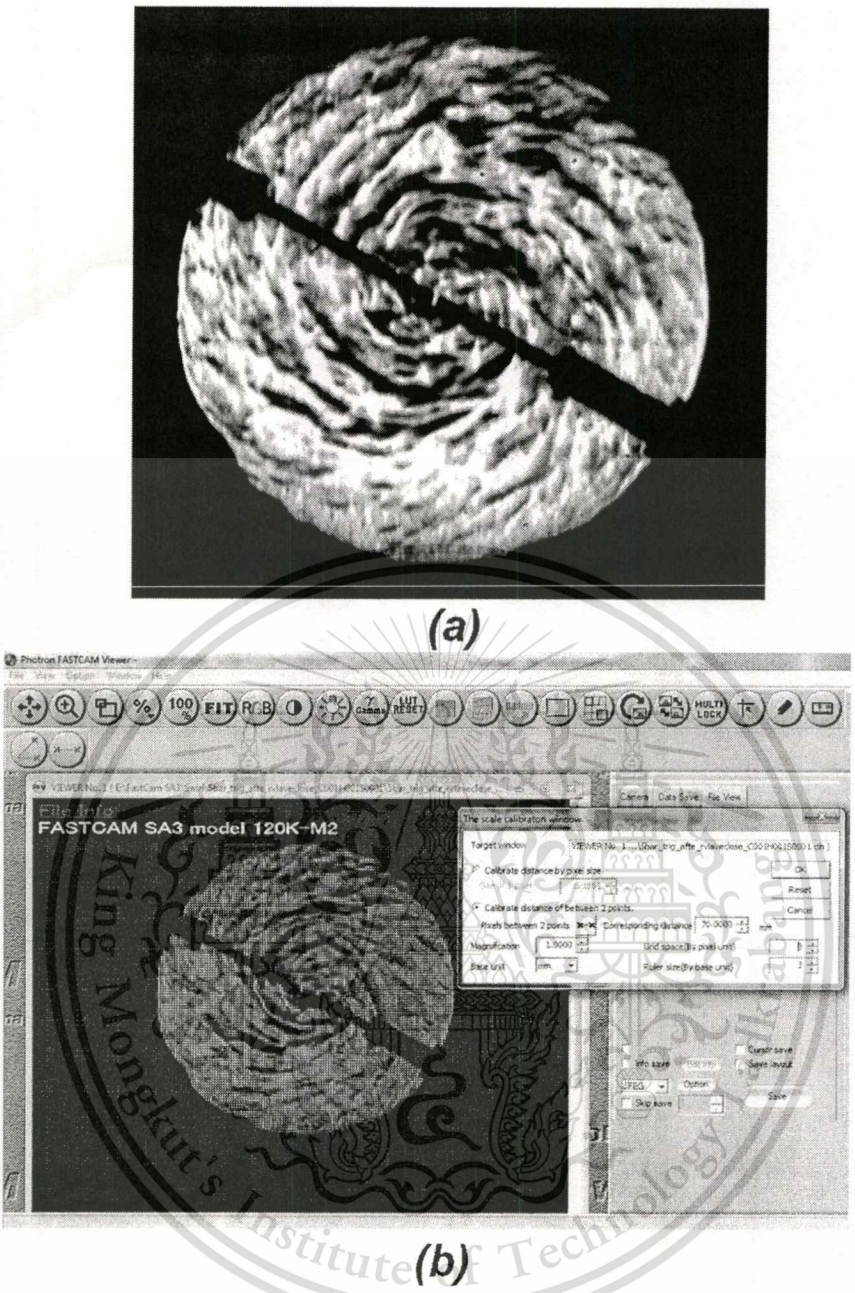

Figure 3.33 (a) Shadowgraph image of air stripes and (b) grid mesh for air velocity calculation.

Figure 3.33 show air stripe image taken from Phrotron SA3 high speed video camera and (b) show the grid mesh that use in Phrotron FASTCAM viewer software. Grid pixels and time elapsed recorded in each video file can be covertly calculated the distance against the time into air stripe velocities. Value of measuring velocity from software was arrange and plotted into velocity chart as show in Figure 3.34

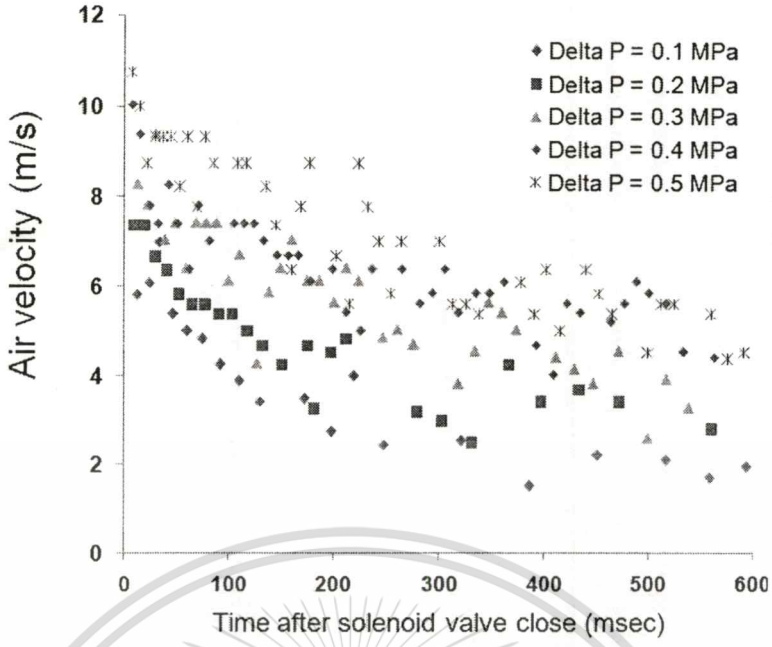

Figure 3.34 Scattering plot of air velocities in various swirl conditions.

From the raw data of velocities plot, regression line may be required. The velocities chart of air velocities against time after solenoid valve closed shown in Figure 3.35

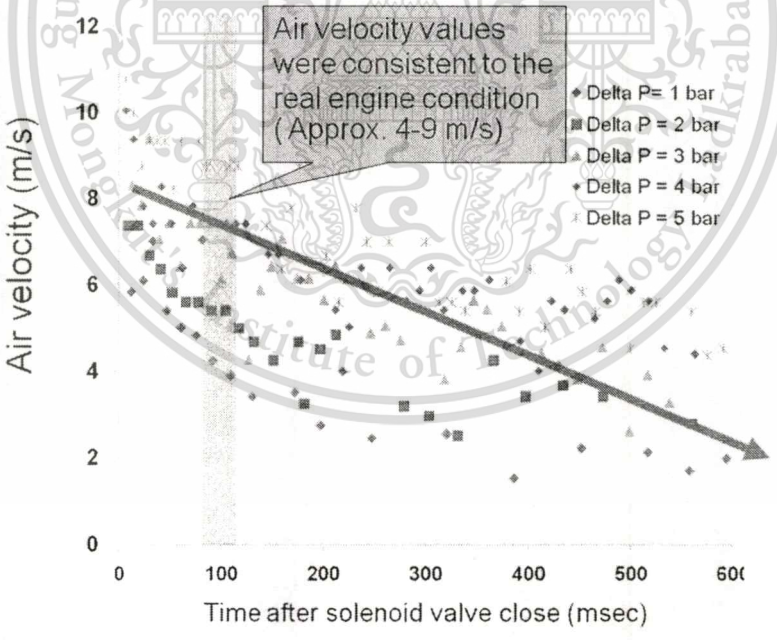

Figure 3.35 Regression plot of air velocities (base on experiment)

As shown in Figure 3.35, later from pressurized air was induced for 1.5 msec.,then, the solenoid valve closed, the swirl flow were deteriorated as shown in Figure 3.34. After the time around 100 msec. Value of swirl velocity consistent with the air velocity at 4.2 – 8.3 m/s. These value were related to the real engine at low

speed and low load condition At this point, the author assume as the start of ignition point. Thus, In this experiment, different in swirl intensities can be reasonable changed by varying the different pressure between chamber and fresh air. Because it related to the air velocity as shown in velocities plot chat.

As can be seen in relative comparison table between swirl value which were displayed in unit of ΔP and air velocities which were quantified in unit of m/sec. when the swirl value change from the lowest one (ΔP=0.1 MPa) to the highest value (ΔP=0.5 MPa), air velocity can be changed only two times or double. Thus, please note that the increasing swirl value for 2 times is not equal to gain double in air velocity. For example when swirl intensity value change from 0.1 MPa to 0.2 MPa (2 times of swirl value). Actually, the air velocity just increase approximately 20% or 1.2 times of original (4.2 m/sec change into 5.0 m/sec).

Table below displayed the air velocities when applying different pressure.

Table 4 : Swirl intensities against air velocities

Swirl intensities in ΔP (MPa)	Swirl intensities in term of air velocities (m/s)
0.1	4.2
0.2	5.0
0.3	6.3
0.4	6.9
0.5	8.3

3.3.2 Equivalence ratio setup

Because of this experiment was conduct on the constant volume combustion chamber. Available air was fixed. Thus, the equivalence ratio were be controlled by varying amount of fuel injected. At the given injection pressure and fuel temperature, mass of fuel injected were depended only on injection duration. In this section, air mass was calculated base on ideal-gas law while fuel mass were prepared in term of calibration chart which was directly obtained by examine in experiment. For the detail of calculation, they were explained through this section.

3.3.2.1 Air mass calculation.

As noted as above, available air mass in this experiment was fixed due to it filled in the constant volume combustion bomb. Thus, air temperature and chamber pressure data were play an important role for calculation available air mass. Air mass were calculated based on ideal-gas law. Following equations show the procedure for calculated these values.

$$P_{atm} + P_{gauge} = P_{abs} \tag{19}$$

Where, $P_{atm} = 1 \text{ bar} = 10^5 \text{ Pa}$ and $P_{initial} = P_{gauge} = 0.5 \text{ MPa}$

Hence,

$$P_{abs} = 0.6 \text{ MPa}$$

From ideal gas law, following equation may be used

$$PV = mR_{air}T \tag{20}$$

Where, $P = P_{abs} = 0.6 \text{ MPa}$, $V =$ Chamber volume $= 385 \text{ cc or } 3.85\text{x}10^{-4} \text{ m}^3$ and $R_{air} =$ Gas constant $= 287.058 \text{ J/mol}\cdot\text{K}$. All condition were examined at ambient air temperature ,Thus, $T =$ Inlet air temperature $= 300 \text{ K}$. After simplified and substitution, air mass can be obtained as follow;

$$m_{air} = \frac{(0.6 \text{ MPa})\cdot(3.85\text{x}10^{-4} \text{ m}^3)}{(287.058 \text{ J/mol}\cdot\text{K})\cdot(300 \text{ K})}$$

$$m_{air} = 2.787 g \tag{21}$$

3.3.2.2 Fuel mass

Mass of tested fuels in this study were directly measured from the injector flow rate. First, tested fuel was feed to the GDi high pressure fuel pump, then it was regulated to approximately 4.5 MPa of injection pressure. This value was consistent to the operation pressure in Mitsubishi GDi engine. Temperature of tested fuel was kept constant as ambient conditions through experiment. Finally, high pressure fuel was injected into measurement beager with the certain time of injection, injection duration. Detail of how to prepare the injection flow rate calibration chart were explained as follow;

E100 Injector flowrate

Injection pressure	45	bar
Bottom mass	22	gram

5 msec → Varied from 5 to 10. 20 and 30 msec.. respectively

time	mass (g)	diff_mass (g)	mass/time (g)
30	26.44	4.44	0.14807
50	33.92	7.48	0.14964
70	44.23	10.31	0.14726
100	58.80	14.57	0.14568
130	77.81	19.01	0.14619
AVG			0.14737

AVG → Fuel mass per one pulse (5msec)

Injection duration (msec)	Fuel mass/time (g)
5	0.14737
10	0.30121
20	0.64160
30	0.95843

Figure 3.36 Investigation of relation between injection duration and fuel mass

From the raw data collected table, injection duration per one pulse was varied form 5 msec. to 10 msec., 20 msec. and 30 msec., respectively. Firstly, fuel was injected for 30 times. Then additional amount of 50 times,70 times ,100 times and 130 times were performed respectively. Total injection times were equal to 30+50+70+100+130 =380 times for each condition. From the measuring fuel mass and neglects the beager mass, it can be convert to relation between fuel mass per pulse or fuel mass against the injection duration time.

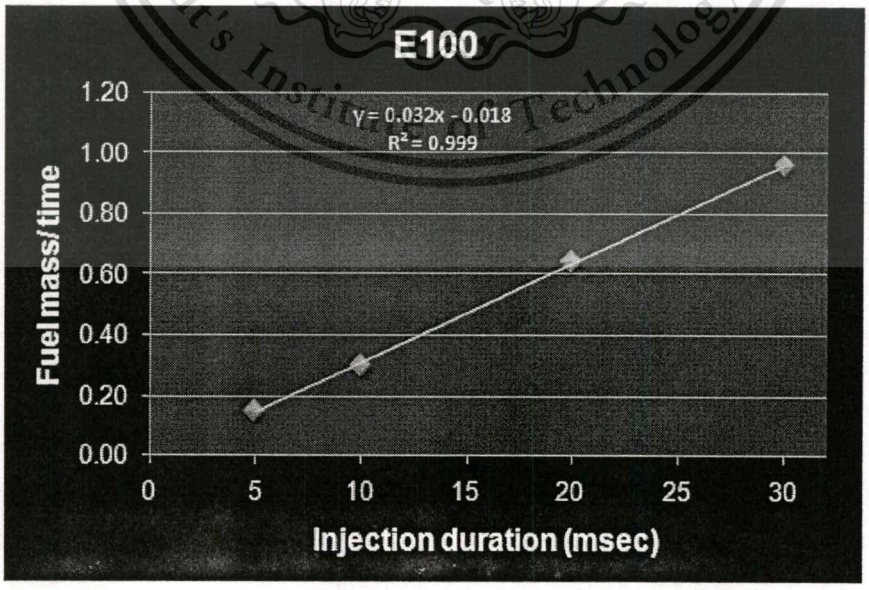

Figure 3.37 Fuel mass calibration chart (E100)

Figure 3.377 show the injection flow rate chart of pure ethanol (E100), in this chart, relation between injection duration in msec. and fuel mass were addressed. In addition, all tested fuel, E0, E20 and E85 were also examined and prepared in form of injection flow rate chart. The measuring point for this test is fixed for 4 values, 5 msec., 10 msec., 20 msec., and 30 msec. of injection duration.

From these chart, relation between fuel mass and injection duration signal, Good linearity of data plot can be achieved from 5 -30 msec. of injection duration with very low variation (R^2=0.9). Furthermore, if available air is fixed and AFR at stoichimetric condition is known, Figure 3.38, fuel mass calibration chart can be converted into relation between equivalence ratio and injection duration.

Due to each tested fuel was different in stoichiometric fraction. Amount of fuel injected for keep the same equivalence ratio value may be changed with the fuel. Thus, Calibration chart for fuel injection in each fuel might be need. Before getting the calibration chart, principal concept of equivalence ratio and stoichemetric mixture were note as follow;

Stoichemetric ratio is the ratio of air to fuel that can be calculated from oxidation equation at adiabatic flame temperature condition. The proper fraction of air to fuel was the mass of air that can be joined with a mole of fuel. Equations below showed stoichemetric ratio for hydrocarbon fuel.

$$C_xH_y+(x+\frac{y}{4})(O_2+3.773N_2)\rightarrow xCO_2+\frac{y}{2}H_2O+N_2 \qquad (22)$$

$$AFR_{Stoi}=\frac{(x+\frac{y}{4})(4.773\cdot 29)}{(12x+y)} \qquad (23)$$

In this study, pure gasoline has the chemical formula as $C_{8.26}H_{15.5}$.thus,

$$\left(AFR_{Stoi}\right)_{E0}=\frac{(8.26+\frac{15.5}{4})(4.773\cdot 29)}{\left((12\cdot 8.26)+15.5\right)}=14.65 \qquad (24)$$

For other ethanol blend such as E20, E85 and also E100 following equations can be used;

$$xC_2H_5OH+yC_{8.26}H_{15.5}+\left(3x+12.13y\right)(O_2+3.773N_2)=aCO_2+bH_2O+cN_2 \qquad (25)$$

Where

x = mole fraction of the Ethanol

y = mole fraction of the Gasoline

And

$$AFR_{Stoi} = \frac{(3x+12.13y)(4.773 \bullet 29)}{46x+114.8y} \quad (26)$$

All of stoichemetric values and mole fraction were drawn in the table as shown below.

Table 5 : Fuel properties table (base on calculation).

Fuel	Mass	Molecular weight	Cp	LHV	Moles	Mole fraction	AFR(stoi)	Molecular weight	LHV
	kg	M	kJ/kg.K	MJ/kg				M	MJ/kg
E0									
C_2H_5OH	0.00	46.07	1.93	26.9	0	0.000			
$C_{8.26}H_{15.5}$	1.00	114.18	1.7	44.0	0.008758	1.000	14.625	114.18	44.0
	1.00				0.008758	1.000			
E20									
C_2H_5OH	0.20	46.07	1.93	26.9	0.004341	0.383			
$C_{8.26}H_{15.5}$	0.80	114.18	1.7	44.0	0.007006	0.617	13.512	88.12	40.6
	1.00				0.011348	1.000			
E85									
C_2H_5OH	0.85	46.07	1.93	26.9	0.01845	0.934			
$C_{8.26}H_{15.5}$	0.15	114.18	1.7	44.0	0.001314	0.066	9.872	50.60	29.5
	1.00				0.019764	1.000			
E100									
C_2H_5OH	1.00	46.07	1.93	26.9	0.021706	1.000			
$C_{8.26}H_{15.5}$	0.00	114.18	1.7	44.0	0	0.000	9.027	46.07	26.9
	1.00				0.021706	1.000			

$$\text{Equivalence ratio } (\phi) = \frac{\text{FAR}_{\text{actual}}}{\text{FAR}_{\text{stoi}}} \tag{27}$$

Or

$$\text{Equivalence ratio } (\phi) = \frac{\text{AFR}_{stoi}}{\text{AFR}_{Actual}} \tag{28}$$

As described in the early part, injection flow rate chart can provide the relationship between injection duration and fuel mass, In equivalence ratio calculation, equivalence ratio directly related to the mass of fuel injected where the available air was fixed. Consequently, relationship between equivalence ratio and injection duration of each tested fuel can be obtained by these concept and fuel calibration chart can be prepared follow these procedures. Figure 3.38 shows the calibration chart of E100, both equivalence ratio and injection duration may be illustrated in this figure. From that chart, if equivalence ratio of E100 is determined, the corrected signal of injection duration can be found with the relationship form this chart.

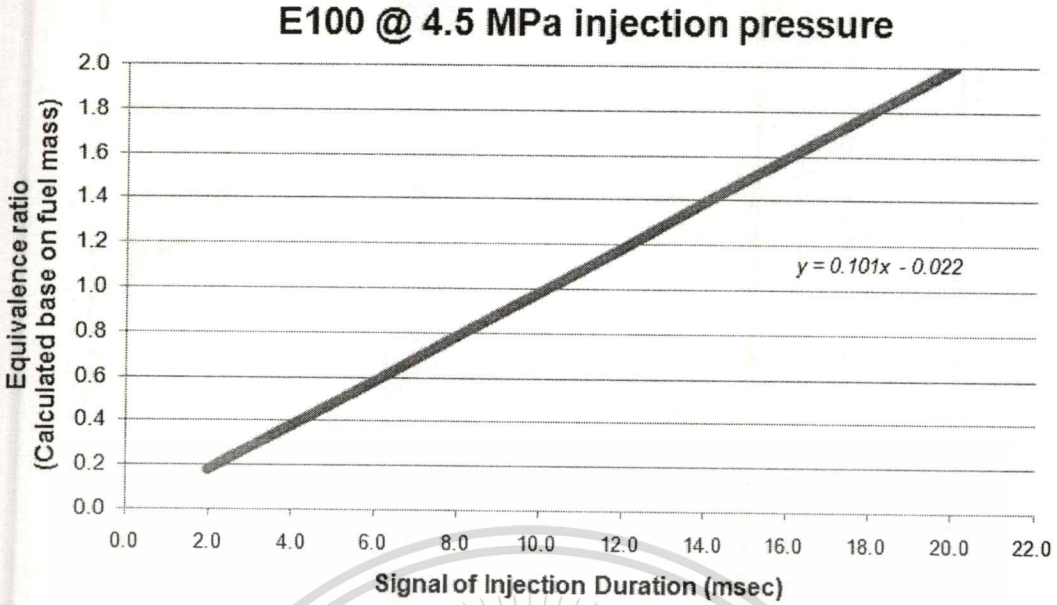

Figure 3.38 Relationship between equivalence ratio of E100 and injection duration.

3.3.3 Timing sequence

First, timing of solenoid was set at 1.5 sec. for ensure that the air intake were filled in the whole chamber. After the solenoid valve closed, the swirl flow were deteriorated as shown in Figure 3.39. In this experiment the strength of swirl motion were varied by applying different pressure between fresh air induced and combustion chamber pressure.

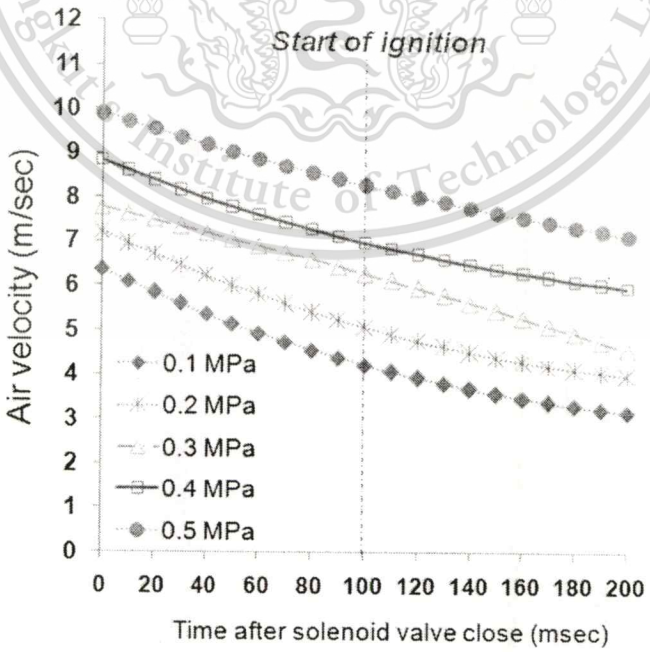

Figure 3.39 Start of ignition point set up.

After the time around 100 msec. Value of swirl velocities were consistent with air velocity at 4.2 – 8.3 m/s. At this point, the author assume as the start of ignition point. Figure 3.40 below displayed the relation timing between solenoid valve and ignition coil signals.

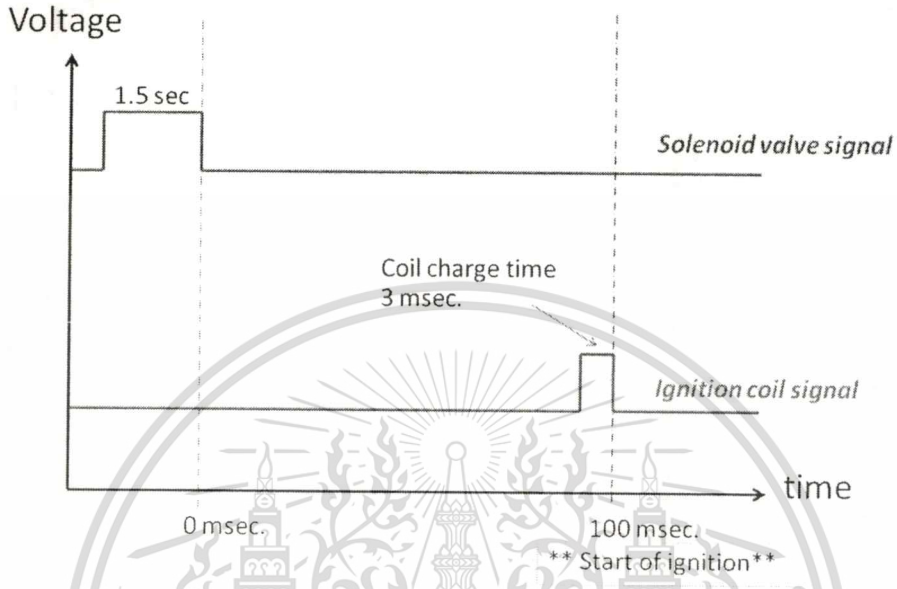

Figure 3.40 Timing of SOI, 100 msec. after solenoid valve closed.

However, In practical, The air velocity didn't measure by LDV or PIV method. But it was measured by observed the air stripes appeared in shadowgraph image of air flow that be taken by high speed video camera. Detail procedure of how to obtain air velocity values have already explained in the beginning of this part. As describe in experimental condition, injection and ignition timing was set constant through the experiment. It equal to 10 msec. Thus, duration end of injection and end of coil charge time were also fixed at 10 msec too. For clearly understand, Figure 3.41 show the signal sequence of injector and ignition coil.

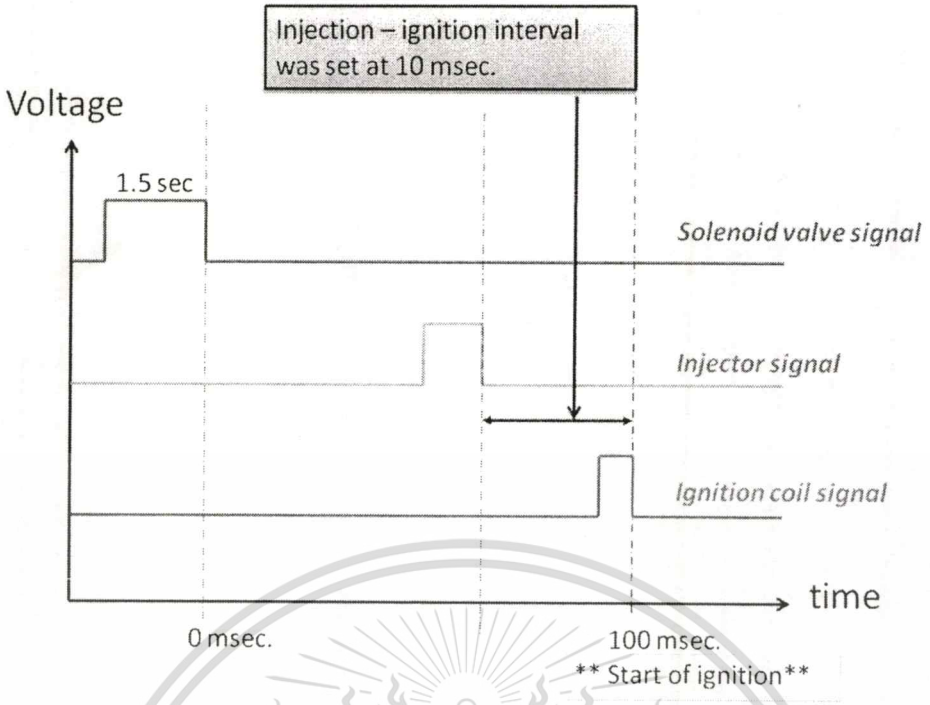

Figure 3.41 Injection – Ignition interval was set as 10 msec. (after EOI).

Injection – Ignition interval was set at 10 msec. after end of injection. This value did not come from the real engine condition. But the author wish to study effect of swirl intensity on the combustion characteristic. So, the experiment setup try to observe the mixing phenomena with different strength of swirl flow.

For conform that the mixture stratification were formed in the chamber and swirl intensities affect to this stratification, Shadowgraph images can be support to the assumption.

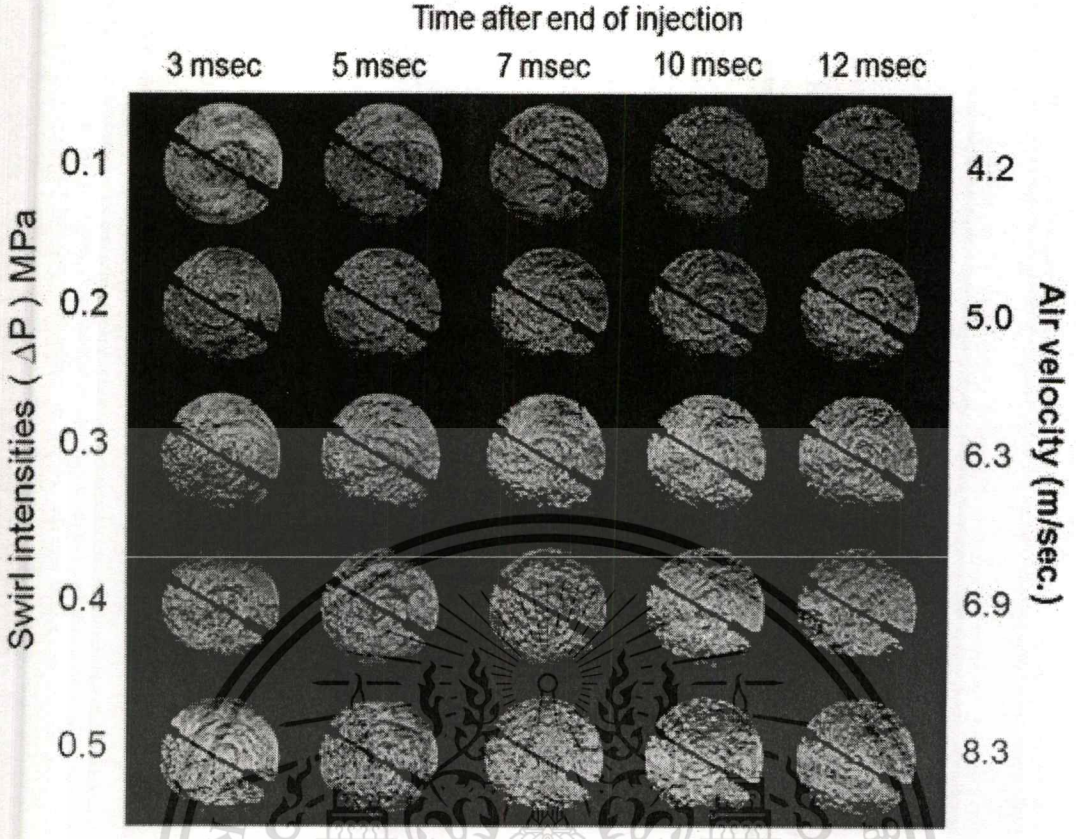

Figure 3.42 Sequence images of mixture stratification under various swirl intensities conditions.

As shown in Figure 3.42, At the 7 msec. after end of injection. We observed that the vapor mixture will be fully form whole the combustion chamber. After that, the author wait for a moment to mixture development in swirl direction. The later 3 msec. the mixture will be affected to the swirl motion. Because of this experiment was conduct on the constant volume combustion chamber. Available air was fixed. Thus, the equivalence ratio were be controlled by varying amount of fuel injected or injection duration. Consequently, start of injection were varied according to equivalence ratio while end of injection was fixed as show in Figure 3.43

However, in this experiment study, effect of mixture stratification may be ignored due to too long interval time during injection and ignition process. In this study, the start of injection (SOInj) can be varied while the end of injection (EOInj) was fixed around 10 msec before ignition start. Thus the fuel and air may be already mixed and the effect of heterogeneous mixture around the spark plug may be regarded. In general, GDi stratified engine, the interval time between the start of injection (SOInj) point and start of ignition (SOIg) is very less. Consequently, effect of mixture stratification on combustion phenomena is quite different from this study.

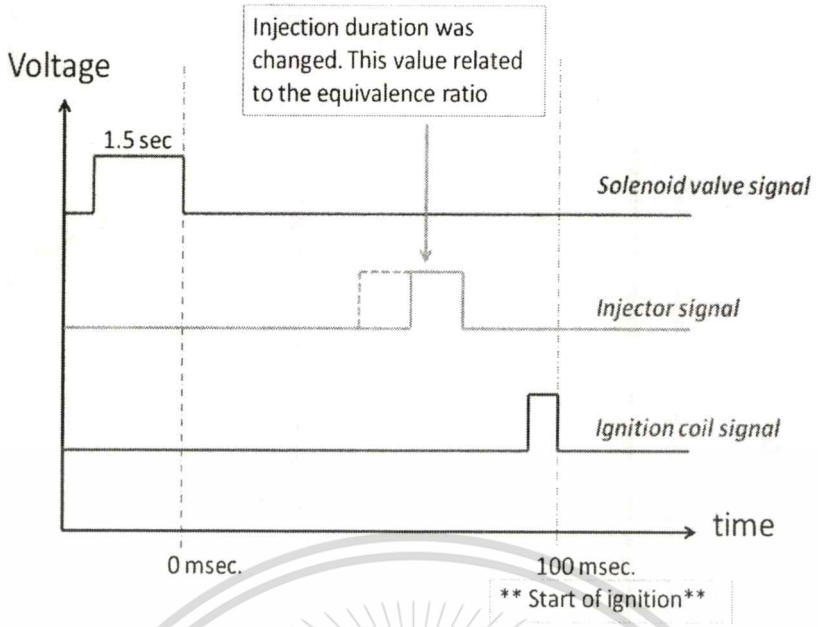

Figure 3.43 Even the injection durations were changed, the injection – ignition interval remained the same.

All of signal sequence timing were be controlled by using the interfacing software. The value of "a", "b", "c", "d" and "e" in fig.3.44 can be set in the software while parameter "x' and "y' were automatically calculated before sent to various actuator. As shown in fig... the strength for a given different pressure can be changed with setting the longer timing "b" because the air motion velocity will be deteriorated as the time left (shown in Figure 3.39) while the injection-ignition timing was controlled by setting the timing "d". The start of injection(x) was not fixed. It depends on injection duration(c) and injection-ignition interval (d). In addition, camera trigger signal was used to control the shutter timing and marking the start of ignition point from high speed video camera. The summarized of timing were also shown in the experiment condition table.

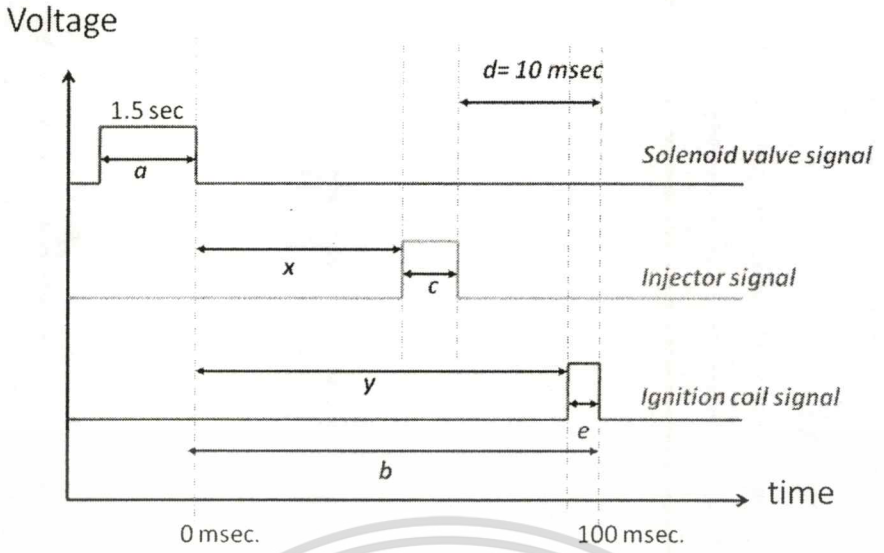

Figure 3.44 Parameters that use for controller software calculation.

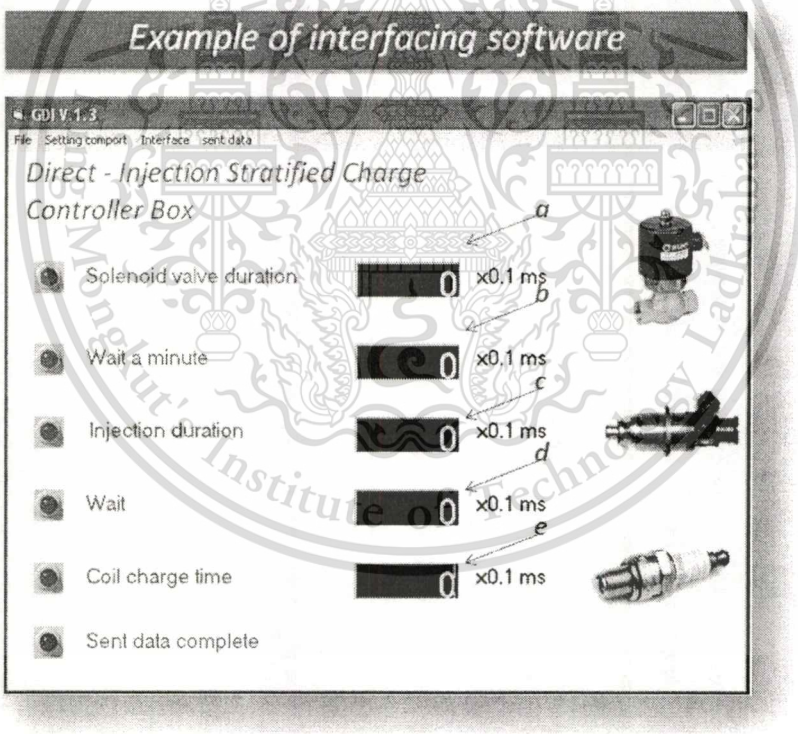

Figure 3.45 Interfacing software window that use in this experiment.

Interfacing software window and timing parameter were illustrated in Figure 3.45

3.3.4 Shadowgraph and Schlieren photography technique with high speed video camera

In this part, detail of setting the high speed video camera were be explained into two part, First, camera setting for flame propagation and another one was the camera setting for visualization of the spray and mixture formation.

For the flam propagation visualization, the resolution was more important than that of the resolution, thus, frame rate of recording was set at 6000 fps and shutter speed were constant as 1/10000 second. Limitation of using high value of speed shutter is the Schlieren image was pre-filtered by a knife edge. Thus, the object images were darken compare with the shadowgraph images.In addition, all of flame propagation images were recorded with 512x512 pixel resolution. For obtained the accuracy of flame edge which is response to the density gradient, Schlieren photography were used to gain this propose. Triggering mode was set to "center trigger", video camera were record the images of flame propagation before received the trigger signal for 352 frames and 352 frames after triggering. The total duration time of recording was equal to 117.333 second.

In spray and mixture formation observation, the camera setting has a little bit different from flame propagation visualization setting. In this practical, the resolution and detail of image were very important. Hence, shutter speed in this experiment was set at 1/60000 second for clearly specific the vapor spray movement and their formations. In addition, Schlieren photography technique was not necessary for this application. Thus, The author prefer to visualize the fuel spray and mixture stratification by Shadowgraph technique rather than Schlieren due to the detail of spray in vapor and liquid phase images can be clearly observed by using more light, and the knife edge was not necessary to filter any scattering light anymore. Other setting such as frame rate, resolution and triggering mode were also the same as setting in flame visualization. However, with higher shutter speed, the buffering capacity (4 GB) to collected spray image were dropped to 50.167 second. Even this recording time was less than the flame propagation observation, the camera can be collected all of event during spray and mixture formation.

3.3.5 Lean limit investigation

As known, the important thing in stratified charge combustion is the stability of the flame. Misfire will occur if the mixture and condition are not suitable to ignite. Overall lean mixture have an opportunity to deteriorate the combustion stability. Due to differences in fuel properties, lean limit of each fuel should be investigated.

Lean limit was the leanest air-fuel mixture that will sustain flame propagation. When relating air-fuel ratio to cylinder pressure or exhaust gas content as the air-fuel ratio increases from stoichiometric, a point is reached where variations increase sharply, approximately the lean misfire limit. The statistic data analysis was chosen in this experiment to investigate the proper lean limit or minimum equivalence ratio that mixture can be ignited at certain pressure and temperature. Variation of peak pressure and area under the pressure versus crank angle curve has been found to be the most sensitive parameter which describes where combustion changes occur. In this study, lean limit was defined as the minimum equivalence ratio that reached the maximum acceptable value of coefficient of variation on peak pressure. For clearly understanding, Figure 3.46 shows the definition of lean limit that use in this study. In this figure, the data of 20 cycles of each condition were collected for investigate the lean limit and maximum acceptable value of CoV was 20% of CoV [10].

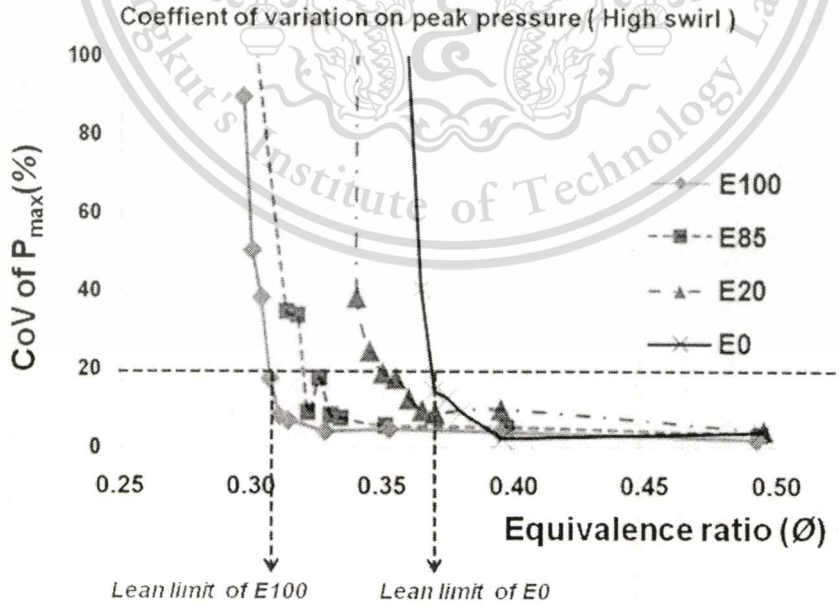

Figure 3.46 Lean limit definition, E0 and E100, based on CoV data.

3.3.6 Mass fraction burn and combustion duration

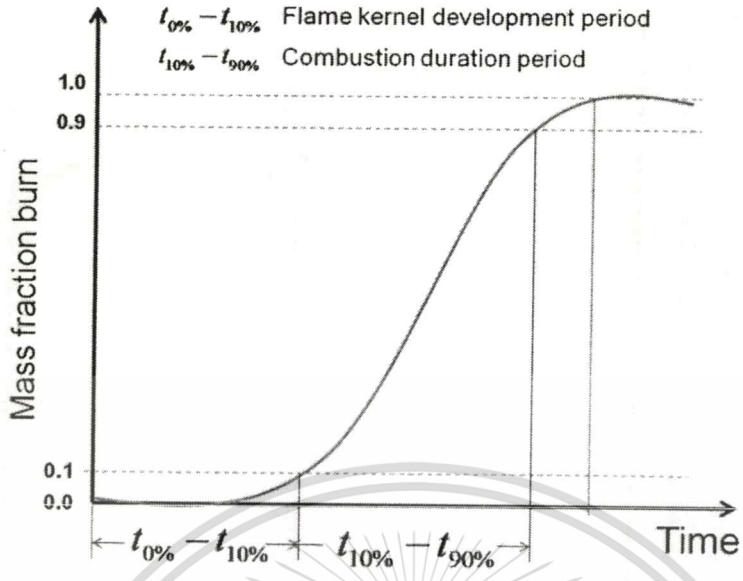

Figure 3.47 Combustion duration defined as 0.1 to 0.9 of mass fraction burned.

Mass burned fraction was calculated based on the pressure data obtained from the experimental results as follows [9].

$$M_f(t) = \frac{P(t) - P_i}{P_{\max} - P_i} \tag{29}$$

Where $P(t)$ is the combustion pressure, P_i is the initial mixture pressure, and P_{max} is the maximum combustion pressure.

If the mixture gas is fully burned when it reaches peak combustion pressure, it can be calculated according to the relative value of the combustion pressure. It is noted that M10 stands for 10 percent combustion and M100 stands for 100 percent combustion [9]. Figure 3.47 shows the definition of combustion duration, which is expressed from 10% mass fraction burn to 90% mass fraction burn [10].

3.3.7 Relation between rate of pressure rise and heat released rate

Due to combustion analysis in constant volume combustion chamber was based on the pressure history data that collect from the high-resolution pressure transducer. Thus, rate of heat release cannot be relatively calculated with the crank angle as same as in the real engine. And also the stratification degree. For applying the Thermodynamics, rate of heat release and stratification degree, can be expressed in term of pressure rise rate $\left(\frac{dP}{dt}\right)$. The relationship between rate of heat release

(ROHR) and pressure rise rate $\left(\frac{dP}{dt}\right)$ was derived from principal of ideal gas law and Thermodynamics as shown equation 5 -9 [10, 11]. This estimation formula is base on assumption that combustion duration is very short.

From the first law of thermodynamics.

$$\text{Heat supply rate} = \text{Heat release rate} + \text{Heat transfer} \tag{30}$$

Neglect the heat transfer during combustion ,The deviation for turbulent combustion by this treatment is small due to the short combustion. Nevertheless, The rate of heat release (ROHR) shown in this thesis might be different from the result of real engine condition which is included the heat transfer or the heat losses term.

$$\text{Heat release rate} = \text{Heat supply rate} \tag{31}$$

Finally, rate of heat release in CVCC (ROHR) can be shown as following equation.

$$\left(\frac{dQ}{dt}\right)_{\text{release}} = \left(\frac{V}{k-1}\right)\frac{dP}{dt} \tag{32}$$

Consequently, if the volume was fixed at constant and specific heat ratio was not change significantly, The rate of heat release can be reflected by the information of rate of pressure rise. In this experimental result, the author try to display only the result of pressure rise rate. For heat release rate, it didn't calculated yet due to lack of specific heat ratio data. However, from the derived equation , it can imply that the heat release rate can explained by pressure rise rate data because these parameters strongly related to each other.

3.3.8 Operation flow

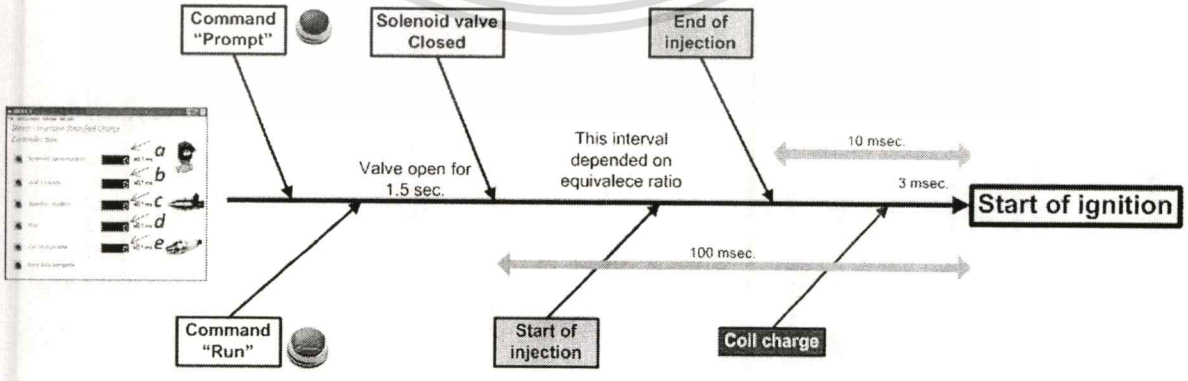

Figure 3.48 Operation flow diagram, Controlled by self-building software.

Summarized of procedure process were described in this section. Figure 3.48 show the process flow diagram of experimental procedure. First, fresh air charge from

the air compressor will be regulated according to swirl intensity by pressure regulator, and then the solenoid valves were allowed to open and closed at certain timing (1.5 second). Second, high pressure fuel will be directly injected to the constant volume combustion chamber. Amount of fuel injected and also its duration were adjusted according to each required air/fuel ratio. After that, ignition coil will be energized for a spark energy at the tip of electrode to initiate the flame kernel. In addition, camera trigger signal was used to control the shutter timing and marking the start of ignition point from high speed video camera.

Chapter 4

Results and Discussions

4.1 Effect of ethanol content on combustion parameters.

4.1.1 Combustion pressure against time after ignition start

Comparison results of effect of ethanol concentration on combustion parameters were investigated in stoichiometric condition. Swirl intensity, ΔP = 0.3 MPa, that conform to real engine condition at low load, air velocity was approximately 6.3 m/s.

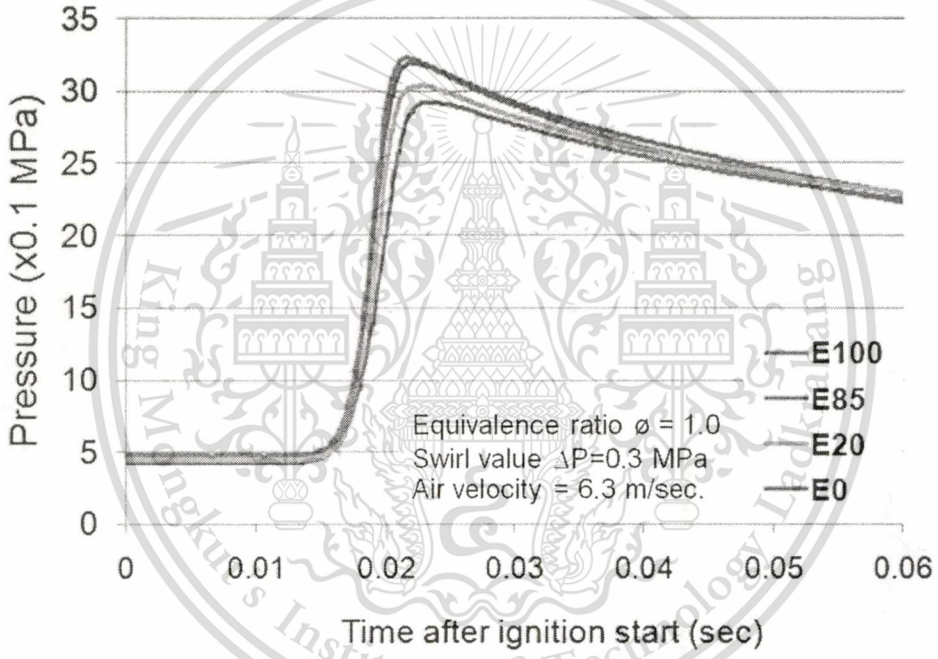

Figure 4.1 Pressure history data of E0, E20, E85 and E100 (ϕ=1.0, Swirl intensity ΔP = 0.3 MPa).

Figure 4.1 shows the effect of the ethanol content on the combustion pressure at medium swirl intensity (ΔP=0.3MPa). As indicated this figure, the maximum pressure appears in pure ethanol (E100) at 3.24 MPa while E85, E20 and pure gasoline (E0) maximum pressure were shown at 3.23 MPa, 3.07 MPa and 2.96 MPa, respectively.

Even though this study the results were compared at the same equivalence ratio. In combustion pressure analysis, energy input, amount of fuel injected cannot

be neglect. Therefore, figure 4.2 shows the energy supply per a kilogram of air at the same equivalence ratio.

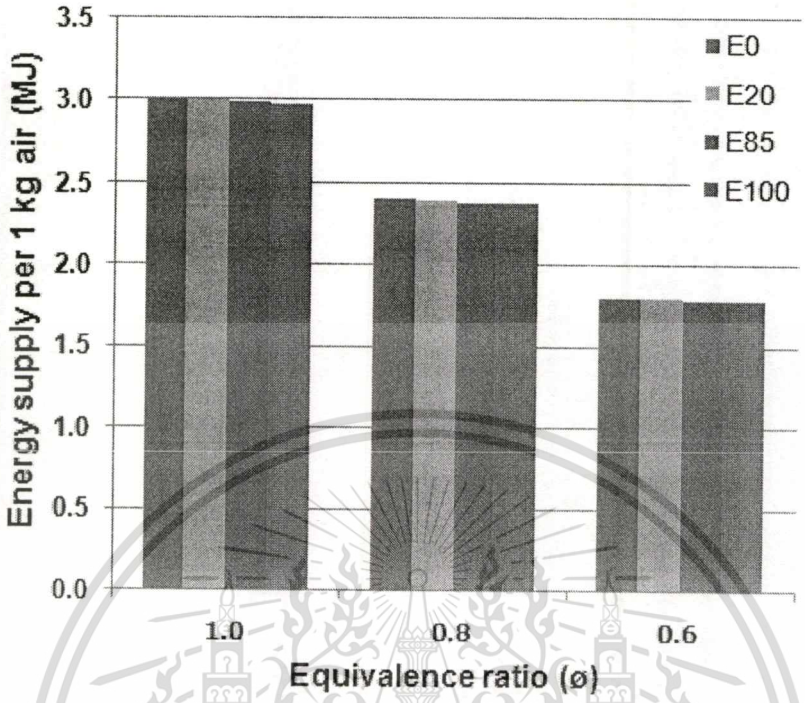

Figure 4.2 Energy supply per 1 kg of available air.

Even through E20, E85 and E100 has less LHV than that of E0 (Gasoline) However, air to fuel ratio of each tested fuel are different as shown in Table 5-6, Thus, in case of E20, E85 and E100, additional fuel injected were required for maintain the same equivalence ratio of E0. Amount of fuel that need to be added for E20, E85 and E100 are 8.24% , 48.15% and 62.01%, respectively.

From the fuel properties table shown in table 5, if available air is fixed at 1 kg, amount of fuel that required for $\emptyset$=1.0 are 68 g, 74 g, 101 g and 110 g in case of E0, E20, E85 and E100, respectively. Total energy input which ware calculated by the multiplication value of fuel mass and LHV of each fuel are 3.01 MJ, 3.01 MJ, 2.99 MJ and 2.98 MJ in case of E0, E20, E85 and E100, respectively.

The comparison of energy supply in term of energy required per a kilogram of air was illustrated in fig 4.2 The values of energy supply were calculated based on lower heating value of each tested fuel required at specific equivalence ratio.

As indicated in fig 4.2 energy input of E0, E20, E85 and E100 were not significant different. However, in high ethanol concentration fuel, energy input tend to be less as increasing percentage of ethanol. For example, in equivalence ratio

equal to 1.0 (ϕ =1.0) condition, energy supply per a kilogram of air of E0, E20, E85 and E100 were 3.01 MJ, 3.01 MJ, 2.99 MJ and 2.98 MJ, respectively.

From these result, figure 4.1, despite the fact that lower ethanol blend, E0 and E20 have an higher energy input as indicated in fig 4.2 the peak value of combustion pressure decreases with decreasing ethanol content in the mixture. Also, the length of time required to reach the maximum value of the combustion pressure is retarded in accordance with the decrease of ethanol percentage. These can imply that when utilizing the ethanol blend fuel, oxygen concentration of each fuel might be different and it might be effect to the combustion process in term of oxidizing performance. High oxygenated fuels such as E100 and E85 have more capability to oxidize with oxygen more than E20 or pure gasoline (E0) which was lack of oxygen concentration of fuel.

4.1.2 Rate of pressure rise

The rate of pressure rise is a very important parameter because this closely relates to heat release rate as described in previous section. Nevertheless, characteristics of $\frac{dP}{dt}$ appeared in this study might be different from the real engine tested result, ROHR, due to $\frac{dP}{dt}$ shown in this thesis was derived from the assumption that heat loss or heat transfer is very less and can be ignored. The effects of ethanol content on the rate of pressure rise were illustrated in fig. 4.3. The peak value of the pressure rise rate was rapidly increased and its timing was shortening at high percentage of ethanol. E20 had not significantly changed in maximum pressure rise rate compared to pure gasoline (E0). However, it can release heat earlier than that of the E0. If consider at the same equivalence ratio, the heat input was not significant changed when changing type of fuel. This demonstrates that ethanol content may accelerate the combustion period and reduce time of heat loss in early stage of the combustion regardless to the amount of energy supply.

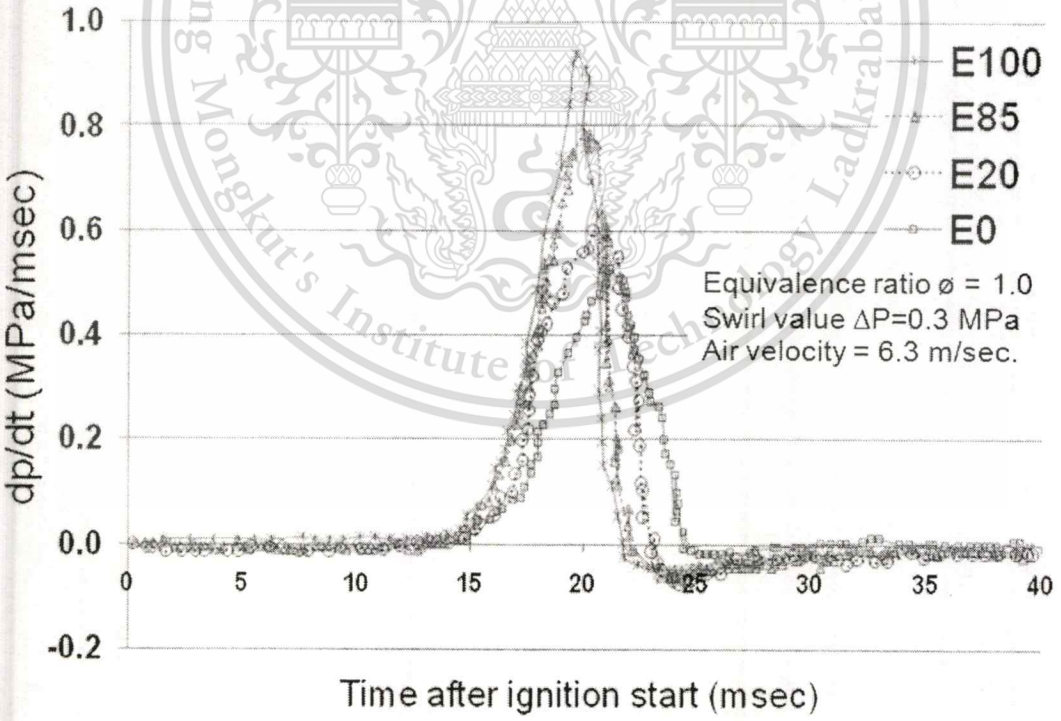

Figure 4.3 Pressure rise rate of various ethanol/gasoline blend fuels.

As shown in fuel properties table, heating value of E20, E85 and E100 are less than E0 but the amount of fuel injected need to be more for maintain the corrected equivalence ratio. However, oxygen content might be different. Fuel properties table

noted that the E0 has 0.0% of oxygen content while E20, E85 and E100, oxygen content were 7.54%, 31.75% and 34.7%, respectively. Consequently, from the results of energy release rate that address as dp/dt in this experiment study, effect of ethanol concentration on pressure rise rate can be discussed as the same manner as in pressure history result, oxygen content within fuel itself can enhance oxidation performance during combustion process.

Table 6 : Fuel properties table.

Fuel	E0	E20	E85	E100
Formula	($C_{8.26}H_{15.5}$)	-	-	(C_2H_5OH)
molecular weight	114.18	88.12	50.60	46.07
Ethanol content (% vol)	0.0	19.9	78.9	100.0
Carbon content (%wt)	84.9	79.85	55.36	52.2
Hydrogen content (%wt)	15.1	12.88	12.89	13.0
Oxygen content (% wt)	0.0	7.54	31.75	34.7
LHV (MJ/kg)	44.0	40.6	29.5	26.9
Air/fuel ratio	14.63	13.51	9.87	9.03
Benzene content (% Vol)	-	2.14	0.24	-
Aromatic content (% Vol)	-	30.3	6.2	-
Heat of vaporization (kJ/kg)	305	-	-	840
RVP (kPa)	58.4	59.0	44.4	16.0
Specific gravity	0.72-0.78	0.7604	0.7830	0.8
RON	92.0-98.0	98.3	101.6	107.0
MON	80.0-90.0	84.6	91.1	89.0

4.1.3 Mass fraction burn rate and combustion duration.

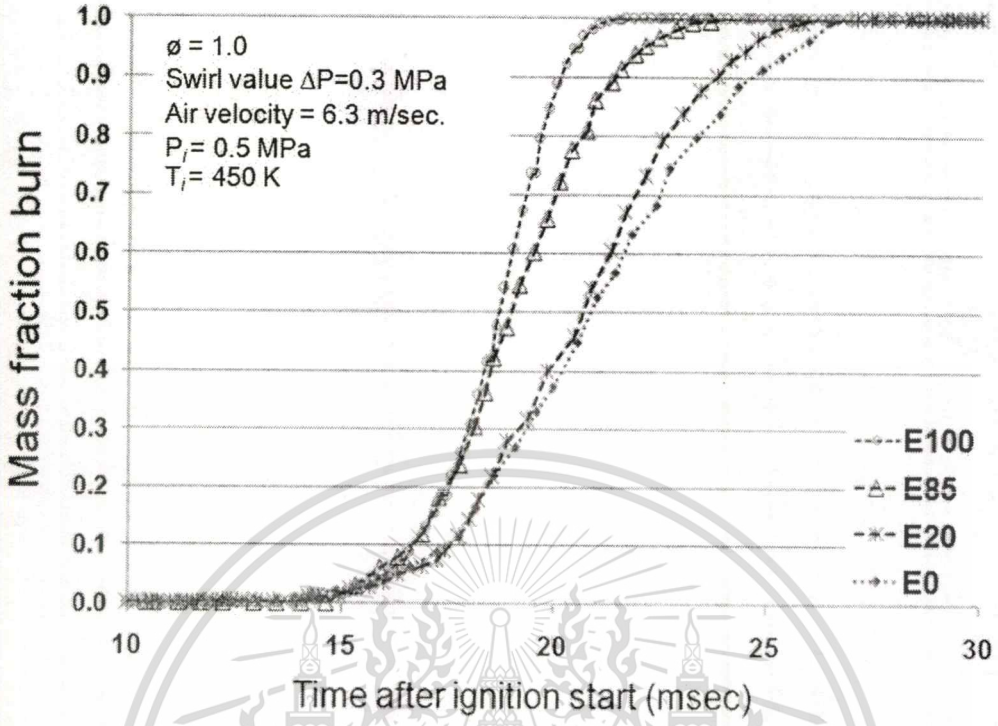

Figure 4.4 Mass fraction burn of various ethanol/gasoline blends

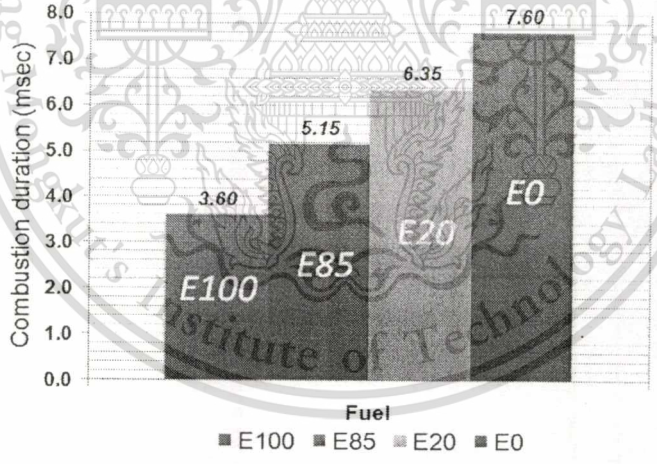

Figure 4.5 Combustion duration at ϕ =1.0, swirl intensity ΔP = 0.3 MPa (6.3 m/sec).

From quantitative analysis, combustion duration may be taken into account by using mass fraction burn rate data. From the mass fraction burned, flame development period and combustion duration are defined as the duration period of 10% and 90 % mass fraction burned respectively. Figure 4.4 and figure 4.5 show the results of mass fraction burn rate and combustion durations of various ethanol-gasoline blended fuels at medium swirl condition (ΔP= 0.3 MPa) in stoichiomatric mode (ϕ =1.0). As indicated in fig. 4.4 - 4.5, the combustion periods were to be shortened and accelerated by high concentration of ethanol in blend fuel. The

combustion duration were 3.6 msec., 5.2 msec., 6.4 msec., and 7.6 msec. in case of E100 (pure ethanol), E85, E20 and E0, respectively.

The mass fraction burn rate results show that E0 and E20 have an closely trend especially in 0.1-0.5 of mass fraction burn. 18.5 -21.0 msec. after ignition start. After that, E20 trend to burn faster than that of pure gasoline. In the same way, E100 and E85, combustion period, especially in 0.1 -0.4 of mass fraction burn, show very closely trend while this period occurs at 17.0 -18.5 msec. after ignition start. From these results, it demonstrates that high ethanol content may accelerate the beginning of combustion period and reduce time of heat loss in early stage of the combustion. Furthermore, after approximately 0.5 of mass fraction burn, slopes of mass fraction burn which were correlated to burn rate tend to be increased as increasing the ethanol content. Comparison results of flame development were shown in fig.4.6 for comprehensive observation.

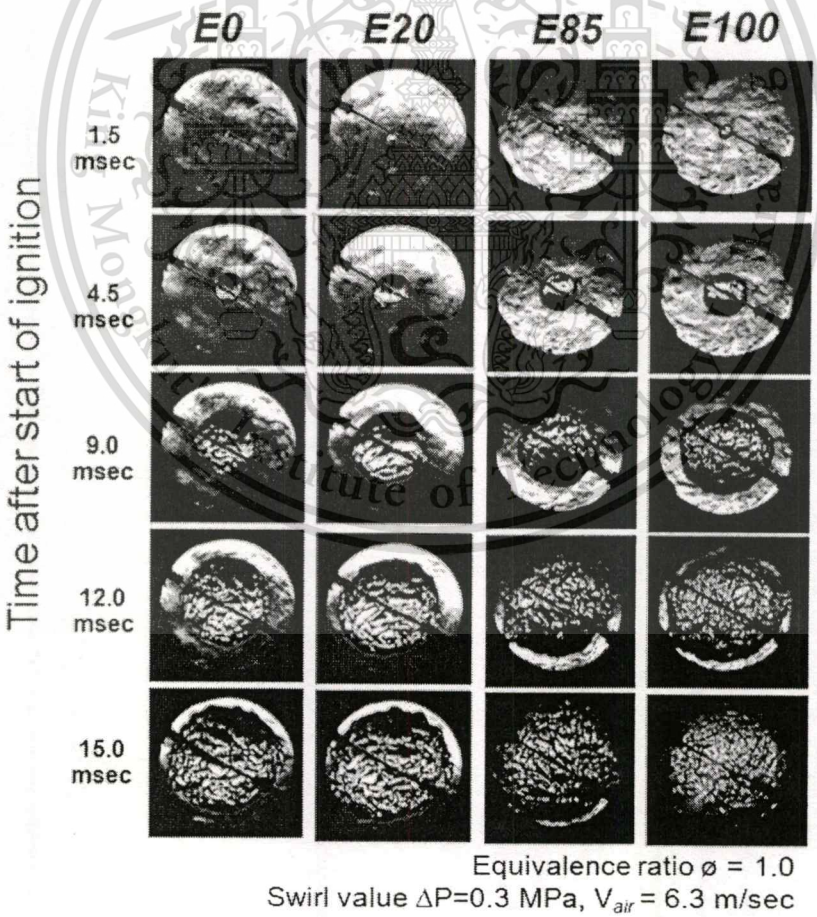

Figure 4.6 Schlieren images of gasoline/ethanol blend and ethanol fuel during flame kernal development process.

This results were the Schlieren images of flame propagation that taken with high speed video camera. All of fuel were tested at stratified condition, swirl intensity was set at 0.3 MPa of different pressure and operate under stoichiometric condition (ϕ =1.0). Flame propagation images just show only flame kernel development process. It was not cover whole combustion process. As shown in fig 4.6, flame development of ethanol fuel showed the fastest rate compare with lower ethanol concentration.

It is well known that the flame speed was related to the air/fuel ratio and mixture has the highest flame speed at equivalence ratio equal to one (ϕ =1.0). From these results, mass fraction burn, combustion duration and flame propagation, it can imply that utilizing ethanol blended fuel can make the stoichiometric in the wider area compare with the pure gasoline (E0). Because blended fuel such as E20, E85 and E100 required more fuel injected and can be completely vaporized easier than conventional gasoline. Consequently, ethanol blended fuel have more change to join the stoichiometric mixture in wider area. In addition,the fuel properties, especially the oxygen content, can affect to the flame speed in term of increasing performance of reaction rate. With increasing the ethanol concentration in the fuel, oxygen content will be also increased as shown in fuel properties table. Due to the ethanol blended fuel (E100, E85 and E20) have more oxygenated properties than the pure gasoline. Thus, flame speeds that were depended on oxidation rate were also increased.

In general, during combustion process, it has many radical reactions, elementary steps, before reactant change into product gas. In each step, the reaction have a specific activation energy (E_a) but the lowest one of each activation energy is defined as the "Rate determining step ($E_{a\text{-min}}$)", the slowest step in a chemical reaction.

Rate determining step ($E_{a\text{-min}}$) of E100, activation energy may less value than E0 due to OH radical is contained within fuel itself. The OH radical is also easily to react with another molecules or species by low E_a. Thus, OH molecules in E100 can lead the faster in reaction rate compare with E0 which isn't containing any OH molecule. Furthermore, E0, it has a large number of aromatic rings than E100. These aromatic content are more difficulty to react with another molecules such as oxygen. Therefore, E_a of rate determining step in E0 is very high. Result in reaction rate of

gasoline fuel is slower than ethanol blend fuel that has less aromatic content and more OH radical. This explanation can be also discussed for the result of mass fraction burn.

Fortunately, it has some investigation for estimate the reaction rate of hydrocarbon in single step. The global model of single step reaction that list in following equation are come from Westbrook and Dryer [24]. This model is very useful for engineering approximations.

$$C_xH_y + (x + \frac{y}{4})O_2 \longrightarrow xCO_2 + (\frac{y}{2})H_2O$$
$$\frac{d[C_xH_y]}{dt} = -Ae^{(-\frac{E_a}{R_uT})}[C_xH_y]^m[O_2]^n \quad (33)$$

For the detail of parameter that use in that equation are listed in table below.

Fuel	Pre-exponential Factor, A^a	Activation Temperature, E_a/R_u (K)	m	n
CH_4	$1.3 \cdot 10^8$	24,358[b]	−0.3	1.3
CH_4	$8.3 \cdot 10^5$	15,098[c]	−0.3	1.3
C_2H_6	$1.1 \cdot 10^{12}$	15,098	0.1	1.65
C_3H_8	$8.6 \cdot 10^{11}$	15,098	0.1	1.65
C_4H_{10}	$7.4 \cdot 10^{11}$	15,098	0.15	1.6
C_5H_{12}	$6.4 \cdot 10^{11}$	15,098	0.25	1.5
C_6H_{14}	$5.7 \cdot 10^{11}$	15,098	0.25	1.5
C_7H_{16}	$5.1 \cdot 10^{11}$	15,098	0.25	1.5
C_8H_{18}	$4.6 \cdot 10^{11}$	15,098	0.25	1.5
C_8H_{18}	$7.2 \cdot 10^{12}$	20,131[d]	0.25	1.5
C_9H_{20}	$4.2 \cdot 10^{11}$	15,098	0.25	1.5
$C_{10}H_{22}$	$3.8 \cdot 10^{11}$	15,098	0.25	1.5
CH_3OH	$3.2 \cdot 10^{12}$	15,098	0.25	1.5
C_2H_5OH	$1.5 \cdot 10^{12}$	15,098	0.15	1.6
C_6H_6	$2.0 \cdot 10^{11}$	15,098	−0.1	1.85
C_7H_8	$1.6 \cdot 10^{11}$	15,098	−0.1	1.85
C_2H_4	$2.0 \cdot 10^{12}$	15,098	0.1	1.65
C_3H_6	$4.2 \cdot 10^{11}$	15,098	−0.1	1.85
C_2H_2	$6.5 \cdot 10^{12}$	15,098	0.5	1.25

[a] Units of A are consistent with concentrations in Eqn. 5.2 expressed in units of gmol/cm^3, i.e., A[=] (gmol/cm^3)$^{1-m-n}$/s.

[b] E_a = 48.4 kcal/gmol.

[c] E_a = 30 kcal/gmol.

[d] E_a = 40 kcal/gmol.

From calculation, reaction rate, reduction rate of hydrocarbon ($\frac{d[C_xH_y]}{dt}$) of E100 or pure ethanol is higher than gasoline (E0). $\frac{d[C_2H_5)OH]}{dt}$ and $\frac{d[C_8H_{18})]}{dt}$ are 0.00148 s^{-1} and 0.000583 s^{-1}, respectively. For the detail of calculation, please see in following figure.

$$C_8H_{18} + (12.5)O_2 \longrightarrow 8CO_2 + 9H_2O$$

$$M_{fuel} = (1)[(8\times12)+(1\times18)] = 114$$

$$M_{O_2} = 12.5[2\times16] = 400$$

$$M_{total} = 514$$

$$[C_8H_{18}] = \frac{114}{514} = 0.22 \qquad [O_2] = \frac{400}{514} = 0.78$$

$$A = 4.6\times10^{11}\ gmol/cm^3 - s \qquad T = 450\ K$$

$$\frac{E_a}{R_u} = 15{,}098\ K \qquad m = 0.25$$

$$n = 1.5$$

$$-\frac{d[C_8H_{18}]}{dt} = (4.6\times10^{11})\, e^{(-\frac{15{,}098}{450})}[0.22]^{0.25}[0.78]^{1.5}$$

$$-\frac{d[C_8H_{18}]}{dt} = 0.000583$$

$$C_2H_5OH + (2)O_2 \longrightarrow 2CO_2 + 3H_2O$$

$$M_{fuel} = (1)[(2\times12)+(6\times1)+(1\times16)] = 46$$

$$M_{O_2} = 2[2\times16] = 64$$

$$M_{total} = 110$$

$$[C_2H_5OH] = \frac{46}{110} = 0.42 \qquad [O_2] = \frac{64}{110} = 0.58$$

$$A = 1.5\times10^{12}\ gmol/cm^3 - s \qquad T = 450\ K$$

$$\frac{E_a}{R_u} = 15{,}098\ K \qquad m = 0.15$$

$$n = 1.6$$

$$-\frac{d[C_2H_5OH]}{dt} = (1.5\times10^{12})\, e^{(-\frac{15{,}098}{450})}[0.42]^{0.15}[0.58]^{1.6}$$

$$-\frac{d[C_2H_5OH]}{dt} = 0.00148$$

Figure 4. 7 Reaction calculation, Isooctane and Ethanol.

In equation 33, pre-exponential factor A is the total number of collisions (leading to a reaction or not) per second, $e^{(-\frac{E_a}{R_uT})}$ is the probability that any given collision will result in a reaction, m and n are reaction order of C_xH_y and O_2 respectively. From these definitions, it can imply that physical properties, number of collision, of fuel is the majority parameter affected to the different in reaction rate. Because of pre-exponential factor A of E100 and isooctane quite different while $e^{(-\frac{E_a}{R_uT})}$, probability, is equal the same. Moreover, Even through m factor of E100 is less than isooctane but the mass concentration, $[C_2H_5OH]$, is higher than isooctane. Consequently, concentration and reaction order, $[C_xH_y]^m[O_2]^n$, of isooctane and ethanol are not different significantly.

The reason why E100 or ethanol has more collision number than isooctane may be discussed that E100 has a smaller size in molecule, Thus, in finite volume,

smaller molecules may have opportunity to react with another around itself more than the larger size in molecules.

4.2 Effect of ethanol content and swirl intensity on lean limit.

4.2.1 Coefficient of variation (CoV) results

Coefficient of variation on peak pressure (CoV_{Pmax}) of each tested fuels were plotted against the equivalence ratio (Ø) as show in fig 4.8. For study effect of swirl intensities on CoV, each chart was show the comparison data in different swirl intensities, they were vary from the lowest swirl intensity (ΔP=0.1 MPa) to the highest swirl intensity (ΔP=0.5 MPa). Initial temperature was 450 K and initial pressure was also constant at 0.5 MPa before ignition start.

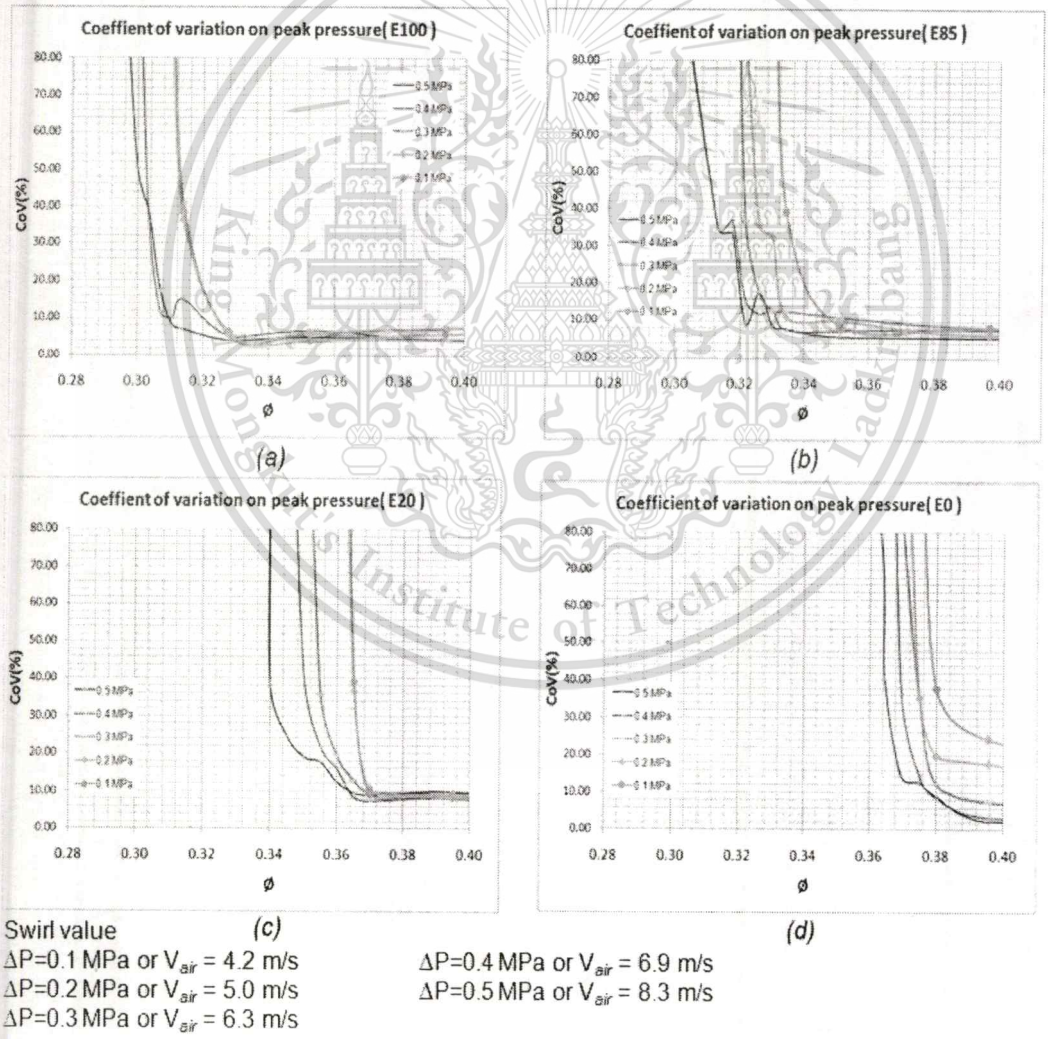

Figure 4.8 Coefficient of variation (CoV) on peak pressure compare with different swirl intensities (a) CoV of E100, (b) CoV of E85, (c) CoV of E20 and (d) CoV of E0.

Figure 4.8 (a) show coefficient of variation on peak pressure of pure ethanol fuel or E100, As indicated in this figure, CoV become less as increase a swirl intensity at specific equivalence ratio. For the given equivalence ratio ϕ =0.32, the CoV of ethanol fuel (E100) were 18.0%, 18.0%, 17.5%, 10.0% and 5.0% at swirl intensity equal to ΔP=0.1 MPa, 0.2MPa, 0.3 MPa, 0.4 MPa and the highest swirl flow ΔP=0.5 MPa, respectively. Influence of swirl flow on CoV data occur in E85, E20, and E100 show the same trend as show in E100 results. However, appropriate equivalence ratio that the mixture can be make the stable combustion (low CoV) even the swirl flow were changed can be found at $\phi > 0.345$ for E100, $\phi > 0.36$ for E85, $\phi > 0.37$ for E20 and $\phi > 0.6$ for E0. Furthermore, addition observation, minimum equivalence ratio that the mixture can be ignited within 20% of CoV can be extended by applying the swirl flow.

4.2.2 Lean limit results.

According to lean limit definition, the maximum set point of (CoV_{Pmax}) that assume as the lean misfire limit was 20% of CoV [10, 22]. At this point, the fuels reach the minimum equivalence ratio that can be ignited and be defined as lean limit point. From the data of CoV lean misfire limit of various blend in deferent swirl condition can be plot as shown in fig 4.9.

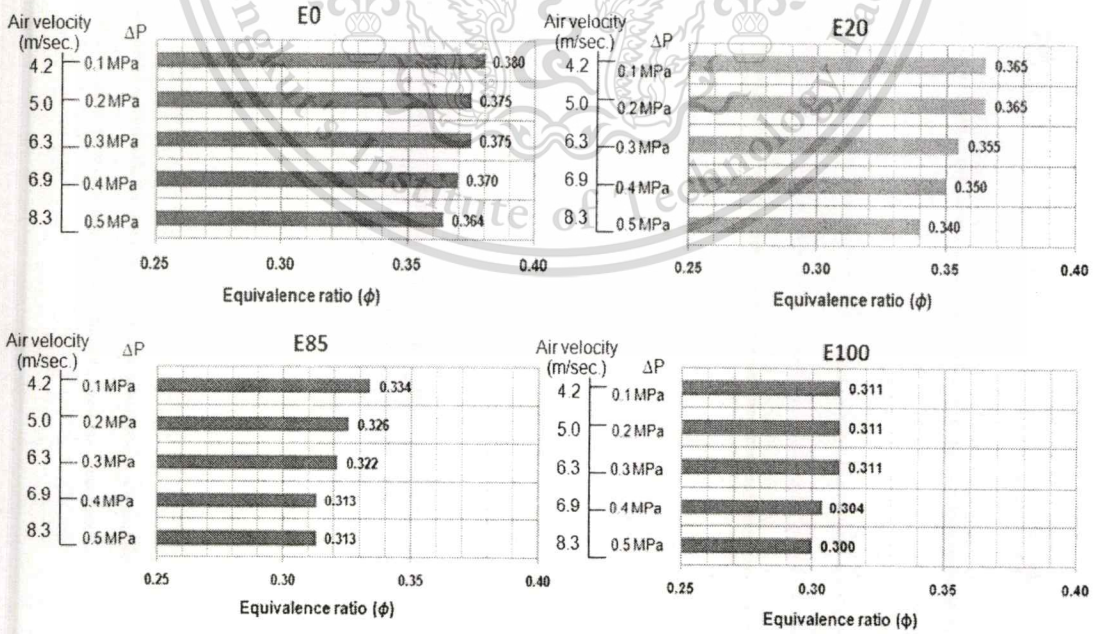

Figure 4.9 lean limit of various blend plot with different swirl intensities.

As illustrated in fig 4.9, E0, lean limit point occur at equivalence ratio (ϕ) equal to 0.38 in the lowest swirl condition (ΔP = 0.1 MPa), whereas, ΔP = 0.2 MPa,

ΔP = 0.3 MPa, ΔP = 0.4 MPa and ΔP = 0.5 MPa, lean limit of E0 are 0.375, 0.375, 0.370 and 0.364, respectively. Similarity results, effect of swirl flow, can be found in E20, E85 and E100 also. As increase the swirl intensity, mixtures have an ability to ignite at lower equivalence ratio. From the results, it can imply that swirl intensity can improve stability of combustion by extending the lean limit range under lean condition. The importance parameter that affect to these phenomena might be the mixture distribution which was strongly affected to the swirl strength. Even in this experiment study, mixture distribution and velocity flow field were not observed by any laser diagnosis technique such as LIF or LDV. Shadowgraph images of mixture spray can show the significant different in stratification mixture during mixture formation process. As show in fig.4.10, ethanol fuel (E100) images show the influence of swirl flow on mixture stratification. These demonstrate that swirl intensity can support the combustion stability in the lean condition by extending the lean limit range. Even though, lean limit of pure ethanol couldn't change with swirl flow. These phenomena may be discussed that atomization and vaporization of fuel was accelerated by the increase of the turbulence intensity and the decrease of the impinged fuel, both of which were caused by the swirling flow. These can imply that swirl flow can enhance the stratification level and this consequent can extend the lean limit range. Further support results also show in Tomita's study [22] that attached in Appendix section.

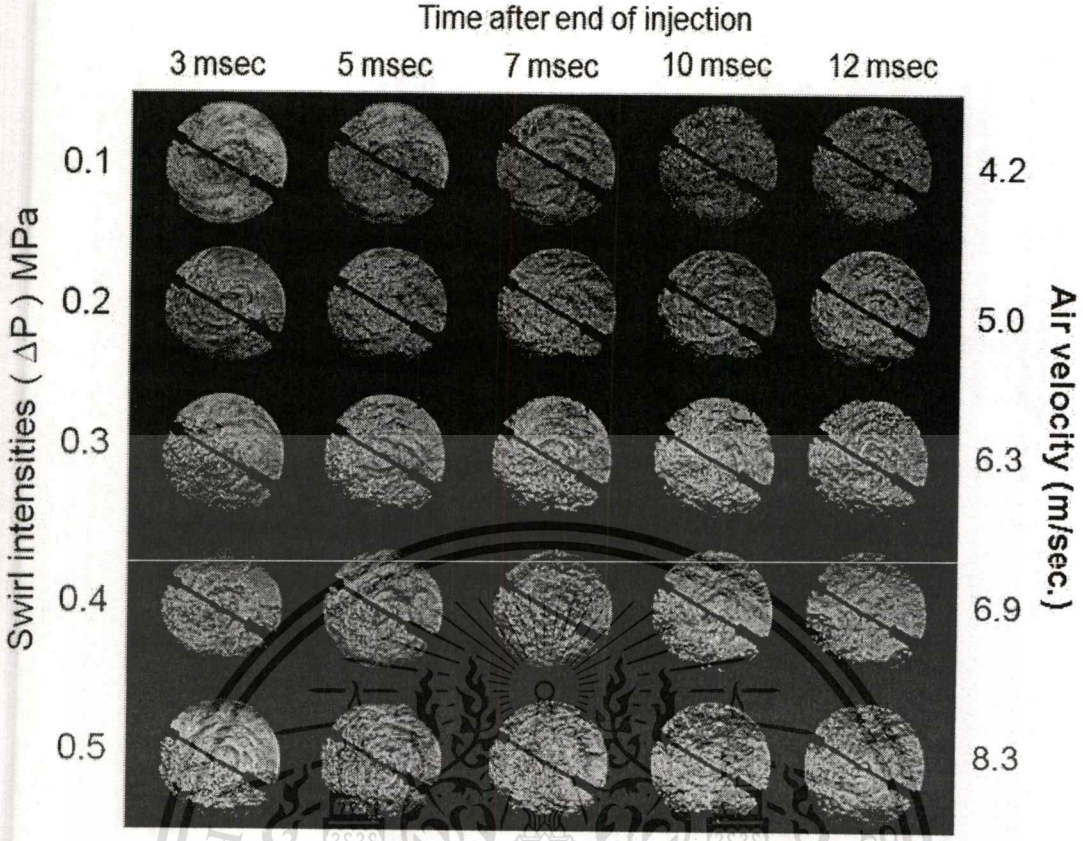

Figure 4.10 Shadowgraph images show the mixture stratification of E100 when applying different swirl conditions.

For an effect of ethanol concentration on lean limit, the results were summarized for clearly compared and shown in fig.4.11.

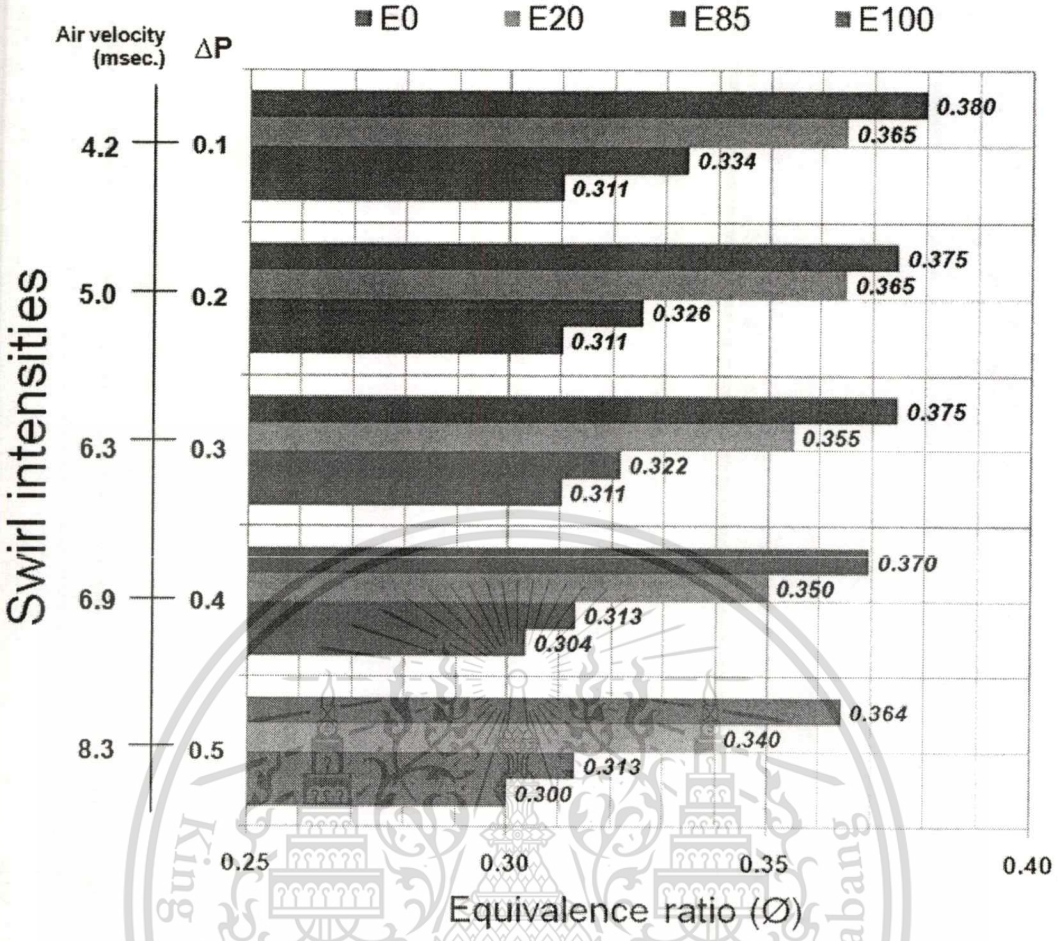

Figure 4.11 Lean limit of various gasoline/ethanol blends – Summarized.

For an given swirl intensity condition, when apply the highest swirl flow, E0, E20, E85 and E100 reached the minimum equivalence ratio at 0.364, 0.34, 0.313 and 0.30 respectively. In the lowest swirl flow condition, E0, E20, E85 and E100 have the lean limit at ϕ = 0.38, ϕ = 0.365, ϕ = 0.334 and ϕ = 0.311, respectively.

However, E100, lean limit was not significant change when applying the swirl intensity. As illustrated in fig 4.9 and fig 4.11, lean limit of E100 were ϕ = 0.31, ϕ = 0.31, ϕ = 0.31, ϕ = 0.304 and ϕ = 0.300 at swirl condition of ΔP = 0.1, ΔP = 0.2, ΔP = 0.3, ΔP = 0.4 and ΔP = 0.5 MPa, respectively. The result shows little change in minimum equivalence ratio since higher percentage of the ethanol has less effect to enhance lean limit range than the lower ethanol content. This behavior can be discussed that ethanol can be ignited and combusted at the lower equivalence ratio because an air/fuel ratio of gasoline and ethanol/gasoline blends are different. Thus, if ethanol/gasoline blends are subjected to the same equivalence ratio as in the pure gasoline, additional amount of the fuel is required for the same equivalence ratio

and get more chance to form stoichiometric mixture in wider area compare with lower ethanol concentration fuels. In other word, ethanol fuel, which is comprised of only one component, has lower carbon atom than the gasoline or E20 and E85. Consequently, it may be diffused by swirl flow easier than the gasoline, E20 or E85 which are comprised of various higher carbon atoms regardless to RVP properties [22]. As ethanol can easily diffuse, vaporization of ethanol fuel may be fully completed since before the ignition start regardless of swirl generation. The comparison result of E0 and E100 spray were shown in fig. 4.12.

From the shadowgraph images, the chamber pressure was set at zero gauge pressure and temperature was 50 °C without swirl flow for clearly detail observation of spray pattern and avoid temperature gradient effect, it can be seen that E0 has start to vaporize earlier that the E100, wider spray cone and short spray penalty, but when the time left, E100 fuel was fully evaporated into vapor phase faster than that the gasoline (E0). It can imply that E0 fuel has more light and heavy fraction than ethanol fuel. Thus, the lighter components tend to be evaporated early in the beginning stage while ethanol fuel wasn't start. After the time past, heavy fraction in gasoline (E0) still remained while ethanol fuel which have only one component already completely change to the vapor phase Even though, lean limit of pure ethanol couldn't change with swirl flow. Other information that support these assumption were address in Appendix , evaporation rate of ethanol and gasoline in term of distillation curve were also noted n that section.

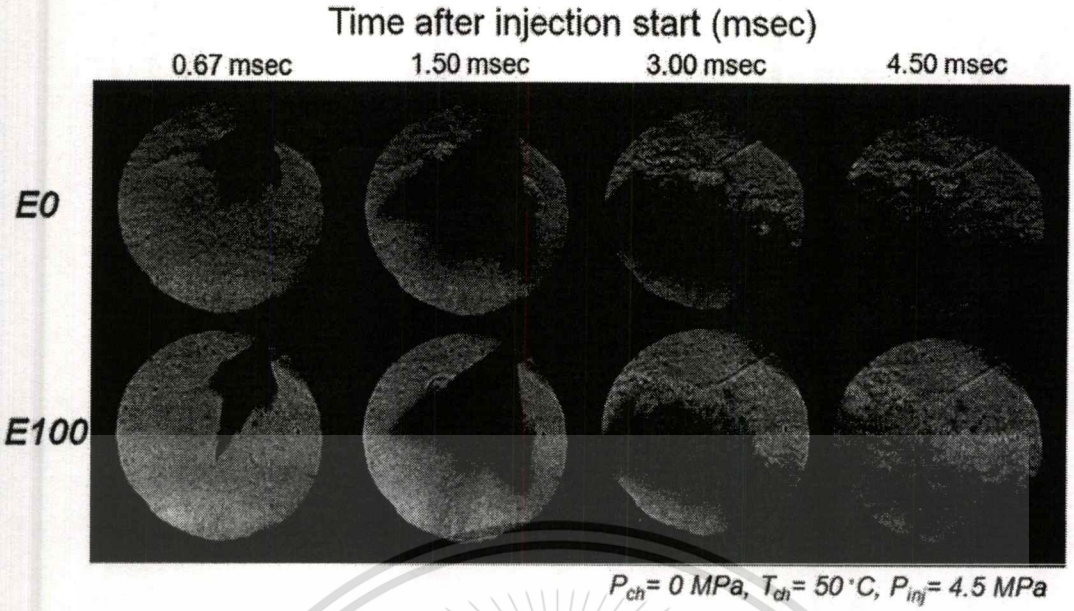

Figure 4.12 Spray images of Gasoline (E0) and Ethanol (E100) fuel.

4.3 Effect of ethanol content and swirl intensity on ignition delay.

As know that the ignition delay time was an important one of combustion parameter. It was not only indicated the time consume during mixture formation process but also it display influence to the time loss in initial stage of the combustion. Especially in spark-ignition engine, less ignition delay can lead the combustion pressure trace close to an ideal P-V diagram in Otto cycle, power stroke. Therefore, heat loss in this period can be deteriorated by reducing in ignition delay time. However, even less time use during early stage of combustion can perform good agreement for combustion behavior but the NOx emission should be taken into account.

From the pressure history data, the definition of combustion duration, injection - ignition interval and ignition delay, were shown by graphical of measured pressure data in fig 4.13. Naoki Shiraishi et al.[4] and Kihyung Lee et al [9]give the definition of injection – ignition interval as elapsed time from start of injection to start of ignition. Then, after the ignition is started, the trace pressure will be decreased until reach the minimum or rate of pressure rise equal to zero. The interval time form ignition start to this point can be defined as ignition delay. For the reason of pressure drop during process, Naoki Shiraishi et al.[4] discussed that this phenomena occurred by latent heat absorption by vaporized fuel just after fuel injection start. Since in this study, it very hard to marking the point that reach zero

slope of P-t chart., Because of lack of measuring device in high resolution condition. Definition of ignition was defined as the time after the ignition start to 10% of maximum pressure. Nevertheless, this period was also including to the initial stage of combustion and might be different to Naoki's definition.

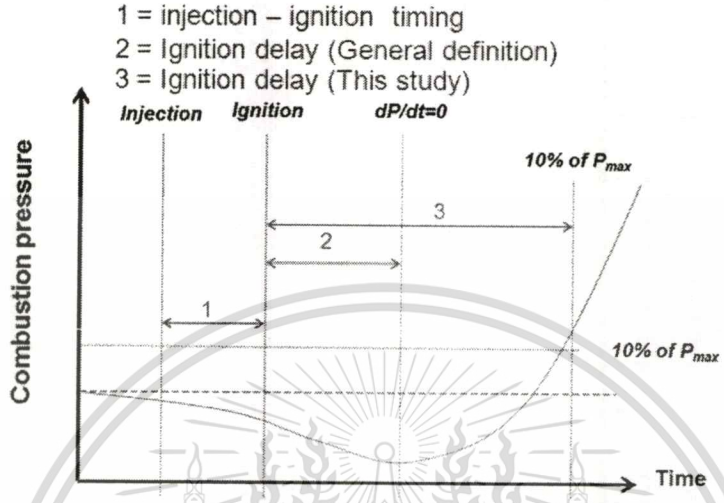

Figure 4.13 Ignition delay definition.

In this experiment, effect of ethanol concentration and swirl intensities on ignition delay were investigated by using a constant volume combustion chamber under stoichiometric condition, initial pressure was start at 0.5 MPa and initial temperature was 450 K before an ignition start. The results were indicated in fig 4.14.

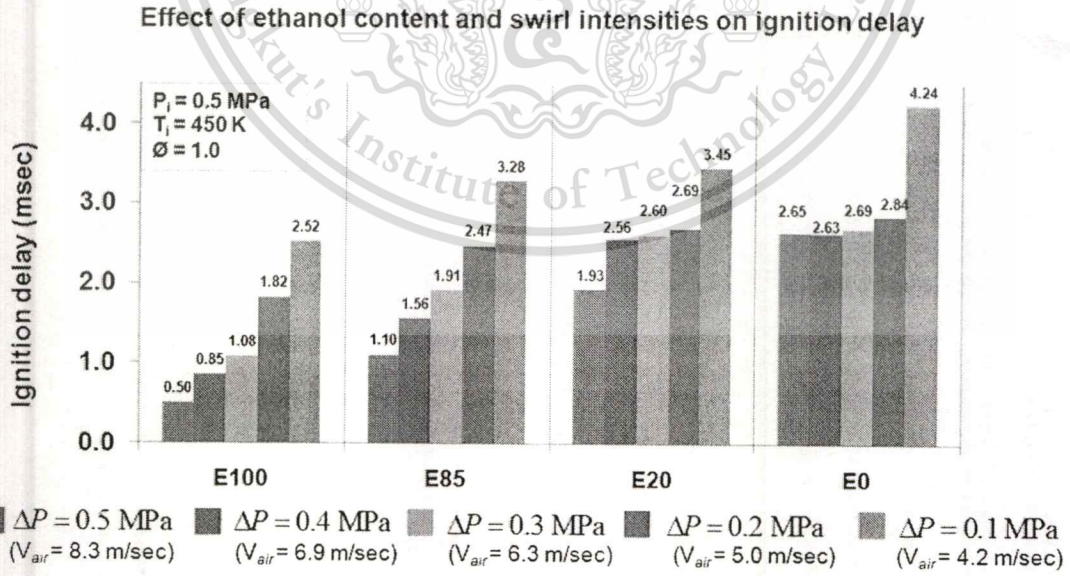

Figure 4.14 Ignition delay of various ethanol/gasoline blends at different swirl intensities.

As indicated in fig.4.14, In the highest swirl intensity, E100, comparing with other blends, ethanol fuel (E100) reach the minimum ignition delay at 0.50 msec.

while E85 ignition delay was 1.10 msec., E20 was 1.93 msec. and pure gasoline (E0) show the longest ignition delay in this swirl condition at 2.65 msec. From these results, it can imply that ignition delay time can be affected by ethanol addition in blend fuel. At an given swirl intensity, as increasing the ethanol fraction, ignition delay time become less. If consider in at the same type of fuel, E100, ignition delay was equal to 0.50 msec. at the highest swirl intensity (ΔP=0.5 MPa), when swirl intensities was reduced to 0.4 MPa, 0.3 MPa, 0.2 MPa and 0.1 MPa, ignition delay become 0.85 msec.,1.08 msec.,1.82 msec. and 2.52 msec., respectively. Hence, the swirl intensity can be considered that have an effect to the ignition delay time. These periods time can be reduced by applying higher intensities. However, result of E0, it didn't show significant change in ignition delay time when applying swirl flow since 0.2 MPa to 0.5 MPa. Even though RVP of E0 show the highest value compare with other, pure gasoline tend to be evaporated early than E100 (pure ethanol) as illustrated in spray images, fig4.12. But, in the end, ethanol fuel was completely vaporized and shifted to vapor phase faster than that of gasoline regardless to the RVP. This phenomenon can be discussed that azeotropic behavior of ethanol/gasoline blends [23] and its distillation can enhance performance in mixture vaporization process. Thus, when the ethanol was subject into base gasoline, evaporation rate was also accelerated.

In pure gasoline, evaporation rate was less, Hence when fuel was injected some of them still remain in liquid phase and didn't evaporate. Especially in spray core, this region contained with over-rich mixture. These over-rich mixture lead the mixture hard to initial an flame kernel. Thus, initial stage of combustion comsumed more time compare with each other blends. In the other hand, in E100, fuel was completely evaporated and might be affected to an swirl flow. Thus, the mixture have more chance to join form near stoichiometric mixture(ϕ =1.0) in wider area compare to E0.

It is well known that the flame propagation speed was related to the air/fuel ratio and mixture has the highest flame speed at equivalence ratio equal to one (ϕ =1.0). From the results, it can imply that utilizing ethanol blended fuel and applying swirl intensities can make the stoichiometric in the wider area compare with the pure gasoline (E0). Because blended fuel such as E20, E85 and E100 required more fuel injected and can be completely vaporized easier than conventional gasoline.

Consequently, ethanol blended fuel have more change to join the stoichiometric mixture in wider area compare with pure gasoline and these lead to reducing in time loss during initial process. Further support information explained effect of swirl on mixture distribution was observed by Tomita [18]. This study was conduct on PLIF method. For the detail, it was included in Appendix section.

Another discussion about ignition delay result may be explained by chemical properties (Heat of Vaporization, Heating Value)and physical properties (Number of molecules, Possibility) of each fuel. First, after the ignition start, E100 or ethanol fuel which has higher HOV than that of the E0 or gasoline may absorb heat during this period more than gasoline for evaporation and change phase from liquid state to gas state. Thus, pressure trace within combustion chamber is decreased. Moreover, decreasing rate of pressure data is more than that of the gasoline fuel which has the lower value of HOV also.

As describe in distillation curve, E100 is completely vaporized at the certain temperature while E0, which is comprise of many H-C chain, the evaporative rate may be less than E100 at a given temperature. Thus, some of fuel remained in liquid phase. These may be lead the small number of molecules ready to react with oxygen. In the other hand, E100, that is completely vaporized, has more quantity of molecules and also more possibility to react with oxygen. During these process (SOIg- $dP/dt = 0$), E100 may take the longer time to complete vaporize every molecules when compare with E0 or pure gasoline. The graphical illustration shown in fig.4.15 describe the pressure trace characteristics occur in CVCC during SOIg - $dP/dt = 0$ process for both in E0 and E100 (notice, A and B period).

In this figure, E0 spend less time to reach $dP/dt = 0$ point but the pressure reduction is less when compare with E100 (Ethanol0 fuel. Consequently, follow to the general definition of ignition delay, noted in A and B period, ignition delay time of E0 may be less than E100. However, in this study, ignition delay was defined as the time from SOIg to 10% of P_{max} point, thus the result displayed in this study may be shown the different characteristic.

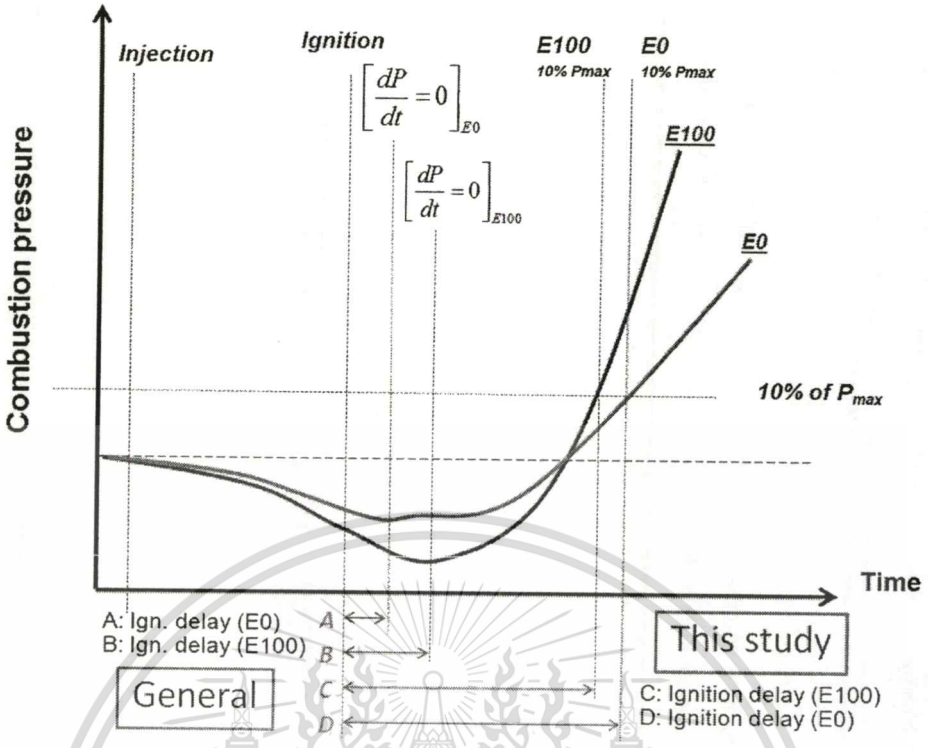

Figure 4. 15 Pressure trace characteristics during start of injection to 10% of P_{max}.

Then, after the pressure reach the minimum point, $dP/dt = 0$, E100 show the sharply increasing in combustion pressure and also pressure rise rate (dP/dt) due to the large number of molecules are ready to react with oxygen. Although lower heating value (LHV) of E100 is less than gasoline but the number H-C element and oxygen that ready to combust are greater than that of the E0. Moreover, E100 molecules that have smaller geometry than E0 will lead more possibility to react with oxygen. Therefore, the combustion pressure and energy release (dP/dt) increase rapidly and it may reach 10% of P_{max} point faster than that of E0 as shown in fig.4.15 (C and D period). As a result, the result of ignition delay shown in this study, E100 show the shortest time during this process. Conversely, E0 or gasoline show the longest time. Because in this study, ignition delay is definition quite different from general definition as describe in early section (Pgs.95-96).

4.4 Effect of ethanol content on flame kernel development.

As a result of lean limit, higher percentage of ethanol blend show the more stability by extending lean limit range. In this section, stability of flame propagations under lean condition were present by means of pressure history data characteristics and Schlieren visualization images. Experiment condition were investigated at a constant swirl condition, 0.5 MPa while equivalence ratio (ϕ) were varied from the stoichiometric condition to 0.8, and 0.6, respectively for observe flame kernel development behavior when operate under lean condition.

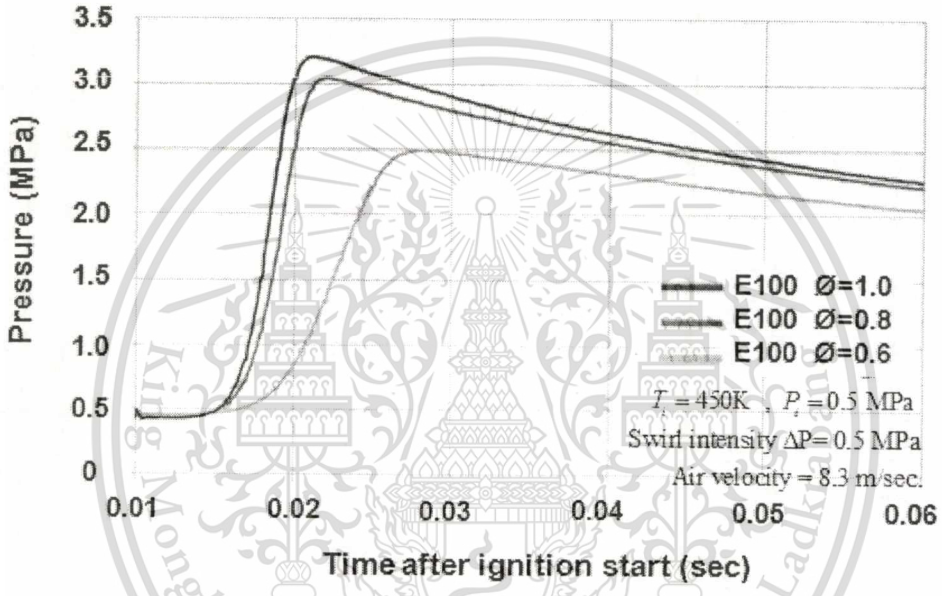

Figure 4.16 Combustion pressure trace of E100 at various equivalence ratios.

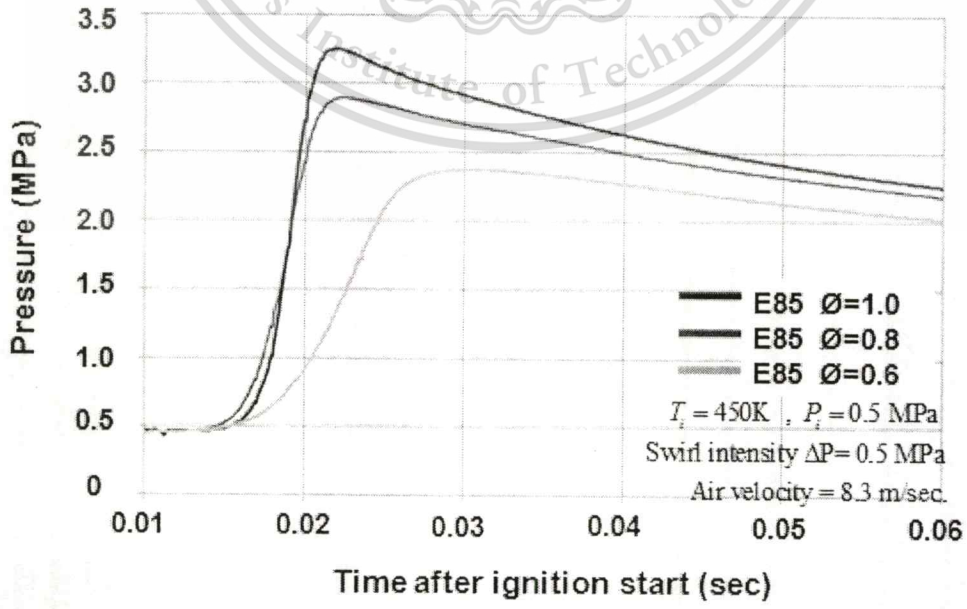

Figure 4.17 Combustion pressure trace of E85 at various equivalence ratios.

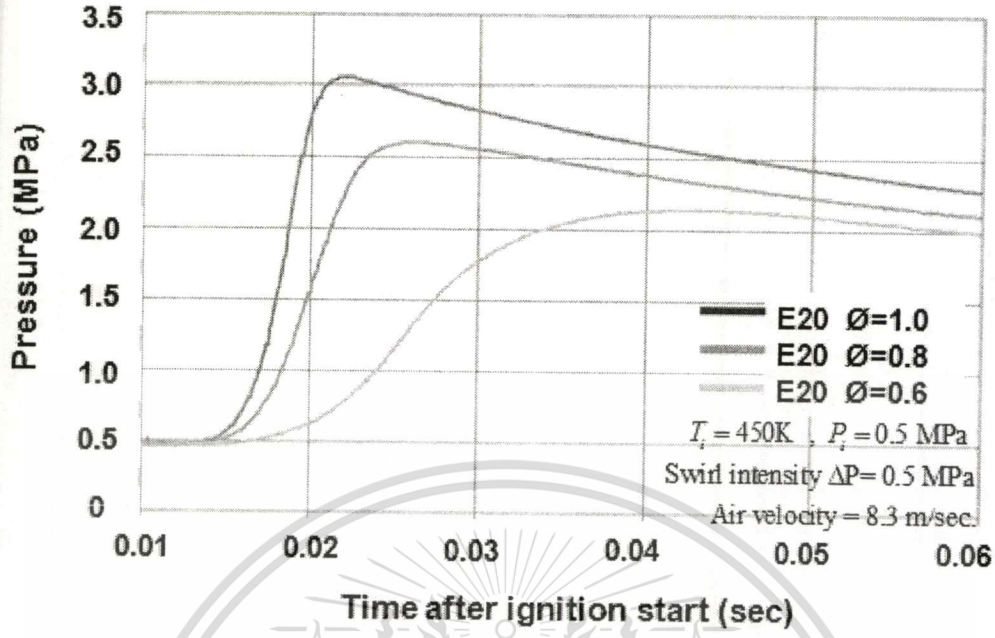

Figure 4.18 Combustion pressure trace of E20 at various equivalence ratios.

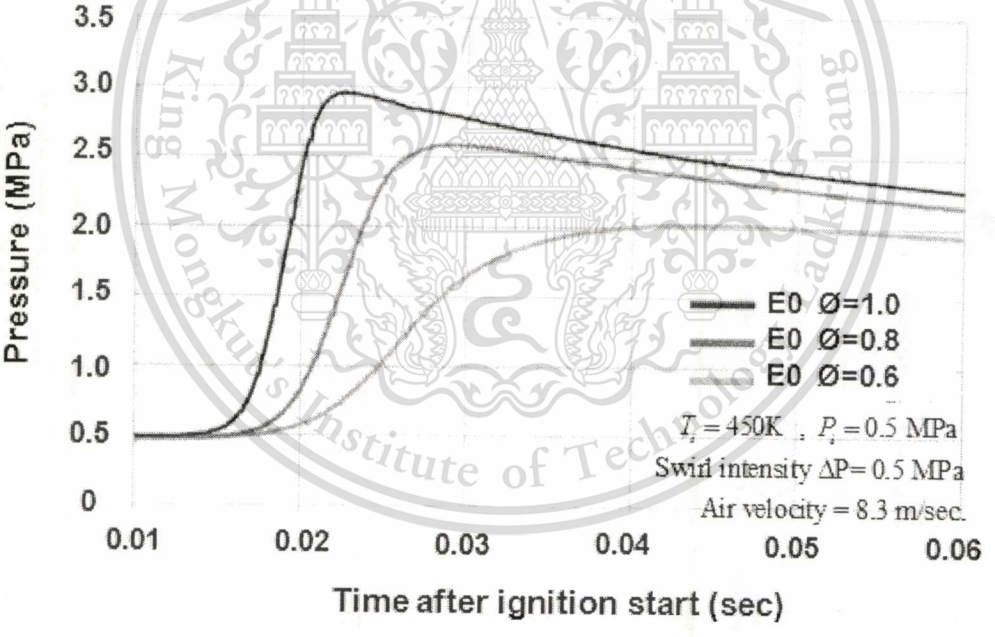

Figure 4.19 Combustion pressure trace of E0 at various equivalence ratios.

Comparing to each tested fuel, as leaner the mixture, combustion pressure also its pressure rise rate were dramatically dropped as decrease an ethanol concentration in blends. As indicated in fig.4.16-4.19, compare with stoichiometric condition, ethanol fuel (E100), peak pressure were reduced approximately 6.6% and 25.7% , when operate under ϕ =0.8 and ϕ =0.6, respectively. E85, peak pressure were reduced approximately 10.5% and 27.6% , when operate under ϕ =0.8 and ϕ =0.6,

respectively. For E20, this were reduced approximately 15.7% and 34.5% , when operate under ϕ =0.8 and ϕ =0.6, respectively.

Finally, E0, peak pressure were reduced approximately 15.5% and 32.3% , when operate under ϕ =0.8 and ϕ =0.6, respectively. These results demonstrate that lower ethanol blends fuels, especially, E20 and E0, combustion were extremely deteriorated when combust under leaner condition. In the other hand, E100 and e85, show the less value of pressure reduction. Furthermore, time to reach the peak pressure, lower ethanol content blends show the considerably longer time to reach its maximum pressure compare with high percentage of ethanol blends. As a result, it can imply that decreasing in ethanol content might make more probability in fluctuation of pressure. Form these results, it can be support to the lean limit result that stability of combustion under lean operation can be enhance by adding more ethanol concentration in base gasoline.

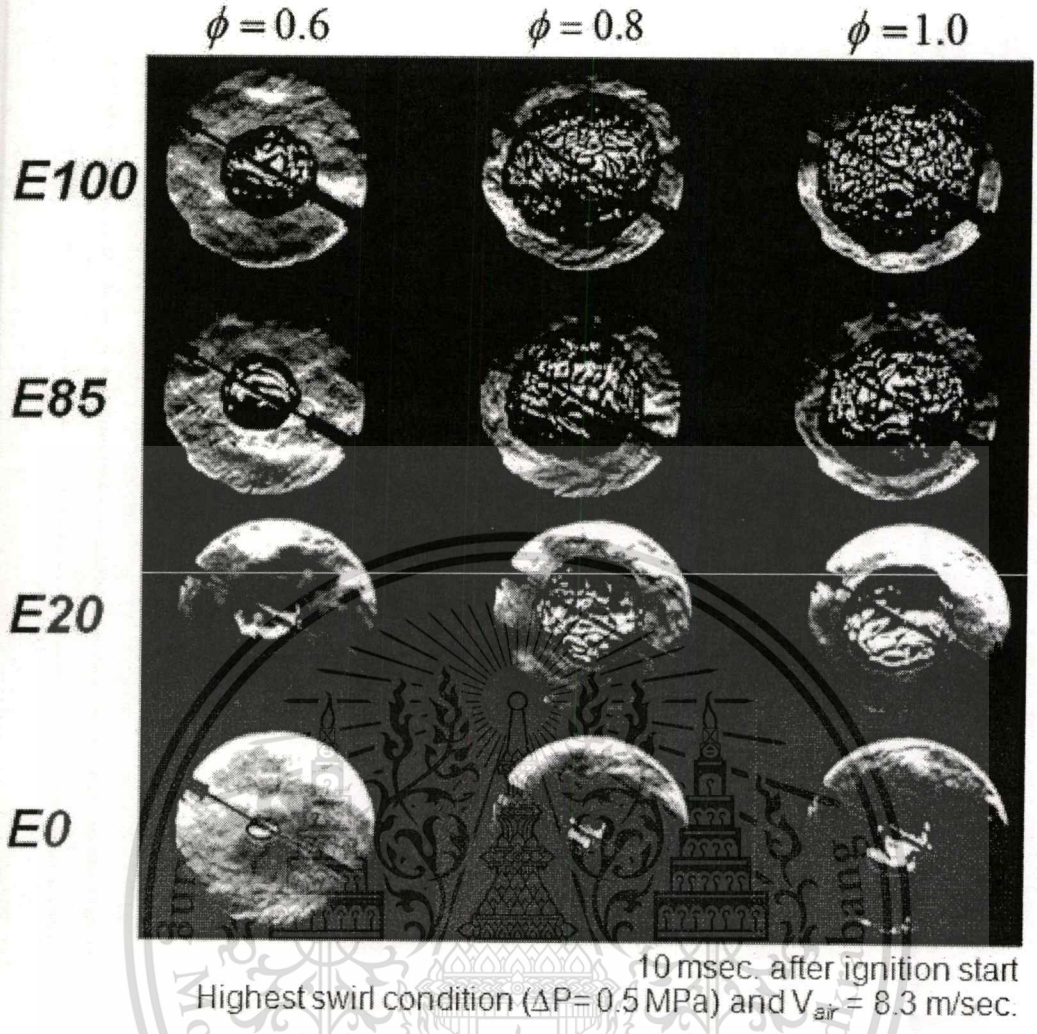

Figure 4.20 Flame kernel development images of E100, E85, E20 and E0 at various equivalence ratio.

For clearly investigation, Flame kernel developments were taken in to account by means of Schlieren photography technique. The results of flame development of each tested fuel were metaphorically shown in fig 4.20. As illustrated in this figure, as decrease the equivalence ratio or operate at leaner condition, flame kernel edge shape of all tested fuel was deteriorated .In addition, compare with E20 and E85, higher ethanol content fuel, and show more stable flame edge. However, circular expanding flame shape were found only in E100 and E85 whereas in E20 and E85 blend, flame development show the unpredictable and non-uniform shapes at all equivalence ratio. In addition, consider in flame area expansion, flame development images result show that the rate of flame development was accelerated by increasing the ethanol concentration in blended fuel. These may discussed that mixture formation capability can be improved by using ethanol fuel.

Furthermore, although ethanol fuel have higher octane number and lower RVP, oxygen content within fuel itself can enhance oxidation rate and accelerate the initial stage of combustion regardless the octane rating and RVP [22]. These comparative results of flame propagation were consistent with Hara Takashi's [15] results which report the laminar flame speed of ethanol compare with n-hapane and iso-octane. For the further information of this study, Appendix can be shown that support assumption and more discussion about flame edge stability (Lewis number). The rate of flame development may be varied with the different equivalence ratio. It can be told that rate of flame development may be influenced by energy input. Due to the equivalence ratio in this experiment was varied by changing amount of fuel injected. Thus, energy supply in each equivalence ratio conditions may be different and its consequently may also affect to the pressure data also. Nevertheless, higher ethanol percentage, especially in E100 and E85, the pressure data result show that the maximum pressure and pressure rise rate show greater value than that of lower ethanol blends, E20 and E0 even though energy supply were comparatively equal at the same equivalence ratio as shown in fig 4.2.

4.5 Effect of swirl intensity on peak pressure and flame development stability.

In combustion characteristics, one of important parameters that present the efficiency was maximum combustion pressure. For this experiment study, peak pressure data were collected by mean of high resolution pressure transducer under following condition. Initial pressure in all tested condition was set at 0.5 MPa while initial temperature was constant at 450K. In order to observe the effect of swirl on flame propagation, swirl intensities were varied from the lowest swirl condition (ΔP=0.1 MPa) to the highest swirl intensity (ΔP=0.5 MPa). Equivalence ratio were changed from stoichiometric condition (ϕ=1.0) to lean mixture condition, ϕ =0.8 and ϕ =0.6, respectively. Following results shown the results of peak pressure of blended fuel at various swirl and equivalence ration condition.

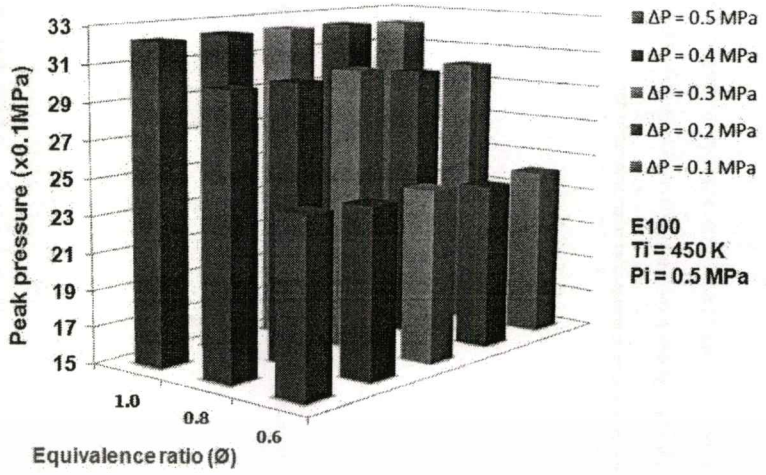

Figure 4.21 Peak pressure of E100 at various swirl and equivalence ratio condition.

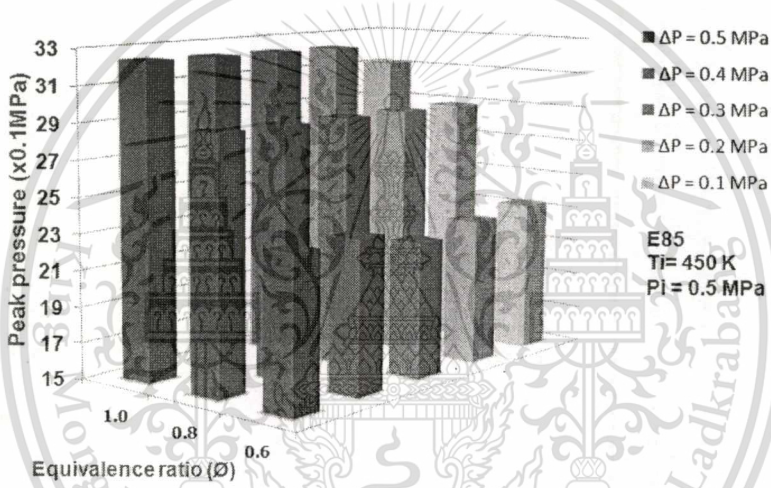

Figure 4.22 Peak pressure of E85 at various swirl and equivalence ratio condition.

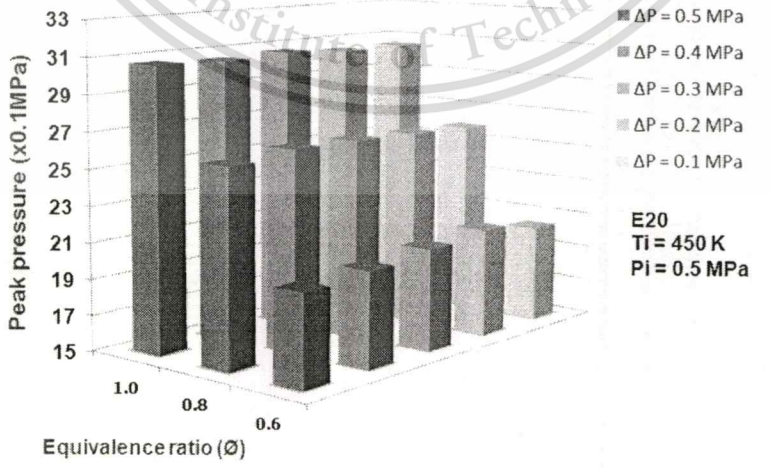

Figure 4.23 Peak pressure of E20 at various swirl and equivalence ratio condition.

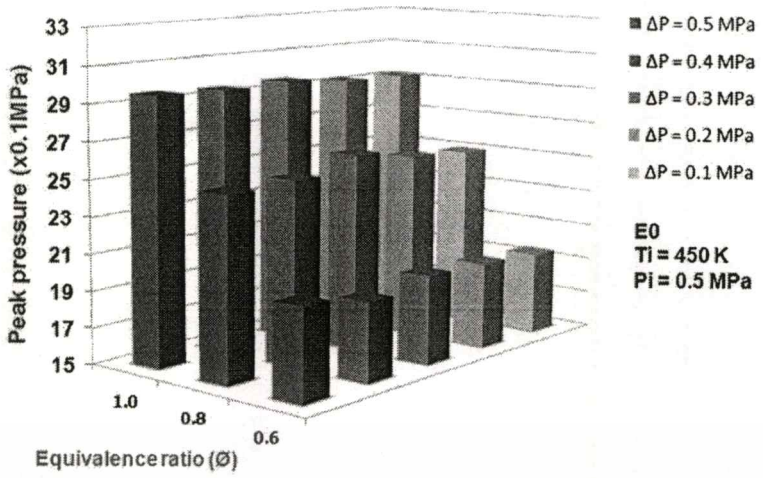

Figure 4.24 Peak pressure of E0 at various swirl and equivalence ratio condition.

As can be seen from the results of peak pressure, maximum combustion pressure occurs within a constant volume bomb rarely change when different swirl intensities were applied. In E100, fig 4.21, standard deviation of peak pressure collected from all swirl condition at ϕ=1.0, ϕ=0.8 and ϕ=0.6 were 0.067, 0.167 and 0.195, respectively. Average maximum pressure of E100 appeared at 32.32 MPa, 30.13 MPa and 24.26 MPa in condition of Ø=1.0, ϕ=0.8 and ϕ=0.6, respectively. In E85 results, fig 4.22, standard deviation of peak pressure shown at ϕ=1.0, ϕ=0.8 and ϕ=0.6 were 0.542, 0.056 and 0.395, respectively. Average maximum pressure of E85 appeared at 32.07 MPa, 28.92 MPa and 23.16 MPa in condition of ϕ=1.0, ϕ=0.8 and ϕ=0.6, respectively. For the low ethanol concentration blended, E20, fig 4.23, standard deviation of peak pressure shown at ϕ=1.0, ϕ=0.8 and ϕ=0.6 were 0.116, 0.152 and 0.343, respectively while average maximum pressure of E20 were 30.57 MPa, 26.0 MPa and 20.50 MPa in condition of ϕ=1.0, ϕ=0.8 and ϕ=0.6, respectively. Compare to pure gasoline, E0, fig 4.24, standard deviation of peak pressure shown at ϕ =1.0, ϕ =0.8 and ϕ = 0.6 were 0.183, 0.376 and 0.266, respectively. Average maximum pressure appeared at 29.40 MPa, 25.23 MPa and 19.69 MPa in condition of ϕ =1.0, ϕ =0.8 and ϕ = 0.6, respectively. These results, standard deviations, demonstrated that the swirl intensities hardly affected to the maximum pressure. However, S.D. (Standard deviation) tends to be increased as decreased the equivalence ratio in all cases, especially in E100 and E20, these may cause from the mixture operate closed to the lean limit range. Hence, variation of combustion may be increased. In addition, high percentage of ethanol fraction blended such as E100 and E85, the average maximum pressure were greater than that of E20 and E0. Thus,

from the results, it can imply that the swirl intensities can't significantly affected to the peak pressure but the ethanol concentration may increase the engine efficiency by increasing the maximum combustion pressure. Furthermore, different in peak pressure when changing the equivalence ratio may be discussed that the amount of fuel injected or ϕ directly affect to the energy release and also the peak pressure.

4.5.1 Swirl intensities and flame development stability.

From the results of peak pressure against the swirl intensities, the results show that swirl intensity hardly affect to the peak pressure. Nevertheless, the results of lean limit demonstrate that swirl intensities can enhance combustion stability by extending the lean limit range. Therefore, the assumption that swirl intensity affects to flame development stability may be taken into account and confirmed by flame visualization technique. Following results were the Schlieren images of flame propagation during flame development period.

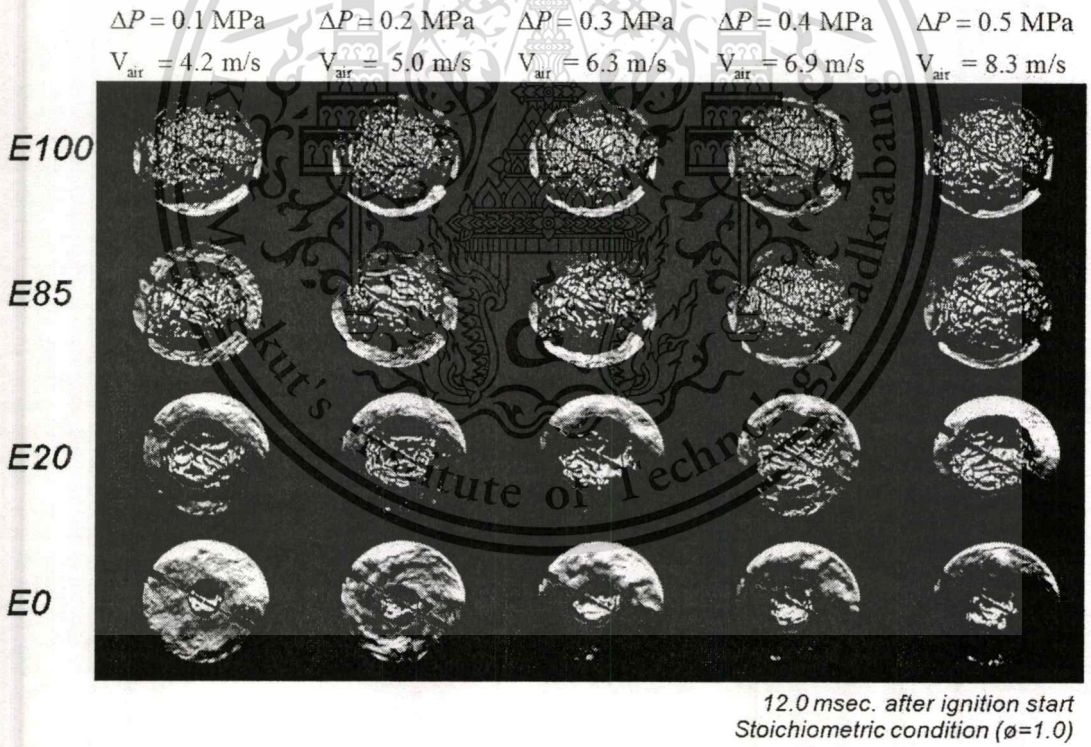

Figure 4.25 Flame propagation images at 12.0 msec. after ignition start and ϕ =1.0

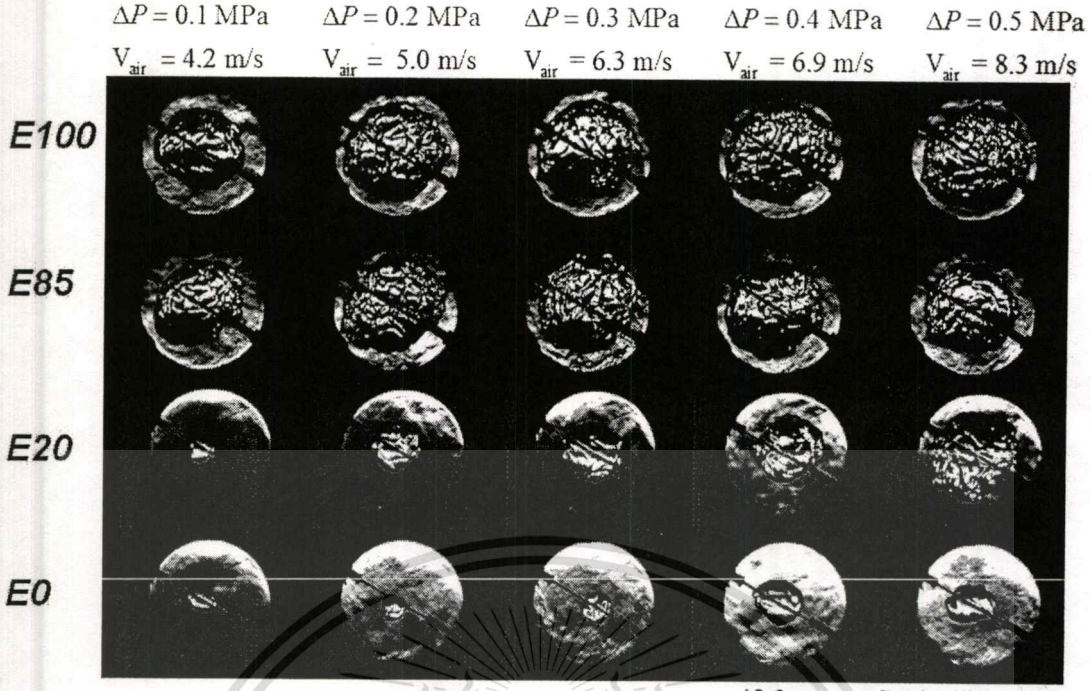

Figure 4.26 Flame propagation images at 12.0 msec. after ignition start and ϕ =0.8

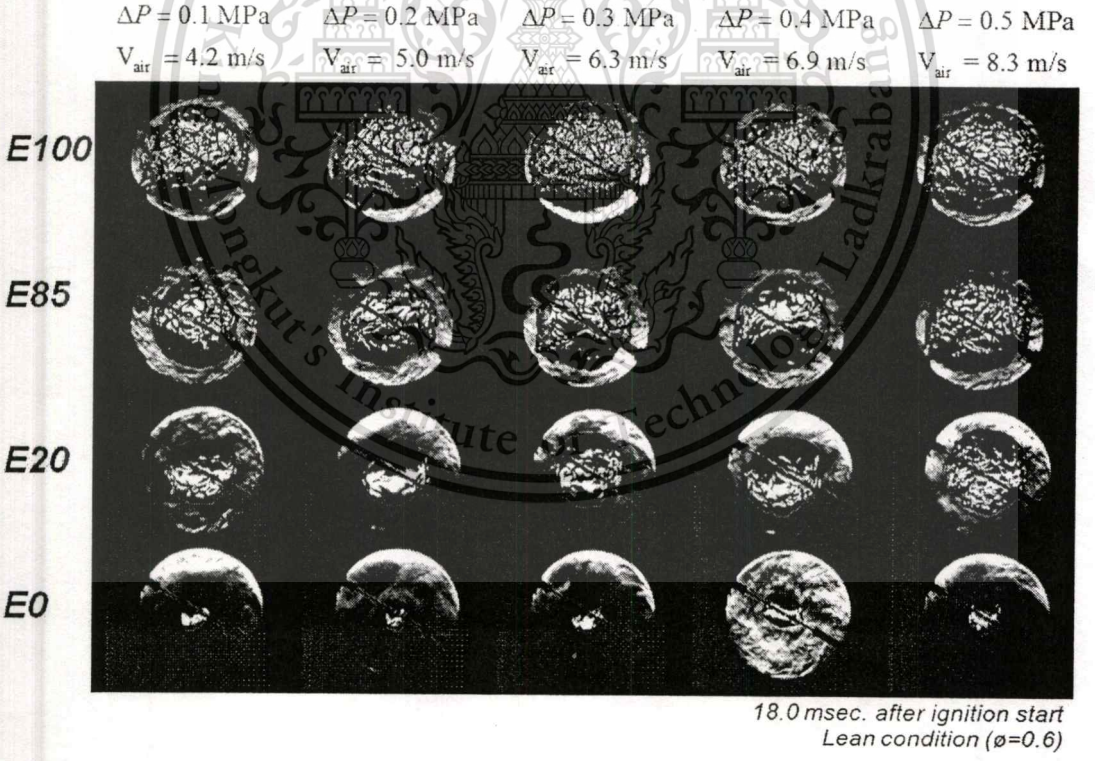

Figure 4.27 Flame propagation images at 18.0 msec. after ignition start and ϕ =0.6

Figure 4.25 -4.27 show the results of flame propagation of E100, E85, E20 and E0 under stoichiometric condition (ϕ =1.0) and lean condition (ϕ =0.8 and ϕ =0.6). As shown in fig 4.25, in stoichiometric condition, flame propagation images didn't

significantly change when varied the swirl condition. Shape and length of flame radius in the highest swirl condition seems to be the same as in the lowest swirl condition. In this figure, flame speed in stoichiometric condition hardly different even more swirl strength were applied. However, when operate at lower equivalence ratio, ϕ =0.8, flame edges in higher swirl intensities found to be more stable and look like uniform grain gather than that of low swirl condition. Spherical flame shape can be found only in high swirl condition, especially in E100 and E85, while in the low swirl condition, flame propagation show the unpredicted shape and lower in flame grain compare with in higher swirl condition flame In fig 4.27, the results at equivalence ratio equal to 0.6 show the same trend as in a condition of ϕ =0.8. Moreover, flame radiuses of E20 and E0 at high swirl intensities seem to be more than in lower swirl condition.

As a results, it can confirm the assumption that swirl intensities hardly affect to the peak pressure because flame propagation images show the same shape and length of flame radius even strength of swirl flow were changed. However, consider in lean condition, as increasing the swirl intensities, flame edge show more uniform grain and spherical shape than that of in low swirl condition. These can imply that the swirl intensity can improve stability of flame development under lean condition by generating uniform grain and spherical expanding flame shape. Furthermore, in lean operation, lower ethanol fraction blended fuel such as E0 and E20, flame propagation speed was accelerated by increasing the swirl intensities. These demonstrate that under lean condition swirl intensity can improve both of flame stability and its speed.

Chapter 5
Conclusions

The combustion characteristics of gasoline/ethanol blends were investigated by using constant volume combustion chamber. Following conclusions can be drawn.

5.1. Despite the fact that lower ethanol blend, E0 and E20 have an higher energy input than that of E85 and E100 as indicated in fig 4.2, the peak value of combustion pressure decreases with decreasing ethanol content in the mixture. Also, the length of time required to reach the maximum value of the combustion pressure is retarded in accordance with the decrease of ethanol percentage. These can imply that when utilizing the ethanol blend fuel, oxygen concentration of each fuel might be different and it might be effect to the combustion process in term of oxidizing performance. Form fuel properties table noted that the E0 has 0.0% of oxygen content while E20, E85 and E100, oxygen content were 7.54%, 31.75% and 34.7%, respectively. High oxygenated fuels such as E100 and E85 have more capability to oxidize with oxygen more than E20 or pure gasoline (E0) which was lack of oxygen concentration of fuel.

5.2. From the results of pressure rise rate, which were corresponding to rate of heat release, blending in higher percentage of ethanol in fuel, can be enhanced combustion characteristics by accelerate flame development process and increasing the peak value of heat release rate. Furthermore, higher ethanol concentration fuel such as E100 and E85, the combustion process occur more advance than that of pure gasoline (E0) when compare with the same equivalence ratio. These may cause from the oxygen content within fuel itself can enhance oxidation rate and accelerate the initial stage of combustion regardless the octane rating.

5.3. In stoichiometric condition, E0 has the longest combustion duration compared with other blends. On the other hand, E100 has the shortest duration, burn rate was 50% faster than E0 while E85 and E20, combustion duration were shorten amount of 30% and 16% when

compare with pure gasoline (E0). It is well known that the flame speed was related to the air/fuel ratio and mixture has the highest flame speed at equivalence ratio equal to one. From the results of combustion duration, it can imply that utilizing ethanol blended fuel can make the stoichiometric in the wider area compare with the pure gasoline (E0). Because blended fuel such as E20, E85 and E100 required more fuel injected, compare with same equivalence ratio of E0, 62.0 % , 48.2 % and 8.3 % additional amount of fuel were required for E100, E85 and E20, respectively. Furthermore, higher ethanol concentration can be completely vaporized easier than conventional gasoline. Consequently, ethanol blended fuel have more change to join the stoichiometric mixture in wider area.

5.4. From these results of mass fraction burn rate, it demonstrates that high ethanol content may accelerate the beginning of combustion period and reduce time of heat loss in early stage of the combustion. Furthermore, after approximately 0.5 of mass fraction burn, slopes of mass fraction burn which were correlated to burn rate tend to be increased as increasing the ethanol content.

5.5. From CoV investigation results, it found that appropriate equivalence ratio that the mixture can be make the stable combustion (low CoV) even the swirl flow were changed can be found at $\phi > 0.345$ for E100, $\phi > 0.36$ for E85, $\phi > 0.37$ for E20 and $\phi > 0.6$ for E0.

5.6. Because of swirl intensity can improve the mixture distribution performance. Thus stratification degree might be increased with applying more swirl intensity. These phenomena may be discussed that atomization and vaporization of fuel was accelerated by the increase of the turbulence intensity and the decrease of the impinged fuel. Under low swirl flow condition, liquid fuel was diffused and impinged to the chamber wall. These fuel droplets formed liquid film on the cylinder wall surface and were not completely vaporized. Thus, less stoichiometric mixture can form in low swirl condition. In other word, swirl intensity can enhance stratification degree that directly affects the lean limit range by diffusing amount of fuel to form stoichiometric mixture in the wider area.

As increase the swirl intensity, coefficient of variations (CoV) on peak pressure were decreased. Since, variations of peak pressure reflect to the combustion stability. Consequently, high ethanol concentration and high swirl intensities can be enhanced the combustion stability by extending the lean limit range.

5.7. Higher ethanol percentages in blended fuel able to extend the lean misfire limit range. Compared with pure gasoline (E0) at low swirl condition, minimum equivalence ratio (ϕ) will be extended amount of 3.95%, 12.01% and 18.30% in case of E20, E85 and E100 respectively. In higher percentage ethanol blend fuel, additional of fuel that required for maintain the same equivalence ratio can increase the chance to form stoichiometric mixture in the chamber. Thus the lean limit range will be extended.

5.8. For mixture stratification, fig 4.10 show the mixture distribution at various swirl intensity. From these results may be discussed that atomization and vaporization of fuel was accelerated by the increase of the turbulence intensity and the decrease of the impinged fuel, both of which were caused by the swirling flow. These can imply that swirl flow can enhance the stratification level and enhance mixture distribution around spark electrode. Consequently, lean limit range may be extended.

5.9. From comparison of ethanol and gasoline spray images, it can be seen that E0 has start to vaporize earlier that the E100, wider spray cone and short spray penalty, but when the time left, E100 fuel was fully evaporated into vapor phase faster than that the gasoline (E0). It can imply that E0 fuel has more light and heavy fraction than ethanol fuel. Thus, the lighter components tend to be evaporated early in the beginning stage while ethanol fuel wasn't start. After the time past, heavy fraction in gasoline (E0) still remained while ethanol fuel which have only one component already completely change to the vapor phase. These can be discussed that ethanol fuel, which is comprised of only one component, has lower carbon atom than the gasoline or E20 and E85. Consequently, it may be diffused by swirl flow easier than the gasoline, E20 or E85 which are comprised of various higher carbon atoms regardless

to RVP properties. As ethanol can easily diffuse, vaporization of ethanol fuel may be fully completed since before the ignition start regardless of swirl generation.

5.10. In pure gasoline, evaporation rate was less, Hence when fuel was injected some of them still remain in liquid phase and didn't evaporate. Especially in spray core, this region contained with over-rich mixture. These over-rich mixture lead the mixture hard to initial an flame kernel. Thus, initial stage of combustion comsumed more time compare with each other blends. In the other hand, in E100, fuel was completely evaporated and might be affected to an swirl flow. Thus, the mixture have more chance to join form near stoichiometric mixture(ϕ =1.0) in wider area compare to E0.

5.11. From the result of pressure history data shown in fig 4.16 – 4.19, it can imply that decreasing in ethanol content might make more probability in fluctuation of pressure. Form these results, it can be support to the lean limit result that stability of combustion under lean operation can be enhance by addition ethanol concentration in base gasoline.

5.12. According to comparative results of flame propagation, although ethanol fuel have higher octane number and lower RVP, oxygen content within fuel itself can enhance oxidation rate and accelerate the initial stage of combustion regardless the octane rating and RVP. As increase the ethanol concentration, flame development seem to be faster.

5.13. Consider in lean condition, more stable flame edge will be obtained by high percentage of ethanol blend, especially in E100 and E85. From Schlieren image, the results show that the percentage of ethanol affect to the sensitivity of flame deterioration. As decrease percentage of ethanol in blended fuel, flame shape will be less stability with reducing the equivalence ratio.

5.14. As can be seen from the results of peak pressure, it can imply that the swirl intensities can't significantly affected to the peak pressure but the ethanol concentration may increase the engine efficiency by increasing the maximum combustion pressure. Furthermore, different in peak pressure when changing the equivalence ratio may be discussed that the

amount of fuel injected or equivalence ratio (ϕ) directly affect to the energy release and also the peak pressure.

5.15. Result of flame propagation and flame kernel development in fig 4.25-4.27 demonstrate that the swirl intensity can improve stability of flame development under lean condition by generating uniform grain and spherical expanding flame shape. Furthermore, in lean operation, lower ethanol fraction blended fuel such as E0 and E20, flame propagation speed was accelerated by increasing the swirl intensities. These demonstrate that under lean condition swirl intensity can improve both of flame stability and its speed.

For better understanding of stratified combustion phenomena, further studies should include advanced method to identify the consistency of the swirl intensities and mixture formation distribution, such as LIF method and flow field simulation as well as optimized the injection-ignition timing for the proper equivalence ratios that mixture form near the spark plug.

References

1. Harry L. Husted, W.P.a.G.R. "Fuel Efficiency Improvements from Lean, Stratified Combustion with a Solenoid Injector." **SAE paper No.2009-01-1485.** 2009.
2. Heywood, J.B. **INTERNAL COMBUSTION ENGINE FUNDAMENTALS.** McGraw-Hill. 1988.
3. F. Zhao, M.-C.L., D.L. Harrington **Automotive spark-ignited direct-injection gasoline engines.** Elsevier Science Ltd. 1999.
4. Naoki Shiraishi, K.S., Syoji Nagasaka,Takayoshi Takano and Hiroshi Sami. "A Study on Direct Injection Gasoline Combustion using Constant Volume Combustion Vessel" **The Fifth International Symposium on Diagnostics and Modeling of Combustion in Internal Combustion Engines (COMODIA 2001).** 2001.
5. Hoimyung Choi, M.K., Kyoungdoug Min and Jonghwa Lee. "THE STRATIFIED COMBUSTION MODEL OF DIRECT-INJECTION SPARK-IGNITION ENGINES." **Proceedings of the Combustion Institute, Volume 29, 2002.** 2002.
6. Michael C. Drake, T.D.F., Andreas M. Lippert. "Stratified-charge combustion: modeling and imaging of a spray-guided direct-injection spark-ignition engine" **Proceedings of the Combustion Institute 30.** 2005.
7. Z. Huang, S.S., T. Ueda, H. Nakamura, T. Ishima, T. Obokata. "Effect of Fuel Injection Timing Relative to Ignition Timing on the Natural-Gas Direct-Injection Combustion" **Journal of Engineering for Gas Turbines and Power.** 2003.
8. Jeonghoon Song, D.H.L. "Experimental Study of Ignition of a Gasoline-Air Mixture in a Constant-Volume Combustion Chamber." **Combustion, Explosion, and Shock Waves, Vol. 39, No. 5.** 2003.
9. Kihyung Lee, C.L., and Haeyoung Jeoung. "A Study on the Effect of Stratified Mixture Formation on Combustion Characteristics in a Constant Volume Combustion Chamber." **JSME International Journal Series B, Vol.48.** 2009.
10. Jinhua Wang, Z.H., Haiyan Miao, Xibin Wang, Deming Jiang. "Study of cyclic variations of direct-injection combustion fueled with natural gas–hydrogen blends using a constant volume vessel." **international journal of hydrogen energy 33 (2008) 7580 – 7591.** 2008.
11. Myung Yoon Kim, D.S.K., and Chang Sik Lee. "Effect of Residual Gas Fraction on the Combustion Characteristics of Butane-Air Mixtures in the Constant-Volume Chamber" **Energy & Fuels 2003, 17, 755-761.** 2003.

12. Masahiko Fujimoto , M.T. "Effect of Swirl Rate on Mixture Formation in a Spark Ignition Engine Based on Laser 2-D Visualization Techniques." **SAE paper No.931905.** 1993.

13. Jinhua Wang, Z.H., Haiyan Miao, Xibin Wang, Deming Jiang. "Characteristics of direct injection combustion fuelled by natural gas–hydrogen mixtures using a constant volume vessel." **International journal of hydrogen Energy 33.** 2008.

14. Bayraktar, H. "Theoretical investigation of flame propagation process in an SI engine running on gasoline–ethanol blends." **Renewable Energy 32 (2007) 758–771.** 2007.

15. Hara Takashi, T.K. "LAMINAR FLAME SPEEDS OF ETHANOL, n-HEPTANE, ISOOCTANE AIR MIXTURES" 2006.

16. Xibin Wang, J.G., Deming Jiang, Zuohua Huang, and Wansheng Chen. "Spray Characteristics of High-Pressure Swirl Injector Fueled with Methanol and Ethanol" **Energy & Fuels 2005, 19, 2394-2401.** 2005.

17. Pulkrabek, W.W. **Engineering fundamentals of the internal combustion engine 2nd edition.** Prentice Hall. 2004.

18. Eiji Tomita, A.N., and Nobuyuki Kawahara "Effects of Swirl Flow and Inhomogeneous Concentration Fields on Combustion of Propane-Air Mixture in a Constant-Volume Vessel" **JSAE paper No.700-8530.** 2000.

19. Wang Xibin, C.W., Gao Jian, Jiang Deming, Huang Zuohua. "Spray characteristics of high-pressure swirl injector fueled with alcohol" **Energy Power Eng. China 2007.** 2007.

20. Nicolas Hadjiconstantinou, K.M., and John B. Heywood. "RELATION BETWEEN FLAME PROPAGATION CHARACTERISTICS AND HYDROCARBON EMISSIONS UNDER LEAN OPERATING CONDITIONS IN SPARK-IGNITION ENGINES" **Twenty-Sixth Symposium (International) on Combustion/The Combustion Institute, 1996/pp. 2637–2644.** 1996.

21. Freudenberger, R. **Alcohol Fuel (Making and Using Ethanol as A Renewable Fuel).** New Society Publishers. 2009.

22. Jian Gao, D.J., Zuohua Huang. "Spray properties of alternative fuels: A comparative analysis of ethanol–gasoline blends and gasoline" **Fuel 86 (2007) 1645–1650.** 2007.

23. Andersen, V.F. "Distillation Curves for Alcohol-Gasoline Blends" **Energy Fuels 2010, 24, 2683–2691.** 2010.

24. Stephen R. Turns. **An introduction to Combustion: Concept and Applications.** McGraw-Hill. 2000.

APPENDICES

Appendix A : Material specification

Steel for constant volume combustion chamber (CVCC)

ASTM A284 Steel, grade D

Categories: Metal; Ferrous Metal; ASTM Steel; Carbon Steel; Low Carbon Steel

Material Notes: Carbon content increases with the thickness of the plate. Maximum thickness is 305 mm. Plates wider than 610 mm are tested in the transverse direction and the elongation requirement is reduced 2.0%

Key Words: AFNOR 35-501 E24-2, AFNOR 35-501 E24-3, BS4360 40(A)B, BS4360 40C, CSAG40-21230 G, DIN 17100 RSt 37-2, DIN 17100 St37-3U, EN10025(90) Fe E360B(FN), EN10025(90) Fe E 360 C, EN10025(93) S235JR(G2), EN10025(93) S235 J0, IS 226, IS Fe 410-S, JIS 3101 SS 400, JIS 3106 SM 400A, JIS 3106 SM 400B, ISO 630 Fe 360 B, ISO 630 Fe 360 C, MNC810E SS 13.11.00, MNC810E SS 13.12.00, NBN21-101 AE235B, NBN21-101 AE235 C, UNI 7070 Fe 360 B, UNI 7070 Fe 360 C

Vendors: No vendors are listed for this material. Please click here if you are a supplier and would like information on how to add your listing to this material.

Physical Properties	Metric	English	Comments
Density	7.85 g/cc	0.284 lb/in³	Typical of ASTM Steel

Mechanical Properties	Metric	English	Comments
Tensile Strength, Ultimate	415 MPa	60200 psi	
Tensile Strength, Yield	230 MPa	33400 psi	
Elongation at Break	21.0 %	21.0 %	in 200 mm
	24.0 %	24.0 %	in 50 mm
Bulk Modulus	140 GPa	20300 ksi	Typical for steel
Shear Modulus	80.0 GPa	11600 ksi	Typical for steel

Component Elements Properties	Metric	English	Comments
Carbon, C	0.270 - 0.35 %	0.270 - 0.35 %	
Iron, Fe	98.0 %	98.0 %	
Manganese, Mn	<= 0.90 %	<= 0.90 %	
Phosphorous, P	<= 0.040 %	<= 0.040 %	
Silicon, Si	0.280 %	0.280 %	
Sulfur, S	<= 0.050 %	<= 0.050 %	

http://www.matweb.com

Quartz glass specification

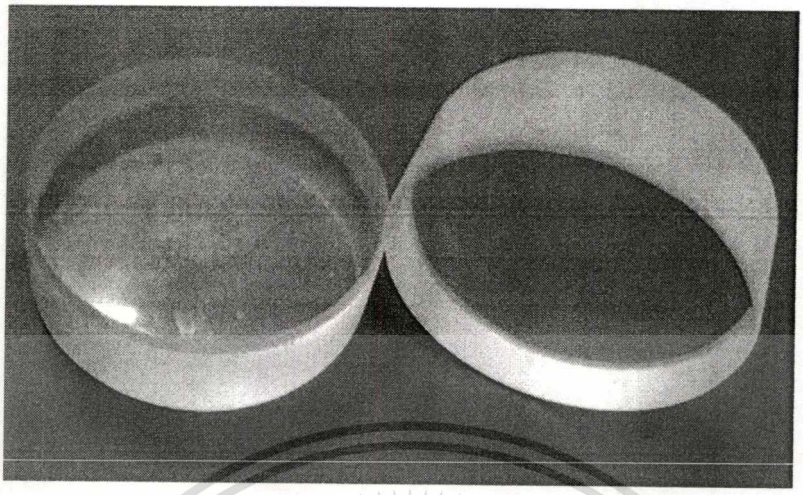

Specifications	Unit	Value
Specific gravity	g/cm^2	2.21
Hardness	Mhos scale	5-7
Rapture strength	Mpa	800-1000
Compressive stress	Mpa	60-700
Young's Modulus 20 °C	Gpa	77.8
Young's Modulus 50 °C	Gpa	82
Young's Modulus 900 °C	Gpa	85
Possion ratio		0.17
Rigid index 900 C	Gpa	36.9
Speed of longinal wave	m/s	$5.72x10^{-3}$

Graphite gasket detail

SealPack Style 300R
FLEXIBLE GRAPHITE ROLLS
Temperature Limits : -200°C to + 1650°C
-200°C to + 850°C Non-Oxidizing atm.
+932°F (500°C) Oxidezing atm.
Chemical Resistance : pH 0-14 except oleum, fuming nitric acid & aqua regia
Thickness (mm) 0.2, 0.35, 0.40, 0.50, 0.8, 1.0, 1.5
Width : 1000 - 1500 mm
Length : 50 - 100 m.

Data acquisition system

Instrument facts:

- AC or DC powered
- High accuracy, 16, 22 or 24 bit resolution
- Fast sampling, 100 kS/s up to 1 MS/s per channel
- Transient recording up to 1 GS/s
- Powerful Intel® Core™2 Duo PC inside
- 80 MB/s stream-to-disk rate
- Bright 17" display
- Spare panel for customization
- 5 available PCI slots

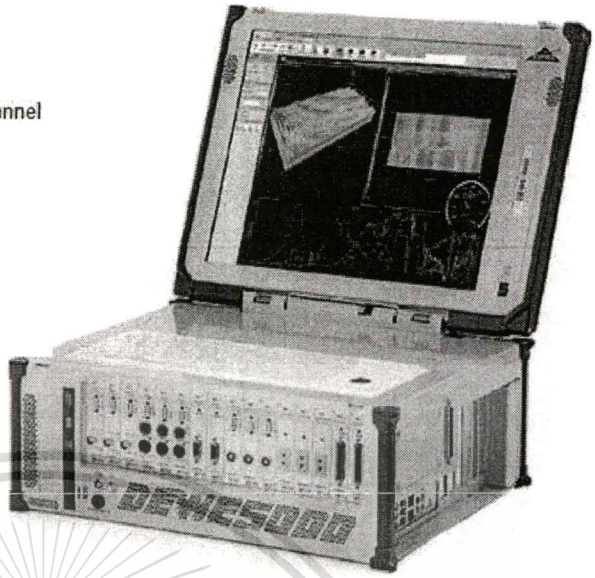

DEWE-5000 series		
Input specifications	DEWE-5000	DEWE-5001
Slots for DAQ or PAD modules	16	-
MDAQ input channels	-	Up to 32
Main system [1]		
Total PCI slots	5	5
Hard disk	1000 GB	
Data throughput	Typ. 70 MB/s [2]	
Power supply	95 to 260 V_{AC}	
Display	17" TFT display, 1280 x 1024 pixel	
Processor	Intel® Core™2 Duo 2 GHz	
RAM	2 GB	
Ethernet	10/100/1000 BaseT	
USB interfaces	4	
RS-232 interface	1	
Storage drive	Internal DVD +/-RW burner	
Operating system	Microsoft® WINDOWS® 7	
Dimensions (W x D x H)	460 x 351 x 192 mm (18.1 x 13.8 x 7.7 in.)	
Weight	Typ. 17 kg (37 lb.)	Typ. 16.5 kg (36 lb.)
Environmental specifications		
Operating temperature	0 to +50 °C, down to -20 °C with prewarmed unit	
Storage temperature	-20 to +70 °C	
Humidity	10 to 80 % non cond., 5 to 95 % rel. humidity	
Vibration [3]	MIL-STD 810F 514.5, procedure I	
Shock [3]	MIL-STD 810F 516.5, procedure I	

Pressure sensor

Technical Data

Range	bar	0 ... 200
Calibrated partial range	bar	0 ... 50
Overload	bar	250
Sensitivity at 200 °C	pC/bar	≈-15
Natural frequency	kHz	≈130
Spark Plug with integrated sensor		
Linearity	% FSO	≤±0,6
Acceleration sensitivity		
Axial	bar/g	<0,005
Radial	bar/g	<0,005
Operating temperature range	°C	≤350
Sensitivity shift		
200 ±50 °C	%	<±1,5
Thermal shock		
At 1500 min -1,9 bar imep		
Δp (short-time drift)	bar	<±0,8
Δimep	%	<±4
ΔPmax	%	<±2
Insulation resistance of sensor		
At 20°	Ω	$>10^{12}$
At 200°	Ω	$>10^{11}$
Insulation resistance of spark plug		
At ambient temperature		
Between central electrode		
and spark plug body at 1000 V	MΩ	>100
Electrical final test of spark plug		
Spark discharge for	7 bar/20 kV	
Break through resistance	kV	<35
Tightening torque of sensor	Nm	1,2 ... 1,3
Tightening torque of spark plug	Nm	20 ... 25
Capacitance for sensor		
with 1 m cable	pF	110
Weight (with protection cartridge)	g	130

Appendix B : Distillation curve for Ethanol and Gasoline

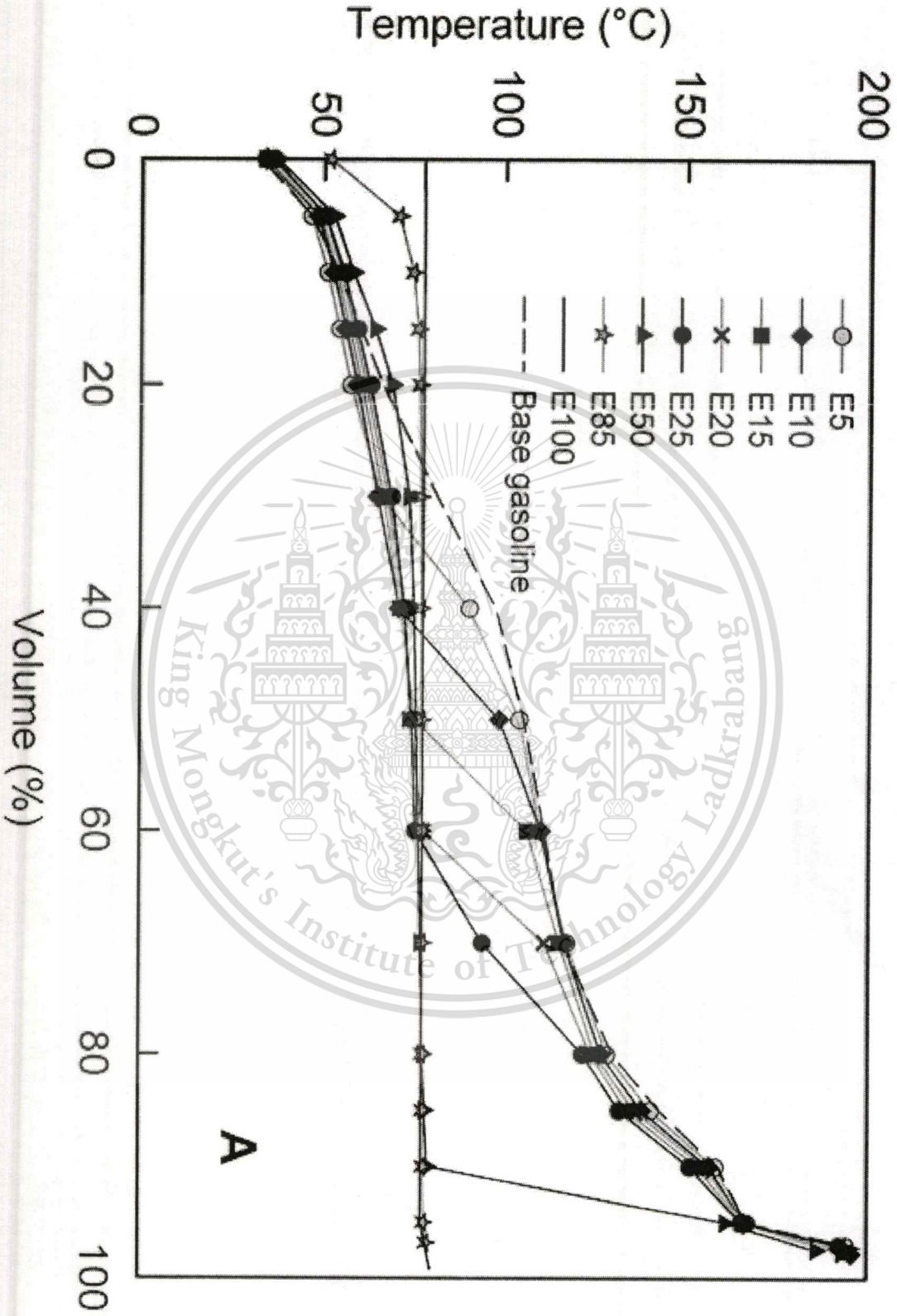

Reff : Andersen, V.F. "Distillation Curves for Alcohol-Gasoline Blends" Energy Fuels 2010, 24, 2683–2691. 2010.

Appendix C : Mixture stratification study (Tomita's study)

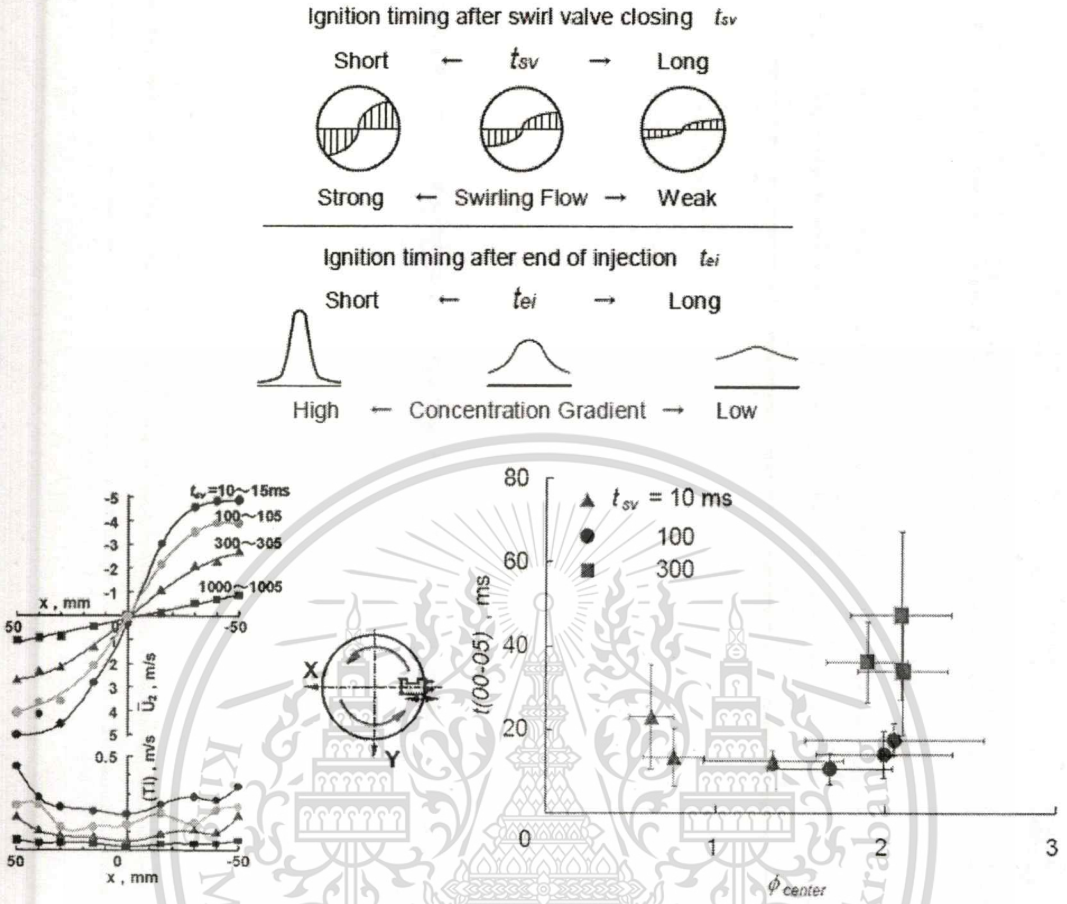

Figure above shows the relation between equivalence ratio near the center measured with the LIF method and the combustion period of initial stage for various conditions in t_{sv}=10, 100 and 300ms in ϕ_{center}=0.3 with error bars that mean the standard deviation of concentration fluctuation near the center of the combustion chamber. In t_{sv}=10ms, the standard deviation was small because the fuel near the center diffused very much. In t_{sv}=100ms, the standard deviation was large while in t_{sv}=300ms, the fuel did not diffuse very much. Therefore, inhomogeneous mixture includes stoichiometric one even if it is lean or rich on the average in t_{sv}=10 and 100ms and the averaged lean and rich limits of flammability became wide.

Source: Eiji Tomita and Nobuyuki Kawahara "Effects of Swirl Flow and Inhomogeneous Concentration Fields on Combustion of Propane-Air Mixture in a Constant-Volume Vessel" **JSAE paper No.700-8530.** 2000.

Appendix D : Flame speed in alcohol fuel study (Takashi's study)

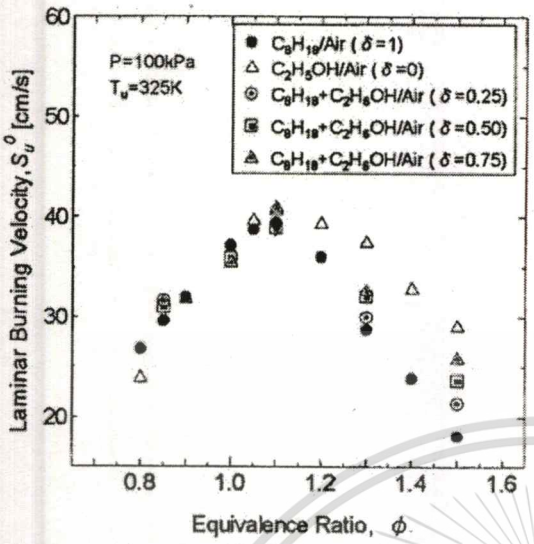

Fig.3 Variations of S_u^0 with ϕ for different δ

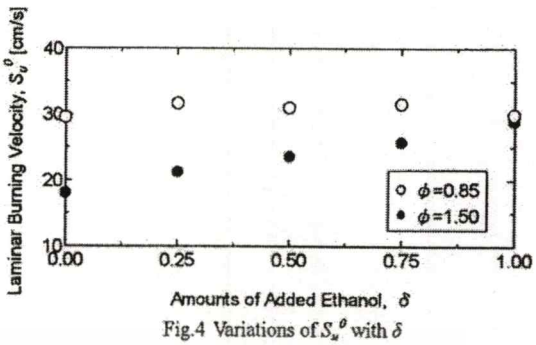

Fig.4 Variations of S_u^0 with δ

Laminar burning velocity of various iso-octane and ethanol blended.

Source: Takashi HARA et.al. "Effect of the ethanol addition on the laminar flame speeds of primary reference fuels" , JSME 4725

Appendix E : Ethanol promotion in Thailand

Alternative Energy Policy for Ethanol Fuel

Ministry of Energy had determined the energy strategies for a country competitiveness, which had been approved by the cabinet on 2 September 2003. One among these strategies is the sustainable alternative energy development that had set the target on increasing the proportion of commercial renewable energy or renewable power generation/industry from 0.5 percent in 2002 up to 8 percent by 2011. Biofuel development, as for ethanol and bio-diesel, is a goal under the Plan of Increasing Proportion of Renewable Energy Use. Ministry of Energy, by DEDE, had established a Gasohol Strategy to propose in the Joint Meeting between Ministers of Energy, of Agricultural and Cooperatives and of Industry and then proposed to the cabinet on 9 December 2003, which the summary is as shown below.

Objectives of Ethanol Strategy

- To create the sustainable energy security of a country and communities
- To enhance the potentials of communities to be energy production sources
- To support a domestic bio-chemical industry development

Target of Ethanol Strategy

Ministry of Energy had set the target on using an ethanol for MTBE substitution in gasoline 95 by 1 ml/d by 2006 and on using an ethanol for 3 ml/d for MTBE substitution in gasoline 95 and for oil substitution in gasoline 91 by 2011.

Alternative energy for energy import reduction.

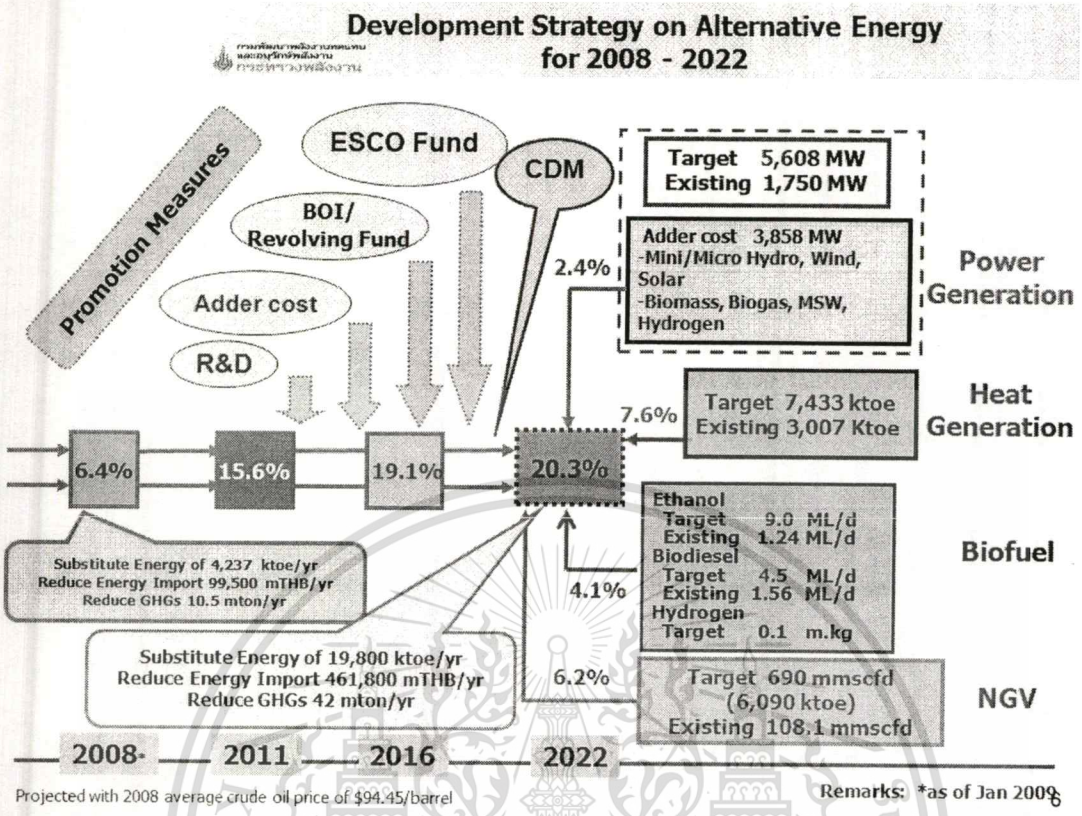

Ethanol promotion strategy

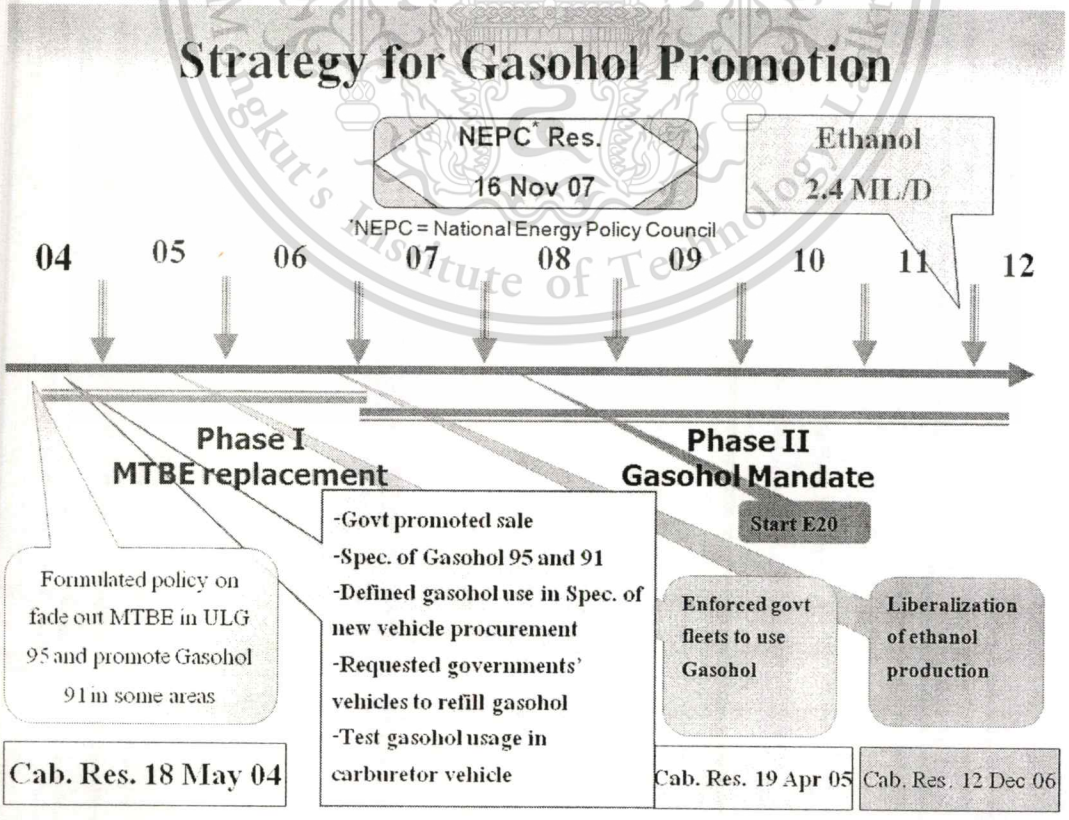

Transportation tax for alternative fuel vehicles.

Thai Automobile Tax Structure

Passenger cars		Light Truck and derivative		*Energy Saving and Alternative Fuel Vehicles	
Duty and taxes		Duty and taxes		Duty and taxes	
Import duty	80%	Import duty	40%	Import duty	40-80%
CEPT (ASEAN)	0%	CEPT (ASEAN)	0%	CEPT (ASEAN)	0%
Excise tax		Excise tax		Excise tax	
- not exceeding 2,000 cc.	30%	- Pick Up Truck	3%	- Hybrid, Electric, Fuel Cell	10%
- 2,001-2,500 cc.	35%	- Double Cab	12%	- ***Eco car***	***17%***
- 2,501-3,000 cc.	40%	- PPV	20%	- NGV	20%
- More than 3,000 cc.	50%	(Pick up passenger vehicle)		- E20**	25%
				- E85	
				1,780-2,000 cc.	22%
				2,001-2,500 cc.	27%
				2,501-3,000 cc.	32%
Municipal tax ***	10%	Municipal tax ***	10%	Municipal tax ***	10%
VAT	7%	VAT	7%	VAT	7%

* Energy Saving and Environmental Tax Incentive *** Municipal Tax calculate from Excise Tax

** E20 5% reduction from normal rate (ex. Normal rate of P-car 2,000 cc. is 30%, E20 is 30-5 = 25%)

Source: T. Boonyamam, Expert meeting on Survey Analysis of the Road Transport Sector for Reducing CO_2 Emission, Bangkok, 15 Feb 2011

Appendix F : Publications

JSAE 20119551 / SAE 2011-32-0551

Experimental investigation in combustion characteristics of ethanol-gasoline blends for stratified charge engine

Chinda Charoenphonphanich[1], Piyaboot Ornman[2], Preechar Karin[3]
[1]Faculty of Engineering, [2]TAIST-TokyoTech Automotive Engineering Program, [3]International College
King Mongkut's Institute of Technology Ladkrabang, THAILAND

Hidenori Kosaka
Tokyo Institute of Technology, JAPAN

Nuwong Chollacoop
National Metal and Materials Technology Center (MTEC), THAILAND

ABSTRACT

The increasing of global energy demand and stringent pollution regulations have promoted research on alternative fuels. In Thailand, ethanol, can be produced from many sources of national agriculture products as renewable fuel, which was strongly promoted by government due to its many merits for use in transportation field. In this study, combustion characteristics of ethanol-gasoline blend (20%, 85%, and 100%) as well as pure gasoline (E0) were investigated by using a swirl-generated constant volume combustion chamber. Flame propagations of different fuel blends were observed by high speed Schlieren photography technique while pressure history data were recorded for detailed combustion analysis. Combustion behavior, combustion duration and rate of pressure rise of all tested fuels were investigated in various swirl intensities and equivalence ratios. In addition, effect of swirl intensities and ethanol concentration on lean misfire limit were also discussed. The results showed that the high concentration of ethanol blend with the high swirl intensity can significantly extended lean misfire limit while lowering combustion variations. Furthermore, combustion duration can be accelerated by increasing the percentage of ethanol in fuel blend. Through this study, a better understanding of stratified charge combustion fuelled with ethanol/gasoline blends can be achieved.

INTRODUCTION

With the increasing concern on fossil fuel shortage and environmental issues from continuously increasing global energy demand, the development of alternative fuel engines has attracted more attention. Alcohol, especially ethanol, was the challenging candidate in alternative fuel since it can be produced from many sources of biomass, and is indeed the renewable energy. In addition, the raw materials for ethanol production, cassava and sugarcane, are also the main economic crops in Thailand. Despite the lower heating value of alcohols compared to that of gasoline, alcohols release a little more heat than gasoline under the same equivalence ratio [1], [2]. Moreover, high octane number allows higher compression ratio; thus, an engine fueled with ethanol can run with higher power output and better thermal efficiency than that of gasoline fueled engines[3].

For stratified charge engine, it is well known that lean, stratified combustion can reduce fuel consumption and gain some merits in gasoline spark-ignited, direct injection engines for several reasons. First, unthrottled operation allows for a significant reduction in pumping loss, especially at low loads. Second, the lean mixture being compressed has a higher ratio of specific heats. This allows for a more efficient compression and expansion process [4]. In theory, for an Otto-cycle engine, the efficiency η_{th} can be written as $\eta_{th} = 1-(1/r_c^{\kappa-1})$, where r_c is compression ratio and κ is specific heat ratio. As an engine operates leaner, the specific heat ratio of combustion mixture becomes higher. If the specific heat ratio (κ) can further be raised, the heat efficiency and engine power output can be improved [2]. In addition, volumetric efficiency in stratified charge engine could be increased by cooling effect from direct injection process [2, 5]. As a result, using ethanol in stratified-charge, spark-ignition, direct-injection engines is capable of achieving significant gains in both volumetric and thermal efficiencies [6].

Although this combustion can achieve many kinds of advantage for combustion characteristics, it produces much unburned hydrocarbon and soot because of inhomogeneous charge mixture in the combustion chamber. The main problem is a misfiring under lean operation even if whole air-fuel mixture is very lean [7]. In stratification, air-fuel ratio tends to be over-rich in the middle of the mixture and over-lean in the periphery bordering surrounding air. It is essential to minimize the above mentioned air-fuel ratio difference by enhancing the stratification degree, defined by the ratio of fuel quantity involved in nearly stoichiometric mixture zone to total fuel quantity. As the stratification degree becomes low, unburned fuel amount increases and

fuel economy deteriorates. Therefore, it is necessary to investigate the combustion characteristics in order to obtain the stable lean combustion.

In this study, the effect of swirl ratio on the combustion characteristics was investigated in the ethanol /gasoline blends, which vary from pure gasoline (E0) to pure ethanol (E100) in the swirl-generated constant volume combustion chamber. With the pressure analysis data, rate of pressure rise (dp/dt), combustion duration and mass fraction burned rate were analyzed while high speed video camera was used to observe flame propagation during combustion processes.

EXPERIMENTAL APPARATUS AND PROCEDURE

EXPERIMENTAL APPARATUS

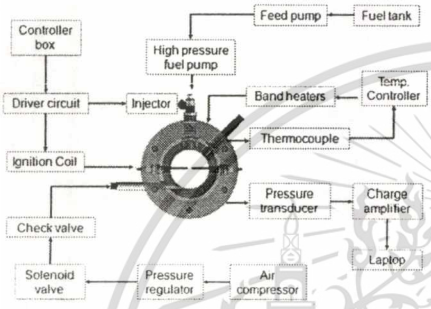

Figure 1: Schematic diagram of experimental apparatus.

Figure1 shows the schematic diagram of the experimental apparatus used in this study. It consists of five major systems. First, air supply system, contains with air compressor and intake swirl port with pressure regulator for making a swirl flow and inducing fresh air charge into the combustion chamber. Second is fuel system, where low pressure fuels were delivered from fuel tank with feed pump. Then, the cam-driven high pressure fuel pump from Mitsubishi GDi engine pressurized the fuel up to 4.5 MPa before sending the fuel to the swirl nozzle injector. Third, heating system, is composed of two band heaters (1300 W) attached outside the chamber wall while initial temperature (Ti) was controlled by the thermo-switching controller. Forth, control module was used to control the signal sequence and to interface with a data acquisition system. Last system was the data acquisition system, A piezo-electronic pressure transducer (Kistler model 611BFD16) was used to measure the combustion pressure and the charge amplified electrical signals including high speed data acquisition system (Dewetron model DEWE-5000) were used to record, filter and condition the signal from the pressure sensor. Details of the measurement and actuator devices of constant volume combustion chamber were shown in fig 2. Figure 2 shows a schematic diagram of the constant volume combustion chamber. The internal diameter and width of this chamber are 70 mm. and 100 mm., respectively. The volume capacity is 385cc. Two quartz glasses windows with 35 mm. thickness are equipped at both sides of the combustion chamber for optical access and visualization of the flame propagation propose. Swirl port allows an induced air to flow into the combustion chamber in tangential direction to realize the swirl flow in the chamber. Graphite gaskets are attached in both side of quartz glasses to absorb impact load from combustion. The spark plugs are located to the central of the combustion chamber to generate the spherically expanding flame and prevent heat transfer to the chamber wall.

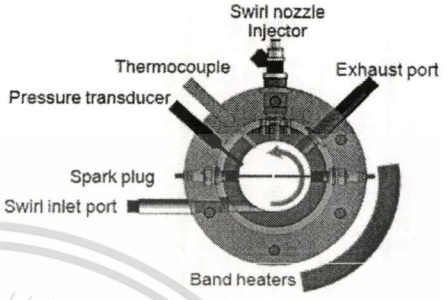

Figure 2 : Actuator and measuring device of constant volume combustion chamber.

Flame propagation during combustion process was visualized by high speed video camera (Photron FASTCAM SA3) with 50 mm. F1.2 lens at 6000 fps and 1/10,000 sec. of shutter speed. For a clearly-defined flame edge, Schlieren photography technique was used in this experimental study, and the result of flame visualization images was analyzed corresponding to pressure history data. Figure 3 shows the arrangement of Schlieren system for flame visualization.

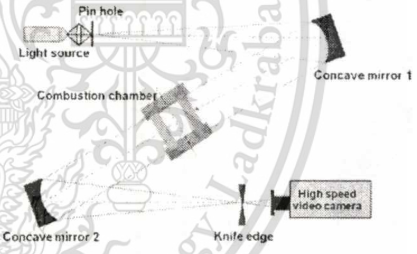

Figure 3 : Schlieren photography setup.

EXPERIMENTAL PROCEDURE

Figure 4 shows the example of signal sequence from control module. First, fresh air charge from the air compressor will be regulated according to swirl intensity, and then the solenoid valve was allowed to open and to close at certain timing. Second, high pressure fuel was directly injected to the constant volume combustion chamber. Amount of fuel injected and also its durations were adjusted according to each required air/fuel ratio. After that, ignition coil was energized for supply spark energy at the tip of electrode to

initiate the flame kernel. In addition, camera trigger signal was used to control the shutter timing and marking the starting point of ignition from high speed video camera.

Because of limitation of utilizing the constant volume vessel thus the timing might be quite different from that in an actual engine condition. However, criterias for setting each timing use in this experiment study were based on the results of Shadowgraph images. First, fresh air charge from the air compressor will be regulated according to swirl intensity, then the solenoid valve was allowed to open and closed at 1.5 second for ensure that the air was filled in the whole chamber. After the solenoid valve closed, the swirl flows were deteriorated as shown in fig.7. In this experiment strengths of swirl motion were varied by applying different pressure between fresh air induced and combustion chamber pressure. After the time around 100 msec., values of swirl velocities were consistent with the air velocity at 4.2 – 8.3 m/s. At this point, the author assume as the start of ignition point. Second, high pressure fuel will be directly injected to the constant volume combustion chamber. Amount of fuel injected and also its durations were adjusted according to each required air/fuel ratio. Because of this experiment study was conduct on constant volume combustion chamber. Therefore, quantity of available air were fixed while equivalence ration or air/fuel ratio were controlled by amount of fuel injected. In addition, fuel pressure was fixed at 4.5 MPa for avoiding the compressible effect of fuel mass and this value was consistent with the real GDi engine condition.

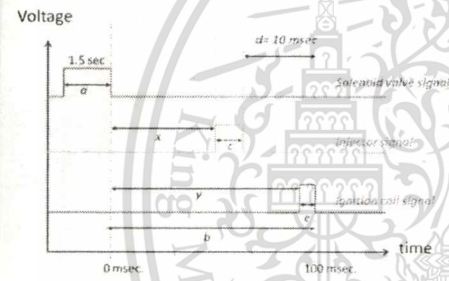

Figure 4 : Signal Sequence from controller

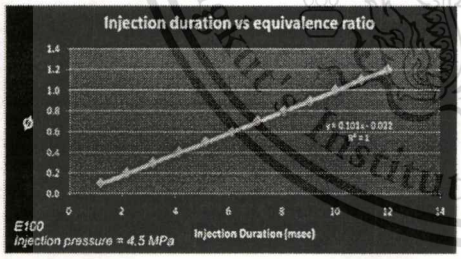

Figure 5 : Calibration chart for setting the injection duration

The relationship between injection duration and equivalence ratio of each tested fuel ware prepared in form of injection calibration charts before the testing as be illustrated in fig.5. After that, ignition coil will be energized for spark energy at the tip of electrode to initiate the flame kernel. Ignition coil charge time was set as constant at 3 msec. for avoid damage from over-charged effect. For the injection and ignition interval, defined as "d" in the fig.4, it was fixed at 10 msec. This timing came from observation of the mixture motion phenomena. At 7 msec. after the end of injection, the mixture vapour have just fully formed whole the combustion chamber. After that, it has to be waited for a moment for mixture development in swirl direction. The later 3 msec. the mixture have been affected to the swirl motion. The mixture motion images against the time after end of injection time were shown in fig.6. All of signal sequences timing were be controlled by using the interfacing software. The value of "a", "b", "c", "d" and "e" in fig. 4 can be set in the software while parameter "x' and "y' were automatically calculated before sent to various actuator. As can be seen in fig.4, swirl strength for a given different pressure can be changed with setting the longer timing "b" because the air motion velocities were deteriorated as the time left (shown in fig.7) while the injection-ignition timing was controlled by setting the timing "d". The start of injection(x) was not fixed. It depends on injection duration(c) and injection-ignition interval (d). In addition, camera trigger signal was used to control the shutter timing and marking the start of ignition point from high speed video camera. The summarized of timing were also shown in the table 1.

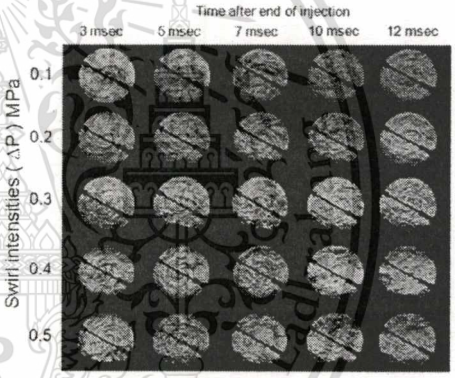

Figure 6 : Mixture motion against the time after end of injection

Table 1 shows the experimental conditions used in this study. Since ethanol-blended gasoline fuels are in the liquid phase at the normal temperature, initial temperature in this experiment was fixed at 450 K, which is higher than evaporation temperature of all tested fuel to avoid a misfire when the fuel was injected into the combustion chamber. Initial pressure in this experiment (P_i) was set at 0.5 MPa. The phenomenon that occurs in this vessel experiment in relation to an engine is to be limited. The initial pressure also quite different from the real engine condition due to lack of pressurized equipment. Thus, the combustion

process will be limited to the early stage of compression stroke. The total equivalence ratios of 1.0, 0.8, and 0.6 were simulated in overall lean condition. Tested fuel in this experiment study were varied from E0 (0% by volume of ethanol fuel), to E20, E85 and E100 (pure ethanol fuel) for an investigation on the effect of ethanol concentration on combustion characteristics.

Table 1 Experimental conditions

Experimental variables	Conditions
Initial temperature (K)	450
Initial pressure (MPa)	0.5
Coil charge time (msec) "e"	3
Injection pressure (MPa)	4.5
Inj – Ign Interval (msec) "d"	10
Ignition start (msec) "b"	100
Solenoid valve duration (sec) "a"	1.5
Tested fuel	E0,E20, E85, E100
Equivalent ratio	1.0, 0.8, 0.6
Swirl intensities in ΔP (bar)	1.0, 2.0, 3.0,4.0 and 5.0
Swirl intensities in velocity (m/s)	4.2, 5.0, 6.3, 6.9, 8.3

Swirl intensity setup

It is known that the mixture distribution and stratification level in stratified engine are strongly related to the injection timing, injector location and turbulence[1, 2]. In this study, Stratification levels were controlled by varying the turbulence strength which was generated by the swirl flow.

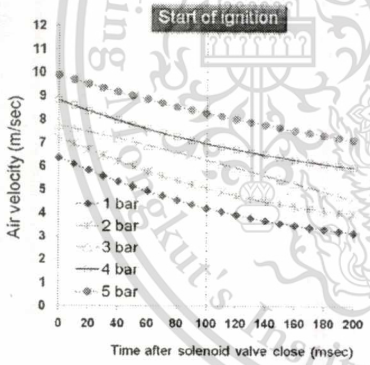

Figure 7 : Regression trace of air velocity against the time after solenoid valve close.

Swirl intensities were varied by adjusting the different pressure between pressurized air inlet and chamber pressure. Low swirl conditions were obtained by less different pressure adjustment while high swirl flows were generated by regulating in more different pressure. Strength of air swirl generated by air induction through tangential inlet port was calibrated by measuring moving speed of stripes appeared in Shadowgraph image of air flow. Figure 7 shows the regression traces of swirl speeds against the time after solenoid valve closed. The timing after solenoid valve closed was set at 100 msec. on each experimental condition while different swirl speeds were changed by varying the different pressure. The images of stratification mixture when applying different pressures were shown in fig.6. In this figure, it can be seen that vapor mixtures were distributed more as the swirl flow increased.

Lean limit investigation

Lean limit is the leanest air-fuel mixture that will sustain flame propagation. When relating air-fuel ratio to cylinder pressure or exhaust gas content as the air-fuel ratio increases from stoichiometric, a point is reached where variations increase sharply, approximately the lean misfire limit. Variation of peak pressure and area under the pressure verses crank angle curve has been found to be the most sensitive parameter which describes where combustion changes occur. In this study, lean limit was defined as the minimum equivalence ratio that reached the maximum acceptable value of coefficient of variations on peak pressure. For better understanding, figure 8 shows the definition of lean limit that use in this study. In this study, the data of 20 cycle of each condition were collected for investigate the lean limit and maximum acceptable value of CoV was 20%.

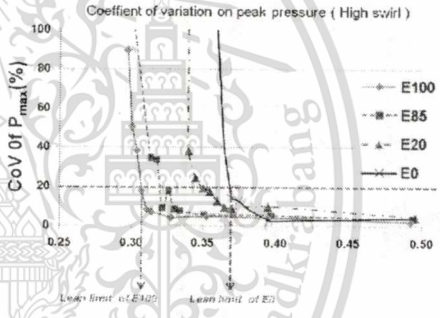

Figure 8 : Lean limit definition.

Rate of heat release, rate of pressure rise and mass fraction burn

In this section, rate of heat release (ROHR) can be calculated by applying the first law of thermodynamics regardless of the heat transfer to the chamber wall. Then, ROHR will be obtained from the following equations.

$$\left(\frac{dQ}{dt}\right)_{release} = mc_v \frac{dT}{dt} + P\frac{dV}{dt} \qquad (1)$$

Apply the ideal gas law, equation (1) becomes [8], [12]

$$\left(\frac{dQ}{dt}\right)_{release} = \left(\frac{c_v P}{R}\frac{dV}{dt}\right) + \left(\frac{c_v V}{R}\frac{dP}{dt}\right) + P\frac{dV}{dt} \quad (2)$$

With a relation between specific heat,

$$\frac{c_p}{c_v} = k \quad \text{and} \quad c_p = c_v + R$$

Since the experiment was conducted in constant volume combustion chamber, the following equation is obtained

$$\left(\frac{dQ}{dt}\right)_{release} = \left(\frac{V}{k-1}\right)\frac{dP}{dt} \quad (3)$$

Where V is the volume of combustion chamber and k as the specific heat ratio?

As for a qualitative analysis, by neglecting the heat transfer during combustion, the deviation for turbulent combustion by this treatment is small due to the short combustion duration [8]. Thus, the rate of pressure rise is proportional to the rate of heat release; and the information of heat release rate can be reflected by the information of pressure rise rate. Hence, heat release rate can be calculated directly with the pressure history data [7, 9-11].

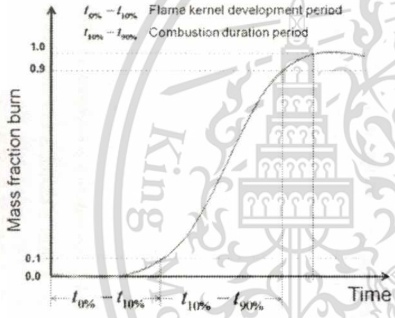

Figure 9 : Investigation of combustion duration using mass fraction burn rate data.

Mass burned fraction was calculated based on the pressure data obtained from the experimental results as follows [9].

$$M_f(t) = \frac{P(t) - P_i}{P_{\max} - P_i} \quad (4)$$

Where $P(t)$ is the combustion pressure
P_i is the initial mixture pressure, and
$P_{\max}$ is the maximum combustion pressure.

If the mixture gas is fully burned when it reaches peak combustion pressure, it can be calculated according to the relative value of the combustion pressure. It is noted that M10 stands for 10 percent combustion and M100 stands for 100 percent combustion [9]. Figure 9 shows the definition of combustion duration, which is expressed from 10% mass fraction burn to 90% mass fraction burn [10].

RESULTS AND DISCUSSIONS

Effect of ethanol content on the rate of pressure rise and mass fraction burn

Figure 10 shows the effect of the ethanol content on the combustion pressure at medium swirl intensity (ΔP=0.3MPa). As indicated this figure, the maximum pressure appears in pure ethanol (E100) at 3.05 MPa. The peak value of combustion pressure decreases with decreasing ethanol content in the mixture due to lack of oxygen concentration of fuel. Also, the length of time required to reach the maximum value of the combustion pressure is retarded in accordance with the decrease of ethanol percentage.

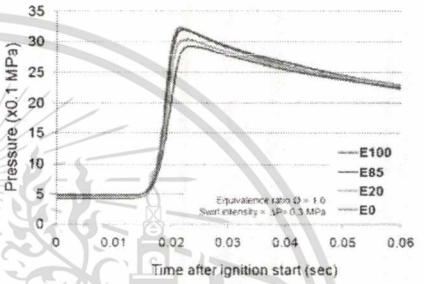

Figure 10 : Pressure data (Ø=1.0, swirl = 0.3 MPa).

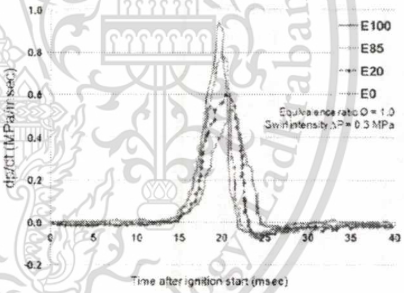

Figure 11 : Rate of pressure rise (Ø=1.0, swirl = 0.3 MPa).

The rate of pressure rise is a very important parameter because this relates to heat release rate, as described in previous section. The effects of ethanol content on the rate of pressure rise were illustrated in fig. 11. The peak value of the pressure rise rate was rapidly increased and its timing was shortening at high percentage of ethanol. E20 had not significantly changed in maximum pressure rise rate compared to pure gasoline (E0). However, it can release heat earlier than that of the E0. Table 2 shows the fuel properties table, from this table,heating value of E20, E85

and E100 are less than E0 but the amount of fuel injected need to be more for maintain the correctted equivalence ratio. If consider at the same equivalence ratio, the heat input was not significant changed when changing type of fuel.

Table 2 Fuel properties table

Fuel	E0	E20	E85	E100
Formula	($C_{8.26}H_{15.5}$)	-	-	(C_2H_5OH)
molecular weight	114.18	88.12	50.60	46.07
Ethanol content (% vol)	0.0	19.9	78.9	100.0
Carbon content (%wt)	84.9	79.85	55.36	52.2
Hydrogen content (%wt)	15.1	12.88	12.89	13.0
Oxygen content (% wt)	0.0	7.54	31.75	34.7
LHV (MJ/kg)	44.0	40.6	29.5	26.9
Air/fuel ratio	14.63	13.51	9.87	9.03
Benzene content (% Vol)	-	2.14	0.24	-
Aromatic content (% Vol)	-	30.3	6.2	-
Heat of vaporization (kJ/kg)	305	-	-	840
RVP (kPa)	58.4	59.0	44.4	16.0
Specific gravity	0.72-0.78	0.7604	0.7830	0.8
RON	92.0-98.0	98.3	101.6	107.0
MON	80.0-90.0	84.6	91.1	89.0

The comparison of energy supply in term of energy required per a kilogram of air was illustrated in fig. 12. Hence, the different of maximum pressure and rate of pressure rise when utilizing the ethanol blend fuel can be discussed that oxygen concentration of each fuel might be different and it might be effect to the combustion process in term of oxidizing performance. High oxygenated fuels such as E100 and E85 have more capability to oxidize with oxygen more than E20 or pure gasoline (E0).

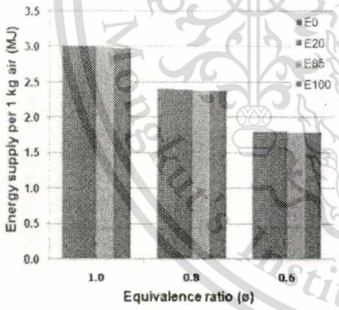

Figure 12 : Comparison of energy input with different equivalence ratio.

From quantitative analysis, combustion duration may be taken into account by using mass fraction burn rate data. Figure 13 and figure 14 show the results of mass fraction burn rate and combustion durations of various ethanol-gasoline blended fuels at medium swirl condition. All fuels were tested with equivalence ratio equal to 1.0. As indicated in fig. 13-14, the combustion periods were to be shortened and accelerated by high concentration of ethanol in blend fuel. The combustion duration were 3.6 msec, 5.2 msec, 6.4 msec, and 7.6 msec in case of E100 (pure ethanol), E85, E20 and E0, respectively. This demonstrates that ethanol content may accelerate the combustion period and reduce time of heat loss in early stage of the combustion.

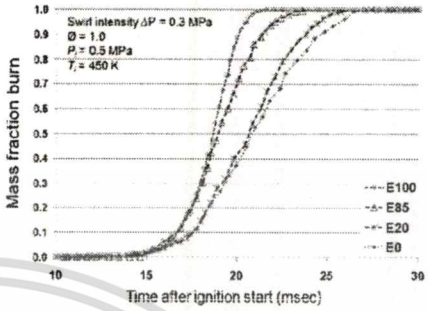

Figure 13 : Mass fraction burn of E100, E85, E20 and E0.

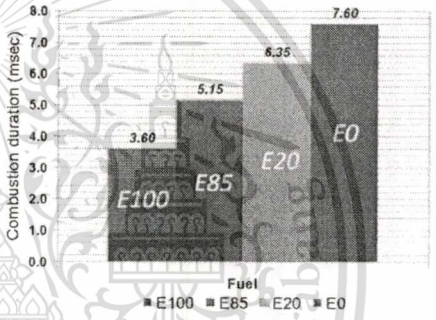

Figure 14 : Combustion duration result (base on mass fraction burn rate data).

Comparing to the images of flame propagation that shown in fig 15. This result were the Schlieren images of flame propagation that taken with high speed video camera. All of fuel were tested at stratified condition, swirl intensity was set at 0.3 MPa of different pressure and operate under stoichiometric condition (Ø=1.0). Flame propagation images just show only flame kernel development process. It were not cover whole combustion process. As shown in fig 15, flame development of ethanol fuel showed the fastest rate compare with lower ethanol concentration. These can be discussed that the fuel properties, especially the oxygen content, can affect to the flame speed in term of increasing performance of reaction rate. With increasing the ethanol concentration in the fuel, oxygen content will be also increased as shown in table 2. Due to the ethanol blended fuel (E100, E85 and E20) have more oxygenated properties than the pure gasoline. Thus, flame speeds that were depended on oxidation rate were increased.

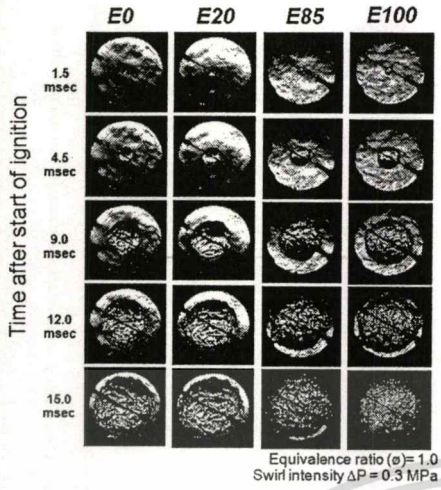

Figure 15 : Schlieren images of gasoline/ethanol blend and ethanol fuel during flame kernal development process.

Effect of ethanol content and swirl intensity on the lean limit

According to definition of lean limit that were discussed in previous section. As the coefficient of variation on peak pressure reached 20% of variation, that point may be assumed as the lean limit point. Figure 16 shows the lean limit of each tested fuel in various swirl intensities. With increasing ethanol concentration in blended fuels, the mixtures have more capability to combust at lower minimum equivalence ratio. In low swirl condition (ΔP=0.1 MPa), E0, E20, E85 and E100 have the lean limit at Ø = 0.38, Ø = 0.37, Ø = 0.33 and Ø = 0.31, respectively. These can imply that ethanol concentration have an effectiveness to improve stability of combustion, especially in overall lean condition by extending the lean limit range. This behavior can be discussed that ethanol can be ignited and combusted at the lower equivalence ratio because an air/fuel ratio of gasoline and ethanol/gasoline blends are different. Thus, if ethanol/gasoline blends are subjected to the same equivalence ratio as in the pure gasoline, additional amount of the fuel is required for the same equivalence ratio.

For the effects of swirl intensity on lean misfire limit, they have many parameters that can affect to the initial flame kernel. Therefore, any effects of temperature or ignition energy were be neglected. The initial temperature was set at 450 K, spark gap was 5 mm for related to standard conventional spark plug. Spark energy is controlled by setting ignition coil charge time which is 3 msec. The results in this study were focused only on the effects of stratification degree, which were realized by the swirl flows, to the lean limit range. From the results, it found that lean limits tend to be lowered as increase swirl strength. E0 has the lean limit at Ø = 0.38 in the lowest swirl condition while high swirl condition, E0 has the lean limit at Ø = 0.36. These results show the same trend as E20 and E85. From the result, when apply the highest swirl flow, E0, E20, E85 and E100 reached the minimum equivalence ratio at 0.36, 0.34, 0.31 and 0.30 respectively. In the lowest swirl flow condition, E0, E20, E85 and E100 have the lean limit at Ø = 0.38, Ø = 0.37, Ø = 0.33 and Ø = 0.31, respectively.

However, E100, lean limit was not significant change when applying the swirl intensities. As illustrated in fig 16, lean limit of E100 were Ø = 0.31, Ø = 0.31, Ø = 0.31Ø = 0.30 and Ø = 0.30 at swirl condition of ΔP = 0.1, ΔP = 0.2, ΔP = 0.3, ΔP = 0.4 and ΔP = 0.5 MPa, respectively.

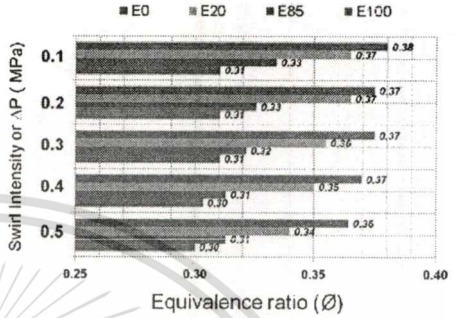

Figure 16 : Effect of ethnaol concentration and swirl intensity on lean limit.

These demonstrate that swirl intensity can support the combustion stability in the lean condition by extending the lean limit range. Even though, lean limit of pure ethanol couldn't change with swirl flow. These phenomena may be discussed that atomization and vaporization of fuel were accelerated by the increasing of turbulence intensity and decreasing of the impinged fuel, both of which were caused by the swirling flow. These can imply that swirl flow can enhance the stratification level. Hence, lean limit of gasoline(E0), E20 or E85 can be extended by swirl flow. In other word, ethanol fuel, which is comprised of only one component, has lower carbon atom than the gasoline or E20 and E85. Consequently, it may be diffused by swirl flow easier than the gasoline, E20 or E85 which are comprised of various higher carbon atoms [12]. As ethanol can easily diffuse, vaporization of ethanol fuel may be fully completed since before the ignition start regardless of swirl generation. The comparison result of E0 and E100 spray were shown in fig. 17. From the shadowgraph images, the chamber pressure was set at zero gauge pressure and temperature was 50 ℃ without swirl flow for clearly detail observation of spray pattern and avoid temperature gradient effect, it can be seen that E0 has start to vaporize earlier than E100 but when the time left, E100 fuel was fully evaporated into vapor phase faster than that of the gasoline (E0). It can imply that E0 fuel has more light and heavy fraction than ethanol fuel. Thus, the lighter components tend to be evaporated early in the beginning stage while ethanol fuel wasn't start. After the time past, heavy fraction in gasoline (E0) still remained while ethanol fuel which have only one component already completely changed into the vapor phase.

Effect of equivalence ratio on flame kernel development

The result effect of equivalence ratio on flame kernel development was shown in fig 18. As decrease the equivalence ratio or operate at leaner condition, flam kernel edge shapes of all tested fuel were deteriorated .In addition, compare with E20 and E85, higher ethanol content fuel, and show more stable flame edge. However, circular expanding flame shapes were found in E100 and E0 but in E85 and E20 blend, flame developments show the unpredictable and non-uniform shape at all equivalence ratio. However, rate of flame development was accelerated by increasing the ethanol concentration in blended fuel. These may discussed that mixture formation capability can be improved by using ethanol fuel. Furthermore, although ethanol blend have an higher octane number, oxygen content within fuel itself can enhance oxidation rate and accelerate the initial stage of combustion regardless the octane rating. The rate of flame development may be varied with the different equivalence ratio. It can be told that rate of flame development may be influenced by energy input.

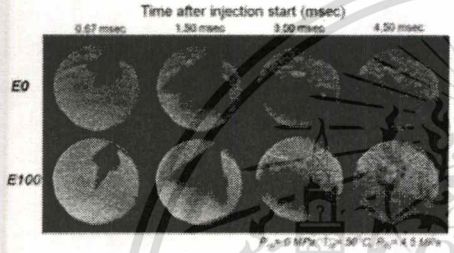

Figure 17 : Spray images of Gasoline (E0) and Ethanol (E100) fuel.

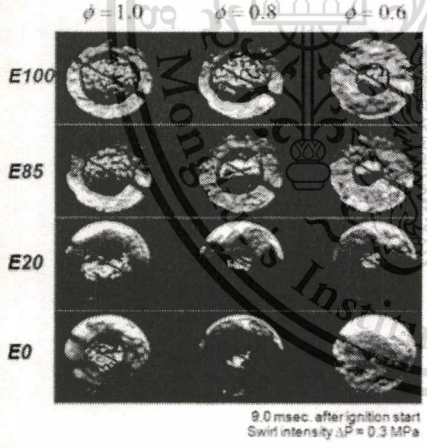

Figure 18 : Effect of equivalence ratio on flame edge stability

CONCLUSIONS

The combustion characteristics of gasoline/ethanol blends were investigated by using constant volume. combustion chamber. Following conclusions can be drawn.

1. From the results of pressure rise rate, which were corresponding to rate of heat release, blending in higher percentage of ethanol in fuel, can be enhanced combustion characteristics by accelerate flame development process and increasing the peak value of heat release rate. Furthermore, higher ethanol concentration fuel such as E100 and E85, the combustion process occur more advance than that of pure gasoline (E0) when compare with the same equivalence ratio. These may cause from the oxygen content within fuel itself can enhance oxidation rate and accelerate the initial stage of combustion regardless the octane rating.

2. In stoichiometric condition, E0 has the longest combustion duration compared with other blends. On the other hand, E100 has the shortest duration, burn rate was 50% faster than E0 while E85 and E20, combustion duration were shorten amount of 30% and 16% when compare with pure gasoline (E0). It is well known that the flame speed was related to the air/fuel ratio and mixture has the highest flame speed at equivalence ratio equal to one. From the results of combustion duration, it can imply that utilizing ethanol blended fuel can make the stoichiometric in the wider area compare with the pure gasoline (E0). Because blended fuel such as E20, E85 and E100 required more fuel injected and can be completely vaporized easier than conventional gasoline. Consequently, ethanol blended fuel have more change to join the stoichiometric mixture in wider area.

3. Higher ethanol percentages in blended fuel able to extend the lean misfire limit range. Compared with pure gasoline (E0) at low swirl condition, minimum equivalence ratio will be extended amount of 3.95%, 12.01% and 18.30% in case of E20, E85 and E100 respectively. Oxidizing performance due to oxygen concentration in fuel may be important parameter to enhance this stability. Furthermore, in higher percentage ethanol blend fuel, additional of fuel that required for maintain the same equivalence ratio can increase the chance to form stoichiometric mixture in the chamber. Thus the lean limit range will be extended.

4. Because of swirl intensity can improve the mixture distribution performance. Thus stratification degree might be increased with applying more swirl intensity. These phenomena may be discussed that atomization and vaporization of fuel was accelerated by the increase of the turbulence intensity and the decrease of the impinged fuel. Under low swirl flow condition, liquid fuel was diffused and impinged to the chamber wall. These fuel droplets formed liquid film on the cylinder wall surface and were not completely vaporized. So, less stoichiometric mixture can form in low swirl condition. In other word, swirl intensity can enhance stratification degree that directly affects the lean limit range by diffusing amount of fuel to form stoichiometric mixture in the wider area. As increase the swirl intensity, coefficient of variations (CoV) on peak pressure were decreased. Since, variations of peak pressure

reflect to the combustion stability. Consequently, high ethanol concentration and high swirl intensities can be enhanced the combustion stability by extending the lean limit range.

5. Consider in lean condition, more stable flame edge will be obtained by high percentage of ethanol blend, especially in E100 and E85. From Schlieren image, the results show that the percentage of ethanol affect to the sensitivity of flame deterioration. As decrease percentage of ethanol in blended fuel, flame shape will be less stability with reducing the equivalence ratio.

6. Even thought the Schlieren image of pure gasoline (E0) shows more uniform shape than that of E85 and E20, the flame kernel development rate was slower than all tested fuel. Due to oxygen content of tested fuel can be increased by blended more ethanol fraction in fuel. So, it can imply that oxygen concentration in fuel, especially in E100 and E85 can enhanced the reaction rate in term of higher flame speed compare with pure gasoline

For better understanding of stratified combustion phenomena, further studies should include advanced method to identify the consistency of the swirl intensities and mixture formation distribution, such as LIF method and flow field simulation as well as optimized the injection-ignition timing for the proper equivalence ratios that mixture form near the spark plug.

CONTACT INFORMATION

Chinda Charoenphonphanich (kchchind@kmitl.ac.th), Piyaboot Ormman (piyaboot.ormman@gmail.com) and Preechar Karin (kkpreech@kmitl.ac.th).

Mechanical Engineering, Faculty of Engineering, King Mongkut's Institute of Technology Ladkrabang Charongkrung 1Rd., Ladkrabang, Bangkok, Thailand 10520 Tel. 0-2326-4197, Fax. 0-2326-4198

ACKNOWLEDGMENTS

This work is supported by the fund of Automotive Laboratory, KMITL and National Science and Technology Development Agency, NSTDA, Thailand. The authors also wish to thank Pathumwan Institute of Technology for their help in measurement of pressure data acquisition.

REFERENCES

1 Thummarat Thummadetsak, C.T., Umaporn Wonggarcenpanit and Pakasit Mannum, Thailand Fuel Performance and Emissions in Flex Fuel Vehicles. SAE paper No.2010-01-2132., 2010.

2. Heywood, J.B., INTERNAL COMBUSTION ENGINE FUNDAMENTALS. 1988: McGraw-Hill

3. Bayraktar, H., Theoretical investigation of flame propagation process in an SI engine running on gasoline–ethanol blends. Renewable Energy 32 (2007) 758–771, 2007

4. Harry L. Husted, W.P.a.G.R., Fuel Efficiency Improvements from Lean, Stratified Combustion with a Solenoid Injector. SAE paper No.2009-01-1485., 2009.

5 F. Zhao, M.-C.L., D.L. Harrington Automotive spark-ignited direct-injection gasoline engines. Progress in Energy and Combustion Science. 1999. Elsevier Science Ltd.

6 Geoff J. Germane, C.G.W., Clay C. Hess Lean Combustion in Spark-Ignited Internal Combustion Engines - A Review. SAE paper No 831694., 1983

7 Naoki Shiraishi, K.S., Syoji Nagasaka,Takayoshi Takano and Hiroshi Sami, A Study on Direct Injection Gasoline Combustion using Constant Volume Combustion Vessel. The Fifth International Symposium on Diagnostics and Modeling of Combustion in Internal Combustion Engines (COMODIA 2001). 2001.

8 Z. Huang, S.S., T. Ueda, H. Nakamura, T. Ishima, T. Obokata, Effect of Fuel Injection Timing Relative to Ignition Timing on the Natural-Gas Direct-Injection Combustion. Journal of Engineering for Gas Turbines and Power, 2003.

9 Kihyung Lee, C.L., and Haeyoung Jeoung, A Study on the Effect of Stratified Mixture Formation on Combustion Characteristics in a Constant Volume Combustion Chamber. JSME International Journal Series B, Vol.48, 2009.

10 Jinhua Wang, Z.H., Haiyan Miao, Xibin Wang, Deming Jiang, Study of cyclic variations of direct-injection combustion fueled with natural gas/hydrogen blends using a constant volume vessel. international journal of hydrogen energy 33 (2008) 7580 – 7591., 2008.

11 Myung Yoon Kim, D.S.K., and Chang Sik Lee, Effect of Residual Gas Fraction on the Combustion Characteristics of Butane-Air Mixtures in the Constant-Volume Chamber. Energy & Fuels 2003, 17, 755-761, 2003.

12 Jian Gao, D.J., Zuohua Huang, Spray properties of alternative fuels: A comparative analysis of ethanol–gasoline blends and gasoline. Fuel 86 (2007) 1645–1650, 2007

13 Eiji Tomita, A.K., and Nobuyuki Kawahara Effects of Swirl Flow and Inhomogeneous Concentration Fields on Combustion of Propane-Air Mixture in a Constant-Volume Vessel. JSAE paper No.700-8530, 2000.

14. Masahiko Fujimoto, M.T., Effect of Swirl Rate on Mixture Formation in a Spark Ignition Engine Based on Laser 2-D Visualization Techniques. SAE paper No.931905, 1993.

The 7th International Conference on Automotive Engineering (ICAE-7)

March 28 – April 1, 2011, Challenger, Impact, Muang Thong Thani, Bangkok, Thailand

Effect of Ethanol Concentration of Gasohol on Lean Flammability Limit in Direct-Injection Stratified Charge Engine

Piyaboot Ornman[1], Chinda Charoenphonphanich[2], Nuwong Chollacoop[3] and Hidenori Kosaka[4]

[1] TAIST TokyoTech Automotive Engineering Program, International College, King Mongkut's Institute of Technology Ladkrabang, THAILAND

[2] Department of Mechanical Engineering, Faculty of Engineering, King Mongkut's Institute of Technology Ladkrabang, THAILAND

[3] National Metals and Materials Technology Center (MTEC), THAILAND

[4] Department of Mechanical Engineering, Tokyo Institute of Technology, JAPAN

ABSTRACT

Lean combustion in spark ignition engine has been recognized as mean of both improving engine efficiency and lowering exhaust emissions. However, combustion stability of this combustion has been challenging. Misfiring due to improper mixture strength in lean operation may be occurred. There are various parameters related to stability on lean combustion such as swirl or tumble flow intensities, ignition timing, spark energy and fuel properties. In this study, effect of ethanol concentration, E0, E20, E85 and E100, on lean limit were experimentally investigated in various swirl intensities by using a constant volume combustion chamber. Coefficient of variation (CoV) and combustion pressure data were observed and analyzed by using high resolution pressure transducer. Experimental results show that the lean limit of gasoline (E0) can be extended by using higher percentage of ethanol content and higher swirl intensity. In addition, high swirl intensities direct injection ethanol fuel combustion can achieve the stable lean combustion along with low cyclic variation due to the mixture stratification in the chamber. The cyclic variation decreases with ethanol concentration and swirl flow intensity.

INTRODUCTION

Due to global energy demand and stringent pollution regulations have been continuously increase, development of internal combustion engine that can be improved both efficiency and fuel economy are very challenge and interesting while ability to reduce pollutant emission should not be neglected.

Lean burn system concept, direct injection stratified charge combustion, is the well known technique for reduce fuel consumption and correspondingly improve engine efficiency. In theory, for an Otto-cycle engine, the efficiency η_{th} can be written as $\eta_{th} = 1-(1/r_c^{\kappa-1})$, where r_c is compression ratio and κ is specific heat ratio. As an engine operate leaner, the specific heat ratio of combustion mixture become higher. If the specific heat ratio (κ) can be further raised, the heat efficiency and engine power output can be improved (1). In addition, volumetric efficiency in stratified charge engine could be increased by cooling effect form direct injection process (1), (2). Furthermore, in this concept, engine is operated under unthrottled operation. Thus, engine load was controlled by amount of fuel injected. Therefore, the engine will significant reduce the pumping loss, especially at low load (3). Although this

combustion technique can achieve many kinds of advantage for combustion efficiency, it produces much unburned hydrocarbon and soot because of inhomogeneous charge mixture in the combustion chamber. The main problem is a misfiring under lean operation. Consequently, unstable driving condition and high unburned hydrocarbon emission will be occurred (4).

To investigate this problem, there were many parameters that influenced on combustion characteristics such as ignition timing, ambient temperature, ambient pressure (5) and spark energy etc (6). Moreover, fuel effect should not be neglected. Alcohol, especially ethanol, was the new challenge candidate in alternative fuel since it can be produced from many source of biomass and is indeed the renewable energy. In addition, the raw materials for ethanol production, cassava and sugarcane, are also the main economic vegetation in Thailand. Although the lower heating value of ethanol is lower than that of gasoline, ethanol release a little more heat than gasoline under the same equivalence ratio. However, the high latent heat will lead to a decrease in in-cylinder temperature and hence result in low NOx emission. Moreover, a high octane number will allow an increase in high compression ratio, thus, an engine fueled with ethanol can have higher power output and better thermal efficiency. Furthermore, these are oxygenated fuels which are beneficial to the reduction of soot emission (7).

In this study, effect of ethanol content on the lean misfire limit in stratified charge combustion, was investigated by means of constant volume combustion chamber. In addition, the effect of swirl intensities on combustion characteristics has also been considered for improving combustion stability purpose.

As mention in the early part, the consumption of using fossil fuel, gasoline, can be reduced by increased engine efficiency and by expanded use of renewable fuels. The concept could also facilitate expanded use of ethanol, a renewable fuel whose use is growing worldwide. Through this study, a better understanding of stratified charge combustion run on ethanol/gasoline blends can be achieved.

EXPERIMENTAL APPARATUS AND PROCEDURE

EXPERIMENTAL APPARATUS

Since, there are many parameters that affect to the combustion behavior. Thus, the fuel effect on combustion characteristics in this experimental were studied and observed by using a constant volume combustion chamber to avoid the error variation from various part in the real engine such as piston geometry, valve timing and ignition timing.

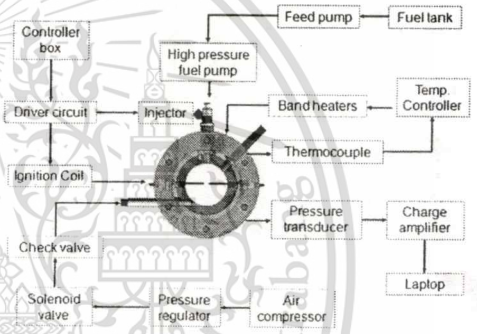

Figure 1 : Schematic diagram of experimental apparatus

Figure 1 shows the schematic diagram of experimental apparatus. This experiment setup comprise of four major systems. First, the air supply system. Pressure regulator was used to regulate the induced fresh air and check valve was use to prevent the combust gas flow back to air inlet system. Second, the fuel system. Low pressure was use to feed the fuel in the first step before sent to high pressure pump. Third, the controller system, in this system, they consist of controller box and injector and also the ignition driver circuit. The last system was the data acquisition system. In addition, for control the initial air temperature, band heater were used and controlled by separated temperature controller box.

Detail of constant volume and combustion chamber and theirs measurement device were

shown in Fig. 2. The internal diameter and width of the chamber are 70 mm and 100 mm, respectively. The volume capacity is 385cc. The quartz glass windows with 35 mm thickness are equipped at both sides of the combustion chamber for optical access and visualization of the flame propagation. Swirl port allows the induced air to flow into the combustion chamber in the tangential direction to realize the swirl flow in the chamber. Graphite gaskets are attached in both side of quartz glass to absorb impact load from combustion. The spark plugs are located to the central of the combustion chamber to generate the spherically expanding flame and prevent heat transfer to the chamber wall.

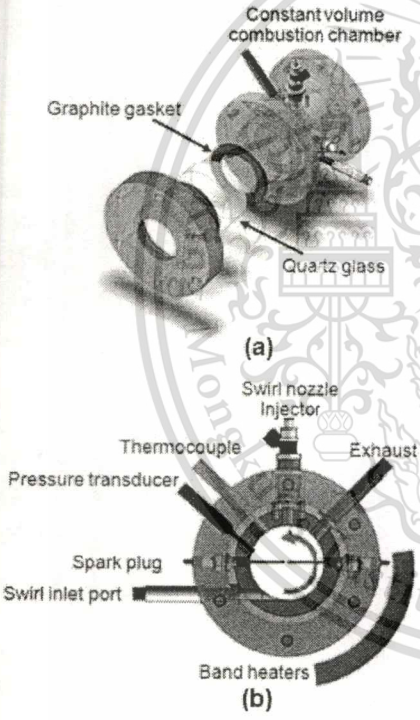

Figure 2: Schematic diagram of the constant volume combustion chamber in (a) disassembly and (b) cross-section views

Ambient pressure (P_a) that is the initial pressure inside the chamber is controlled by adjusting the pressure regulator, which also induces pressure corresponding to the swirl intensities. A piezo-electronic pressure transducer (Kistler model 611BFD16) was used to measure the combustion pressure and the charge amplified electrical signals including high speed data acquisition system (Dewetron model DEWE-5000) were used to record the signal from the pressure sensor .Two band heaters (1300 W) were attached to the chamber wall to control the initial temperature (T_i).

EXPERIMENTAL PROCEDURE

First, pressurized air induced from air compressor tank was regulated according to No. of swirl intensity by pressure regulator. Then, flow though to the combustion chamber by the swirl inlet port for realizing the swirl flow with combustion chamber. Then, tested fuel were delivered from fuel tank to high pressure pump by low pressure feed pump. After that, the cam-driven high pressure fuel pump will pressurize the fuel up to 40 MPa before deliver to the direct injection injector.

Since ethanol-blended gasoline fuels are in the liquid phase at the normal temperature, initial temperature in this experiment was fixed at 450K, which is higher than evaporation temperature of all tested fuel for avoid misfire when the fuel was injected into the combustion chamber (8). To observe combustion behavior in early stage of combustion, the initial pressure (P_i) was set at 0.5 MPa. The total equivalence ratio was varied from 1.0 to minimum combustible value.

Table 1. Experiment condition

Experimental variables	Conditions
Initial temperature (K)	450
Initial pressure (MPa)	0.5
Ignition time (msec)	10
Injection pressure (MPa)	4.5
Inj – Ign Interval (msec)	12
Equivalent ratio	Less than 1.0
Swirl intensities or ΔP (MPa)	0.5,0.4,0.3,0.2,0.1

According to table 1, the ignition duration was set at 10 msec. Time duration from injection to ignition in this experiment was fixed at 12 msec to ensure that the fuel spray can be fully developed.

In order to manage the air induction timing, injection duration, injection – ignition interval and also the camera triggering, The controller box was use to interface with self-building software via laptop or PC. As show in Fig. 3, the signal sequences from controller command to the air solenoid valve, injector and ignition coil according to the given timing.

Finally, during the combustion process. The combustion pressure signal that was recorded by the pressure transducer will be conditioned and sent to the charge amplifier. Then these signals were analyzed by data acquisition software in laptop or PC.

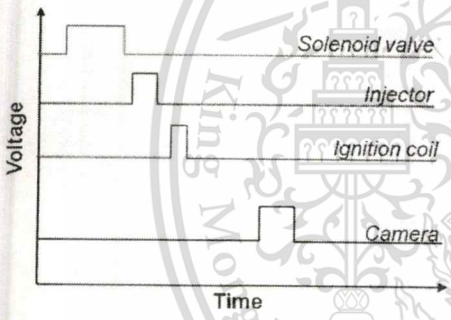

Figure 3: Signal sequence pattern

Setup of equivalent ratio (Ø)

For calculation of the equivalent ratio, the following equation can be used (1).

$$\phi = \frac{(m_f / m_a)_{actual}}{(m_f / m_a)_{theory}}$$

Where $(m_f / m_a)_{actual}$ is real fuel /air ratio and

$(m_f / m_a)_{theory}$ is theoretical fuel /air ratio

$(m_f / m_a)_{theory}$ can be calculated by means of chemical equilibrium of combustion. The fuel properties and their air/fuel ratio are shown in table 2 while actual air mass $(m_a)_{actual}$ were calculated base on ideal gas law using initial pressure, initial temperature and combustion chamber volume. Thus, equivalent ratio (ϕ) will be varied by changing in fuel mass injected $(m_f)_{actual}$ the mass of the injected fuel was calibrated with the injection duration time as shown in Fig. 4

Table 2 Fuel properties (9), (10), (16), (17)

Fuel	E0	E20	E85	E100
Formula	($C_{8.26}H_{15.5}$)	-	-	(C_2H_5OH)
molecular weight	114.18	88.12	50.60	46.07
Ethanol content (% vol)	0.0	19.9	78.9	100.0
Oxygen content (% wt)	0.0	7.54	31.75	34.7
LHV (MJ/kg)	44.0	-	-	26.9
Air/fuel ratio	14.63	13.51	9.87	9.03
Heat of vaporization (kJ/kg)	305	-	-	840
RVP (kPa)	58.4	59.0	44.4	16.0
Specific gravity	0.72-0.78	0.7604	0.7830	0.8
RON	92.0-98.0	98.3	101.6	107.0
MON	80.0-90.0	84.6	91.1	89.0

Lean limit investigation

As known, the important thing in stratified charge combustion is the stability of the flame. Misfire will occur if the mixture and condition are not suitable to ignite. Overall lean mixtures have an opportunity to deteriorate the combustion stability. Due to differences in fuel properties, lean limit of each fuel should be investigated.

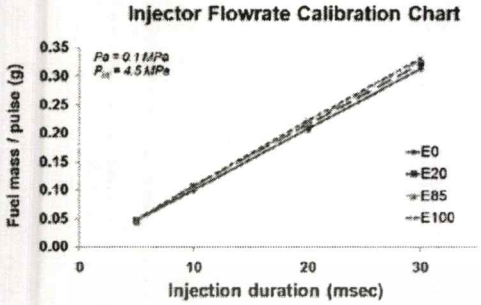

Figure 4: Calibrated chart for injection duration against the fuel mass

The statistic data analysis was chosen in this experiment to investigate the proper lean limit or minimum equivalence ratio that mixture can be ignited at certain pressure and temperature. From pressure data, 10 data from each condition were collected for each fuel. If the misfire occurs, it will increase the coefficient of variation (CoV). Therefore, if it exceeds the acceptable value, which was set to 20% of CoV (12) (13) in the current study. It implies that mixture does not ignite. In this experimental analysis, minimum equivalence ratio at the maximum acceptable CoV is assumed as the lean limit (4). In addition, CoV can be derived by following equation (1).

$$\mathrm{CoV}_x = \frac{\sigma_x}{\bar{x}} \times 100\%$$

Where,

$$\bar{x} = \frac{1}{N}\sum_{i=1}^{N} x_i$$

And the standard deviation

$$\sigma_x = \sqrt{\frac{\sum_{i=1}^{N}\left(x_i - \bar{x}\right)^2}{N}}$$

RESULT AND DISCUSSION

EFFECT OF ETHANOL CONCENTRATION ON LEAN MISFIRE LIMIT

According to lean limit investigation that be described in experimental procedure part, Coefficient of variation on peak pressure (CoV_{Pmax}) of each tested fuel were plotted against the equivalence ratio (Ø) as show in Fig 5. In this graph, it was shown only in medium swirl flow condition but the test fuel were varied from zero ethanol content or pure gasoline (E0) to hundred percentage of ethanol blend or pure ethanol (E100).

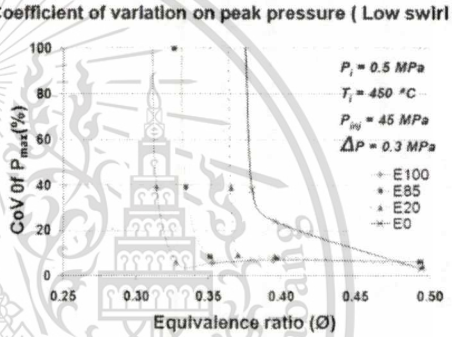

Figure 5: Coefficient of variation on peak pressure in medium swirl condition

The maximum set point of (CoV_{Pmax}) that assume as the lean misfire limit was 20% of CoV (12), (13). At this point, the fuels reach the minimum equivalence ratio that can be ignited. The lean misfire limit of various blend in deferent swirl condition were shown in Fig 6.

As indicated in Fig 6, for low swirl condition (ΔP = 0.1 MPa), Gasoline or E0 has the highest value of equivalence ratio (Ø) equal to 0.38; whereas, those of E20, E85 and E100 are 0.365, 0.334 and 0.310, respectively. The result shows little change in minimum equivalence ratio since higher percentage of the ethanol has less effect to enhance lean limit range than the lower ethanol content.

Pure ethanol (E100) has minimum lean limit in all swirl intensities compared with other fuels.

On the other hand, pure gasoline or E0 shows the highest value of lean limit in every swirl condition.

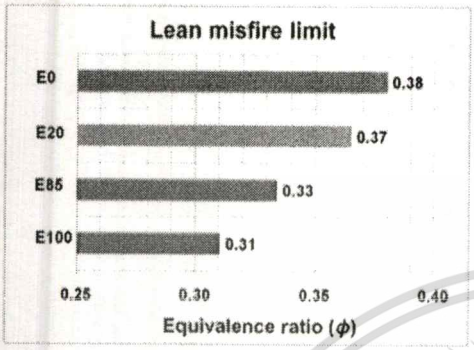

(a) Low swirl condition (ΔP=0.1 MPa)

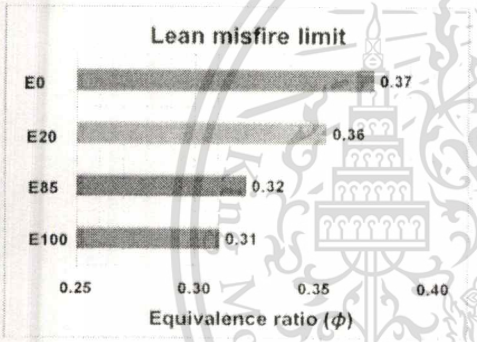

(b) Medium swirl condition (ΔP=0.3 MPa)

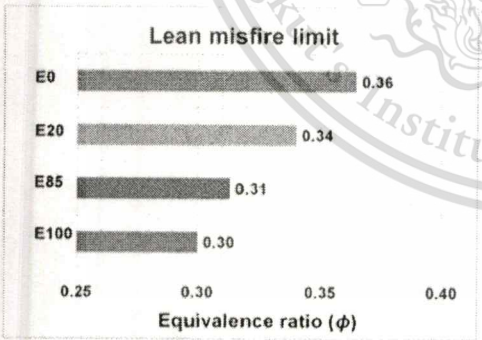

(c) High swirl condition (ΔP=0.5 MPa)

Figure 6: Lean misfire limit of various blends in deferent swirl condition

As the ethanol content increases, the mixtures will combust in lower equivalence ratio. Pure ethanol reaches lowest equivalence ratio of 0.30, in the highest swirl condition which means that ethanol content can support the combustion stability in the lean condition. This behavior can be discussed that ethanol can be ignited and combusted at the lower equivalence ratio because an air/fuel ratio of gasoline and ethanol/gasoline blends are different. Thus, if ethanol/gasoline blends are subjected to the same equivalence ratio as in the pure gasoline, additional amount of the fuel is needed for the same equivalence ratio. For example, at equivalence ratio equal to 1.0, the stoichiometric air/fuel ratio of each fuel in Table 2. Shows that AFRE0=14.6, AFRE20=13.5, AFRE85=9.87 and AFRE100=9.0. When compare to the same equivalence ratio as pure gasoline (E0), additional amount 8.24%, 48.15% and 62.01% of fuels were required to E20, E85 and E100 respectively. Consequently, the mixture which have the higher percentage of ethanol in constant volume chamber will have more chance to form mixture near stoichiometric ratio than that the pure gasoline (E0). Furthermore, ethanol fuel was the oxygenated fuel and also comprised of only one component, while gasoline is a mixture of many components with various carbon atoms and structures. The components with relatively low boiling points evaporate easier and faster, while the components with higher boiling points will evaporate more slowly. Thus, the mixture formation preparations in injection process of ethanol blend were more effective than the pure gasoline (E0) and allow the mixture to be ignited at the lower equivalence ratio (14), (7).

EFFECT OF SWIRL INTENSITIES ON LEAN MISFIRE LIMIT

Figure 7 shows the lean limit of each tested fuel in various swirl intensities. As the swirl intensities increase, the fuels tend to be ignited at the lower equivalence ratio. For pure gasoline (E0), the minimum equivalence ratio or lean misfire limit was 0.38 at low swirl condition (ΔP = 0.1 MPa), while in the highest swirl condition (ΔP = 0.5 MPa), lean misfire limit is 0.36. In higher ethanol content, the

same trend as the pure gasoline (E0) was obtained but the result was less than expected.

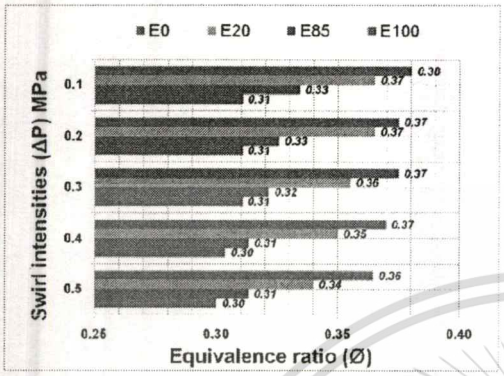

Figure 7: Lean misfire limit of each tested fuel in various swirl intensities

For pure ethanol (E100), equivalence ratio at lean limit were 0.310, 0.310, 0.310, 0.304 and 0.300 at swirl intensity equal to ΔP = 0.1 MPa, 0.2 MPa, 0.3 MPa, 0.4 MPa and the highest swirl flow (ΔP = 0.5 MPa), respectively. These results demonstrate that the swirl intensities can be improved the combustion stability by means of extending the lean misfire limit of the mixtures. From the result, when apply the highest swirl flow, E0, E20, E85 and E100 reached the minimum equivalence ratio at 0.364, 0.340, 0.310 and 0.30 respectively. From these results, we can discuss in that in for stratified combustion, it was just some amount of mixture, which can be ignited, especially that of stoichiometric mixture. In higher swirl intensity, stratification degree (8), (15) which are characterized by a ratio of stoichiometric mixture over the overall lean mixture became higher, therefore, rich and lean limit of the mixture become wider (15).

CONCLUSION

The lean misfire limit on gasoline/ethanol blend was investigated by using constant volume combustion chamber. Following conclusion can be drawn.

Higher ethanol percentages in blended fuel able to extend the lean misfire limit range. Compare with pure gasoline (E0) at low swirl condition, minimum equivalence ratio will be extended amount of 3.95%, 12.01% and 18.30% in case of E20, E85 and E100 respectively. These demonstrate that ethanol fuel able to improve combustion stability in lean operation. These can be discussed that, for operate at the same equivalence ratio, additional fuel injected of ethanol blended fuel may increase the chance of fuel to form near stoichiometric.

In the same manner as increase the swirl intensity, coefficient of variation (CoV) on peak pressure will be decrease with increasing ethanol percentage in fuel. Since, variations of peak pressure reflect to the combustion stability. Consequently, high ethanol concentration and high swirl intensities can be enhance the combustion stability by extending the lean limit range.

As increase the swirl intensity, lean misfire limit (minimum equivalence ratio which corresponding to 20% of CoV) of all blended fuel tend to be decreased. These may be cause from the atomization and vaporization of fuel was accelerated by the increase of the turbulence intensity and the decrease of the impinged fuel, both of which were caused by the swirling flow. Under low swirl flow condition, liquid fuel was diffused and impinged to the chamber wall. This fuel droplets formed liquid film on the cylinder wall surface and was not completely vaporized. So, less stoichiometric mixture can form in low swirl condition. In other word, swirl intensity can enhance stratification degree that directly affects the lean limit range by diffusing amount of fuel to form stoichiometric mixture in the wider area. However, high ethanol concentration fuel e.g. E100, Lean limit was not significantly change with swirl intensities. Compare between the lowest and the highest swirl condition, lean limit of E0, E20, E85 and E100 can be extended approximately 4.1%, 6.1 %, 6.3% and 3.4% respectively.

ACKNOWLEDGMENTS

This work is supported by the fund of Automotive Laboratory, KMITL and National Science and Technology Development Agency, NSTDA – Thailand. The authors also

wish to thank Pathumwan Institute of Technology for their help in measurement of pressure data acquisition

REFERENCES

[1] John B. Heywood, "Internal Combustion Engine Fundamental" ISBN: 0-07-100499-8, 1988.

[2] Zhao F., "Automotive spark-ignited direct-injection gasoline engines", Progress in energy and combustion science 25 (Pgs. 437-562), 1999.

[3] Zhao F., Lai M.C., Harrington D.L., "Automotive spark ignited direct injection gasoline engines", ISBN: 0-08-043676-5, 1999.

[4] Wood G., Germanw J., Carl G., "Lean combustion in spark ignition internal combustion engine –A Review", SAE paper No. 831694, 1983

[5] Shiraishi N., Sakai K., Nagasaka S., "A Study on Direct Injection Gasoline Combustion using Constant Volume Combustion Vessel", The Fifth International Symposium on Diagnostics and Modeling of Combustion in Internal Combustion Engines, 2001

[6] Jeonghoon S., Lee D.H., "Experimental Study of Ignition of a Gasoline Air Mixture in a Constant-Volume Combustion Chamber" Combustion, Explosion, and Shock Waves, Vol. 39, No. 5, 2003.

[7] Xibin W., Wansheng C., Jian G., Deming J., "Spray characteristics of high-pressure swirl injector fueled with Alcohol", Higher Education Press and Springer-Verlag, 2007.

[8] Kihyung L., Changhee L., Haeyoung J., "A Study on the Effect of Stratified Mixture Formation on Combustion Characteristics in a Constant Volume Combustion Chamber", JSME International Journal No 2, Vol. 48, 2005.

[9] Ganesan V., " Internal combustion engine" 2nd edition, McGrw-Hill publishing Co,ltd, ISBN 007-123656-2, 2004

[10] The Government gazette,Thailand, "Determination of Gasohol fuel characteristics and qualities", 2003.

[11] Jinhua W., Zuohua H., Haiyan M., Xibin W., Deming J., "Characteristics of direct injection combustion fuelled by natural gas–hydrogen mixtures using a constant volume vessel", International journal of hydrogen energy,Vol 33, 2008

[12] Jinhua W., Zuohua H., Haiyan M., Xibin W., Deming J., "Study of cyclic variations of direct injection combustion fueled with natural gas–hydrogen blends using a constant volume vessel", International journal of hydrogen energy, Vol. 33, 2008.

[13] Jian Gao et.al. "Spray properties of alternative fuels: A comparative analysis of ethanol–gasoline blends and gasoline", Fuel 86, No 1645–1650. 2007.

[14] Tomita E., Nishiyama A., "Effects of Swirl Flow and Inhomogeneous Concentration Fields on Combustion of Propane-Air Mixture in a Constant-Volume Vessel ", JSAE paper No 700-8530, 2000.

[15] Tabata M., Fujimoto M., "Effecft of swirl rate on mixture formation in a spark ignition engine based on laser 2-D visualization techniques", SAE technical paper paper No 931905, 1993.

[16] Larsen U., Johansen T., Schramm J., International Energy Agency (IEA),"Ethanol as a Fuel for Road Transportation", 2009 .

[17] Thummadetsak T., Tipdecho C., Wongjareonpanit U., Monnum P., "Thailand Fuel Performance and Emissions in Flex Fuel Vehicles", SAE paper No.2010-01-2132, 2010.

General Announcement and Call for Abstracts

The First TSME International Conference on Mechanical Engineering (TSME - ICoME)

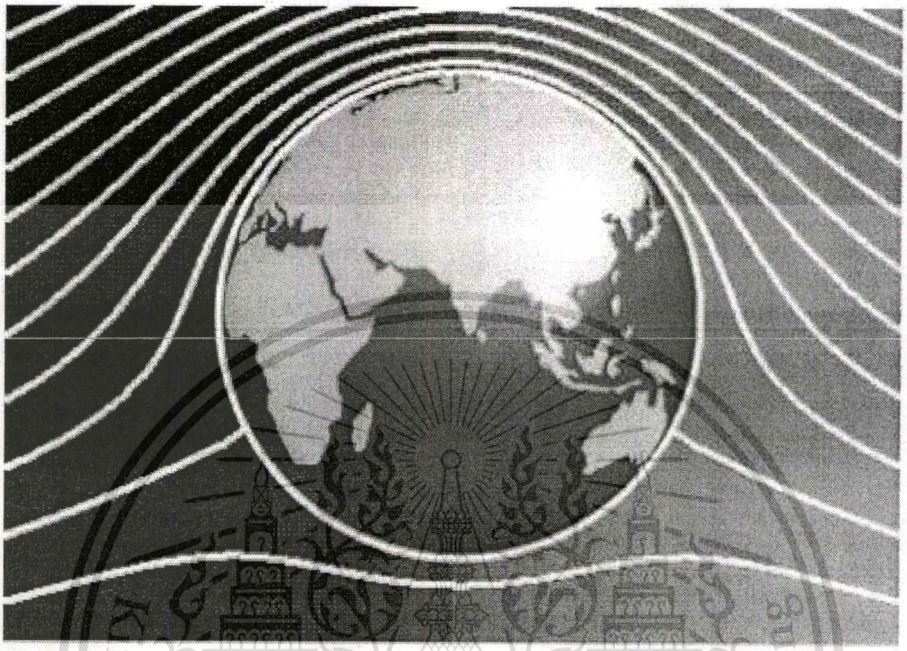

TSME - ICOME

1st International Conference on Mechanical Engineering

October 20-22, 2010
Sunee Grand Hotel
Ubonratchathani, Thailand

The First TSME International Conference on Mechanical Engineering
20-22 October, 2010, Ubon Ratchathani

Study on Combustion Characteristics of Direct Injection Stratified Charge in Ethanol/Gasoline Blends

Piyaboot Omman[1], Assoc.Prof. Hidenori Kosaka[2],
Dr.Nuwong Chollacoop[3] and Chinda Charoenphonphanich[*1]

[1] Department of Automotive Engineering (International Program),
Faculty of Engineering, King Mongkut's Institute of Technology Ladkrabang, Bangkok,
Thailand 10520
[2] Department of Mechanical Engineering, Tokyo Institute of Technology, Japan
[3] National Metals and Materials Technology Center (MTEC), Pathumthani, Thailand 12120
[*1] Corresponding Author: Tel: 0-2326-4197, Fax: 0-2326-4198 E-mail: piyaboot.omman@gmail.com

Abstract

In this research, combustion characteristics of gasoline/ethanol blends in direct injection stratified charge engine were carried out using a constant volume combustion chamber. To evaluate the influence of blending on the combustion behavior .The flame propagation of different blends of ethanol–gasoline blends (20%, 85% and 100% ethanol) as well as pure gasoline were investigated under various swirl intensities and equivalence ratios. Pressure data taken during the testing allowed for detailed analysis. The different blend of fuels were compared in terms of combustion characteristics , rate of pressure rise, combustion duration, flammability limit also stratification degree that demonstrate the stability of combustion in lean operation will be investigated and discussed.

Key words: Constant volume combustion chamber, direct injection, stratified charge, Ethanol/gasoline blends, Swirl intensities

1. Introduction

In the recent years, Trend of consumption in energy was increasing continuously. Alcohols, especially ethanol was the new challenge candidate in alternative fuel due to it can be produced from many source of biomass and were the renewable energy. In addition, the raw material for produced ethanol, cassava or sugarcane was the main economic vegetation in Thailand. Although the lower heating value of alcohols is lower than that of gasoline, alcohols release a little more heat than gasoline under the same equivalence ratio. Moreover, a high octane number will allow an increase in high compression ratio; thus, an engine fueled with ethanol will have high power output and better thermal efficiency.

For stratified charge engine, it is well know that lean, stratified combustion can reduced fuel consumption and gain some merits in

gasoline spark-ignited, direct injection engines for several reasons. First, unthrottled operation allows for a significant pumping loss reduction, especially at lower loads. Second, the lean mixture being compressed has a higher ratio of specific heats. This allows for a more efficient compression and expansion process. Third, there are lower wall heat losses in the cylinder because of the centralization of the mixture away from the walls [1].

This challenge to utilize ethanol and ethanol-gasoline blends to direct injection gasoline engines .It were very interested because ethanol has an anti-knock properties also it has higher heats of vaporization compared to pure gasoline and it can combust with higher compression ratio[2], follow to its consequences, using ethanol in Stratified-charge, spark-ignition, direct-injection engines are capable of achieving significant gains in efficiency both volumetric efficiency and thermal efficiency[3].

Although this combustion can achieve many kinds of advantage to combustion characteristics, it produces much unburned hydrocarbon and soot because of inhomogeneous of the charge mixture in the combustion chamber and the main problem is misfiring under lean operation [4]. Even if whole air-fuel mixture is very lean. In stratification, air-fuel ratio tends to be over-rich in the middle of the mixture and over-lean in the periphery bordering surrounding air. It is essential to minimize the above air-fuel ratio difference by enhancing the stratification degree which represents the ratio of fuel quantity involved in nearly stoichiometric mixture zone to total fuel quantity. As the stratification degree becomes low, unburned fuel amount increases and fuel economy deteriorates. Therefore, it is necessary to investigate the combustion characteristics in order to obtain the stable lean combustion.

In the combustion characteristics of stratified charge combustion, they have much kind of influences factors that effect to the combustion process such as physical properties of the fuel, swirl intensity, ignition timing, equivalent ratio, ambient temperature and pressure etc.

In this study, the effect of swirl ratio, on the combustion characteristics are investigated to the gasoline/ethanol blends which vary from pure gasoline (E0) to pure ethanol (E100) in the constant volume combustion chamber. With the pressure analysis data, the rate of pressure rise (dp/dt), combustion duration and mass fraction burned rate were analyzed. Through this study, a better understanding of stratified charge combustion run on gasoline/ethanol blends can be achieved.

2. Experimental apparatus and procedure

2.1 Experimental apparatus

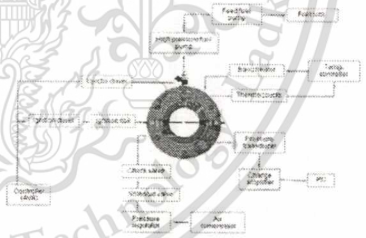

Fig.1. Schematic diagram of experimental apparatus

Fig.1 shows the schematic diagram of the experimental apparatus used in this study. The following equipments were used: a constant volume combustion chamber, cam-driven pump

provide the high pressure fuel to the injector, an air compressor and a intake swirl port with pressure regulator for making a swirl intensities and inducing the fresh air charge into the combustion chamber, a swirl nozzle injector, heating system for controlling the air temperature in combustion chamber, an conventional ignition system of the CDI (capacitor discharge ignition) type for generating ignition energy, pressure and temperature measuring equipment, Controller box was used to control the signal sequence and to interface with a data acquisition system.

2.1.1 Constant volume combustion chamber

Fig. 2 shows a schematic diagram of the constant volume combustion chamber. The internal diameter and width of the chamber were 70 mm and 100 mm, respectively. The volume capacity was 385cc. The quartz glass windows with 35 mm thickness are equipped at both end sides of the combustion chamber for optical access and visualize the flame propagation. Swirl port is allowed the induced air to flow into the combustion chamber in the tangential direction to realize the swirl flow in the chamber .Graphite gasket are attached in both side of quartz glass to absorb impact load from combustion. The spark plug are located to the central of the combustion chamber for generate the spherically expanding flame and prevent heat transfer to the chamber wall.

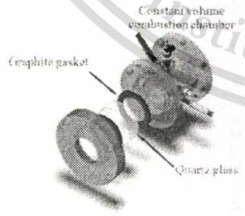

Fig.2 (a) Disassembly of the constant volume

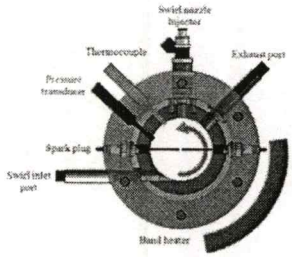

Fig.2 (b) Detail of measuring devices

Figure 2. Schematic diagram of the constant volume combustion chamber.

Ambient pressure (Pa) that is the initial pressure inside the chamber is controlled by adjusting the pressure regulator, also the induced pressure which corresponding to the swirl intensities. A piezo-electronic pressure transducer (Kistler model 611BFD16) is used to measure the combustion pressure and the charge amplified electrical signals including high speed data acquisition system (Dewetron model DEWE-5000) are used to record the signal from the pressure sensor .Two band heaters (1300 W) were attached to the chamber wall to control the initial temperature (Ta).

2.2 Experimental procedure

Table.1 is shown the experimental condition

Experimental variables	Conditions
Ambient temperature (K)	450
Ambient pressure (MPa)	0.5
Ignition time (msec)	10
Injection pressure (MPa)	4.5
Ignition time (msec)	12
Equivalent ratio	1.0,0.8,0.6
Swirl intensities or ΔP (MPa)	0.0,0.1,0.2,0.3,0.4

Because of gasoline and ethanol blends fuel are in the liquid phase at the normal temperature, initial temperature in this experiment is fixed at 450K, which is higher than evaporation

temperature of all tested fuel for avoid misfire when injected the fuel into the combustion chamber. For observe combustion behavior in early stage of combustion, the initial pressure (Pa) is set at 0.5 MPa. The total equivalence ratio was simulating in overall lean condition, since they were adjust to 1.0, 0.8, and 0.6.

2.2.1 Setup of equivalent ratio (Ø)

The mass of the injected fuel will be calibrated in additional chart that relate to the time of injection as shown below in Fig.3

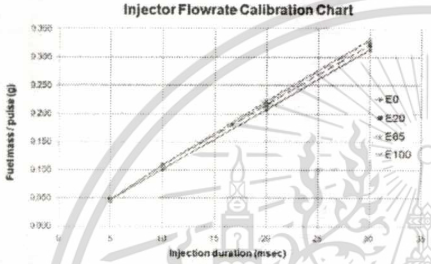

Fig.3. Calibrated chart for injector

The injection duration can be controlled by the controller according to the air mass which is prior induced into the combustion chamber. Air mass in this experiment can be calculated follow these equations.

$$m_{(air\ total)} = m_{initial} + m_{swirl} \quad (1)$$

Where, $m_{initial}$ can be calculated from ideal gas law at initial pressure and m_{swirl} can be directly measured by anemometer

For calculate the equivalent ratio, this equation can be use

$$\phi = \frac{(m_f / m_a)_{actual}}{(m_f / m_a)_{theory}} \quad (2)$$

Where, $(m_f / m_a)_{actual}$ is real fuel /air ratio

$(m_f / m_a)_{theory}$ is theory fuel /air ratio

From equation (2) theory air/fuel ratio can be calculated from the chemical equilibrium. And following table is shown the fuel properties.

Table.2 is shown the fuel properties[6]

Fuel	E0	E20	E85	E100
Formula	$(C_{8.25}H_{15.5})$	-	-	(C_2H_5OH)
molecular weight	114.18	88.12	50.6	46.07
LHV (MJ/kg)	44	-	-	26.9
Air/fuel ratio (stoi)	14.625	13.51	9.872	9.027
Heat of vaporization (kJ/kg)	305	-	-	840
Specific gravity	0.72-0.78	-	-	0.8
RON	92-98	-	-	107.0
MON	80-90	-	-	89.0

The ignition duration time is set at 10 msec. Duration time from injection to ignition in this experiment is fixed at 12 msec for ensure that the fuel spray can be fully developed. Swirl intensities were controlled by the different pressure between the air induced pressure and the chamber pressure. All of time parameters and sequence of signal were controlled by the PC interface program as show in Fig.4

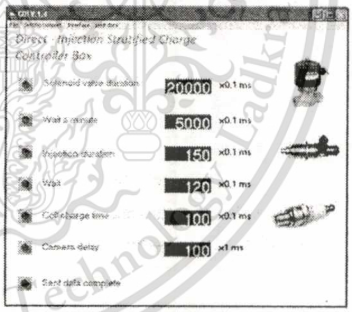

Fig.4 Interface window for controlling the signal sequences

After induce the pressurized air into the chamber for generate swirl flow, the swirl nozzle injector will injected the fuel directly in to the combustion chamber, then, spark plug will be

ignited the mixture as the same time as the data acquisition record the pressure data. This signal sequences are shown in Fig.5.

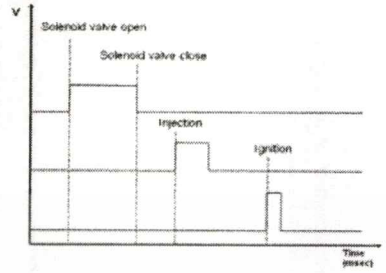

Fig.5 Pattern of signal sequence

2.2.2 Lean limit investigation

As we know, the important thing in stratified charge combustion is the stability of the flame. Misfire will be occur if the mixture and condition aren't suitable to ignite. Overall lean mixture have an opportunity to deteriorate the combustion stability and because of different in fuel properties . Since , Lean limit of each fuel should be investigated

The statistic data analysis is choose in this experiment for investigate the proper lean limit or minimum equivalence ratio that mixture can be ignited at certain pressure and temperature. From pressure data, we collect 10 data from each condition and each fuel. If the misfire occurs it will increase the coefficient of variation (CoV) .Therefore, if it exceed the acceptable value, in this experiment is set at 20% of CoV[8], it means mixture does not ignite. In this experimental analysis ,minimum equivalence ratio at the maximum acceptable CoV is assumed as the lean limit.

2.2.3ROHR and Mass fraction burn calculation

In this section, rate of heat release (ROHR) can be calculated by applying the first law of thermodynamics and regardless the heat transfers to the chamber wall. Then ROHR will be obtained by following equations.

$$\left(\frac{dQ}{dt}\right)_{release} = mc_v\frac{dT}{dt} + P\frac{dV}{dt} \qquad (3)$$

Apply the ideal gas law , equation (3) will rearrange and become[8],[12]

$$\left(\frac{dQ}{dt}\right)_{release} = \left(\frac{c_v P}{R}\frac{dV}{dt}\right) + \left(\frac{c_v V}{R}\frac{dP}{dt}\right) + P\frac{dV}{dt} \qquad (4)$$

Relation between specific heat ,

$$\frac{c_p}{c_v} = k \quad \text{and} \quad c_p = c_v + R$$

The experiment were conduct in constant volume combustion chamber, Then, the following equation is obtained

$$\left(\frac{dQ}{dt}\right)_{release} = \left(\frac{V}{k-1}\right)\frac{dP}{dt} \qquad (5)$$

Where V is the volume of combustion chamber And k as the specific heat ratio.

As a qualitative analysis, by neglecting the heat transfer during combustion is made. The deviation for turbulent combustion by this treatment is small due to the short combustion duration [14]. Thus, the rate of pressure rise is proportional to the rate of heat release and the information of heat release rate can be reflected by the information of pressure rise rate. So , heat release rate can be calculated directly with the pressure history data[4-5],[8],[11]

Mass burned fraction is calculated based on the pressure data obtained from the experimental results as follow[5],[13].

$$M_f(t) = \frac{P(t) - P_i}{P_{max} - P_i} \qquad (7)$$

Where $P(t)$ is the combustion pressure P_i is the initial mixture pressure, and P_{max} is the maximum combustion pressure.

If the mixture gas is fully burned when it reaches peak combustion pressure, it can be calculated according to the relative value of the combustion pressure, where M10 stands for 10 percent combustion and M100 stands for 100 percent combustion[5].

Fig.6(a) shows the definition of combustion duration . It express from 10% mass fraction burn to 90% mass fraction burn[8].

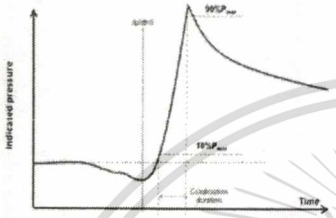

Fig.6 (a) Combustion duration

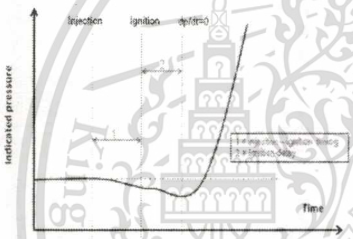

Fig.6 (b) ignition delay and ignition timing

Fig.6 Schematic behavior of indicated pressure

The traces of indicated pressure P was schematically drawn in Fig. 6, where is expressed exaggeratedly the pressure drop caused by latent heat absorption by vaporized fuel just after fuel injection start[4].

Spark gap is discharged at the aimed injection-sparking interval time later from injection start, and then ignition occurs at further later time by ignition delay. Ignition timing determined by combustion observation coincides with the timing when dP/dt takes zero as shown in Fig.6 [4].

3. Result and discussion

3.1 Lean limit according to the swirl intensities and percentage ethanol content

Fig.7 shows the lean limit of each tested fuel in various swirl intensities. Pure ethanol (E100) has minimum lean limit in every swirl intensities compare with other fuel. On the other hand, pure gasoline or E0 is the highest lean limit in every swirl conditions. In the low swirl flow (2600 rpm), Gasoline or E0 is the highest value at ø equal to 0.38 and for E20,E85 and E100 are 0.365,0.334 and 0.310 respectively. In case of higher swirl intensities, each fuel trend to ignite in the lower equivalence ratio. At the highest swirl flow (8800 rpm), Pure ethanol (E100) can be ignited at the lowest equivalence ratio at 0.300 which is Air/fuel ratio equal to 30.0 while E20,E85 and E0 can be ignited at 0.34,0.313 and 0.364 respectively.

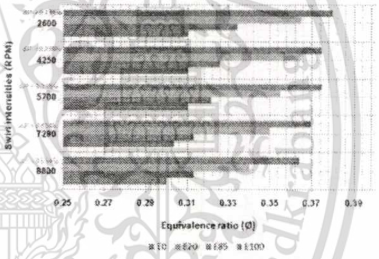

Fig.7 Lean limit in different swirl intensities

At the certain swirl value, medium swirl (5700 rpm), Pure gasoline (E0) can combust in the highest equivalence ratio compare with each other. And as the ethanol content increase, the mixture will combust in lower equivalence ratio at 0.375. Pure ethanol reach lowest equivalence ratio at 0.3105 that mean ethanol content can be support the combustion stability in the lean condition. If we consider in each fuel, in higher swirl intensity ,the minimum equivalence ratio at

lean condition will become less compare with the lower swirl flow. In case of E0, equivalence ratio at lean limit were 0.380,0.375,0.374,0.369 and 0.364 at swirl intensity equal to 2600 ,4250, ,5700, 7280 rpm and the highest swirl flow was 8800 rpm, respectively. In higher ethanol content, we obtain the same trend as the pure gasoline(E0) but the result less than expect. For pure ethanol (E100), equivalence ratio at lean limit were 0.310, 0.310, 0.310, 0.304 and 0.300 at swirl intensity equal to 2600 ,4250, ,5700,7280 and the highest swirl flow 8800 rpm, respectively. The result show rarely change in minimum equivalence ratio. Since, Higher percentage of the ethanol is less effect to enhance lean limit range than the lower ethanol content. From these results, we can discuss in two aspects, first , for stratified combustion, The whole of mixture did not combust completely, It just some amount of mixture which can ignite, especially one is stoichiometric mixture. In higher swirl intensity ,Stratification degree[5,7] which characterized ratio amount of stoichiometric mixture over the overall lean mixture became higher, Therefore ,rich and lean limit of the mixture become wider[7] or we can said that the swirl intensity can enhance stratification degree that directly effect to the lean limit range. Second aspect ,if we consider only one swirl intensity, we will found that the ethanol can ignite and combust at the lower equivalence ratio. As we know, because of air/fuel ratio of gasoline and ethanol/gasoline blends are different. So, if we need to test ethanol/gasoline blends fuel in the same equivalence ratio as the pure gasoline, we must add amount of the fuel to make it equal to same equivalence ratio. For example, at equivalence ratio equal to 1.0, the stoichiometric air/fuel ratio of each fuel in table 2. are shown that AFR_{E0}=14.6 , AFR_{E20}=13.5, AFR_{E85}=9.87 and AFR_{E100}=9.0 that means if we need to test gasoline/ethanol blends at the same equivalence ratio as pure gasoline (E0) we should add 8.24% , 48.15% and 62.01% to E20, E85 and E100 respectively. Consequently, the mixture of ethanol/gasoline in constant volume chamber will have more change to form mixture near stoichiometric ratio than that the pure gasoline (E0).

3.2 Effect of ethanol content and swirl intensity on the ignition delay

In Fig.8, Pure gasoline (E0) have the longest ignition delay in all swirl intensity and ignition delay will be decrease if the ethanol content are increase. At swirl intensity equal to 2600 rpm (or ΔP=0.1 MPa), ignition delay time of E0 is 4.24 msec and it became as 3.45 ,3.28 and 2.52 msec in case of E20, E85 and E100. respectively.

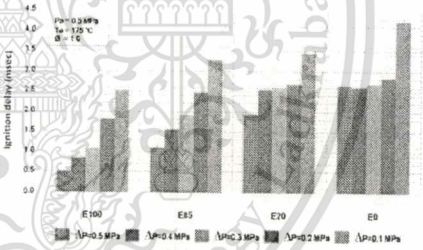

Fig.8 Effect of ethanol content and swirl intensities on ignition delay

These phenomena demonstrate that higher ethanol content can vaporize easier than lower ethanol content .

From table 2, Although ethanol has higher octane number and has low rate of vaporization , ethanol is comprised of only one

component , while gasoline is a mixture of many components with various carbon atoms and structures.

The components with relatively low boiling point which evaporate easier and faster, while the components with higher boiling point will evaporate more slowly. thus, gasoline has the longest ignition delay regardless of the higher vapor pressure of gasoline[9,10]

As show in the fig.8, ignition delay time of the ethanol (E100) will be decrease in the higher swirl flow. The result show that the ignition delay time of E100 are 2.52 msec at 2800 rpm,1.82 msec at 4250 rpm,1.08 msec at 5700 rpm ,0.85 msec at 7280 rpm and reach the shortest at 0.50 msec at 8800 rpm. These result demonstrate that swirl intensity can effect to the ignition delay by diffuse the fuel injected to the wider area. So, the mixture near the stiochiometric ratio which can easily combust will be greater than the case of low swirl flow. In case of low swirl flow, the amount of fuel injected will be form the very rich mixture near the center of combustion chamber. Therefore, the initial combustion also the ignition delay became long[7]. In the lower ethanol content such as E85 and E20 also the E0, The different of ignition delay time between each swirl intensity step will decrease as the ethanol content decrease except low swirl flow (2200 rpm) case. These may be discussed that ethanol comprised of only one component and has lower carbon atom than the gasoline or E20 and E85, Consequently, it may be diffused by swirl flow easier than that the gasoline , E20 or E85 which is comprised of various higher carbon atom[9]. As it can easily diffused , it has more change to form the stoichiometric mixture in broader area.

3.3 Ethanol content according to rate of pressure rise and mass fraction burn

Figures 9-11 shows the effect of the ethanol content on the combustion pressure at 8800 rpm swirl intensity (ΔP = 0.3 MPa). As indicated in Fig.9, the maximum pressure appears in the pure ethanol (E100) at 3.05 MPa. the peak value of combustion pressure decreases with a decrease of the ethanol content in the mixture because of lack of oxygen concentration of fuel. Also, the length of time required to reach the maximum value of the combustion pressure is retarded in accordance with the decrease of ethanol percentage.

Fig.9 Pressure data of E0 ,E20 ,E85 and E100 at equivalence ratio = 0.8

The rate of pressure rise is a very important parameter because this has a very significant influence on heat release rate as described in previous section. The effects of ethanol content on the rate of pressure rise are illustrated in Figure 10. As indicated in the figure, the peak value of the pressure rise rate was rapidly increase and its timing was shorten at high percentage of ethanol. E20 has not significantly change in maximum pressure rise rate compare with pure gasoline (E0). However, it can release heat early than that of the E0. This demonstrate that ethanol content may accelerate

the combustion period and reduce time of heat loss in early stage of the combustion.

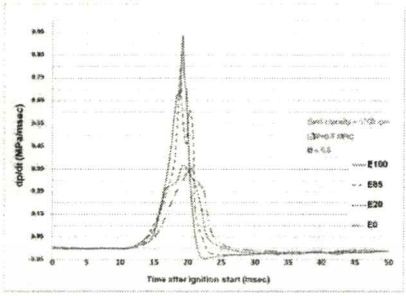

Fig.10 Rate of pressure rise of E0, E20, E85 and E100

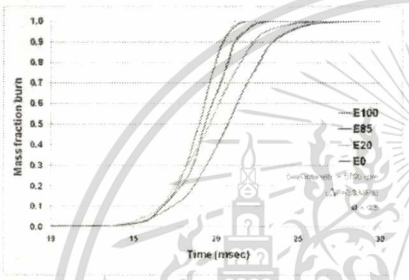

Fig.11 (a)

Fig.11 (b)

Fig. 11 Effect of ethanol content on mss fraction burn and combustion duration. Fig.11 (a) Mass fraction burn, Fig.11 (b) Combustion duration

Thermodynamic analysis of measured cylinder pressure data is a very powerful tool used for quantifying combustion parameters.[11] The important one is often referred to as "burn-rate analysis". Burn-rate analysis is used mainly to obtain the mass fraction burned, which is a normalized quantity with a scale of 0 to 1.

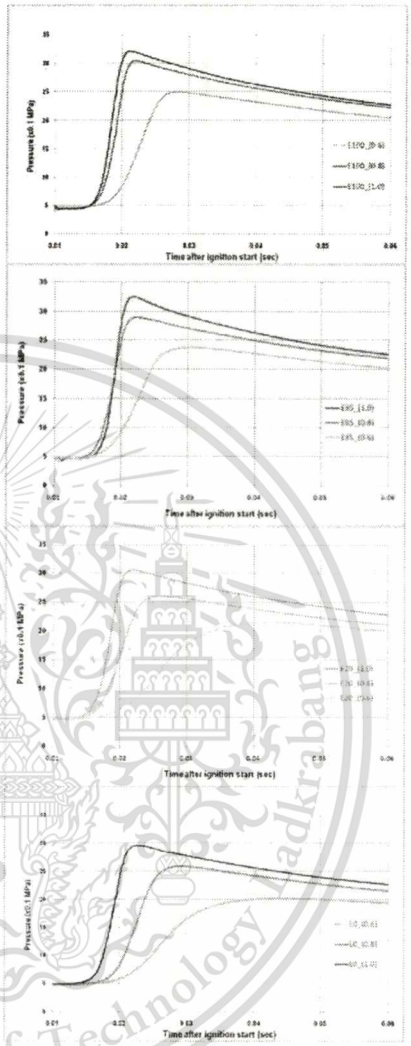

Fig.12 Effect of equivalence ratio on combustion pressure (at swirl = 8800 rpm)

Fig.11 shows the effect of ethanol content on mass fraction burned at the equivalence ratio 0.8 and 8800 rpm swirl flow. With an increase of ethanol blend, the total combustion duration

decreases, as shown in the comparison of mass fraction burned. Fig.11 (b), combustion duration of E100 was 5.44 msec this value define as 10% to 90% of trace pressure data while E85, E20 and E0 were 6.41 msec, 8.39 msec and 9.17 msec ,respectively

Fig.12 shows the influence of equivalence ratio and ethanol concentration on combustion pressure. As the equivalence ratio of mixture decrease, peak pressure were decrease and combustion duration were increase also. These result were displayed the same trend in every tested-fuel. However, Low alcohol fuel-blended ,especially in E20 and E0, the combustion pressure and combustion duration were dramatically change at low equivalence ratio.

From the result in fig. 11 and fig.12, it can be inferred that the decrease in ethanol fraction and equivalence ratios plays an important role in the decrease of maximum pressure in the chamber.

4. Conclusion

1. She swirl intensity can enhance stratification degree that directly effect to the lean limit range by diffuse amount of fuel to form stoichiometric mixture in the wider area.

2. Higher ethanol percentage in fuel will lead to extend the lean limit range because additional fuel injected may increase the change of fuel to form near stoichiometric

3. , Although ethanol has higher octane number and has low rate of vaporization , ethanol is comprised of only one component , while gasoline also the ethanol/gasoline blends are the mixture of many components with various carbon atoms and structures. The components with relatively low boiling point which evaporate easier and faster, while the components with higher boiling point will evaporate more slowly. Thus , pure ethanol trend to be evaporated faster than other blends.

4. In case of low swirl flow, the amount of fuel injected did not diffused very much. Thus, the fuel and air charge will be form the very rich mixture near the center of combustion chamber. Consequently, the initial combustion also the ignition delay became long.

5. The decrease in ethanol fraction and equivalence ratios plays an important role in the decrease of maximum pressure in the chamber. The combustion duration of pure ethanol (E100) is less than that of E85, E20 and E0 respectively. In the other hand, peak pressure of pure ethanol (E100) is higher than that of E85, E20 and E0 respectively.

Combination both high swirl flow and high ethanol content can enhance stability of the combustion in overall lean mixture.

Further studies will include advanced method to identify the consistency of the swirl intensities and mixture formation distribution, such as LIF method and flow field simulation as well as optimized the injection-ignition timing for the proper equivalence ratios that mixture form near the spark plug.

5. Acknowledgement

This work is support by the fund of Automotive Laboratory, KMITL and National Science and Technology Development Agency, NSTDA – Thailand.

Author wish to express their gratitude to Dr. Chinda Charoenphonphanich and Dr.Nuwong Chollacoop for their valuable suggestion in this research. The authors also wish to thank

Pathumwan Institute of Technology for their help in measurement such as pressure data acquisition.

6. References

[1] Harry, L. Husted, W. Piock and Ramsay, G. (2009). Fuel efficiency improvements from lean stratified combustion with a solenoid injector, SAE paper No.2009-01-1485

[2] Paul E. Kapus and Fuerhapter, Alois. (2007). Ethanol direct injection on turbocharged SI engines - potential and challenges, SAE paper No. 2007-01-1408, 2007.

[3] Geoff J. Germane, Carl G. Wood and Clay C. Hess (1989). Lean combustion in spark-ignited internal combustion engines--A Review, SAE paper No. 831694, 1989.

[4] Naoki, S. et.al (2001). A study on direct injection gasoline combustion using constant volume combustion vessel, The Fifth International Symposium on Diagnostics and Modeling of Combustion in Internal Combustion Engines, (COMODIA 2001), July, 2001.

[5] Kihyung, L., Changhee, L. and Haeyoung J. (2005). A study on the effect of stratified mixture formation on combustion characteristics in a constant volume combustion chamber. *JSME International Journal* Series B, Vol. 48, No. 2, 2005.

[6] Internal combustion engine 2nd edition (2004), V.Ganesan, McGrw-Hill publishing Co,ltd: ISBN 007-123656-2

[7] Tomita, E. and Nishiyama, A. (2000). Effects of Swirl Flow and Inhomogeneous Concentration Fields on Combustion of Propane-Air Mixture in a Constant-Volume Vessel, JSAE paper No.700-8530

[8] Jinhua Wang et.al (2008) .Study of cyclic variations of direct-injection combustion fueled with natural gas hydrogen blends using a constant volume vessel, international journal of hydrogen energy 33

[9] Jian Gao et.al (2007) ,Spray properties of alternative fuels: A comparative analysis of ethanol–gasoline blends and gasoline, Fuel 86 No.1645–1650(2007)

[10] Wang Xibin et.al (2007), Spray characteristics of high-pressure swirl injector fueled with alcohol, Energy Power Engineering China 2007, 1(1): 105–112

[11] M.Kim ,D.Kim and C.Lee (2003), Effect of residual gas fraction on the combustion characteristics of butane-air mixture in the constant0volume chamber , Energy & Fuel , 2003 *17*, 755-761

[12] Huang Z. et.al (2003), Combustion characteristics of a direct-injection engine fueled with natural gas-hydrogen blends under various injection timings, Energy & Fuels 2006, 20, 1498-1504

[13] Chareonphonphanich, C and Srichai, P. (2009). Flame Propagation of Bio-Ethanol in a Constant Volume Combustion Chamber, JSAE paper No. 2009-32- 0113 / 20097113

[14] Huang Z, Shiga S, Ueda T, et al (2003). Effect of fuel injection timing relative to ignition timing on the natural-gas direct-injection combustion. Gas Turbines Power 2003; 125(3):783–90.

AUTHOR BIOGRAPHY

Author: Mr.Piyaboot Ornman

Date of Birth: 30th January 1986

Address: 35/25 Chareonwittaya Rd. T. Sobtui A.Meuang Lampang 52100

Education:

2004 – 2007: Bachelor Degree in Mechanical Engineering, King Mongkut's Institute of Technology Ladkrabang.

2008 – 2011: Master Degree, Automotive Engineering (International Program), International College, King Mongkut's Institute of Technology Ladkrabang.

Publications:

1) P.Ornman, H.Kosaka, N.Chollacoop and C.Charoenphonphanich., "Combustion Characteristics of Direct Injection Stratified Charge of Gasohol Fuels", The 1st TSME International Conference on Mechanical Engineering, 20-22 October, 2010, Ubon Ratchathani, THAILAND.
2) P.Ornman, C.Charoenphonphanich, N.Chollacoop and H.Kosaka., "Effect of Ethanol Concentration of Gasohol on Lean Flammability Limit in Direct-Injection Stratified Charge Engine", The 7th International Conference on Automotive Engineering (ICAE-7), March 28 – April 1, 2011, Challenger, Impact, Muang Thong Thani, Bangkok, THAILAND.
3) C.Charoenphonphanich, P.Ornman, P.Karin , N.Chollacoop and H.Kosaka., "Experimental investigation in combustion characteristics of ethanol-gasoline blends for stratified charge engine", The 17th Small Engine Technology Conference (SETC2011), November 8-10, 2011, Sapporo Convention Center, Sapporo, Hokkaido, JAPAN.